CHIRAL METAL COMPLEXES OF

1,4,7-triazacyclononane AND RELATED LIGANDS

John Robb (B.Sc.)

A thesis submitted to the University of Glasgow for the degree of Doctor of Philosophy.

Department of Chemistry

August 1987

There are a number of people whom I should like to thank for their help in the course of this project. Firstly I would like to thank my supervisor Dr R.D. Peacock for his encouragement and expertise over three years in Glasgow and for his continued support during the remainder of the work. I would also like to thank Dr. L.J. Farrugia for his enthusiasm and for the patience which he showed in "cracking" the crystal structure of $[\{Co(S\text{-}Methetacn)\}_2(\mu H)_3](PF_6)_3$. I am indebted to my colleague Dr. B.C. Noble for conveying this thesis, in embryonic form, across the border on several occasions and more particularly for rescuing it during two fire alarms. My gratitude is also due to the SERC for supplying the research studentship which allowed me to carry out this work.

On a more personal level I am grateful to my parents, for their support and encouragement throughout my academic life, and to Jenifer, my wife, for her encouragement and love as we travelled this path together.

To my wife, Jenifer,

and my mother and father

ABBREVIATIONS

abs	absorbance
c.d.	circular dichroism
c.p.l.	circularly polarised luminescence
cyclam	1,4,8,11-tetraazacyclotetradecane
cyclen	1,4,7,10-tetraazacyclododecane
d	doublet
dien	diethylene triamine
dientt	N,N',N''-tritosyl diethylene triamine
DMF	Dimethyl formamide
DMSO	Dimethyl sulphoxide
dpt	N-(3-aminopropyl)-1,3-diamino propane
EDTA	ethylenediaminetetraacetic acid
en	ethylenediamine
LFSE	ligand field stabilisation energy
m	multiplet
m.d.	magnetic dipole
MEA	monoethanolamine
Metacn	2-methyl-1,4,7-triazacyclononane
Metcta	2-methyl-1,4,7-triazacyclononane-N,N',N''-triacetate.
Methetacn	N,N',N''-tris(2-hydroxyisopropyl)-1,4,7-triazacyclononane.
m.p.	melting point
NIR	near infra-red
n.m.r.	nuclear magnetic resonance
PEM	photo-elastic modulator
p.m.r.	proton magnetic resonance
pn	propylene diamine
ppl	plane polarised light
ppm	parts per million

sep	sepulchrate
SERC	Science and Engineering Research Council.
TACD	1,4,7-triazacyclodecane
TACDD	1,5,9-triazacyclododecane
tacn	1,4,7-triazacyclononane
tacntt	N,N',N''-tritosyl-1,4,7-triazacyclononane
TACUD	1,4,8-triazacycloundecane
taetacn	N,N',N''-tri(2-aminoethyl)-1,4,7-triazacyclononane
tart	tartrate
tcta	1,4,7-triazacyclononane-N,N',N''-triacetate
thetacn	N,N',N''-tri(2-hydroxyethyl)-1,4,7-triazacyclononane
tn	1,3-diaminopropane
tosyl	p-toluene sulphonyl
Ts	p-toluene sulphonyl
U.V.	ultra-violet
vis.	visible

CONTENTS

		PAGE
Chapter 1	Introduction	1
1.1	Macrocycles	1
1.2	Transition Metal Complexes	4
1.3	Synthesis of Macrocycles	6
1.4	Metal Complexes of Triazamacrocycles	15
1.5	Optical Activity of Metal Complexes	16
1.6	Optical Activity of Triazamacrocyclic Complexes	26
1.7	Ligands With Pendant Arms	37
1.8	Electronic Spectroscopy	46
1.9	Luminescence	50
1.10	Circular Dichroism and Circularly Polarised Luminescence	51
1.11	Objectives	57
Chapter 2	Experimental	59
2.1	Instrumentation	60
2.2	Materials	65
2.3	Experimental Procedure	67
Chapter 3	Complexes of tacn	91
3.1	$Co(tacn)_2Cl_3.5H_2O$	92
3.2	$Cr(tacn)_2Br_3.5H_2O$	115

Chapter 4	N,N',N''-tris(hydroxyalkyl)-1,4,7-triazacyclononanes and related complexes.	150
4.1	Introduction	151
4.2	N,N',N''-tris(2-(S)-hydroxyisopropyl)-1,4,7-triazacyclononane	152
4.3	Co^{III}((S)-Methetacn)]$^{3+}$-Results	154
4.4	[{Co(S-Methetacn)}$_2$ (μH)$_3$](PF$_6$)$_3$ - Crystal Structure	160
4.5	Discussion of Cobalt Complexes of Methetacn	162
4.6	Conclusions Relating to Cobalt Complexes of Methetacn	179
4.7	[Co(thetacn)]$^{3+}$	183
4.8	Copper Complexes of (S)-Methetacn	186
4.9	[Ni^{II}((S)-Methetacn)]$^{2+}$	189
Chapter 5	The Ligands tcta and Metcta and their Metal Complexes.	193
5.1	Introduction	194
5.2	[Co(tcta)]	195
5.3	[Co(S-Metcta)]	198
5.4	Discussion of [Co(tcta)] and [Co(S-Metcta)]	199
5.5	[Cr(tcta)]	202
5.6	[Cr(S-Metcta)]	203
5.7	Discussion of [Cr(tcta)] and [Cr(S-Metcta)]	204
5.8	The Rôle of Tartrate in Chiral Induction	208
5.9	[Cu(S-Metcta)]$^-$	209
5.10	[Ni(S-Metcta)]$^-$	212
5.11	Conclusions	215

SUMMARY

The aim of this project was to investigate some metal complexes containing the 1,4,7-triazacyclononane moiety, particularly in respect of their optical activity. The species $[Co(tacn)_2]Cl_3.5H_2O$ was investigated and its circular dichroism spectrum decomposed into $A_2(T_1)$ and $E(T_1)$ components. The analogous chromium complex was prepared and was found to spontaneously resolve on crystallisation. Optically active crystals were investigated by absorption, circular dichroism, luminescence and circularly polarised luminescence spectroscopies. The c.p.l. spectra of $[Cr(tacn)_2]Br_3.5H_2O$ represent only the third use of this technique on a crystalline sample.

The bulk of the work reported relates to derivatives of tacn with pendant arms such that they constitute N_3O_3 donors. Two groups of tacn derivatives fulfilling this criterion may be distinguished: those possessing three acetate arms and those possessing three alcohol arms. Of the latter class the ligands thetacn and Methetacn were prepared and their novel metal complexes reported. Particular attention was paid to the cobalt complexes of the chiral ligand S-Methetacn; an X-ray crystal structure of one form being reported. The acetate ligands tcta and Metcta were used to prepare chiral complexes with various first row transition metals.

For all the species involved investigation centred on chiral properties and extensive use was made of circular dichroism and to a lesser extent circularly polarised luminescence

spectroscopies, as means of probing the optical activity of metal complexes. On the basis of the optical activity observed in the visible region of the spectra of several first row transition metal complexes, empirical means of determining the absolute configuration of novel MN_3O_3 complexes, from their c.d. spectra, are suggested.

CHAPTER 1

Introduction

1. INTRODUCTION

1.1 Macrocycles

Macrocycles, and their metal complexes, play an important part in many biological processes. Extensive research has been conducted for over a century to identify the systems involved and to elucidate the processes in which they take part. Interesting though this field is however, a vast new area of research has built up around synthetic macrocycles. Unlike naturally occurring macrocycles, such as the porphyrins, synthetic macrocycles are often saturated and so the chemistry of their metal complexes is, in many ways, markedly different from natural systems.

The term macrocycle refers to heterocyclic ring systems containing a minimum of nine atoms of which two or more are non-carbon atoms. The main hetero-atoms encountered are; oxygen in the crown ethers, (Ref 1), sulphur in the cyclic polythioethers (Refs 2 & 3) and nitrogen in the polyazamacrocycles (Refs 4 & 5). Combinations of hetero-atoms of various types within a ring have also been studied (Ref 6). The presence of electronegative donor atoms allows macrocycles to behave as ligands towards metal ions while the ring often imposes constraints on the geometry of the metal complexes formed.

It has become apparent that a number of factors are responsible for determining the stability of a given metal-ligand complex (Ref 7). The important features are;

the type of binding site (amine, ether, amide etc), the number of binding sites (denticity), the size of the ion and the cavity, the physical placement of the sites, the degree to which the ion and the ring are solvated and, finally, the charge on the ion.

Often the properties of a macrocyclic complex are markedly different from those of the metal salt from which it was derived. Complexes incorporating macrocycles with large hydrophilic tails, for example, may be used to solubilise metal ions in organic solvents (Ref 8). It is also possible, by accurately modelling the correct macrocycle, to create a cavity which favours otherwise unstable oxidation states so that Ni(III) complexes, for example, may be prepared.

This volume is primarily concerned with the polyazamacrocycles, their derivatives and their first row transition metal complexes. Prior to 1974 there were two important synthetic routes to azamacrocycles; template synthesis (Fig 1.1, Ref 10) and free ligand cyclisation (Fig 1.2, Ref 11). In the former case the ligand is formed on a metal ion which holds the reactants, typically a carbonyl containing molecule and a polyamine, such that their relative positions are conducive to cyclisation. The problems with this method were a lack of general applicability and difficulty in obtaining the free amine from its metal complex. Before 1974 free ligand cyclisation was achieved using halide leaving-groups. The major

deficiency in this method was the yield which typically ranged from one to five per cent.

Since 1974 a route has been available which gives high yields of free ligand over a wide range of macrocyclic molecules (Refs 4 and 5). The Richman Atkins cyclisation differs from previous syntheses in utilising the bis (sulphonamide sodium) salt on one of the two reacting fragments to displace two sulphonate ester leaving groups on the other fragment (Fig 1.3).

With yields ranging, typically, from 50% to 80% for most azamacrocycles this synthesis was clearly superior to either of its predecessors, and by dispensing with the need for high dilution during cyclisation it provided a convenient multigram synthesis of polyazamacrocycles which rendered study of metal complexes of these interesting molecules more feasible.

Since most biological systems involving macrocycles employ molecules containing four nitrogen atoms it is not surprising that the first polyazamacrocycles to be investigated were those closely resembling the natural systems. The ligands cyclam (Ref 12) and cyclen (Ref 13) (Fig 1.4) have attracted considerable interest. More recently larger macrocycles have been produced which contain six or more nitrogen atoms while polyazamacrocycles with three identical donor atoms have been of particular interest to spectroscopists as a result of the high symmetry of their metal complexes.

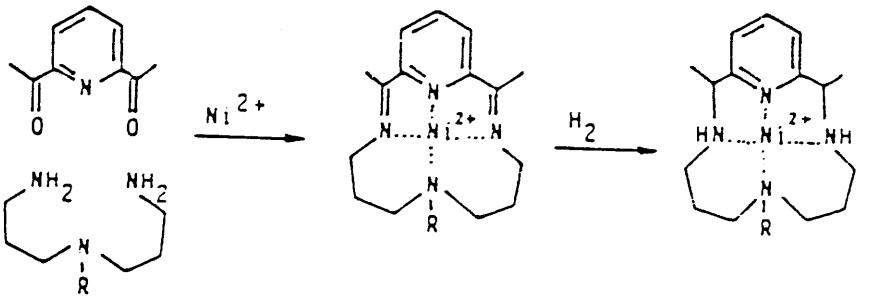

FIGURE 1.1
An example of the use of template synthesis in macrocycle formation. (Taken from ref. 9)

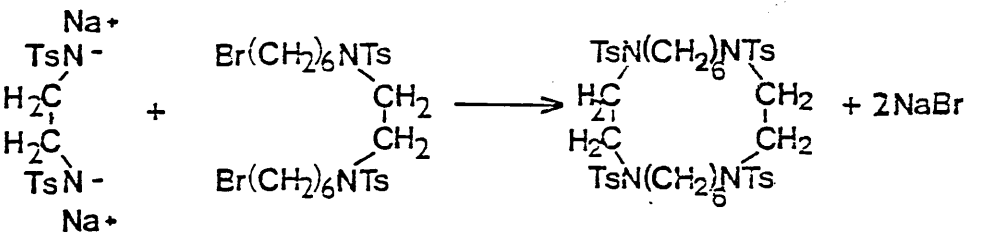

FIGURE 1.2
An example of Free Ligand Cyclisation as a route to polyazamacrocycles. (Taken from ref. 11)

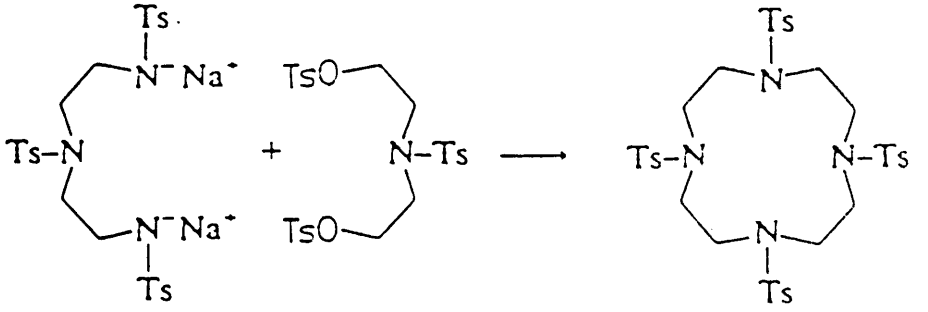

FIGURE 1.3
An example of the cyclisation step from a Richman Atkins synthesis of a tetraazamacrocycle.

1.2 Transition Metal Macrocyclic Complexes

Much of the initial interest in this area of chemistry derived from the desire to mimic biochemical reactions such as the uptake of oxygen by haemoglobin. However the field of macrocyclic chemistry continues to grow with interest centred on unusual oxidation states, the geometry and spectroscopy of metal complexes and thermodynamic aspects relating to complexation.

It has been evident for many years that these complexes enjoy greater stability than those of straight chain analogues or those containing an equivalent array of unidentate donors. This increased stability derives from two effects; the chelate effect and the macrocyclic effect. The first of these affects all complexes containing chelating ligands and this effect is largely entropic as shown in the metathesis below;

$$[Ni(NH_3)_6]^{2+} + 3\ en\ (aq) = [Ni(en)_3]^{2+} + 6NH_3(aq)$$

Simplistically there are more species in solution on the right hand side thus the reaction from left to right has a positive entropy change. This leads to a more favourable value of the Gibbs Free Energy and so the nickel tris ethylene diamine species predominates in such a solution. The macrocyclic effect is responsible for the observation that metal complexes of an open chain chelating ligand are less stable than those of the corresponding macrocycle. It is now known (Ref 14) that enthalpy and entropy make varying contributions to the macrocyclic effect depending

on the system, although research continues into the nature of these contributions (Refs 15 & 16).

Many early studies of macrocyclic metal complexes concentrated on those systems in which a ring containing four nitrogen donor atoms was bound to the metal ion. In such cases the macrocycle often coordinates meridionally (Fig 1.5) with two unidentate ligands occupying the remaining coordination sites trans to one another. However it is also possible, in these complexes, for the macrocycle to coordinate facially leaving the remaining ligands cis to one another. In the former case the symmetry approaches D_4 however in the latter it is approximately C_{2v} , and if the two forms are in equilibrium assignment of spectra becomes difficult.

From a spectroscopic view - point a more satisfying chromophore is that resulting from complexation of a metal ion with two tridentate macrocycles to give a sandwich type complex (Fig 1.6). In order to favour such complexes the tridentate ligand should have its nitrogen donor atoms connected by short carbon chains. This has the effect of preventing meridional coordination of the type observed with diethylene triamine and would thereby constrain the macrocycle to bind the metal ion facially.

The ligand 1, 4, 7 - triazacyclononane (Fig 1.6) fulfils these criteria since its three donor atoms are connected by three ethylene chains resulting in a highly symmetric

cyclen

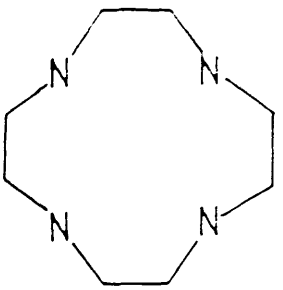

cyclam

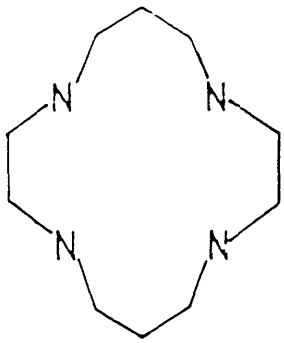

FIGURE 1.4
The tetraazamacrocycles cyclen and cyclam.
(1,4,7,10-tetraazacyclododecane and
1,4,8,11-tetraazacyclotetradecane)

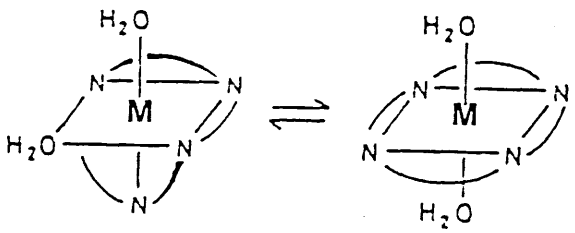

FAC MER

FIGURE 1.5
The two modes of coordination , facial and meridional , of a tetraazamacrocycle.

a)

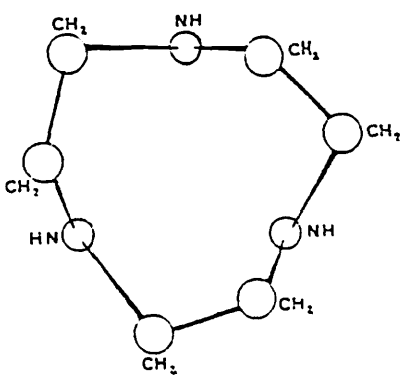

b)

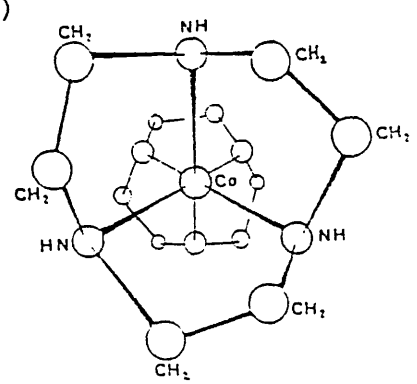

FIGURE 1.6
a) An example of a triazamacrocycle : the ligand 1,4,7-triazacyclononane.
b) A sandwich type complex comprising a metal ion and two triazamacrocyclic ligands.

ligand. Indeed in the first report of the ligand and its bis complex with cobalt(III) a sandwich structure of this type was postulated (Ref 17).

1.3 Synthesis of Triazamacrocycles

1,4,7 - triazacyclononane

The first account of the 1,4,7-triazacyclononane moiety appeared in 1937 (Ref 18) when Peacock and Gwan reported that on treating

N,N'-di(p-toluene sulphonyl)-N,N'-bis-(β - chloroethyl) ethylene diamine with alcoholic ammonia (Fig 1.7) they obtained, as a major by-product, a compound which was 'almost certainly',

1,4-di(p-toluene sulphonyl)-1,4,7-triazacyclononane in the form of its hydrochloride salt.

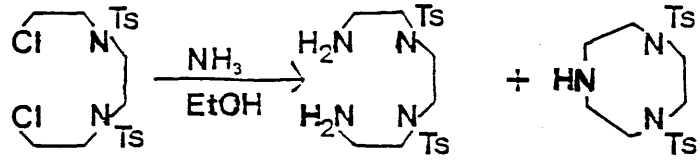

FIGURE 1.7
The Peacock and Gwan route to 1,4-di(p-toluene-sulphonyl)-1,4,7-triazacyclononane.

The product was characterised by chloride content and its melting point was recorded. However, since no detosylation to the amine was reported it must be assumed that the yield was not high.

In 1972 Koyama and Yoshino (Ref 17) prepared four triazamacrocycles, and characterised the hydrobromide salts along with selected cobalt complexes. Their aim was to assess the extent to which the strain resulting from a nine membered macrocyclic ring affected the stability of metal ion complexes whose formation would result in three mutually adjacent chelate rings. The ligands which they chose to study were;

1,4,7-triazacyclononane (tacn);

1,4,7-triazacyclodecane (TACD);

1,4,8-triazacycloundecane (TACUD) and

1,5,9-triazacyclododecane (TACDD).

A general route to the 10,11 & 12 membered rings was reported: however this method was not extended to the tacn case.

The synthetic route for preparing the larger ring sizes involved tosylating the appropriate linear triamine in basic aqueous solution by addition of a solution of p-toluene sulphonyl chloride in diethyl ether. A solution of the tritosyl triamine with 1,3-dibromo ethane in dimethyl formamide was then added to a solution of anhydrous sodium carbonate in D.M.F. at 120 degrees centigrade under conditions of high dilution. The resulting tritosylates of the cyclic polyamines were extracted into benzene which was removed to leave an oil which was redissolved in benzene and allowed to crystallise. The tacn synthesis was via the ditosyl tacn preparation reported by Peacock and Gwan (Ref 18) and no yield was reported. Koyama and Yoshino, however, were first to prepare the ligand

tacn. They did this by a detosylation which was effected, as in the case of the larger macrocyclic rings, by refluxing the tosylated macrocycle in a mixture of 9 volumes of glacial acetic acid and 16 volumes of 47% hydrobromic acid for 2 days. The yield for the detosylation of tacn was reported as 88% for the trihydrobromide salt.

Two years later, in what was perhaps the most significant paper on tacn synthesis, Richman and Atkins offered a general route to polyazamacrocycles which gave yields for the cyclisation step far superior to those available by earlier syntheses. Prior to 1974 cyclisation steps used displacement of terminal halides in order to achieve condensation. While limited success was achieved by using this technique for producing larger macrocycles there is no account in the literature of it being successfully applied to tacn synthesis.

The new synthesis, on the other hand, achieved a 71% reported yield for cyclisation of tritosyl diethylene triamine disodium salt with ditosyl ethylene glycol in dimethyl formamide (D.M.F.).

The innovative aspect of this route was the use of bis (sulphonamide sodium) salts to displace sulphonate ester leaving groups. This reaction was necessarily conducted in an aprotic solvent which was typically dimethyl formamide, although dimethyl sulphoxide has also been used in the case of a C-methyl substituted macrocycle (Ref 19).

The tritosyl tacn produced was insoluble in water and was recovered by addition of a concentrated solution in D.M.F. to a large volume of water. The work-up reported by Richman and Atkins involved hydrolysis of the tritosyl tacn using sulphuric acid in reflux over 48 hours. The ligand was obtained as its hydrochloride salt by boiling the hygroscopic tacn. $3/2H_2SO_4$, obtained from the reflux, with 6N HCl. Yields of greater than 90% for the hydrolysis step were reported.

Since Richman and Atkins reported their method there has been considerable interest in finding the best conditions and reagents for each stage in the preparation. It should be pointed out that within the Richman Atkins framework there are two alternative routes to 1,4,7-triazacyclononane as shown in Figures 1.8 and 1.9.

Route 2 is the one commonly used because it gives higher yields and consequently cleaner product. However, Searle and Geue (Ref 20) reported having attempted several syntheses by route 1. They found that at the condensation stage variable amounts of tacky solid were produced which proved to be mixtures of tacntt and starting materials along with by-products involving 2:1 and 1:2 combinations of the tosylated reagents.

The first stage in route 1 involves tosylation of diethanolamine which was reported by Hay and Norman (Ref

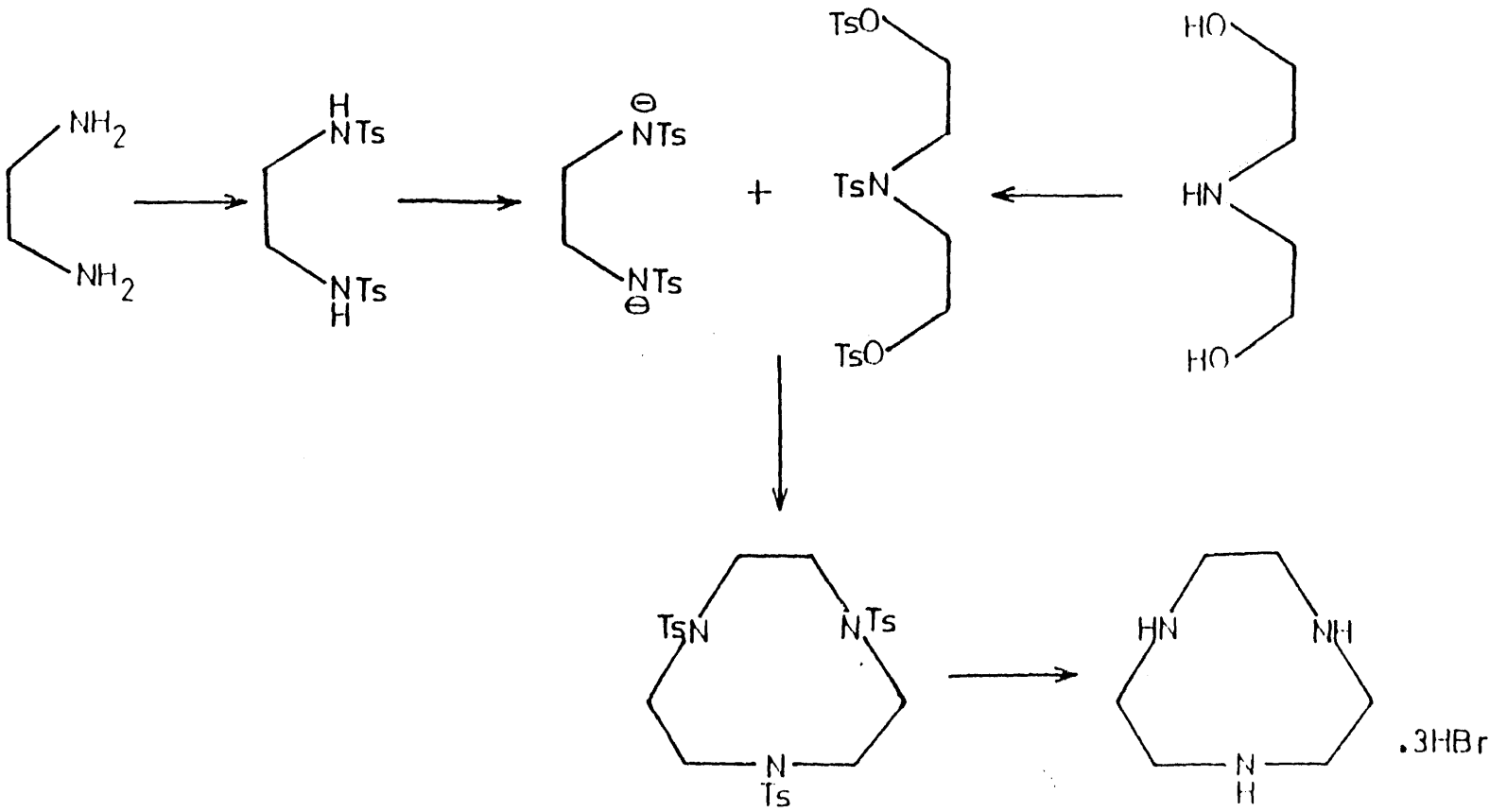

FIGURE 1.8
Route 1 to tacn : cyclisation from N,N'-di(p-toluenesulphonyl) ethylene diamine and N,O,O'-tri(p-toluenesulphonyl) diethanolamine.

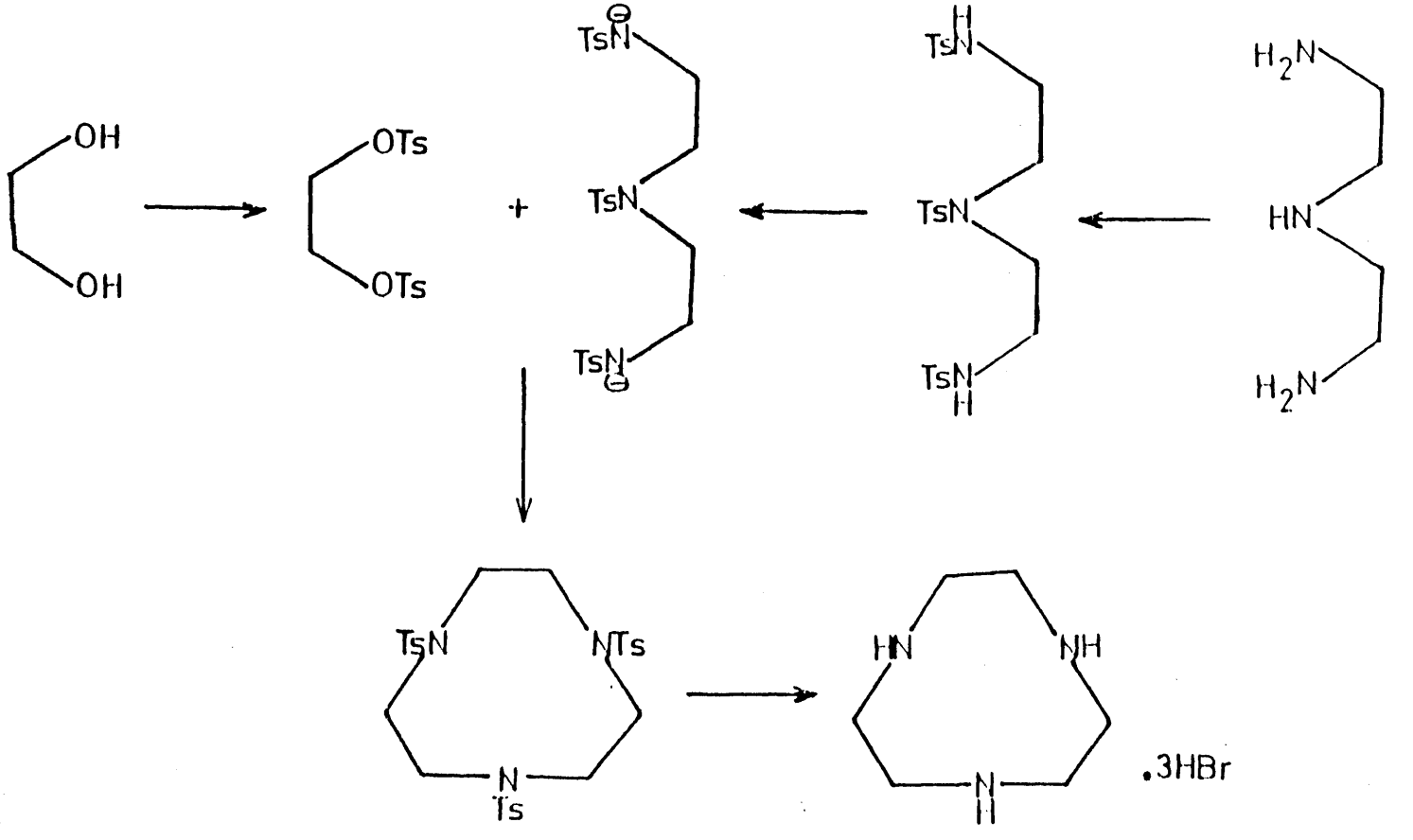

FIGURE 1.9
Route 2 to tacn : cyclisation from 1,2-di(p-toluenesulphonyloxy) ethane and N,N',N''-tri(p-toluenesulphonyl)diethylenetriamine .

21) following a technique used by Atkins. In this synthesis solid p-toluene sulphonyl chloride was added, under nitrogen, to a solution of diethanolamine in dry pyridine in an ice bath such that the temperature did not exceed 10 degrees centigrade. On slow addition of HCl precipitation was reported to give a yield of 85%. A simpler preparation, though one which affords only a 60% yield, is that of Fabbrizzi (Ref 22). In this synthesis an ether solution of tosyl chloride was added to a stirred solution of diethanolamine in triethylamine in an open beaker. Addition of water dissolved excess starting material and the precipitate was recrystallised from ethanol.

The universally used route to ditosyl ethylene diamine involves addition of an ether solution of p-toluene sulphonyl chloride to a basified (NaOH) aqueous solution of the amine. This reaction gives high yields (71%) and can be generally applied to the tosylation of amines.

Searle and Geue (Ref 20) reported that on cyclisation of the disodium salt of di(p-toluene sulphonyl) ethylene diamine with tritosyl diethanolamine, the product was an impure tacky solid.

Route 2, then, is generally preferred and is extensively cited in the literature. This method involves condensation of the disodium salt of tritosyl diethylene triamine (made by an analogous manner to that used to prepare disodium ditosyl ethylene diamine) with ditosyl ethylene glycol. The

formation of the disodium salt of the tosylated amine was often conducted as a separate step in early syntheses (Ref 23) and the disodium ditosyl oligo-amine was isolated and characterised. By addition of the tosylated amine to a solution of sodium ethoxide in ethanol a precipitate of the disodium salt was obtained. However, as a result of the ease of hydrolysis of this product it was found advantageous in later syntheses to prepare the salt and then to effect an in-situ cyclisation. The first report of a tacn preparation using this method was by Searle and Geue (Ref 20). It involved adding solid sodium hydride, in a nitrogen atmosphere, to a solution of tosylated diethylene triamine in dry dimethyl formamide. The solution was heated to complete the reaction and filtered, to remove any excess sodium hydride, taking care to exclude water. The filtrate was heated to 105 degrees centigrade and to it was added, dropwise, a dry D.M.F. solution of 1,2-di(p-toluene-sulphonyloxy) ethane. The dropping took place over several hours in order to ensure optimum yield of 1:1 stoichiometry reaction product (ie tritosyl tacn). Higher cyclic and linear products are often reported from tacn preparations (Refs 24 & 25).

Route 2 was reported by Searle and Geue (Ref 20) to be superior in terms of both yield and purity of product. Synthesis by route 1 was attempted in the belief that, were it as good as route 2, any residual tosylated amine starting material would be ditosyl ethylene diamine which would be more easily separated from the product than the

tritosyl diethylene triamine contaminant in route 2. The poor results from route 1 are rationalised in terms of a two step reaction mechanism (Fig 1.10) in which the two fragments in each case combine by an intermolecular reaction to give the same linear intermediate monosodium salt which then cyclises in an intramolecular fashion to give tritosyl tacn (Ref 20).

Since the linear salt is the same in both cases the authors reasoned that the initial joining of the two fragments is inhibited for route 1. They offer three possible reasons for this. Firstly they considered steric and electronic factors, pointing out that in the dianion of ditosyl ethylene diamine the two negative charges are closer together than in the dianion of tritosyl diethylene triamine. Secondly they postulate, on the basis of higher products, that the linear intermediate may be more reactive towards the route 1 starting materials than towards those in route 2. Finally they do not rule out the possibility of greater sensitivity to water of the disodium salt of ethylene diamine. Hydrolysis of this salt would effectively destroy one of the reagents in route 1.

Detosylation of tosylated cyclic triamines may be achieved by either of the two methods in general usage. The more common detosylation technique involves reductive cleavage by refluxing the tosylated amine in a mixture of hydrobromic acid and acetic acid over approximately three days. The trihydrobromide salt obtained is often converted

to the trihydrochloride by several recrystallisations from concentrated hydrochloric acid. The alternative detosylation involves refluxing the tosylated amine for two days in concentrated sulphuric acid in order to achieve hydrolysis and produce tacn.3/2H_2SO_4 which is hygroscopic. Again conversion to the hydrochloride may be achieved by recrystallisation from concentrated HCl. A variation on the HBr detosylation was reported by Graham and Weatherburn (Ref 26) who conducted the experiment in a sealed tube and achieved good yields (80%).

2(R)Methyl-1,4,7-triazacyclononane.

The ligand R-Metacn (Fig 1.11) was originally prepared by Mason and Peacock in 1975 (Ref 27). It differs from tacn in that it is C-methyl substituted to give a chiral centre on one of the potential chelate rings. The intention was that this chiral centre should force sandwich type bis complexes of the ligand to be optically pure in solution rather than exist as a racemic mixture as observed for solutions of $[Co^{III}(tacn)_2]^{3+}$. The complexes would have effective C_3 symmetry since the methyl group is sufficiently far from the chromophore to allow it to be regarded as a minor perturbation on the systems.

The synthesis first employed was based on the Richman Atkins cyclisation. R(-)propylene diamine, resolved by the method of Dwyer and co-workers (Ref 28), was tosylated and converted to its disodium salt before being isolated. The resulting salt was dissolved in dry dimethyl formamide at

100 degrees centigrade and to it was added one equivalent of tritosyl diethanolamine, in D.M.F. The product, N,N',N''-tritosyl-2-Methyl-1,4,7-triazacyclononane, was detosylated by refluxing it in a mixture of hydrobromic acid and glacial acetic acid.

This preparation has been extensively used and was examined in detail by Graham and Weatherburn (Ref 19) in 1983. They reported that the method gave yields of approximately 20% for the cyclisation step with the remainder of the product comprising linear and higher cyclic combinations of the tosylated starting materials. Graham and Weatherburn attempted to use an alternative route (Fig 1.12) involving condensation of ditosyl propane-1,2-diol with the disodium salt of tritosyl diethylene triamine.

The failure to achieve cyclisation using a di(p-toluene sulphonyloxy) alkane derived from a secondary alcohol may be explained by postulating an inability on the part of the $-\overset{\ominus}{N}Ts$ moiety to attack the sterically hindered tertiary carbon atom on which the -OTs leaving group was situated (Fig 1.13).

The conclusion was drawn that while the Mason and Peacock route was still the best available for production of

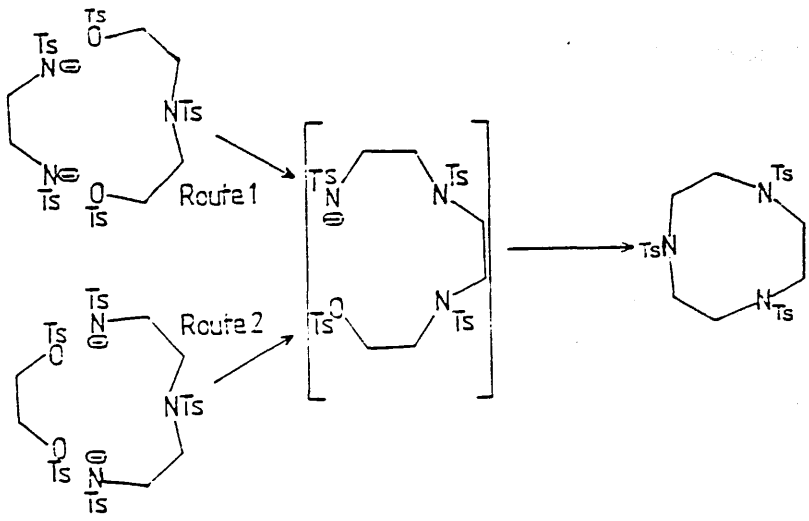

FIGURE 1.10
Both routes to 1,4,7-triazacyclononane are postulated to pass through the same intermediate.

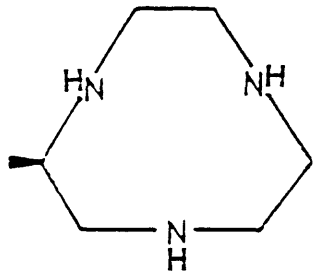

FIGURE 1.11
The ligand 2-R-methyl-1,4,7-triazacyclononane : abbreviated R-Metacn.

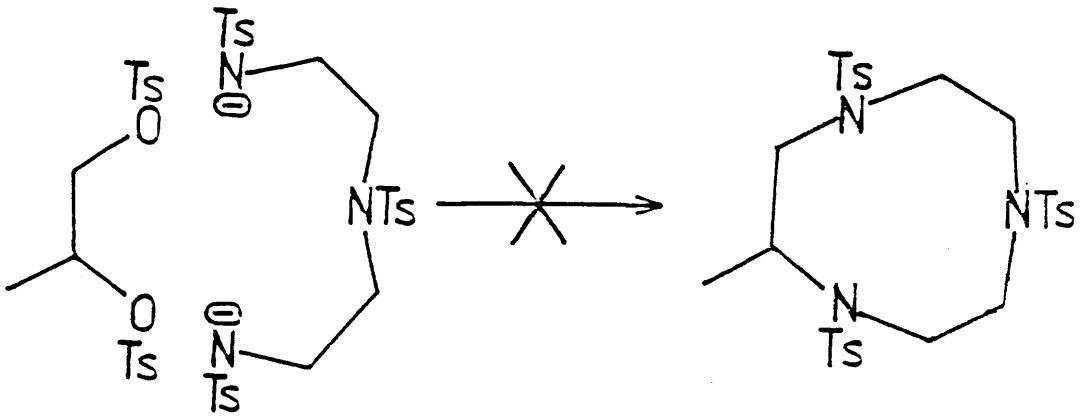

FIGURE 1.12
The high-yield route to tacn was found to be inapplicable to the C-methyl substituted analogue, R-Metacn.

C-methyl substituted triazamacrocycles, the yields are smaller, and the quantity and variety of by-products greater, than would be acceptable for unsubstituted analogues.

1.4 Metal Complexes of Triazamacrocycles

First row transition metal complexes of triazamacrocycles fall into two broad categories; mono complexes and bis complexes. Mono complexes (Ref 29) adopt the structure in figure 1.14a, with the terdentate ring facially coordinated to the metal ion and the three remaining coordination sites also constituting a facial arrangement. So pronounced is the tendency of tacn to coordinate facially that the ligand dpt;(N-(3-aminopropyl)-1,3-diamino propane), which shows a strong preference to bind meridionally, was found (Ref 30), for the first time, to have assumed a facial coordination in the complex $[Co^{III}(tacn)(dpt)]^{3+}$.

Bis complexes of triazamacrocycles tend to have sandwich structures whereby both of the ligands bind facially (Fig 1.14b). These sandwich structures raise several points of interest. In contrast with most tris diamine complexes (Ref 31) they do not exhibit trigonal compression: indeed trigonal elongation resulting from replusive interactions of hydrogen atoms is a feature of these systems.

A second consequence of the interactions between hydrogen atoms on the two ligands in bis complexes is that the conformation of a chelate ring on one of the ligands exerts

an influence resulting in adoption of the same conformation by neighbouring chelate rings on the other ligand. This can most clearly be seen in the case of complexes involving the ligand R-Metacn where one of the chelate rings is constrained in the λ conformation (Ref 32). However, it has been found that $[Co^{III}(tacn)_2]Cl_3.5H_2O$ forms enantiomeric single crystals from racemic solutions indicating that the conformations, while being fixed in the solid state, are mobile in aqueous solution. The process of racemisation in this case involves simple flipping of the chelate rings. In 1983 Wieghardt et al (Ref 33) outlined a preparation of $[Cr(tacn)_2]^{3+}$ and recorded its absorption spectrum. Surprisingly however, no work was conducted on the optical activity of this species.

In addition to mono and sandwich structures involving triazacyclononane ligands several other geometries are known; from the square planar platinum bis tacn complex (fig 1.15a, Ref 34) to hydroxo bridged chromium complexes (Fig 1.15b, Ref 35).

1.5 Optical Activity of Metal Complexes (Ref 36)

Certain substances have the power to rotate the plane of plane polarised light. In order to do this it is necessary for a substance to contain molecules, or arrangements of molecules, which are chiral, that is non-superposable on their mirror images. Molecules, or arrangements, which have this property exist in two enantiomeric forms, one rotating plane polarised light to the right, the other rotating it

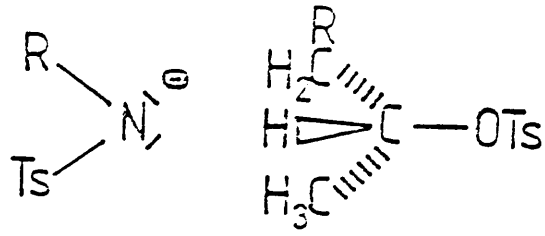

FIGURE 1.13
The apparent inability of 1,2-di(p-toluenesulphonyloxy) propane to react with the disodium salt of a secondary amine may be the result of steric crowding.

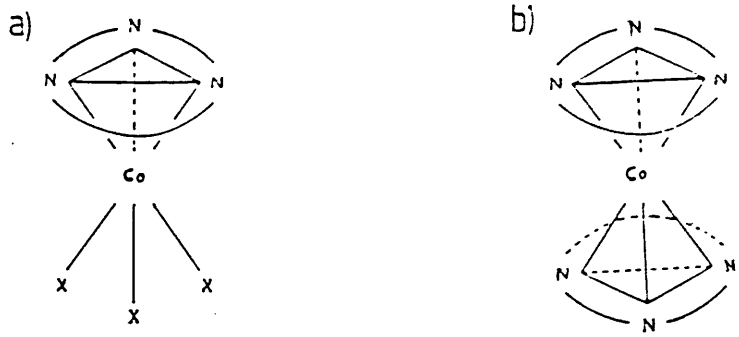

FIGURE 1.14
Schematic diagrams of a) mono-macrocyclic and b) bis-macrocyclic complexes showing in each case the facial nature of the coordination. (Adapted from ref 17)

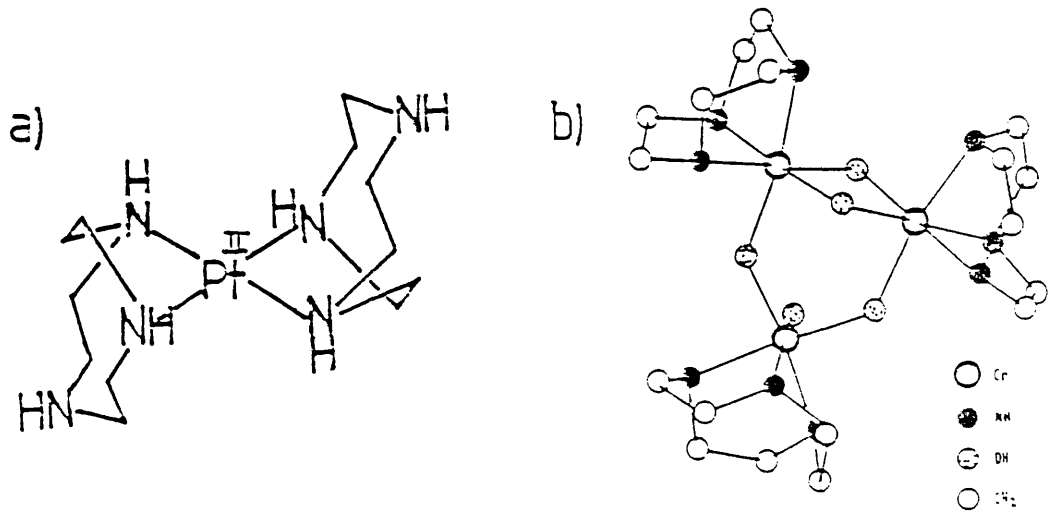

FIGURE 1.15
Two complexes involving tacn in unusual geometries: a) a square planar platinum complex (adapted from ref 34) and b) a hydroxo bridged chromium trimer (taken from ref 35).

by the same degree to the left. Any imbalance in the two enantiomers will result in a rotation.

Molecules which are chiral are said to be dissymmetric and possess no improper axes of rotation (σ, S_n, i). In organic chemistry dissymmetry normally entails the two possible arrangements of four substituents about a central carbon atom: however in the chemistry of metal complexes, which are often six coordinate, there is a greater variety of sources of dissymmetry.

Perhaps the most studied example of a chiral transition metal complex is $[Co(en)_3]^{3+}$ (Fig 1.16). In this case the dissymmetry results from two sources. Firstly there is a chiral mutual disposition of the planes of the chelate rings. This is observed as the twist of the 'propeller blades' looking down the C_3 axis of the molecule. Concentrating on one of the three near nitrogen atoms it is seen to be connected to one of the rear nitrogens. If the connected rear nitrogen is to the right of the front nitrogen then the molecule has a Δ configuration. If it is rotated to the left the configuration is Λ . The second source of dissymmetry is the chelate rings which may adopt either of two possible chiral conformations (Fig 1.17): λ or δ.

By IUPAC convention (1970) the conformation has the δ form if the C-C bond forms a segment of a right handed helix with respect to the N-N direction in the chelate ring. The

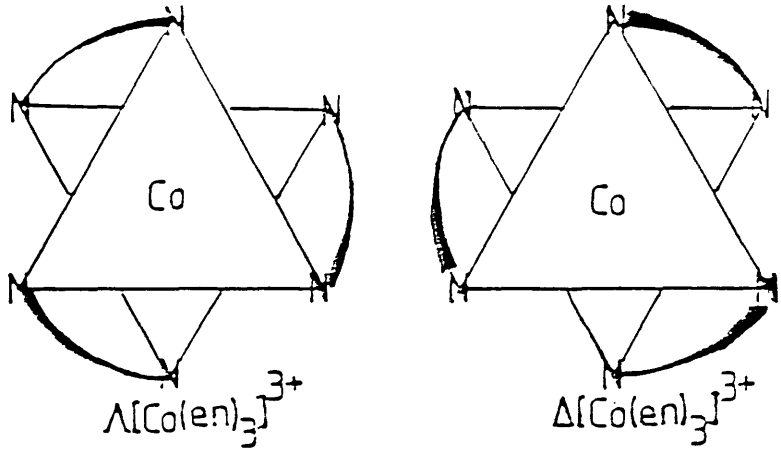

FIGURE 1.16
A schematic representation of the two possible configurational isomers Λ and Δ of $[Co(en)_3]^{3+}$.

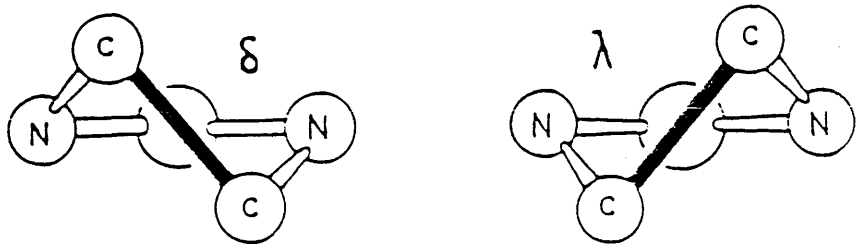

FIGURE 1.17
The two conformational enantiomers (δ and λ) resulting from a five membered chelate ring.
(Taken from ref 37)

λ conformation involves a similar left handed helix. While λ and δ conformations can be equal in energy, and indeed interconvert at room temperature for certain complexes in solution: chelate rings are often locked in either the λ or δ form in the solid state.

Other sources of optical activity encountered in transition metal complexes involve chiral configurations about atoms in the ligand. Ligands involving chiral carbon atoms give rise to optically active complexes while nitrogen atoms carrying three different substituents constitute centres of chirality, on coordination.

The preparation of an optically pure sample of a particular stereo-isomer of a complex may be accomplished by several techniques. Perhaps the simplest is to use an optically active ligand in synthesis of the complex. Such ligands may occur naturally in one enantiomerically pure form or racemic mixtures of ligands may be resolved using properties such as the differential solubility of diastereo-isomers. An example of the former case is tartaric acid which is obtained from grapes as its **L**(+) form. Dwyer and co-workers (Ref 28) resolved propane-1,2-diamine by forming its (+) tartrate salts (-)pn(+)tart and (+)pn(+)tart which,being diastereo-isomers, had different solubilities in water.

Many transition metal complexes with non-optically-active ligands may, nevertheless, be resolved. It has already been

mentioned that $[Co(tacn)_2]Cl_3.5H_2O$ gives crystals containing one or other enantiomer, but not both. This is a relatively rare situation where a racemic solution gives rise to enantiomeric crystals (around 250 such cases are known (Ref 36)). The complex racemises on dissolution of the single crystal. In the case of complex ions resolution of stereo-isomers can often be achieved by ion exchange chromatography using media such as SP-Sephadex. The use of eluting agents such as sodium(+)tartrato antimonate gives diastereomeric interactions between agent and sample thus causing the various stereoisomers to move at different rates through the column (Ref 38). While this technique is suitable for ions it is not widely applicable to neutral species.

A similar method which allows optically active complexes to be obtained is that involving diastereomeric precipitation. The technique gives varying yields of the required enantiomer and relies on a diastereomeric interaction. The principle is best considered by reference to an example (Ref 39), the formation of dextro $[CoIII(en)_3]^{3+}$ by a partial asymmetric synthesis. The chirality of the starting material Co(d-tart) is important because it determines that of the product. The reaction sequence is outlined in Figure 1.18.

The yield of (4) is further enhanced by the reaction;
(5) + (2)$\longrightarrow$(4)$\downarrow$ + (3) which is an electron transfer reaction. The $[Co(en)_3]^{3+}$ unit is stable in solution and is

independent of the d-tart ion which may later be replaced by iodide, for example, without loss of chirality. (Racemisation is effected at 110 degrees centigrade in a sealed tube using a charcoal catalyst.)

Having obtained an optically active sample of a metal complex it is normal to obtain its circular dichroism spectrum. A vast amount of research, both theoretical and experimental, has been carried out into the circular dichroism of metal complexes. The aim of such research has been to explain c.d. spectra in terms of the transitions involved and then to predict, from a theoretical or empirical basis, a relation between c.d. spectra and absolute configuration which will hold for related complexes. In order to understand c.d. spectra it is necessary to understand the transitions involved. By observing electronic transitions in absorption spectra and assigning them (by reference to known complexes or to Tanabe Sugano diagrams) it is possible, in turn, to assign bands in the corresponding c.d. spectra.

The metal complexes considered in this work are those containing Co(III), Cr(III), Cu(II) and Ni(II) so it is worth examining the c.d. spectra of some complexes of these metals.

Complexes involving Co(III) are generally octahedral and exhibit two d→d transitions in the visible region. The higher in energy of these bands is assigned to

$^1A_{1g} \longrightarrow {}^1T_{2g}$ and is electric and magnetic dipole forbidden. It corresponds to a transition from $d_{xy} \longrightarrow d_{z^2}$, $d_{xz} \rightarrow d_{y^2}$ or $d_{yz} \rightarrow d_{x^2}$. The other transition is $^1A_{1g} \rightarrow {}^1T_{1g}$ which is magnetic dipole allowed and arises from $d_{xy} \longrightarrow d_{x^2-y^2}$. Since the complexes considered in this work possess pseudo D_3 symmetry it is necessary to consider the effect of this lowering of symmetry. In the absorption spectrum no splitting is observed for CoIII, however in the c.d. spectrum splitting is evident for the $^1T_1$ state. In D_3 symmetry $^1T_2$ splits into ^1E and $^1A_1$. Transitions from the $^1A_1$ ground state to the $^1A_1$ excited state are forbidden so that for the $^1T_2$ transition a single c.d. band corresponding to a $^1A_1 \longrightarrow {}^1E$ transition is observed. The $^1T_1$ state splits into ^1E and $^1A_2$, both of which have magnetic dipole allowed transitions from the $^1A_1$ ground state and as a consequence two bands are normally observed under the $^1A_1 \longrightarrow {}^1T_1$ transition in D_3 symmetry.

The transitions under the $^1T_1$ state are of interest because the two energy levels may, in favourable conditions, be resolved. The $^1A_1 \longrightarrow {}^1E$ transition is caused by light propagated parallel to the C_3 axis: the $^1A_1 \longrightarrow {}^1A_2$ transition is excited by light propagated perpendicular to the C_3 axis. The first consequence of this is that the two bands have opposite signs since light travelling in these two directions encounters opposite helicities within a given molecule. This follows from the property of a helix (of which a C_3 molecule is an example) that its axial helicity is opposite to its equatorial helicity (Fig 1.19).

The second consequence of the lowering of degeneracy of the $^1T_1$ state is that light propagated down the C_3 axis of the molecule excites only the transition $^1A_1 \longrightarrow {}^1E$. This is significant because if the molecules were alligned it would be possible to observe this transition in isolation and indeed this has been done on several occasions (Refs 31 & 40) using single crystals in which the orientation of the molecular C_3 axis within the crystal was known. The importance of decomposing the rotational strengths due to these two transitions results from the observation that the observed c.d. spectra of $^1A_1 \longrightarrow {}^1T_1$ transitions represent an approximately 90% mutual cancellation of the two contributions.

For a crystalline solid Kuroda and Saito (Ref 31) showed that for a molecule with C_3 symmetry, where the three fold axis of the molecule was inclined to the optic axis at an angle α, the differential molar extinction coefficient for the $^1A_1 \longrightarrow {}^1T_1$ transition could be split into components for A_2 and E transitions. The molar extinction coefficient for a single crystal with light propagated down the highest fold axis is given by:

$$1a) \qquad \Delta\varepsilon = \frac{(1+\cos^2\alpha)}{4}\Delta\varepsilon(E_x) + \frac{(1+\cos^2\alpha)}{4}\Delta\varepsilon(E_y) + \frac{\sin^2\alpha}{2}\Delta\varepsilon(A_2)$$

For a crystal where the C_3 axis is parallel to the crystal c-axis the equation simplifies to;

1b) $\Delta\varepsilon_s = \frac{1}{2}\Delta\varepsilon(E_x) + \frac{1}{2}\Delta\varepsilon(E_y) + 0 \quad = \Delta\varepsilon(E)$

In order to assess $\Delta\varepsilon(A_2)$ it is necessary to obtain the value $\Delta\varepsilon(T_1)$, for a randomly oriented sample; a solution or preferably a microcrystalline sample (supported in KBr). In this case:

1c) $\Delta\varepsilon_m = \frac{1}{3}\Delta\varepsilon(E_x) + \frac{1}{3}\Delta\varepsilon(E_y) + \frac{1}{3}\Delta\varepsilon(A_2)$

Which simplifies to:

1d) $\Delta\varepsilon_m = \frac{2}{3}\Delta\varepsilon(E) + \frac{1}{3}\Delta\varepsilon(A_2)$

From the two equations (1b & 1d) it is possible to obtain absolute values for $\Delta\varepsilon(E)$ and $\Delta\varepsilon(A_2)$.

Peacock and Stewart, in a review (Ref 41) of c.d. of transition metal complexes, listed several parameters in the spectra which could be related, theoretically and empirically, to structural features of Co(III) complexes. The first such parameter considered was the sign of the $E(T_1)$, transition which was found to be negative for most $\Lambda[Co(\widehat{N\ N})_3]^{3+}$ complexes but positive for $\Lambda[Co(tn)_3]^{3+}$ (Ref 42). By introducing the concept of an angle, ω, being the lesser of the two angles between any front donor atom and its back neighbour (Fig 1.20) it was possible to formulate a relation which held for all known amine complexes, including the bis triamines.

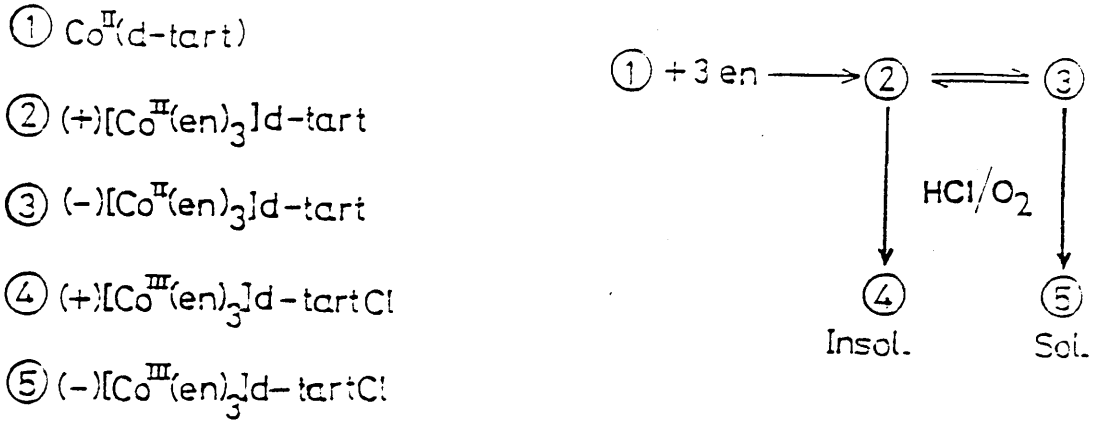

FIGURE 1.18
The separation of optically stable enantiomers by use of diastereomeric interactions with a chiral reagent. The salts formed have different solubilities.

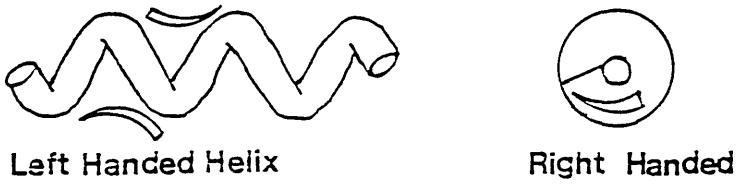

FIGURE 1.19
The same helix viewed from orthogonal directions exhibits different helicities.

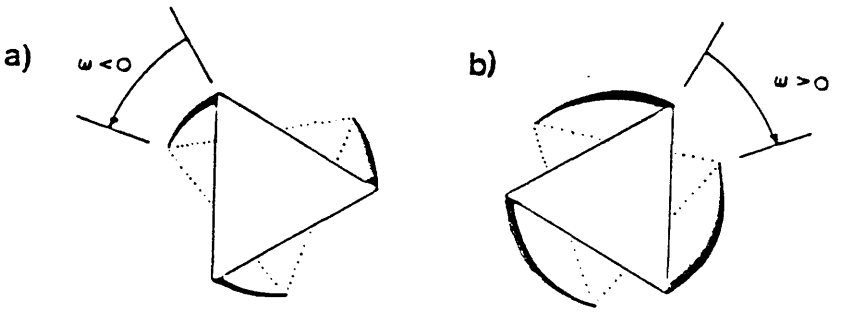

FIGURE 1.20
The angle ω determines the sign of the E and $A_2(T_1)$ transitions of Co(III) and Cr(III) complexes. There is no rule relating the sign of the c.d. of these transitions to the absolute configurations, Λ and Δ.

Figure 1.20 shows how ω can be positive or negative for the same absolute configuration. The $[CoIII(tn)_3]^{3+}$ case is no longer anomalous in terms of the signs of A_2 and E if it is considered to be similar to figure 1.20b while the other $[Co(\widehat{N\ N})_3]^{3+}$ species have shorter chelate rings and correspond to type 1.20a.

Another c.d. parameter which the authors related to structure is the relative energies of the A_2 and E polarised transitions. It would appear that complexes exhibiting compression along their C_3 axes have the E component at lower energy than the A_2 component. In elongated complexes the opposite situation obtains. For the third parameter, the ratio $R(A_2):R(E)$, the authors were reluctant to draw conclusions.

Chromium(III) complexes are d^3 species and consequently have high octahedral ligand field stabilisation energies. Two transitions are normally observed in the visible region of the spectrum, although a third spin-allowed d→d transition is hidden under the charge transfer bands. The transitions observed are, at lower energy $^4A_2 \longrightarrow {}^4T_2$ ($d_{xy} \longrightarrow d_{x^2-y^2}$ etc) and at higher energy $^4A_2 \longrightarrow {}^4T_1$ (F) ($d_{xy} \longrightarrow d_{z^2}$ etc). The higher energy, $^4A_2 \longrightarrow {}^4T_1$ (P) transition is not usually observed. As in the case of Co(III) the trigonal distortion splits the T states into A and E so that T_2 gives A_1 and E while T_1 gives A_2 and E. The A and E states resulting from any T state have oppositely signed bands. Since $^4A_2 \longrightarrow {}^4A_2$ is

forbidden the observed c.d. spectrum consists of a single high energy band $^4A_2 \longrightarrow {}^4E\ (^4T_1)$ and two oppositely signed lower energy bands, $^4A_2 \longrightarrow {}^4E\ (T_2)$ and $^4A_2 \longrightarrow {}^4A_1\ (^4T_2)$. In addition to these spin allowed bands chromium(III) also exhibits spin forbidden bands at lower energy (~15,500cm^{-1}) which may be observed by both c.d. and c.p.l. spectroscopies. These characteristically sharp bands represent transitions to doublet states: $^4A_2 \longrightarrow {}^2T_1$ and $^4A_2 \longrightarrow {}^2E$.

Cu(II) has nine d-electrons and as a result its octahedral ligand field is not significantly stabilised and tetragonal complexes predominate.

Unlike Co(III) and Cr(III), Cu(II) gives complexes which are optically labile in solution. The absorption spectra of copper complexes consist of a broad band at about 14300cm^{-1}, often with a shoulder, and normally unsymmetrical. This band corresponds to the $^2E \longrightarrow {}^2T_2$ transition in octahedral symmetry.

Ni(II) has eight d-electrons and a consequent tendency to form square planar complexes. Transitions may be observed, in octahedral symmetry, from the ground state $^3A_2$ to three excited triplet states; $^3T_1(P)$, $^3T_1(F)$ and $^3T_2(F)$. In D_3 symmetry the transitions to the first two states (ie the two higher energy transitions) have symmetry E (and A_1 forbidden). The $^3T_2$ state gives rise to transitions of symmetry E and A_2 and should therefore give two

opposite signed c.d. bands. Of the three transitions in the visible spectrum of nickel(II) only the low energy $^3A_1 \longrightarrow {}^3T_2$ has a zero order magnetic dipole. Often the lowest energy transition is split by spin-orbit coupling into three terms, $^3F_4$, $^3F_3$ & $^3F_2$.

1.6 Optical Activity of Triazamacrocyclic Complexes

The optical activity of metal complexes of triazamacrocycles has received considerable attention over the years. The cobalt complexes in particular are of interest because of their lack of lability. While the ligand R-Metacn was designed (Ref 27) to form optically active complexes, the ligand tacn has also been used to give optically active species (Ref 36). $[Co^{III}(tacn)_2]Cl_3.5H_2O$, for example, forms enantiomorphic crystals although it is optically labile in aqueous solution.

While interest has centred on the Co(III) complexes of triazamacrocycles the Cr(III) species, which should be similar in many respects, have received little attention, presumably because of synthetic difficulties. No work has been reported on the optical activity of $[Cr^{III}(tacn)_2]^{3+}$ type complexes.

The first circular dichroism studies on metal complexes of triazacyclononanes were carried out by Mason and Peacock (Ref 27) on the complex $[Co^{III}(R\text{-Metacn})_2]^{3+}$ in 1975. In the paper the optical activity of chiral diamine and polyamine complexes is reported to result from two sources;

a dissymmetric puckering of the chelate rings (λ , δ) and a chiral mutual disposition of chelate rings (Λ , Δ). The conformational effect was assumed to be additive over all chelate rings present whereas the configurational effect was believed to be dependent on the number of ring-ring interactions. In complexes of diamines the two effects are inseparable, however models of the then recently prepared $[Co(tacn)_2]^{3+}$ suggested that no configurational effect would be present, but that within the chelate rings belonging to one ligand the conformations would be the same (i.e. $\lambda\lambda\lambda$ or $\delta\delta\delta$). The influence of the conformations of one macrocyclic ligand ring on those of another had not been discovered and it was expected that $[Co(tacn)_2]^{3+}$ would exist in (λ_3 , λ_3),(δ_3 , δ_3) and (λ_3 , δ_3) forms. Since the meso form would predominate the ligand R(-)2-methyl - 1,4,7- triazacyclononane was designed and prepared to allow chiral cobalt complexes of these ligands to be observed. It was intended that the methyl group would impose a conformation on the chelate ring to which it was appended and consequently on all six chelate rings of the bis complex. Models suggested that R-Metacn would give a λ puckering of the chelate rings. The c.d. spectrum of $[Co(R\text{-}Metacn)_2]^{3+}$ in solution showed a positive rotational strength in the $^1A_1 \longrightarrow {}^1T_1$ region of Co(III) which for the $Co(III)N_6$ chromophore was known to be characteristic of λ puckering.

The magnitude of the circular dichroism band for $^1A_1 \longrightarrow {}^1T_1$ was greater than that expected from adding six

λ conformations and to explain this a synergistic effect resulting in trigonal distortion was postulated and supported by preliminary X-ray results. The magnitude of the negative band under the $^1A_{1g} \longrightarrow {}^1T_{2g}$ (O_h) transition was much less than that of the positive band due to the lower energy $^1A_{1g} \longrightarrow {}^1T_{1g}$ transition.

Mikami et al subjected $[Co^{III}(R\text{-Metacn})_2]I_3.5H_2O$ to X-ray crystal analysis and discovered both an elongation along the C_3 axis ($\hat{NCoC}$ 51.3° cf 54.7° for octahedral) and a twist of the lower donor set of some 7.6 degrees in the clockwise direction. A note is made of the fact that the single crystal c.d. spectrum with light propagated parallel to the optic axis shows a single negative band under the $^1A_1 \longrightarrow {}^1T_1$ transition at 487nm, whereas the solution spectrum by Mason and Peacock has a positive band at 477nm for this transition. Since light parallel to the optic axis should excite the $^1A_1 \longrightarrow {}^1E(T_1)$ transition it appeared that this transition was at lower energy than the $^1A_1 \rightarrow {}^1A_2(T_1)$ and had a lower rotational strength.

The next important work on the optical activity of these complexes was also concerned with Metacn. Nonoyama (Ref 44) investigated the Ni(II) and Cu(II) bis complexes of the ligand and also conducted further examinations on the cobalt(III) bis complex. The work reported concerned the optical activity due to six λ conformations of the chelate rings of a complex which was presumed to have no configurational chirality. In the case of copper(II), the

circular dichroism spectrum was that expected; however in the nickel case some evidence of trigonal splitting was observed which the author attributed to the expected D_3 symmetry of the molecule.

Much of the work reported related to the cobalt(III) bis complex for which nine isomers were shown to be possible as a result of two coordination modes (a & b in Fig 1.21) and 3 relative orientations of the methyl groups. Chromatographic separation on SP-sephadex using Na_2SO_4 & Na_2HPO_4 eluting agents yielded five fractions which were characterised by nmr, ir, U.V./vis. and c.d. spectroscopies. The circular dichroism spectra of all the fractions were found to be similar in the visible region although from the energies of the d→d transitions it appeared that complexes involving two ligands in the a mode (Maa) had the strongest ligand field, Mab being intermediate and Mbb being weakest. In both a and b modes the methyl group was equatorial with respect to the mean plane of its chelate ring. An interesting feature of the two modes is that in mode a the nitrogens have S,R,S, configurations whereas in mode b they are in R,S,R, configurations. The similarities observed for the visible c.d. spectra of complexes involving the two modes would suggest that nitrogen configuration is not of great importance to the optical activity observed in the visible region.

Kuroda and Mason (Ref 45) recorded the single crystal c.d. spectrum of $[Co(R\text{-Metacn})_2]^{3+}$ and used the information

obtained to calculate the rotational strengths $R(A_2)$ and $R(E)$ in D_3 symmetry resulting from splitting of the degeneracy of the $^1A_{1g} \longrightarrow {}^1T_{1g}$ transition in octahedral symmetry. They were able to do this because $[Co(R\text{-}Metacn)_2]^{3+}$ forms uniaxial crystals with the C_3 axis of the complex parallel to the crystal c-axis. By propagating light parallel to that axis it was possible to excite only the $A_1 \longrightarrow E$ transition and so to obtain the rotational strength $R(E)$. The solution spectrum represented the total rotational strength $R(T_1) = R(A_2) + R(E)$ and so by subtraction $R(A_2)$ was obtained.

It was found that while for $[Co(en)_3]^{3+}$, $R(E) > R(A_2)$, the reverse was the case for $[Co(R\text{-}Metacn)_2]^{3+}$. The difference was attributed to the presence of chelate rings in the xy plane of the complex enhancing $R(E)$ at the expense of $R(A_2)$ in the former case and of chelate rings in a more polar position enhancing $R(A_2)$ at the expense of $R(E)$ in the latter case. For $[Co(R\text{-}Metacn)_2]^{3+}$ the $^1A_1 \longrightarrow {}^1E$ component has a negative sign while $^1A_1 \longrightarrow {}^1A_2$ necessarily has the opposite sign.

The presence of phosphate ions in solutions containing $[Co(en)_3]^{3+}$ was known to enhance A_2 because the ion occupies a polar position, effectively elongating the molecule (Refs 46 & 47). By observing the effect, on the c.d. spectrum of $[(Co(R\text{-}Metacn)_2]^{3+}$, of adding various anions it was hoped to determine the position of the anion relative to the complex ion in solution.

As a starting point the crystal structure of the iodide salt showed that the halide occupied a polar position. In solution if this situation was maintained then addition of iodide would enhance the A_2 component and would be expected to result in a more positive band due to the octahedral $^1A_{1g} \longrightarrow {}^1T_{1g}$ transition. By addition of 0.01M iodide this was found to be the case. Addition of oxy anions such as selenite or perchlorate reduced the observed rotational strength of the transition indicating an enhancement of R(E) relative to $R(A_2)$. This suggested that in solution these oxy anions act as hydrogen bonded "chelate rings" linking the top and bottom triazacyclononane ligands and increasing the bulk in the xy plane of the complex. Models confirmed that the amino protons were capable of such hydrogen bonding but that no feasible polar positioning of the oxy anions existed. The possibility of the changes in the observed c.d. being due to conformational lability of the chelate rings was discounted following the observation that the c.d. of $[Co(R\text{-}Metacn)_2]^{3+}$ in methanolic solution is invariant to temperature over the range 120K to 300K suggesting that there is no significant conformational freedom in the complex.

In a subsequent paper (Ref 48) Drake, Kuroda and Mason reaffirmed the above theory and applied the ligand polarisation model to the complex ion $[CoIII(R\text{-}Metacn)_2]^{3+}$. In addition to the chirality resulting from 6 λ chelate rings they also took into account the 7.6 degrees trigonal

twist and the elongation observed in the crystal structure. However, using the first order ligand polarisation model, the values obtained theoretically for $R(A_2)$, $R(E)$ and $R(T_1)$, though of the correct sign, were not in good agreement with those obtained experimentally. The first order ligand polarisation treatment is based on the fact that the leading electric multipole aligns the electric dipoles of all the ligand groups (C-H etc) where these dipoles are induced by the radiation field causing the transition. The magnitude of an induced dipole is proportional to the mean polarisability of the ligand group concerned at the transition frequency. The rotational strength in the first order approximation is then taken to be the scalar product of the electric dipole moment with the magnetic dipole transition moment. The results obtained by this treatment are given in table 1.1.

TABLE 1.1

c.d of $[Co(R\text{-}Metacn)_2]^{3+}$ (From Ref 48)

	$R(A_2)$	$R(E)$	$R(T_1)$
Theoretical	0.66	-0.64	0.02
Experimental	0.32	-0.16	0.16

In order to explain the discrepancies the authors hoped to perform a second order ligand polarisation treatment which would take account of mixing between d-electron and charge transfer transitions and which would require a knowledge of the frequencies of transitions in the charge transfer region. The c.d. spectrum in the vacuum U.V. region was measured and three bands observed, one of which was attributed to a $^1A_1 \rightarrow {}^1E$ transition. In the case of $\Lambda[Co(en)_3]^{3+}$ assignment of the bands was facilitated by the restricted sum rule;

$$R(A_2) + R(E) = 0 \qquad (1e$$

which was found to be correct to within 10%. Thus two transitions of opposite sign and similar magnitude could be assumed to have arisen from a common $^1A_{1g} \longrightarrow {}^1T_{1g}$ octahedral parentage. In the case of $[Co(R\text{-}Metacn)_2]^{3+}$ the restricted sum rule was found to be inapplicable and so such assignment was not possible. As a result no second order ligand polarisation treatment was conducted.

In a deviation from the mainstream research in the area of optical activity of metal complexes of triazacyclononanes, Shimba, Fujinami and Shibata used tacn to form a novel type of chiral complex (Ref 49). The chirality of the complex $[Co(Br)(CN)(NH_3)(tacn)]Cl_3$ results from having four different groups round a centre, as in the case of chiral carbon compounds. The complex was produced as a racemic mixture and resolved into its enantiomers by column chromatography using a solution of potassium d-tartrato antimonate. The same group later published 17 similar

$[CoIII(a)(b)(c)(tacn)_2]^{3+}$ complexes (Ref 50).

In 1980 Dubicki, Ferguson, Geue and Sargeson (Ref 43) reported a study on the dependence on outer sphere coordination of the c.d. spectra of Co(III) complexes. One of the complexes studied was $[CoIII(tacn(\delta\delta\delta))_2]Cl_3.5H_2O$ which was obtained by spontaneous resolution on crystallisation from HCl. The main purpose of the paper was to demonstrate that the inability of the various theories to explain observed solution c.d. was due to the outer sphere complexes formed in solution. By the use of axial single crystals as c.d. samples it was hoped to eradicate this problem and show, at the same time, the validity of the static coupling model of optical activity.

According to the static coupling model the first order rotatory strength for axial single crystals is given by

1f) $R^1 = 3/2\ Im[P^1_x M^o_x + P^1_y M^o_y]$,

where X and Y are directions perpendicular to the propagation axis, P^1_x is the transition electric dipole in the X direction and M^o_x is the transition magnetic dipole in the X direction. In solution the first order rotational strength, $R(A_2) + R(E)$ should sum to approximately zero so that what is observed is largely second and third order rotatory strengths.

An interesting series of experiments was reported by Nonoyama and Sakai (Ref 51) who produced the complexes

$[Co(tacn)(NH_3)_3]^{3+}$, $[Co(R\text{-}Metacn)(tacn)]^{3+}$ and $[Co(R\text{-}Metacn)(NH_3)_3]^{3+}$. This work was largely concerned with the additivity rule for the conformational chelate ring effect in c.d. spectra. For $[CoIII(R\text{-}Metacn)_2]^{3+}$, the optical activity may, to a first approximation be regarded as deriving from six chelate rings with a common λ conformation. Thus the total $\Delta\varepsilon$ under the $^1A_1 \longrightarrow {}^1T_1$ transition of 4.35 to 4.77 may be regarded as comprising six contributions of between 0.72 and 0.80 from the rings.

In the case of both the a and b coordination modes in the complex $[Co(Metacn)(NH_3)_3]^{3+}$ the c.d. spectra are similar. The $\Delta\varepsilon$ value of 0.78 to 0.87 for this complex is consistent with one λ chelate ring indicating that in the absence of a second triazacyclononane ligand in the complex there is no preferred conformation of the two chelate rings which do not carry methyl groups. In the case (again of both a & b modes) of $[Co(R\text{-}Metacn)(tacn)]^{3+}$ the $\Delta\varepsilon$ value of 3.98 to 4.06 is approximately 90% of that observed in the $[Co(R\text{-}Metacn)_2]^{3+}$ case indicating the importance of inter-ligand interactions in determining the conformations of the chelate rings.

The values obtained (table 1.2) confirm that the modes of coordination (a and b) do not have a pronounced effect on the conformations adopted. This was expected since it was known (Ref 44) that in both modes the methyl group was equatorial with respect to its chelate ring when the λ conformation was adopted. In addition to the

$[Co(Metacn)(NH_3)_3]^{3+}$ complex having a circular dichroism spectrum consistent with one conformationally chiral chelate ring, this is also reported (Ref 29) to be the case for several other $[Co(Metacn)(X)_3]^{3+}$ species.

TABLE 1.2

c.d. of Various Macrocyclic Cobalt (III) complexes

(Taken from Ref 51)

Mode	Complex	λ (nm)	$\Delta\varepsilon$
b	$Co(Metacn)(NH_3)_3Cl_3.3/2H_2O$	471	0.78
a	$Co(Metacn)(NH_3)_3Cl_3.\ H_2O$	465	0.87
b	$Co(Metacn)(tacn)Cl_3.5H_2O$	474	3.98
a	$Co(Metacn)(tacn)Cl_3.5H_2O$	471	4.06
bb	$Co(Metacn)_2Cl_3.5H_2O$	481	4.35
aa	$Co(Metacn)_2Cl_3.5H_2O$	476	4.72

The deficiencies of the additivity rule for conformational chirality in chelate rings are shown by reference to the complex $[Co\ (R\text{-propane-1,2-diamine})\ (NH_3)_4]^{3+}$ with $\Delta\varepsilon = 0.5$ compared to 0.8 from $[Co(R\text{-Metacn})(NH_3)_3]^{3+}$. The discrepancy may be explained by a trigonal twist in the Metacn complex and to a small extent by configurational chirality in the secondary nitrogens of the Metacn ring.

1.7 Ligands With Pendant Arms

One of the interesting features of the azamacrocyles, which sets them apart from other macrocyclic systems, is the ability of the ring nitrogens to carry groups other than hydrogen. Compounds derived in this way are described as N-functionalised to distinguish them from ligands where the additional groups are linked to the ring system via a ring carbon atom. In the C-substituted cases the additional groups are usually introduced prior to cyclisation, as in the case of R-Metacn, however N-functionalised derivatives are normally prepared using a preformed macrocycle as one of the reagents. The groups attached to nitrogen are often described as pendant arms and they provide the possibility of introducing additional ligating groups to a ligand. A wide variety of pendant arms is available including: carboxylic acid, alcohol, nitrile (Ref 52) and amine containing groups.

Some work has been carried out on triazamacrocycles with pendant arms. The first report of such work, by Hama and Takamoto,is in Japanese[53] and concerns the ligand 1,4,7-triazacyclononane-N,N',N''-triacetate (tcta), (Fig 1.22) and its divalent metal complexes. The stability constants of metal complexes of the ligand were obtained by measuring minute quantities of free ligand in solutions of the complexes. In a subsequent paper (Ref 54) the preparation of the ligand is described. The macrocycle 1,4,7-triazacyclononane, as its trihydrochloride salt, was dissolved in aqueous solution with an excess over three

equivalents of chloroacetic acid. The solution was heated to 45 degrees centigrade while the pH was maintained at 10 by means of lithium hydroxide. On taking the solution to dryness and recrystallising from ethanol a yield of 55% was achieved.

The authors confirmed, by electronic spectra, that both Co(III) and Cr(III) complexes of tcta, and of ligands derived from larger terdentate macrocycles, closely resembled tris (glycinato) complexes with facial arrangements of both the N_3 and O_3 donor sets.

In 1982 Wieghardt et al (Ref 55) published the results of a comprehensive investigation into the chemistry of the ligand tcta with a wide variety of first row transition metals. Complexes reported were [OV(tcta)]$^-$, [Cr(tcta)] , [Mn(tcta)] , [Mn(tcta)]$^-$, [Fe(tcta)], [Fe(tcta)]$^-$, [Co(tcta)], [Co(tcta)]$^-$, [Ni(tcta)]$^-$, [Cu(tcta)]$^-$ and [Al(tcta)]. [NiIII(tcta)] was reported to have been generated but was not discussed. The electronic and infrared spectra and the reduction potentials of the species were recorded and the crystal structures of the Cr(III), Fe(III) and Cu(II) species determined.

The complexes were formed by addition of simple metal salts to solutions of the ligand and subsequent addition of base. The more air sensitive complexes required oxygen free conditions and in most cases heat was required to drive the formation reaction. It was found that the M^{3+} salts were

relatively insoluble in water in contrast to the M^{2+} salts which were precipitated by addition of ethanol to their aqueous solutions.

Perhaps the most interesting feature of these complexes was the twist about the central metal ion, as observed in the crystal structures. An angle φ (Fig 1.23) is reported for the Fe(III), Cr(III), Ni(II) and Cu(II) species. A value of 30 degrees for φ gives an octahedral configuration while a value of 0 degrees represents the trigonal prismatic situation.

From these values it can be seen that while the Cr^{3+} and Ni^{2+} complexes are only slightly distorted from octahedral geometry the Fe(III) and Cu(II) complexes approach a trigonal prismatic disposition of donor atoms. The observed twists are explained in terms of two factors: the ligand field which favours an octahedral environment, and the short exocyclic chelate rings of the complex (Fig 1.24) which try to impose a trigonal prismatic arrangement. Since the ligand is the same in all cases it is the ligand field stabilisation energy which determines the extent to which the molecule is twisted.

The relationship between twist and LFSE is demonstrated in table 1.3. X-ray studies of powder samples of Mn(III), Co(III) & Al(III) showed that they crystallised isotypically with the Cr(III) species. This indicates a similar octahedral type environment to that which the Cr(III) is seen to possess and is in agreement, for the transition metals, with the theory proposed.

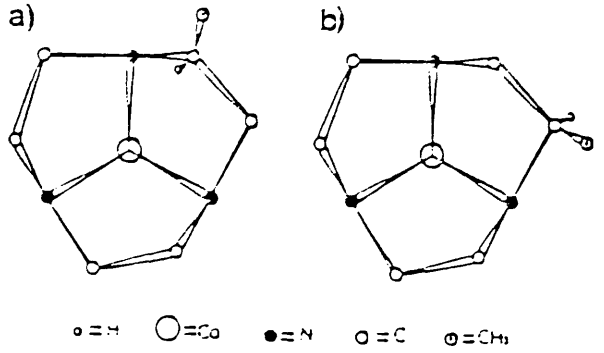

FIGURE 1.21
The a and b coordination modes of the ligand R-Metacn which give three possible isomers in bis complexes : aa, ab and bb.

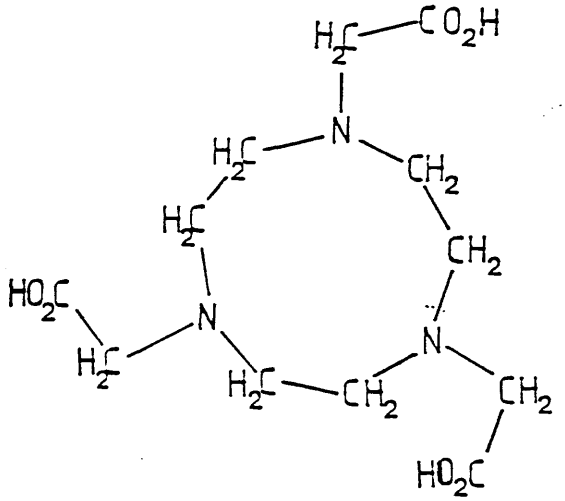

FIGURE 1.22
The ligand tcta :- 1,4,7-triazacyclononane-NN'N''-triacetate.

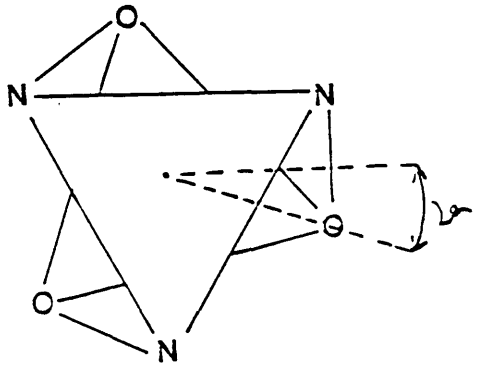

complex	γ
[Fe(tcta)]	12·6°
[Cr(tcta)]	24·5°
[Cu(tcta)]⁻	13·3°
[Ni(tcta)]⁻	22·5°

FIGURE 1.23
The extent of the twist in transition metal complexes of the ligand tcta showing the significance of the angle γ. (Taken from ref. 56)

TABLE 1.3

LFSE/twist correlations for some tcta complexes (Taken from Ref 56)

Ion	d^n	LFSE	Twist from octahedral
Cr(III)	d^3	-1.3Dq	11.0°
Fe(III)	d^5	0	34.8°
Ni(II)	d^8	-1.3Dq	15.0°
Cu(II)	d^9	-0.5Dq	33.4°

In 1983 Hancock et al (Ref 56) reported a route to Ni(III)(tcta), (in their reference tcta is referred to as TACNTA). The preparation involved dissolving [NiII(tcta)] in dilute nitric acid. With time the resulting solution turned from blue to pink and precipitated crystals of [NiIII(tcta)]. The authors believed that the hexadentate nature of the macrocyclic derivative would enable it to bind strongly to the metal and that the small cavity afforded by the N_3O_3 donor set of tcta would be conducive to oxidation of Ni(II) to the smaller Ni(III) ion.

The crystal structure obtained for [NiIII(tcta)] showed, once again, the propensity of the ligand to trigonally distort from octahedral configuration in metal ion complexes. The ORTEP diagram (Fig 1.25) shows a Λ configuration about the metal as defined by the exocyclic rings. In addition the conformation of the endocyclic rings is δ. Thus the complex may be described as $\Lambda(\delta)$. It is postulated that the tacn moiety, on coordination is chiral (λ_3 or δ_3) and that two structures

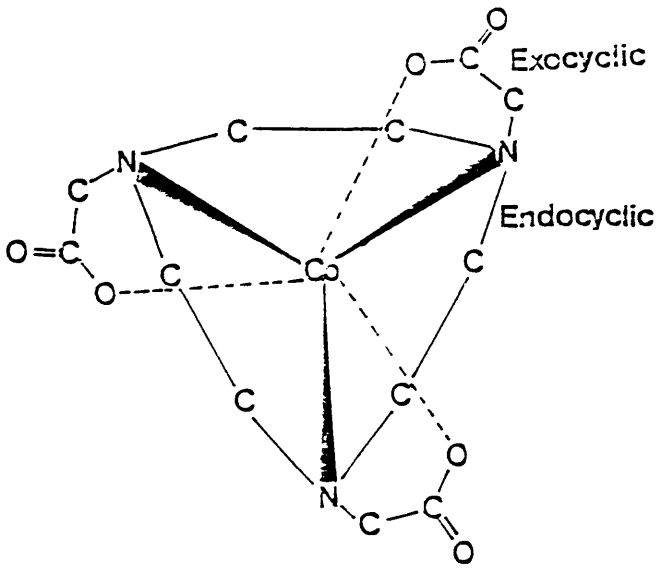

FIGURE 1.24
The two distinct chelate ring types in $[M(tcta)]^{n-}$ species: endocyclic and exocyclic. Short exocyclic rings cause trigonal distortion of the MN_3O_3 chromophore.

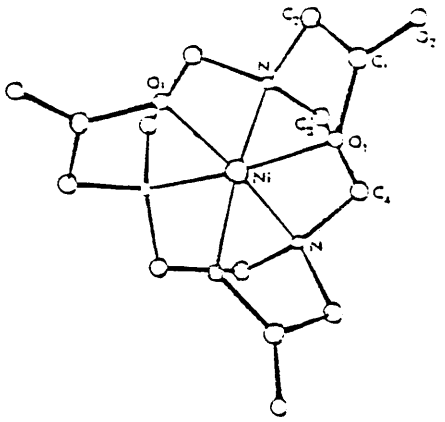

FIGURE 1.25
The ORTEP diagram of $[Ni(tcta)]^-$ showing the "type 1" $\Lambda(\delta)$ structure.(Taken from ref. 57)

are possible depending on the arrangement of the acetate bearing chelate rings. Hancock reports that a type I structure $\Lambda(\delta)$ or ($\Delta(\lambda)$) is less trigonally distorted than the type II structure $\Lambda(\lambda)$, or more fully $\Lambda(\lambda\lambda\lambda)$. The type II may be visualised by mentally disconnecting the acetates, which are arranged in a counter clockwise fashion in Fig 1.25; and reconnecting them to the metal in a clockwise manner. Wieghart's structures of Cr(III) and Ni(II) tcta complexes (Ref 55) showed them to be of type I similar to the Ni (III) case. Hancock carried out Empirical Force Field analyses and found that for the NiII species the type I form is approximately 4kcal/mol more stable than the type II. It was concluded that while the small cavity of tcta favours nickel(III) it is larger than the optimum cavity size for stabilising this species.

In a more recent paper (Ref 57) on tcta complexes Hancock et al report the crystal structure of $H_3O^+[Ni(tcta)]^-$ which is unusual in that the H_3O^+ species is present in the crystal while all three acetate arms were found to coordinate to the metal ion. (This is contrary to evidence with, for example, EDTA complexes where the presence of acid protonates acetate groups). Further to this it is reported that while Ni(II), Ni(III) and Cr(III) adopt the type I structure $\Delta(\lambda)$: the Cu(II) and Fe(III) structures, reported by Wieghardt (Ref 55) are of type II (distorted in the case of copper). In table 1.4 the apparent relationship between the length of the M-N bonds and the switch from type I to type II is shown. It is postulated that as the M-N distance increases the metal ion is forced towards the oxygens which distort towards an

almost trigonal prismatic arrangement which in turn causes the complex to adopt a type II structure. The type II structure is reported to have the acetate units in a more vertical position relative to the horizontal plane containing the nitrogen donors,thus allowing the oxygens to distance themselves from the metal. Apart from the structure of $H_3O[Ni(tcta)]$ the structure of $[CuCl(tctaH_2)]$ was also reported. In the latter structure one of the pendant arms of the ligand is protonated and has dissociated from the metal to be replaced by a chloride ion. This structure is compared to that of $[Cu(tcta)]^-$, in which the ligand is hexadentate, which is less distorted. The conclusion was drawn that coordination by tcta effectively prevents the Cu(II) ion from distorting its coordination sphere to attain a more favourable configuration. On dissociation the system is less constrained and distortion towards a tetragonally distorted arrangement of the donor atoms occurs.

TABLE 1.4

M-N bond length/type relations for tcta complexes

	M-N(Å)	M-O(Å)	twist from octahedral	type
NiIII	1.92	1.92	6.9°	I
NiII	2.04	2.08	12.0°	I
CrIII	2.06	1.96	11.0°	I
CuII	2.12	2.07	33.4°	II
FeIII	2.18	1.96	35.0°	II

Another system involving pendant arms on a tacn moiety is the ligand thetacn first reported by Hancock in 1983 (Ref 58) (Fig 1.26). This ligand with three hydroxyethyl arms is potentially hexadentate.

Like tcta it is an N_3O_3 donor with the potential for forming highly symmetric complexes. Preparation of the ligand was achieved by reaction of free tacn with three equivalents of ethylene oxide in basified ethanolic solution. The ligand was obtained as its monohydrobromide salt. The paper deals with the chemistry of Cu(II) and Zn(II) complexes of thetacn and with the ligand itself. The ligand has two pKa values; pK_1 = 11.52 and pK_2 = 3.42 compared with tacn; pK_1 = 10.42, pK_2 = 6.82. This would imply that at high pH the lone pairs on the nitrogen atoms of thetacn are more available than those of tacn. This was not expected since the hydroxyethyl groups should be electron withdrawing. The reason for this observation was, according to the authors, that at high pH there is extensive intramolecular hydrogen bonding which breaks down at lower pH.

The Cu(II) complex of thetacn has the same stability constant as that of tacn while for the Zn(II) case the thetacn complex is more stable than the tacn analogue. This is reported to be remarkable in view of the twist associated with $[Cu(tcta)]^-$ which had recently been reported. Similar twists were expected for the thetacn complexes so that the apparent higher stability of thetacn

complexes (strained) compared to tacn complexes was unexpected. No mention was made of the possible distortion and consequent strain in complexes such as $[Cu(tacn)_2]^{2+}$. The conclusion was drawn that the high stability of these complexes implied that the ligand was hexadentate.

The amine analogue of thetacn; N,N',N''-tris(2-aminoethyl)-1,4,7-triazacyclononane (taetacn) was first reported by Hammershoi and Sargeson (Ref 59) in 1983. The preparative route (Fig 1.27) involved adding phthalimido-acetaldehyde (4 equivalents) to 1 equivalent of a slurry of tacn.3HBr in dry acetonitrile. Anhydrous tetramethyl ammonium acetate and sodium cyanoborohydride were added and the mixture was left to stir for 15 hours in anhydrous conditions. Following work up with HBr the ligand taetacn was obtained as its hexahydrobromide.

The synthesis relied on reductive alkylation in the first step and acid hydrolysis of the amide in the second.

The cobalt(III) complex of taetacn was obtained by aerial oxidation of Co(II) in the presence of H^+, taetacn and activated charcoal. The complex was purified by column chromatography. By using a chiral eluting agent (sodium (+)tartrate) separation of the two enantiomers of the cobalt(III) complex was achieved. Both a crystal structure (Ref 60) and a circular dichroism spectrum of the complex are available. The complex labelled Δ (on the basis of the $[Co(en)_3]^{3+}$ moiety) was found to have both a positive

and a negative band in the area of the $A_1 \longrightarrow T_1$ transition (Fig 1.28).

The positive band is at lower energy and has the same sign as the unique c.d. band due to the $A_1 \longrightarrow T_2$ transition. The observed c.d. is opposite in sign to that obtained for $\Delta[Co(en)_3]^{3+}$ which the authors (Ref 59) took as evidence of factors, other than those associated with the $[Co(en)_3]^{3+}$ moiety, affecting the observed c.d. The sepulchrate derived from taetacn (azasartacn) is also reported along with two related novel cage complexes. The c.d. spectra of all four are reported and commented upon.

In a second paper from 1983 on taetacn Stewart, Snow and Hambley (Ref 60) reported the crystal structure of $(-)[Co(taetacn)](ClO_4)_3$ and also performed energy minimisation calculations for the various conformations.

The crystal structure showed that $[Co(taetacn)]^{3+}$ exists in the $\Delta(\lambda\delta)$ conformation (endocyclic λ, exocyclic δ).

The geometry shows a trigonal twist of approximately 12 degrees The torsion angles in the chelate rings are less than those associated with $[Co(en)_3]^{3+}$ but close to those observed for ethylene diamine chelate rings of "ob" configuration.

In the energy minimisation calculations the four conformers of C_3 symmetry, namely $\Delta(\lambda\delta)$, $\Delta(\lambda\lambda)$, $\Delta(\delta\delta)$ and $\Delta(\delta\lambda)$ were

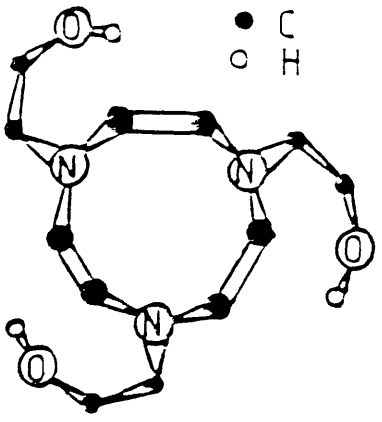

FIGURE 1.26
The hexadentate ligand N,N',N''-tris(2-hydroxyethyl)-1,4,7-triazacyclononane (abbreviated thetacn).

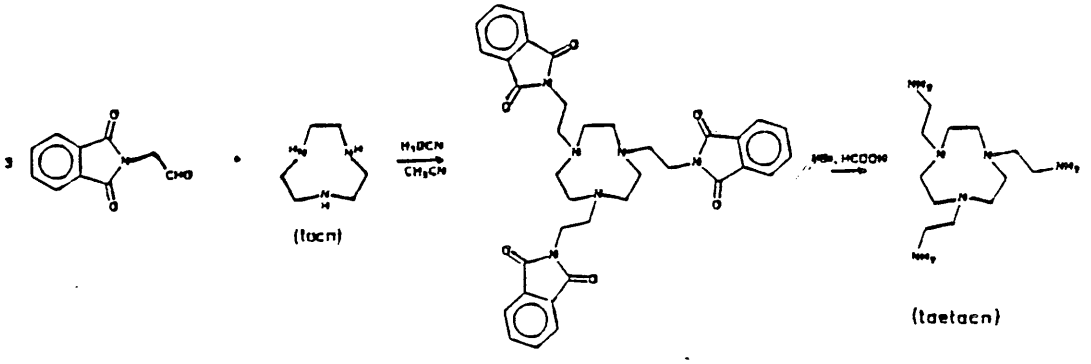

FIGURE 1.27
The synthetic route to N,N',N''-tris(2-aminoethyl)-1,4,7-triazacyclononane (abbreviated taetacn).

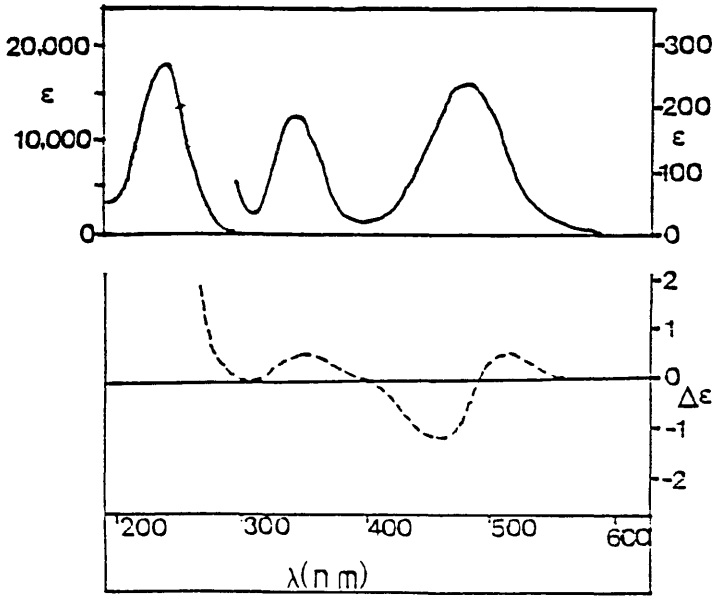

FIGURE 1.28
The absorption (top) and circular dichroism (bottom) spectra of $[Co(taetacn)](ClO_4)_3$ in water. (Adapted from ref. 60).

considered. $\Delta(\delta\lambda)$ was found not to possess a minimum energy form. Of the other three $\Delta(\lambda\delta)$ was lowest in energy largely because of a lack of trigonal strain expressed at the nitrogen atoms linking the two types of chelate rings in the $\Delta(\lambda\lambda)$ and $\Delta(\delta\delta)$ cases. The $\Delta(\lambda\delta)$ conformer which appears, from the calculations, to be most stable was indeed found in the crystal structures. The authors concluded that the strain of lel rings was infeasible and so the ob, $\Delta(\lambda\delta)$ complex should be conformationally stable.

1.8 Electronic Spectroscopy

In transition metal complexes three classes of transition occur which give rise to visible/U.V. absorption; d⟶d (or f⟶f) metal ion transitions, charge transfer transitions between a ligand and a metal ion and internal ligand transitions.

In order for an electronic transition to have intensity it must result in a change in the dipole moment of the species undergoing excitation. The three principal mechanisms involved are; electric dipole, magnetic dipole and electric quadrupole mechanisms. The intensity observed in absorption spectra of d-block transition metal complexes is derived largely from electric dipole transitions: magnetic dipole and electric quadrupole mechanisms give low intensities. The intensity of such absorption spectra is, in general, dependent on the change in the electric dipole moment which accompanies the transition being observed.

In a transition from a non-degenerate ground state a to a non-degenerate excited state b the matrix element of the transition is termed the transition moment μ_{ab} and is given by:

1g) $$\mu_{ab} = \langle a | \underset{\sim}{\mu} | b \rangle$$

where $\underset{\sim}{\mu}$ is the electric dipole moment vector. The intensity is related to the dipole strength, D_{ab} which is in turn related to the transition moment by:

1h) $$D_{ab} = |\mu_{ab}|^2$$

The total intensity under a band is given by the oscillator strength, f_{ab}, which is related to the dipole strength by:

1i) $$f_{ab} = \frac{8\pi^2 m c}{3he^2} \tilde{\nu} D_{ab} = k \tilde{\nu} D_{ab}$$

Substituting for D_{ab} gives

1j) $$f_{ab} = k \tilde{\nu} (\langle a | \underset{\sim}{\mu} | b \rangle)^2$$

1k) $$= k \tilde{\nu} [(\langle a | \underset{\sim}{\mu}_x | b \rangle)^2 + (\langle a | \underset{\sim}{\mu}_y | b \rangle)^2 + (\langle a | \underset{\sim}{\mu}_z | b \rangle)^2]$$

It follows that if, for a given transition, any of $\langle a | \underset{\sim}{\mu}_x | b \rangle$, $\langle a | \underset{\sim}{\mu}_y | b \rangle$ or $\langle a | \underset{\sim}{\mu}_z | b \rangle$ is non-zero then the transition will be electric dipole allowed. The integrals are non-zero provided that the direct product $\langle a | \underset{\sim}{\mu} | b \rangle$, contains the totally symmetric representation of the molecular point group to which the molecule belongs. That

is, if the direct product ab belongs to the same symmetry species as one of the components of $\underset{\sim}{\mu}$. The representations of the wave functions are known and hence the direct product can be obtained.

Three selection rules govern electronic transitions:

i] The electric dipole moment operator is odd with respect to inversion and as a result can only couple an odd and even combination of wave-functions. Thus transitions between states of equal parity are forbidden. This rule precludes transitions which involve redistribution of electrons within a single subshell (e.g. d$\rightarrow$d, f$\rightarrow$f). This is the Laporte selection rule which is often expressed as

$\Delta l = \pm 1$

ii] Transitions involving simultaneous excitation of two or more electrons are forbidden since the electric dipole moment operator operates on only one electron at a time.

iii] Electronic Eigen functions may be expressed as the product of an orbital function and a spin function (in the absence of spin-orbit interactions). Thus for the ground state, a, and the excited state,b;

1l) $\quad a = a^{o}\, a^{s}$ and $b = b^{o}\, b^{s}$

The transition moment integral is given by:

1m) $\langle a | \underset{\sim}{\mu} | b \rangle = \langle a^o a^s | \underset{\sim}{\mu} | b^o b^s \rangle$

1n) $= \langle a^o | \underset{\sim}{\mu} | b^o \rangle \langle a^s | b^s \rangle$

Since the electric dipole moment operator cannot couple electronic spins, $\langle a^s | b^s \rangle$ vanishes for states of different spin because the functions corresponding to different s values are orthogonal. As a result transitions involving a change in spin state are forbidden. Thus the number of unpaired electrons must be the same in the ground and excited states for a transition to be spin allowed. This gives the spin selection rule $\Delta S = 0$.

Table 1.5 shows typical values of the molar extinction coefficients for various classes of transition.

TABLE 1.5

Molar extinction coefficients of typical forbidden transitions

SPIN	LAPORTE	($l\,cm^{-1}\,mol^{-1}$)
Forbidden	Forbidden	0.001 ⟶ 1
Allowed	Forbidden	1 ⟶ 10
Allowed	Partially Allowed*	100 ⟶ 1000
Allowed	Allowed	1000 ⟶ 1,000,000

*Partially allowed by orbital mixing

1.9 Luminescence

When a molecule has been raised in energy by visible or U.V. radiation to an excited electronic level it must return to the ground state. It may do so by a number of routes as shown in Fig 1.29 (Ref 61). The molecule may externally quench by collision with other molecules in solution or it may internally quench, by vibrational mechanisms, to the ground state. However, if these processes are sufficiently slow the phenomenon of luminescence may be observed as the emission of visible light. Two types of luminescence may be defined; fluorescence and phosphorescence. Fluorescence is decay from the lowest excited state with the same spin multiplicity as the ground state. Since this process is spin allowed it is fast, typically in the range 10^{-8} to 10^{-4}s. Phosphorescence is emission from a state which is lower in energy than the lowest spin-allowed transition state and which is spin forbidden. Consequently it is a slower process (several seconds in extreme cases) and may be observed after absorption has ceased. Since phosphorescence requires a radiationless transition by inter-system crossing, which is spin forbidden, only a very small fraction of molecules phosphoresce. Phosphorescence is favoured by paramagnetic centres which relax the spin selection rule.

The value of luminescence spectoscopy is that it allows the structures of excited states to be investigated in much the same way that absorption spectra allow elucidation of ground state structures.

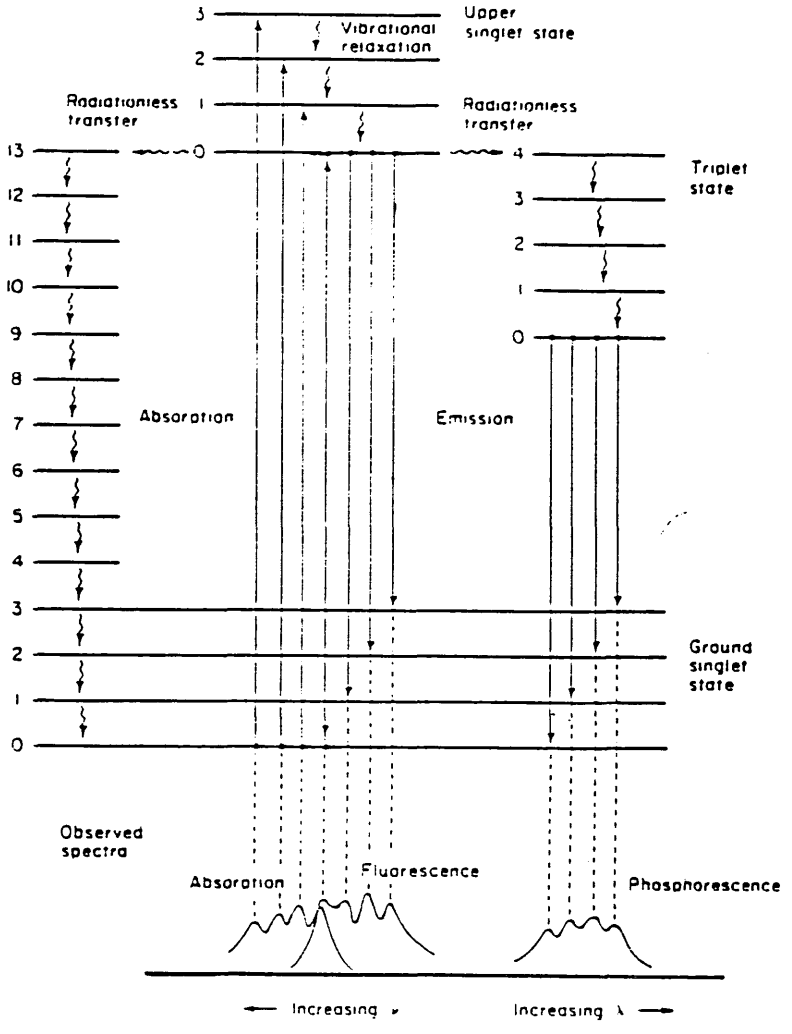

FIGURE 1.29
A species in an excited state may return to the ground state by a number of mechanisms of which fluorescence and phosphorescence involve emission. (Taken from ref. 61).

1.10 Circular Dichroism and Circularly Polarised Luminescence.

Circular Dichroism (Refs 62 & 63)

In general, the refractive index of a transparent medium is greater than that of a vacuum, the reason being that light is slowed by polarisable electrons. Plane polarised light may be regarded as the sum of two enantiomeric circularly polarised components (Fig 1.30). If circularly polarised light passes through a chiral medium the interaction is diastereomeric: that is, the interaction of left circularly polarised light with the medium is different from that of right circularly polarised light. This effect is manifested in two ways. Firstly, since the refractive indices for the two helicities are different in a chiral medium, one wave is retarded relative to the other and so the two waves are out of phase by an angle ϕ. When the waves recombine to form plane polarised light the plane is rotated by an angle, α, given by the Fresnel equation;

1.o) $$\alpha = \frac{1800\ (n_l - n_r)}{\lambda_{VAC}}$$

α in degrees dm^{-1} n_l Refractive index for left circularly polarised light

λ_{VAC}: wavelength of light.

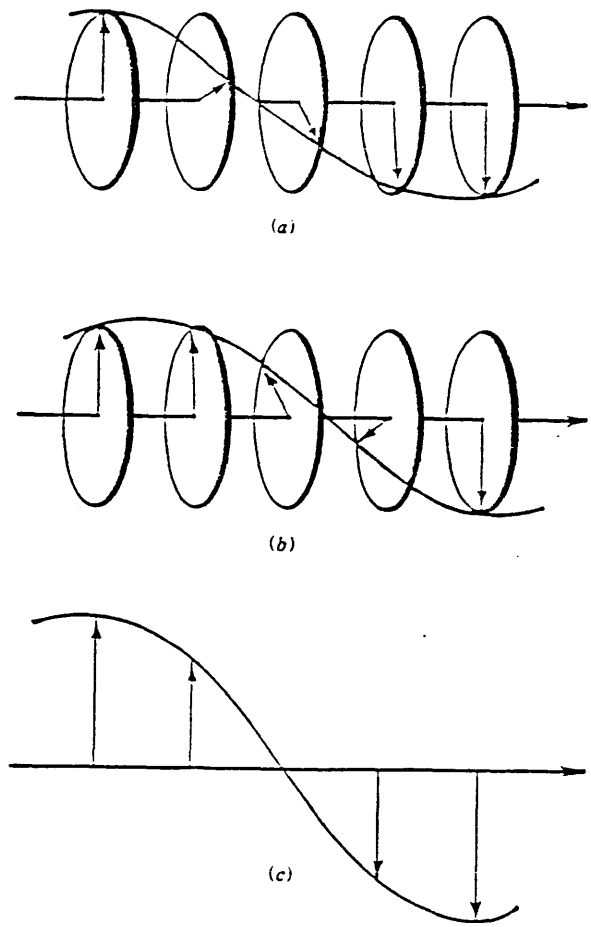

FIGURE 1.30
a) Right handed circularly polarised light and b) left handed circularly polarised light may combine to give c) a resultant of plane polarised light. Horizontal arrows indicate the direction of propagation while arrows perpendicular to this direction denote the instantaneous disposition of the electric vector of the radiation. (Taken from ref. 63).

Clockwise rotation of the plane as measured by a polarimeter is, by convention, positive so that $n_l > n_r$.

Near to absorption bands a second effect becomes important. Besides being out of phase the extinction coefficients of the two helicities are unequal so that the magnitudes of the two waves are different. This is observed on recombination as the formation of elliptically, rather than plane, polarised light. (Fig 1.31)

The value of tan Ψ is given by the ratio of the minor axis of the ellipse to the major axis where Ψ is the angle of ellipticity. The magnitudes of these axes are related to the amplitudes of the right and left circularly polarised components of the light so that;

1p) $$\tan \Psi = \frac{(a_l - a_r)}{(a_l + a_r)}$$

where;

1q) $$a = a_o e^{(-2\pi k / \lambda_{vac})}$$

for unit path length a_o = initial amplitude, λ is the wavelength and k is the absorption index $(k_l - k_r)$ which is a measure of the circular dichroism. Equations 1p & 1q may be approximated to:

1r) $$\Psi = \frac{180(k_l - k_r)}{\lambda_{vac}}$$

where Ψ is in degrees per unit path length.

In practice extinction coefficients are used, rather than absorption indices, the two being related by:

1s) $$k = \frac{2.303}{4\pi} \lambda_{vac} c \varepsilon$$

where c is the concentration in moles per litre. The differential molar extinction coefficient is given by;

1t) $$\Delta\varepsilon = \varepsilon_l - \varepsilon_r$$

The rotation of the plane of polarised light is the basis for Optical Rotatory Dispersion (ORD) while the dependence of the minor axis of the ellipse on wavelength gives rise to the phenomenon of circular dichroism (c.d.). ORD, though useful in quantitative assessments of optical purity, has been surpassed by c.d. spectra in structure elucidation. The main reason for this is that c.d. bands are at a maximum close to corresponding electronic transitions while ORD curves have a value of zero in this region. Another advantage of c.d. bands is that they are localised whereas ORD curves have magnitude far from the corresponding absorbance.

c.d. spectra consist of plots of $\Delta\varepsilon$ against wavelength (or wavenumber).

Figure (1.32) shows a typical relationship between absorbance, c.d. and ORD for a single absorbance band.

The amplitude of the ORD curve, [A], where $[A] = \alpha_{max} - \alpha_{min}$ is given by $4028 \times \Delta\varepsilon_{max}$ so that the two forms of measuring optical activity may be interconverted in simple cases.

History of Optical Activity

In the 1840's Pasteur suggested helicity, as constituted by four different groups round a central atom, as a criterion for molecular dissymmetry (Ref 64). In 1847 Haidinger made the first circular dichroism measurements, on a sample of amethyst (Ref 65). In the 1890's Drude (Ref 66) put optical activity on a sound theoretical footing by showing that a helical charge displacement of an electron in an electromagnetic field would result in optical activity. He reasoned that translation of the electron would give an electric dipole moment whereas rotation would give a magnetic dipole moment. If these two moments are parallel a right handed helix is formed and leads to a positive rotational strength: if they are anti-parallel then a left handed helix is formed leading to a negative rotational strength and $\Delta\varepsilon$ negative (Fig 1.33).

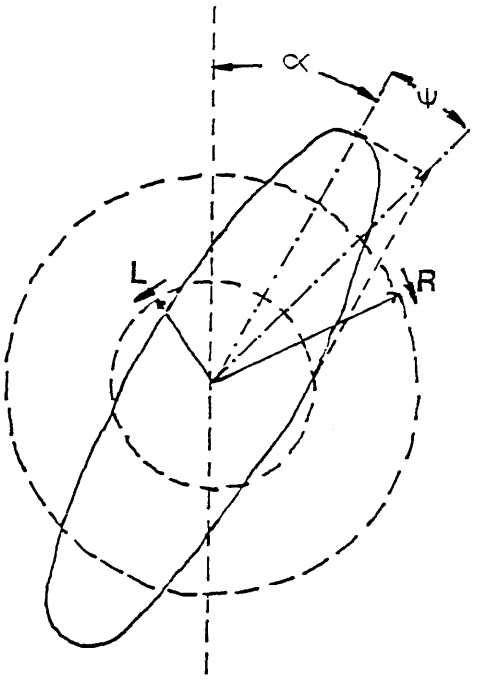

FIGURE 1.31
The combination of optical rotation ∝ and differential dichroic absorption gives rise to elliptical polarisation. Ψ is the ellipticity.

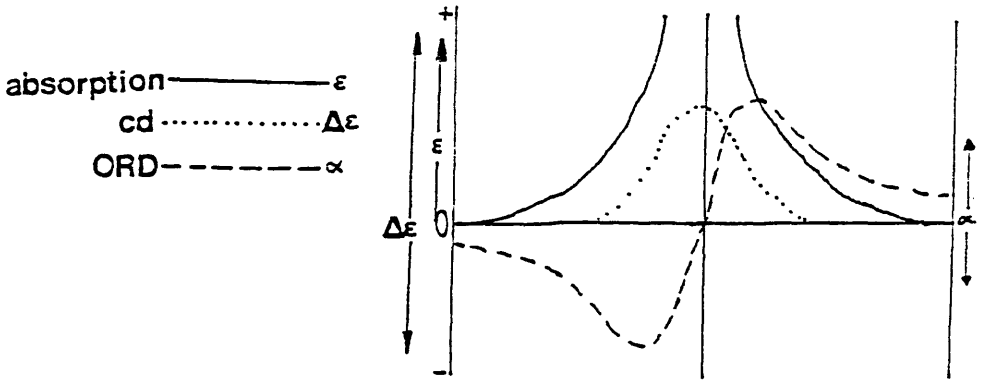

FIGURE 1.32
The absorption , circular dichroism and Optical Rotatory Dispersion associated with a single transition.

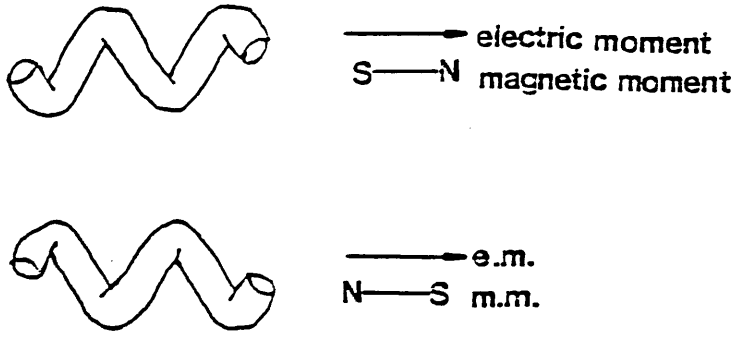

FIGURE 1.33
Right circularly polarised light results when the electric and magnetic dipoles of the radiation are parallel: left circularly polarised when they are anti-parallel.

In 1895 the Cotton Effect was discovered (Ref 67). The effect comprises different refractive indices for the two helicities of light and, in the region of absorbance bands, different molar extinction coefficients. In 1928 Rosenfeld developed a quantum mechanical treatment of optical activity (Ref 68) relating the rotational strength R_{ab} for an electronic transition from b to a, to the electric and magnetic dipole operators of the molecule:

1u) $R_{ab} = Im \langle a| \underset{\sim}{\mu} |b\rangle . \langle b| \underset{\sim}{m} |a\rangle$

where a and b are the wavefunctions of the two states, $\underset{\sim}{\mu}$ is the electric dipole moment operator, $\underset{\sim}{m}$ is the magnetic dipole moment operator and Im indicates that only the imaginary part of the product is to be taken.
For practical purposes R_{ab} is given by

1v) $R_{ab}=\mu m \cos\theta$

where μ & m are the magnitudes of the electric and magnetic dipole transition moments and θ is the angle between them. The rotational strength is measured experimentally as the area under a c.d. band and is given by:

$$R_{ab}=22.9 \times 10^{-40} \int \frac{(\varepsilon_l - \varepsilon_r)}{\bar{\nu}} d\nu \qquad \text{c.g.s. units} \qquad (1w$$

where $\bar{\nu}$ is the absorption wavenumber. R_{ab} may be positive

($\varepsilon_l > \varepsilon_r$) or negative ($\varepsilon_r > \varepsilon_l$). The rotational strength sums to zero over all transitions.

Just as the total intensity under a c.d. curve is given by the rotational strength R_{ab}, so the total intensity under an electronic transition is given by D_{ab}, the dipole strength. Quantum mechanically D_{ab} is given by:

1x) $$D_{ab} = |\langle a|\, \underset{\sim}{\mu}\, |b\rangle|^2$$

Rather than measuring and quoting R_{ab} and D_{ab} for transitions it is more convenient to use the Kuhn Dissymmetry Factor, g, which is dimensionless.

1y) $$g = \frac{|\varepsilon_l - \varepsilon_r|}{\varepsilon} = 4R_{ab}/D_{ab}.$$

Thus the ratio of the rotational strength to the dipole strength may be ascertained by inspection of absorption and c.d. spectra.

Circularly Polarised Luminescence (Ref 69)

Many of the above principles also apply to the phenomenon of Circularly Polarised Luminescence. However, it is the emission of circularly polarised light which gives rise to the observed spectrum of ΔI versus λ. ΔI is termed the emission circular intensity differential.

1z) $$\Delta I = I_l - I_r$$

The emission dissymmetry factor g_{em} is given by:

1@) $$g_{em} = 2\Delta I/I = 2(I_l - I_r)/(I_l + I_r)$$

Electronic c.p.l is analogous to electronic c.d. but differs from it in probing the forbidden excited states of the sample molecule.

1.11 Objectives

At the time of commencement of this work there had been considerable activity in the field of triazamacrocyclic metal complexes. The ligand tacn and many of its complexes had been characterised and interest was turning to derivatives of tacn possessing three pendant arms. The ligands tcta and thetacn had been synthesised and their metal complexes prepared and investigated. No work on the optical activity of such $[M(N_3O_3)]$ systems had been reported; however it was envisaged that the c.d. spectra of these species would be of particular interest in view of the geometries reported for $[M(tcta)]^{n-}$ complexes by Wieghardt et al (Ref 55). The complex ions were twisted relative to octahedral geometry and it was hoped that the twist angle would be reflected in the circular dichroism spectra.

Investigations of the optical activity of triazamacrocyclic complexes had been restricted to complexes of the inherently chiral ligand.
2(R)-methyl -1,4,7-triazacyclononane and single crystal studies of $Co(tacn)_2Cl_3.5H_2O$

The primary aim of this work was to investigate complexes with the N_3O_3 donor set, paying special attention to the optical activity of such species. Optically active samples were to be obtained by designing novel chiral ligands, analogous to tcta and thetacn, and also by preparing resolved samples of complexes containing the achiral ligands.

Work had been carried out on cobalt tris diamine complexes to decompose the c.d. spectra in the region of the T_1 (O_h) transition into A_2 (D_3) and E (D_3) components. It was an aim of this work to extend these studies by decomposing the circular dichroism spectra of $[Co(tacn)_2]^{3+}$. The complex $[Cr(tacn)_2]^{3+}$ had been prepared and its absorption spectra reported. It was envisaged that this species would have interesting luminescence and solid state c.p.l. and c.d. spectra. The overall aim was to prepare complexes containing the 1,4,7-triazacyclononane moiety and to investigate them spectroscopically, with particular regard to their optical activity.

CHAPTER 2

Experimental

2. EXPERIMENTAL

2.1 Instrumentation

2.1.1 Electronic Absorption Spectra

Electronic absorption spectra were recorded on a Beckman U.V. 5270 UV-visible-NIR spectrophotometer. Spectra of samples in solution were generally run in 1cm quartz cuvettes which were also suitable for the circular dichroism spectrometer. Solid samples, other than single crystals, were run as discs of 13mm diameter. The discs were prepared by grinding the sample, along with a salt support (e.g. KCl) to the required degree of homogeneity. The mixture was then pressed between two metal plates for five minutes at a pressure of 6 tons per cm^2.

2.1.2 Circular Dichroism Measurement (Ref 63)

The circular dichroism (c.d.) spectrometer (Fig 2.1) is constructed around a Jobin Yvon 0.6m monochromator. The source is a 150 watt horizontally mounted xenon arc lamp which is focussed by means of a parabolic reflector. The light energy from the monochromator is plane polarised in the vertical plane by a quartz rochon prism and is circularly polarised by passing through a photo-elastic modulator comprising a crystal of calcium fluoride held such that the electric vector of the plane polarised light is at 45° to the fast and slow axes of the crystal.

The circularly polarised light passes through the sample and is collected by the photo-multiplier. The modulated

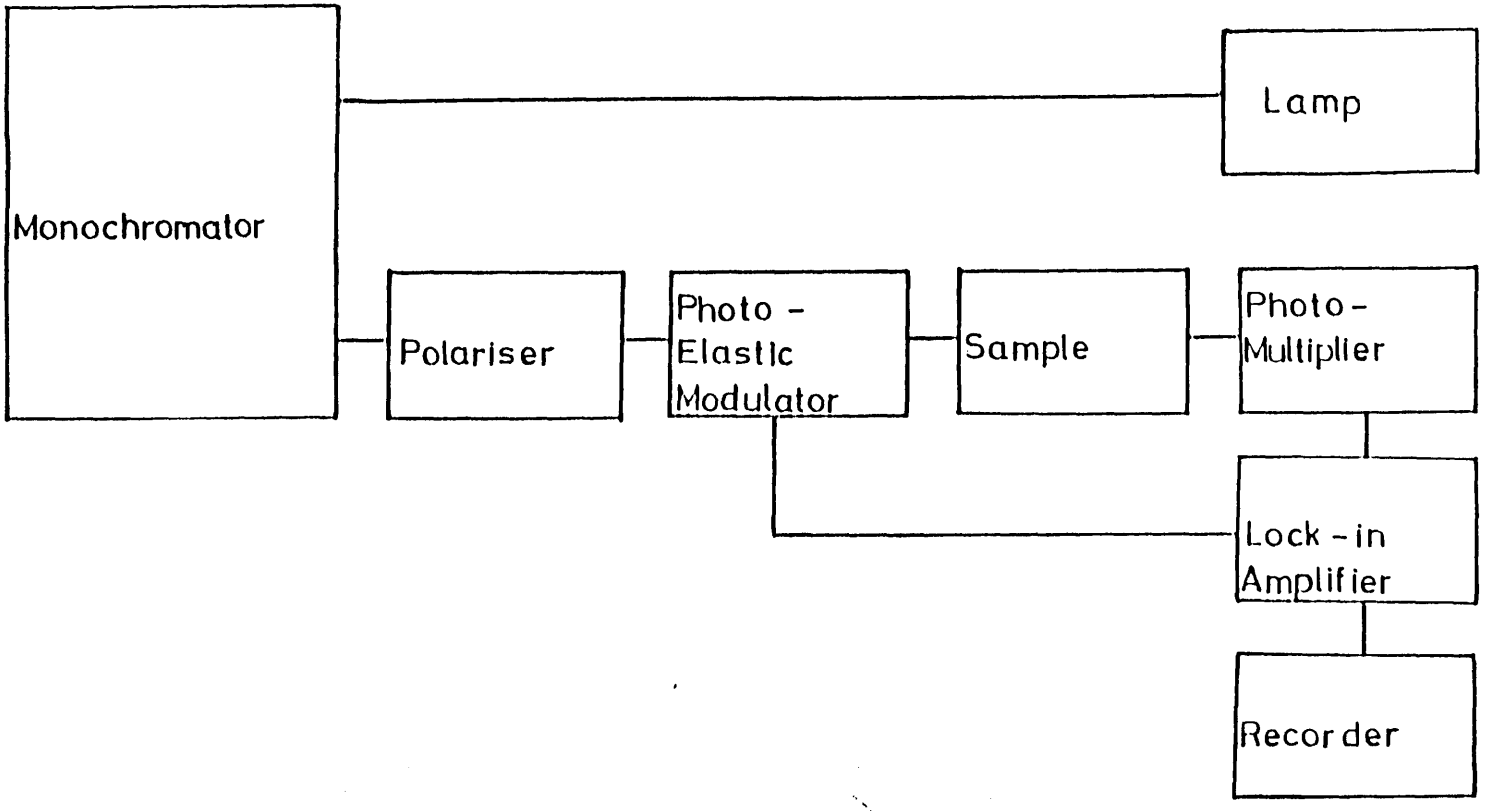

FIGURE 2.1
A schematic diagram of a circular dichroism spectrometer.

signal is measured using a synchronous lock-in amplifier, [referenced to the photo-elastic modulator (PEM) vibration frequency of 50KHz]. The lock-in amplifier detects the periodic difference in light intensity due to an optically active sample in the path of the light beam. The output of the lock-in amplifier is plotted on a chart recorder as the monochromator is scanned in wavelength. The resulting spectrum shows the differential dichroic absorption (ΔA) varying with wavelength. The light sensitivity of the spectrometer is $\Delta A = 10^{-6}$ (arbitrary units).

2.1.3 Operation of the photo-elastic modulator

The Photo-elastic Modulator consists of a bar shaped crystal of calcium fluoride or fused silica which is driven into oscillation by mechanical coupling to a bonded-on piezo - electric transducer made of crystalline quartz. The stretching and compression of the optical element results in an oscillating birefringence ($n_x - n_y$). This is due to a time varying difference between the two refractive indices n_x and n_y applying to light polarised parallel or perpendicular to the x and y axes in figure 2.2.

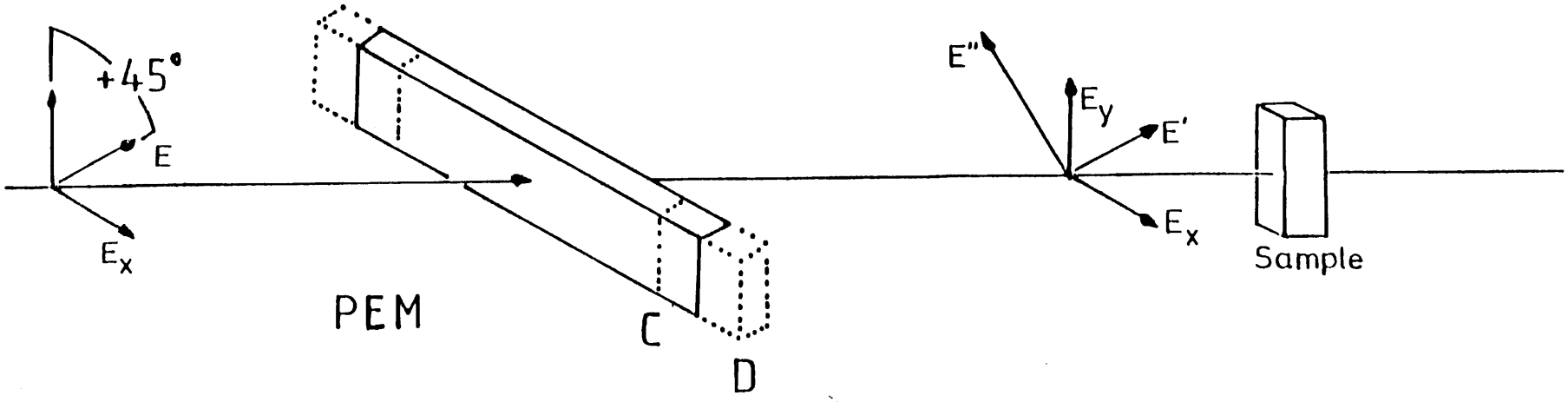

FIGURE 2.2
Operation of the photo-elastic modulator.

The extensional displacements along the x-axis of the bar are given by:

2a) $\delta = \delta^{\circ} \sin (2\pi x/\lambda) \sin \omega t$

δ°= maximum extension λ= wavelength of incident light

ω= oscillating frequency ; t = time

The corresponding strain is proportional to $\left(\frac{\delta\delta}{\delta x}\right)$, that is, to cos $\left(\frac{2\pi x}{\lambda}\right)$ and is at a maximum at the centre of the bar. The birefringence $(n_x - n_y)$ is proportional to the strain and varies with time as sin ωt.

The birefringence causes a phase difference to accumulate between the x and y electric vector components of a light wave traversing the crystal. If incident light, polarised at 45° to the bar axis, passes through the modulator which is vibrating at a frequency such that at the extrema C and D (Fig 2.2) the relative phase shift is 90°, (ie quarter wave modulation), the light is converted to circularly polarised light. In Figure 2.2 the vector E' rotates counter-clockwise in case C and clockwise in case D. This light, alternating between right and left circularly polarised, passes through the sample.

2.1.4 Luminescence

Coherent 52G Kr^+ and Ar^+ ion lasers were used as light sources for recording both luminescence spectra and circularly polarised luminescence spectra. The apparatus

employed for luminescence studies is represented schematically in figure 2.3. The laser beam passes through an aperture in the mirror and strikes the sample which is in the form of a single crystal. The resulting luminescence scatters in all directions so that the proportion of emitted light scattered onto the mirror is constant. The mirror reflects the light onto a lens which focusses it into a beam directed through the monochromator to the photo-multiplier. The photo-multiplier is connected to a chart recorder which outputs a plot of luminescence intensity against wavenumber.

2.1.5 Circularly Polarised Luminescence

In the case of circularly polarised luminescence (cp.l.) spectroscopy the luminescence apparatus is modified as shown in figure 2.4. On emerging from the lens the circularly polarised light enters the photo-elastic modulator which is oriented at 45° to the plane of the light. The effect of the PEM is the reverse of that employed in recording c.d. spectra. Just as the c.d. spectrometer's PEM converts plane polarised light (ppl) to circularly polarised light, so the PEM in this case converts circularly polarised light to ppl as shown in table 2.1.

Table 2.1: The Effect on Circularly Polarised Light of the PEM.

	Case 1	Case 2
Left circularly polarised	$\perp^{r}$ ppl	$\parallel^{d}$ ppl
Right circularly polarised	$\parallel^{d}$ ppl	$\perp^{r}$ ppl

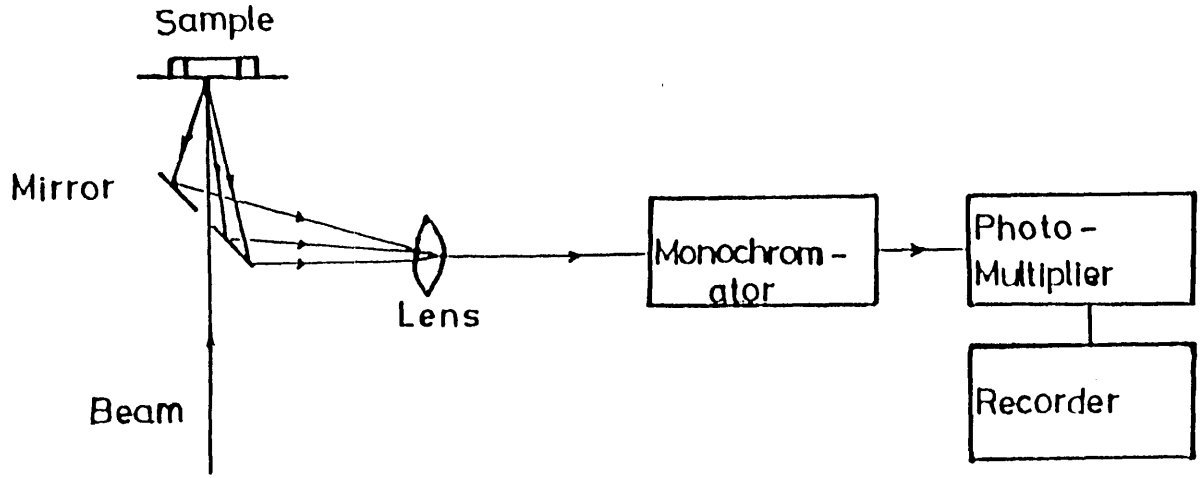

FIGURE 2.3
A schematic diagram of the apparatus for recording luminescence spectra.

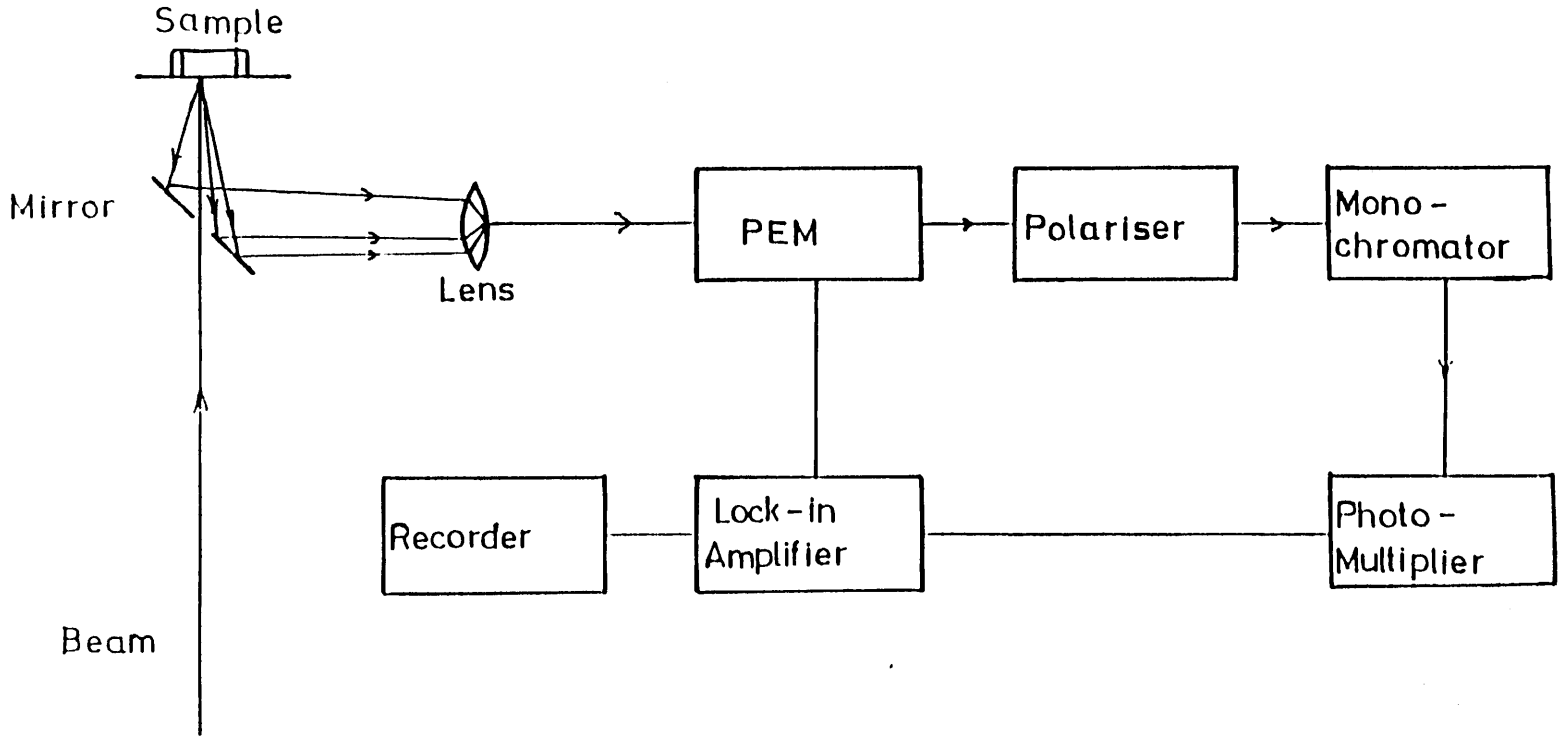

FIGURE 2.4
A schematic diagram of the apparatus for recording circularly polarised luminescence spectra.

Interconversion between the two cases is effected by physically rotating the PEM through 90°. In practice the PEM remains fixed in orientation so that one of the two cases applies and the machine is calibrated to determine which. Thereafter the relative intensities of left and right circularly polarised light can be determined, for example in case 1, from the ratio of perpendicular ppl to parallel ppl.

On leaving the PEM the light passes through a polariser which is set to cut out all radiation other than parallel ppl (or perpendicular ppl). The plane polarised light then passes through a monochromator to a photo-multiplier which is connected to the PEM through a lock-in amplifier. The output of the photo-multiplier, corrected to take account of modulation, is then output by the recorder as a plot of differential intensity versus wavenumber.

2.1.6 pH Measurements

Determination of pH values was carried out on a digital PHM62 standard meter from Radiometer Copenhagen using a GK2301C saturated calomel electrode. Buffer solutions used are listed in Table 2.2 and were made by adding 0.2M solutions of the reagents listed until the required pH was attained.

Table 2.2 Buffer Solutions

pH Range	Buffering Agents
2.5-4	Formic Acid/Sodium Formate
4-6	Acetic Acid/Sodium Acetate
6-8	Sodium Dihydrogen Phosphate/Disodium Hydrogen Phosphate
8-10	$HCl/Na_2B_4O_7.10H_2O/NaOH$

2.2 Materials

Table 2.3 Solvent Purification

Solvent	Purification Method
Chloroform	Stored in the dark
Methanol, Ethanol, Isopropanol	Stored over activated 3Å molecular sieves
Diethyl Ether	Sodium wire added
Dimethyl Formamide	Stirred overnight with BaO. Fractionated *in vacuo*
Dimethyl Sulphoxide	Stored over 3Å molecular sieves
Acetic Acid	Used without further purification

Table 2.4 lists some of the chemicals used in this work along with the suppliers and purities of the materials.

Table 2.4

Sources of some materials used

Chemical	Supplier	Purity
ethylene glycol	Riedel De Haen	99.5%
ethylene diamine	BDH	98%
propylene diamine	Aldrich	99%
diethylene triamine	Aldrich	95%
diethanolamine	Aldrich	97%
triethylamine	Koch Light	Anhydrous
ethylene oxide	BDH	pure
S-propylene oxide	Aldrich	99%
R-propylene oxide	Fluka	>99%
l-tartaric acid	Aldrich	99%
d-tartaric acid	May & Baker	99.8%
bromoacetic acid	Koch Light	Pure
p-toluene sulphonyl chloride	Koch Light	Pure A.R.
sodium hydride	Koch Light	50% (in oil)
hydrobromic acid	BDH	A.R.
$CoCl_2.6H_2O$	Hopkin & Williams	99%
$CrCl_3.6H_2O$	Hopkin & Williams	95%
$CuCl_2.2H_2O$	Hopkin & Williams	99%
$NiCl_2.6H_2O$	BDH	97%
NH_4PF_6	Aldrich	99.5%
H_2O_2	May & Baker	99%
NaOH	Formachem	96%
HCl	May & Baker	A.R.

Electronic absorption spectra were used to characterise known compounds. Analysis of new compounds was carried out by the micro-analysis service of Glasgow University.

2.3 Experimental Procedure

2.3.1 Preparation of 1,4,7-triazacyclononane: tacn.

The cyclic triamine, tacn, was prepared by two routes both of which are based on Richman Atkins (Refs 4 & 5) type cyclisations.

Route 1 (Fig 1.8)

N,N'-di(p-Toluene sulphonyl) ethylene diamine

In a two litre round bottomed flask equipped with a mechanical stirrer was placed ethylene diamine (12g, 0.2 moles) and sodium hydroxide (16g, 0.4 moles) dissolved in 200 mls of water. The resulting solution was stirred vigorously over 2 hours during which time p-toluene sulphonyl chloride (76.2g, 0.4 moles) in 500 mls of diethyl ether was added dropwise. The mixture was stirred for a further 2 hours at room temperature, to ensure complete reaction, after which addition of 300 mls of methanol precipitated an off-white solid. The solid was washed with water and methanol to give a white solid which was air dried. Yield 53.0g, 72.0% mp 173-175°C. Found; C 51.9, H 5.4, N 7.7. Calc. for $C_{16}H_{20}N_2O_4S_2$; C 52.2, H 5.4, N 7.6.

N,O,O'-tri(p-toluene sulphonyl) diethanolamine

Preparation of the reagent was by the method reported by Fabbrizzi (Ref 22). A 3 litre beaker equipped with a

mechanical stirrer was charged with diethanolamine (20.4g, 0.2 moles) and triethylamine (200 mls). The solution was stirred and a second solution comprising 114.4g (0.6 moles) of p-toluene sulphonyl chloride in 600 mls of diethyl ether was added slowly from a dropping funnel at room temperature. The addition of a slight excess of tosyl chloride was found to result in a pink coloration. Stirring was continued for one hour after dropping was complete and after this period the solution was added with vigorous stirring to 200mls of water which dissolved the unchanged starting material from the solid precipitate. The remaining white precipitate was recrystallised from the minimum quantity of ethanol.

Yield 64.3g, 58% mp 92-95°C. Found; C 52.9, H 5.2, N 2.5. Calc. for $C_{25}H_{31}NO_8S_3$; C 52.7, H 5.4, N 2.5.

N,N,'N"-tri(p-toluene sulphonyl)-1,4,7-triazacyclononane (Ref 20)

36.8g, 0.1 moles, of N,N'-ditosyl ethylene diamine was dissolved in 1000 mls of dry dimethyl formamide in a two litre 3 necked round bottomed flask equipped with a mechanical stirrer, a nitrogen inlet and a heating mantle. The flask containing the solution was purged with dry nitrogen for 10 minutes and thereafter sodium hydride (11g of 50% suspension in oil) was added slowly with vigorous stirring in such a manner that the exothermic reaction remained under control. When the NaH had been added and the effervescence had subsided the temperature of the solution was raised to 70°C to allow the reaction to go to

completion. Excess sodium hydride was filtered, under vacuum, so that the solution of N,N'-disodium N,N'-di (p-toluene sulphonyl) ethylene diamine passed into a second round bottomed flask suitable for the next stage of the synthesis. Early literature syntheses advocate retrieval of the salt at this stage. However any delay appears to allow hydrolysis to the starting material and so it has been found to be essential to proceed without delay to the cyclisation reaction.

The temperature of the DMF solution of the di-sodium salt of ditosyl ethylene diamine was raised to 110°C, to exclude moisture, and a second solution containing tritosyl diethanolamine (56.7g, 0.1 moles) in dry DMF (500 mls) was added over 4 hours with stirring. After a further 2 hours of stirring at 110°C the solution was allowed to cool before being rotary-evaporated to 300 mls. Addition of this solution of tritosyl-1,4,7-triazacyclononane to 1 litre of water gave a tacky white precipitate which was washed with water and ethanol and used without further treatment in the next stage of the preparation. Mass spectroscopy provided evidence that the major impurity was the dimer [18]aneN_6 and that quantities of starting material were also present. This was consistent with reports by Searle and Geue (Ref 20).

1,4,7-triazacyclononane trihydrochloride

12.3g of the tacky solid obtained in the cyclisation step was dissolved in a mixture of 400 mls glacial acetic acid

and 1100 mls HBr (Ref 17) which was refluxed for 3 days during which time a black scum formed on the darkening solution. The scum was removed by filtration and the solution was rotary-evaporated to 100 mls whereupon 50 mls of concentrated HCl was added. The solution was then heated on a steam bath at 80°C for 1 hour and allowed to cool before being added, dropwise, to a mixture of 250 mls ethanol and 500 mls diethyl ether. The precipitate, tacn .3HCl, was in the form of a tacky solid which was twice recrystallised from concentrated HCl and on trituration gave a white solid. Yield 0.5g, 10.2%, mp 258-271°C (dec). Found; C 29.6, H 7.9 ,N 17.7, Cl 44.9. Calc. for $C_6H_{18}N_3Cl_3$; C 30.2, H 7.5, N 17.6, Cl 44.6 ; m/e 128.

Route 2 (Figure 1.9)

This method is substantially that used by Searle and Geue (Ref 20) although the synthesis has been modified at various points. This route has been found to be far superior to route 1 both in the yields obtained and in the purity of the product.

1,2-di(p-toluene sulphonyloxy) ethane

p-toluene sulphonyl chloride (100g, 0.526 moles) was added slowly to a stirred solution of ethane-1,2-diol (16.3g, 0.263 moles) in triethylamine (300 mls) over a period of 2 hours. The mixture was stirred for a further hour at room temperature during which time a white precipitate formed. 100 mls of water was added to dissolve residual starting material and the resulting tacky solid was washed with

water and then recrystallised from 170 mls of hot acetone by addition of ether on cooling. Yield 66.2g, 67.7% mp 123-126°C. Found; C 52.1, H 4.7, S 17.1 Calc. for $C_{16}H_{20}O_6S_2$; C 51.9, H 4.9, S 17.3.

N,N',N''-tri (p-toluene sulphonyl) diethylene triamine

p-toluene sulphonyl chloride (100 g, 0.526 moles) in diethyl ether (600 mls) was added dropwise to a vigorously stirred solution of diethylene triamine (18.1g, 0.175 mol) and NaOH (20 g) in water (800 mls). Vigorous stirring is essential if separation into an aqueous phase and an organic phase, with consequent drop in yield, is to be avoided. After stirring for three hours the solution suddenly solidified and methanol was added to remove starting materials. The product was filtered and washed with water then methanol before being air dried. Recrystallisation was found to be unnecessary. Yield 62.9g, 63.6%. mp 173-174°C. Found; C 53.1, H 5.6, N 7.5, S 17.2 Calc. for $C_{25}H_{31}N_3O_6S_3$; C 53.1, H 5.5, N 7.4, S 17.0.

N,N',N''-tri(p-toluene sulphonyl) - 1,4,7-triazacyclononane

As in route 1 the disodium salt of the tosylated amine was not isolated since hydrolysis to the tosylated amine was found to be significant on occasions when the salt was isolated. The in-situ preparation reported by Searle and Geue (Ref 20) was therefore used and was found to have considerable advantages over preparations in which the salt was isolated, both in terms of purity of product and in the yield obtained.

A 1 litre 3 necked round bottomed flask was charged with N,N',N''-tri(p-toluene sulphonyl) diethylene triamine (28.3g, 0.05 moles) and 550 mls of dry dimethyl formamide. The vessel was purged with nitrogen for 10 minutes after which sodium hydride (8g of 50% suspension in oil 0.17 mol) was added sufficiently slowly to ensure that the reaction remained under control. When the initial effervescence had died down (approximately 1 hour) the solution was heated to 70°C and maintained at that temperature until the reaction was complete and hydrogen evolution had ceased. The excess NaH was filtered under dry nitrogen so that the filtrate passed into a 2 litre 3 necked round bottomed flask as a yellow solution which was raised, without delay, to a temperature of 105°C. This solution was stirred vigorously while a second solution containing 1,2-di(p-toluene sulphonyloxy) ethane (18.5g, 0.05 moles) in dry DMF (250 mls) was added over four hours. The mixture was maintained at 105°C for a further 2 hours after which the volume was reduced to 200 mls and addition of the resulting concentrated solution to water in a beaker gave a white tacky precipitate which was filtered and washed with water, ethanol and diethyl ether before being dried at 100°C. Recrystallisation from a small volume of chloroform on addition of ethanol gave a white crystalline precipitate. Yield 22.8g, 77% mp 218-220°C.

Found; C 54.8, H 5.7, N 7.1, S 16.3. Calc. for $C_{27}H_{33}N_3O_6S_3$; C 54.8, H 5.6, N 7.1, S 16.2.

1,4,7-triazacyclononane trihydrochloride (tacn.3HCl)

N,N',N''-tri(p-toluene sulphonyl)-1,4,7-triazacyclononane (22.8g, 0.040 mol) was dissolved in a mixture of 1100 mls glacial acetic acid and 600 mls HBr. This solution was refluxed for 7 days during which it darkened progressively. The volume was then reduced, by rotary - evaporation, to 300 mls and the resulting solution was added dropwise to a mixture of 600 mls ethanol and 300 mls diethyl ether in an open beaker. The grey/white precipitate was substantially tacn.3HBr.

The hydrobromide salt was dissolved in the minimum quantity of boiling concentrated hydrochloric acid and on cooling a white precipitate formed which, after two recrystallisations, gave tacn.3HCl.

The trihydrochloride salt was washed with ethanol and ether and air dried. Yield 8.0g, 87%.mp 263-267°C (dec). Found; C 30.1, H 7.5, N 17.6

Calc. for $C_6H_{18}N_3Cl_3$; C 30.2, H 7.5, N 17.6.

2.3.1.1 $CoIII(tacn)_2Cl_3.5H_2O$

To 1g (4.2 mmol) of tacn.3HCl in 3 mls of water was added 0.72g (12.6 mmol) of KOH in such a way that the temperature remained well below 100°C. To the cooled free ligand solution was added 20 mls of ethanol which precipitated the potassium chloride of neutralisation. After filtration the filtrate was added to a solution of $CoCl_26H_2O$ (0.5g, 2.10 mmols) in 5 mls of water. 0.48g of KOH was added to basify the solution. A brown coloured solution resulted which

turned yellow after approximately 30 minutes during which air was bubbled through it. Slow reduction of volume yielded yellow hexagonal platy crystals. Yield 1.8g, 82%.

Found; C 28.0, H 7.7, N 16.4.

Calc. for $C_{12}H_{40}Cl_3CoN_6O_5$; C 28.0, H 7.8, N 16.4.

2.3.1.2 $Cr^{III}(tacn)_2Br_3.5H_2O$

Chromium (III) bis tacn was formed by two methods; the first based on a published route by Weighardt (Ref 33): the second a novel approach. In both cases exclusion of moisture was found to be essential during complex formation.

(i) 1.0g tacn.3HCl (4.19 mmoles) was dissolved, with warming, in 3 mls of water. To this solution was added, slowly to avoid excessive heating, KOH (0.72g). The resulting solution was extracted with toluene (5 x 10 ml aliquots) and the toluene was removed under reduced pressure to leave the free ligand 1,4,7-triazacyclononane. The free ligand is likely to be susceptible to oxidation and so the addition of 5 mls of ethanol to give a 0.84M solution was carried out immediately.

$CrCl_3.6H_2O$ (0.48g, 1.8 mmoles) was dissolved in 30 mls of dry dimethyl sulphoxide which was taken to 190°C in order to dehydrate the chromium salt. The solution changed colour almost immediately from green to purple. This temperature was maintained until 5 mls of the solvent had evaporated. The solution was then cooled to 70°C in a dry nitrogen atmosphere and the

solution of tacn in ethanol which was prepared previously was added. The temperature was raised slowly to 170°C and maintained for 30 minutes after which a crystalline yellow precipitate was observed to have formed under a red solution. Recrystallisation from concentrated sodium bromide solution gave yellow hexagonal crystals which were observed to fluoresce red under U.V. light. Yield 0.73g 68%.

(ii) 0.90g (3.8 mmol) tacn.3HCl was dissolved in 5 mls of water and 0.46g of sodium hydroxide was added to effect neutralisation. To the aqueous free ligand solution was added 30 mls of dimethyl sulphoxide and the resulting solution was taken to 150°C and maintained until the volume reduced to 20 mls. A second solution containing 0.50g (1.88 mmoles) of $CrCl_3.6H_2O$ in 20 mls of DMSO, the volume of which had been reduced to 15 mls by evaporation at 190°C, was added to the first. The temperature of the combined solution was maintained at 170°C for 1 hour after which a yellow crystalline solid had precipitated. The solid was filtered and recrystallised from the minimum quantity of water by addition of solid sodium bromide. Yield 0.72g, 75% Found; C 22.47, H 6.28, N 13.21. Calc. for $C_{12}H_{40}Br_3CrN_6O_5$; C 22.61 H 6.28, N 13.19. (The complex was found to be subject to long term dehydration).

2.3.2 Preparation of R-2-methyl-1,4,7-triazacyclononane; Metacn.

The preparation of R-Metacn was first reported in 1976 by Mason and Peacock (Ref 27). A modified version of this synthesis was used to prepare the ligand and is outlined below and represented schematically in figure 2.5. The synthesis is analogous to the low yield, low purity, route 1 to tacn. However it has been found that due to difficulties in the cyclisation step the more successful tacn preparation cannot be adapted for use in Metacn synthesis.

R-(-) Propylene diamine

Propylene diamine was resolved by the method of Dwyer and co-workers (Ref 28). Propylene diamine (260g, 3.5 mol) was added, slowly, to a stirred solution of 700 g (4.67 mol) of d-tartaric acid in 750 mls of cold water. The reaction mixture was allowed to cool to 40°C and was then cooled rapidly in ice to a temperature of 5°C which was maintained for 45 minutes. The diastereomeric salt,

(-) - propylene diamine(d-tartrate) precipitated and was filtered and washed with ice water (250 mls). The product was recrystallised three times from the minimum quantity of 5% acetic acid (1, 900 mls, 2, 850 mls, 3, 800 mls). Yield 560g, 85.2%, mp 137-139°C.

The tartrate salt (37.4g, 0.1 mol) was added with stirring to 300 mls of boiling water and on dissolution 15.0g (0.2 moles) of potassium chloride was added. The potassium tartrate salt which formed was insoluble and was removed by filtration. The filtrate was reduced in volume to 100 mls and refiltered before being taken to dryness to give

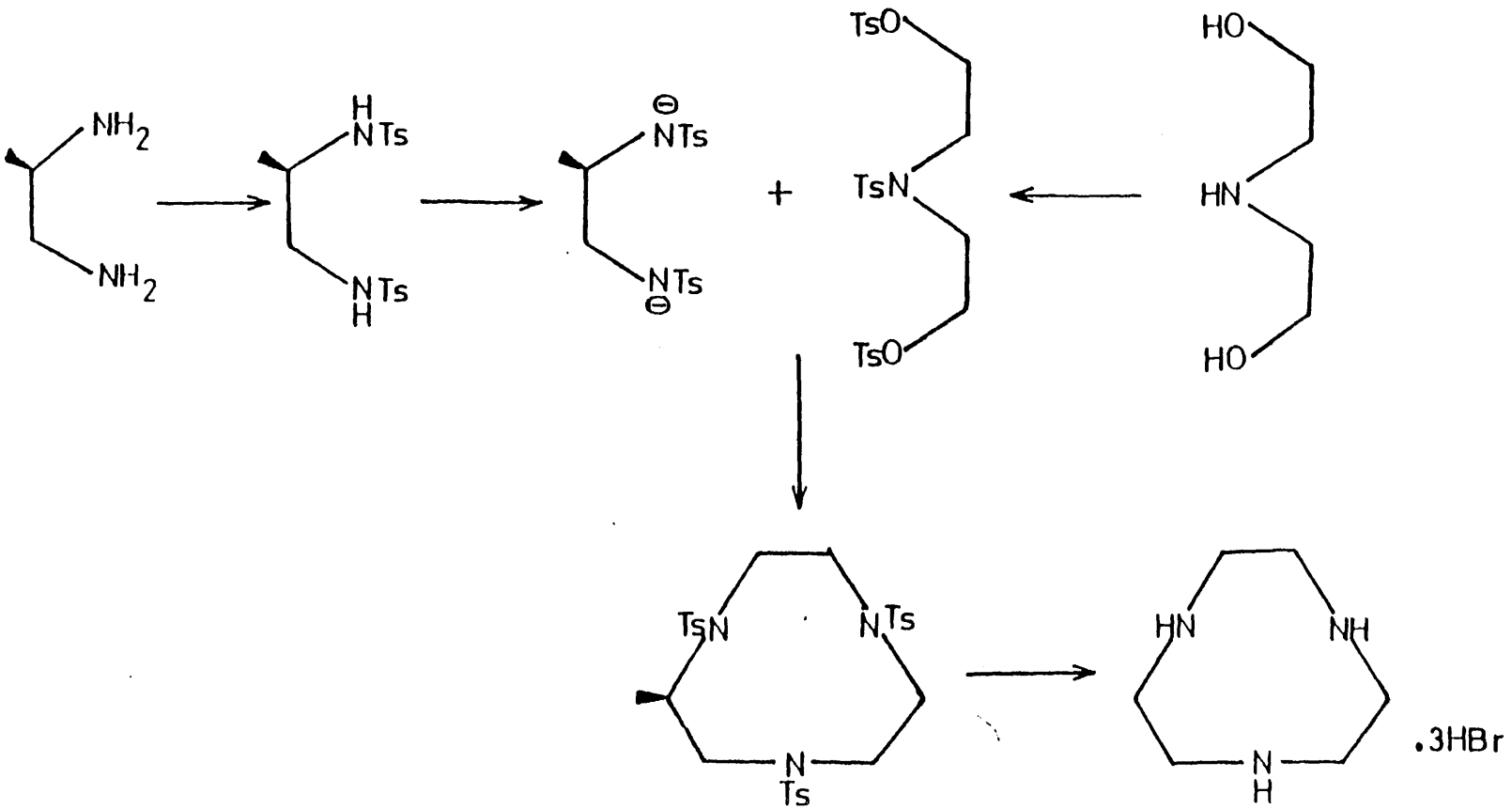

FIGURE 2.5
The synthetic scheme leading to Metacn.

(-)propylene diamine dihydrochloride. Yield 12.6g, 87% . mp 222-225°C.

The dry dihydrochloride salt (14.7g, 0.1 moles) was mixed intimately with dry sodium hydroxide powder (32g, 0.8 moles) in a round bottomed flask.

When the mixing process was complete and before a significant amount of the exothermic neutralisation reaction had occurred the flask was connected to a distillation apparatus,equipped with a heating mantle, and raised in temperature so that dry distillation occurred. The major fraction, a clear liquid at 121°C, was (-)propylene diamine which was stored over KOH for 24 hours prior to use. Yield 6.1g, 82%.

Found; C 46.2, H 13.4, N 36.0.

Calc. for $C_3H_{10}N_2$;C 48.6, H 13.5, N 37.8 (5% aqueous impurity)

Synthesis of S-(+)- propylene diamine was achieved in the same way by the use of l-tartaric acid in the initial diastereomeric salt formation.

N,N'-di(p-toluene sulphonyl) - (S)-propane- 1,2-diamine

The tosylation of the resolved diamine was by a route analogous to that used by Bencini et al (Ref 70) for similar amines. 100g, 0.52 moles of p-toluene sulphonyl chloride in 550 mls of diethyl ether was added dropwise over 6 hours to a vigorously and mechanically stirred solution of 18.9 g (0.26 moles) of (+)-propylene diamine and 21.0g (0.52 moles) of sodium hydroxide in 250 mls of water. The stirring was necessarily vigorous to ensure

thorough mixing of the two phases. When the 6 hour dropping period had elapsed stirring was continued for approximately one hour longer, at which time the reaction mixture solidified indicating completion of reaction. The white precipitate was recrystallised from a large volume of ethanol by slow addition of water.

Yield 80g, 80.5%. mp 100-104°C.

Found; C 53.4, H 5.7, N 7.3, S, 16.7

Calc. for $C_{17}H_{22}N_2O_4S_2$;C 53.7, H 5.8, N 7.4, S 16.7.

N,O,O'-tri(p-toluene sulphonyl)bis(2-hydroxyethyl) amine

114.4g (0.6 moles) of p-toluene sulphonyl chloride in 600 mls of diethyl ether was added over one hour to a stirred solution of bis (2-hydroxyethyl) amine (20.4g, 0.2 moles) in triethylamine (200 mls) in an open beaker. The solution was stirred for a further 1 hour after which 200 mls of water was added to dissolve unchanged starting material. The white precipitate was recrystallised from the minimum quantity of hot ethanol.

Yield 64.3g, 58% mp 93-93°C.

Found; C 52.9, H 5.0, N 2.5, S 17.0.

Calc. for $C_{25}H_{29}NO_8S_3$;C 52.9, H 5.1, N 2.5, S 16.9.

N,N',N"-tri(p-toluene-
sulphonyl)-2(S)-methyl-1,4,7-triazacyclononane

As was the case in the tacn synthesis the disodium salt of the tosylated amine was found to be prone to hydrolysis and so no attempt was made to isolate it and there was the minimum possible delay between formation of the disodium

salt and commencement of the cyclisation step. Exclusion of water at these two stages was found to be essential.

To a stirred solution of 38.2g (0.1 moles) of N,N'-di (p-toluene sulphonyl)-(S)-propane-1,2-diamine in 700 mls of dry dimethyl formamide was added slowly 16g of a 50% suspension in oil (0.34 moles) of sodium hydride. After 1 hour the initial effervescence had subsided and the solution, which was yellow in colour, was raised to 70°C for approximately one hour in order to ensure that the disodium salt of the tritosylated amine would be present in the highest possible yield. The excess sodium hydride, which was present as a precipitate was filtered under nitrogen so that the filtrate passed directly into a second reaction vessel. The solution was raised to 110°C immediately and the cyclisation reaction commenced.

To the solution of disodium N,N'-di(p-toluene sulphonyl) propane-1,2,-diamine at 110°C was added, over 4 hours with stirring, a second solution of N,O,O'-tri(p-toluene sulphonyl)bis(2-hydroxyethyl) amine, 56.7g (0.1 moles), in 350 mls of dry dimethyl formamide. When the four hours had elapsed the solution was maintained at 110°C for a further 2 hours after which it was reduced in volume to 250 mls and added slowly to 2 litres of water. A tacky oil precipitated which, on stirring under methanol, gave an off-white solid of tritosyl-(S)-Metacn.

Yield 7.1g, 11.7% mp 199 - 203°C

Found; C 55.6 H 5.8 N 6.8, S 15.5.

Calc. for $C_{28}H_{35}N_3O_6S_3$; C 55.5, H 5.8, N 6.9, S 15.8.

2(S)-methyl-1,4,7-triazacyclononane.3HBr

Detosylation to the trihydrobromide salt of the ligand was effected by refluxing 5g of tritosyl Metacn (8.3 mmoles) in a 1 litre round bottomed flask charged with 500 mls of glacial acetic acid and 200 mls of hydrobromic acid. The solution was observed to darken over the 7 days of refluxing. On completion the volume was reduced to 100 mls and the solution was added dropwise, with stirring, to a mixture of 200 mls of diethyl ether and 400 mls of ethanol. A grey coloured precipitate of Metacn.3HBr precipitated and was filtered and dissolved in the minimum quantity of boiling hydrochloric acid to give Metacn.3HCl.

Yield (Metacn.3HBr) 1.97g, 62%.mp 235-238°C

Found; C 21.7, H 10.9, N 5.2.

Calc. for $C_7H_{20}N_3Br_3$; C 21.8, H 5.2, N 10.9, m/e 143.

2.3.3 1,4,7-triazacyclononane-N,N',N''-triacetate; (tcta)

This ligand (Fig 2.6), first reported by Arishima, Hamada and Takamoto in 1973 (Ref 71), was prepared using the method of Wieghardt et al (Ref 55). tacn.3HCl (2.38g, 0.01 moles) was dissolved in 5 mls of water containing 1.20g (0.03 moles) of sodium hydroxide. To this solution was added, with stirring, at 20°C a second solution comprising 4.7g (0.034 moles) of bromoacetic acid and 1.2g NaOH in 10 mls of water. The resulting solution was heated to 80°C on a steam bath and a solution of 1.2g NaOH in 5 mls of water was added dropwise. The temperature was maintained for 1 hour after which the reaction was considered to be complete. On cooling the pH was adjusted to 7 using

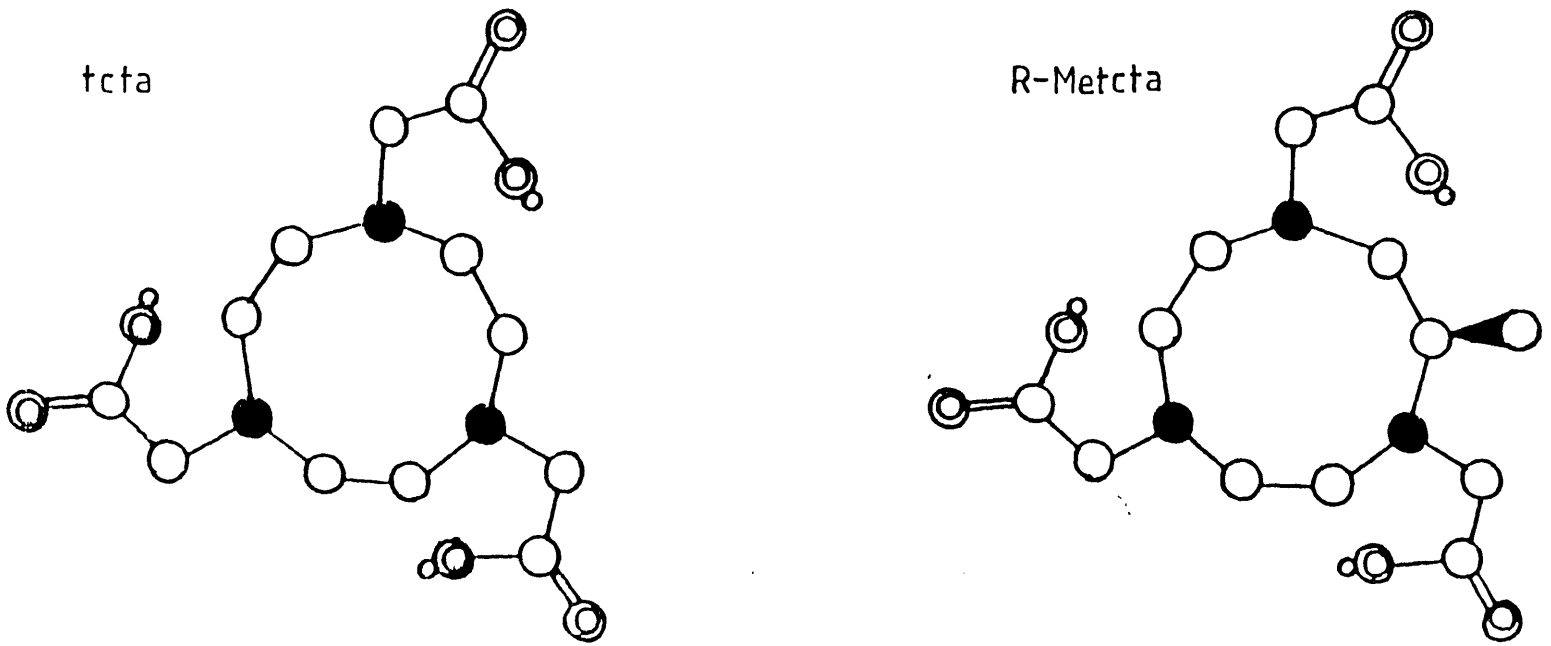

FIGURE 2.6
The ligands tcta and R-Metcta .

concentrated hydrochloric acid. No attempt was made to isolate the ligand and the solution was used in all subsequent preparations (Molarity = 0.5M assumed). m/e = 300.

2.3.3.1 Optically Active CoIII(tcta)

Takahashi & Takamoto in 1977 (Ref 54) and Wieghardt et al in 1982 (Ref 55) both prepared racemic CoIII(tcta): the following preparation gives rise to an imbalance of the two enantiomers of the complex.

The chiral induction derives from the optical activity present in the starting material CoII(l-tart). CoII (l-tart) was made by a method based on that used by Broomhead et al (Ref 39). $CoCl_2.6H_2O$ (23.8g, 0.1 moles) was dissolved in 50 mls of water and heated to 65°C. A second solution comprising 23.0g of sodium l-tartrate in 50 mls of water was added to the first and the temperature was maintained for one hour during which a purple/red precipitate developed. The mixture was cooled in ice, filtered and washed with acetone before being air dried.

Yield 20.7g, 92%

Found; C 23.2, H 1.9.

Calc. for $C_4H_4CoO_6$; C 23.2 H 1.9.

CoII(l-tart), (1.04g, 5 mmoles), was added to 10 mls of the 0.5M solution of tcta stirred at 80°C. The initial precipitate of CoII(l-tart) decreased as the reaction proceeded until a red solution was obtained. Hydrogen peroxide was added at this point to ensure complete oxidation. On cooling some crystals separated out leaving a red solution. The volume was reduced to 5 mls and on

overnight refrigeration the solution became pale pink having deposited more crystals. The second crystal sample was optically active.

Yield 0.32g, 18%.

Found; C 39.9, H 4.8, N 11.8.

Calc. for $C_{12}H_{18}CoN_3O_6$; C 40.1, H 5.0 N 11.7. (Note - the (d-tart) synthesis was also used.)

2.3.3.2 Optically Active Cr(tcta)

To 0.67g (2.5 mmoles) of $CrCl_3.6H_2O$ in 5 mls of water was added, with stirring, a solution comprising 0.375g (2.5 mmoles) of l-tartaric acid in 5 mls H_2O. The green solution darkened whereupon 5 mls of 0.5M tcta solution was added and the resulting solution was refluxed until a dark red colour was observed (approximately 2 hours). On cooling crystallisation occurred leaving an optically active mother liquor which was refrigerated overnight to give more crystals. The second crystal sample was optically active.

Yield 0.36g, 41%.

Found; C 40.9, H 4.9, N 11.9.

Calc. for $C_{12}H_{18}CrN_3O_6$; C 40.9, H 5.1, N 11.9. (The enantiomeric form was prepared using d-tartaric acid).

2.3.4. 2-(S)-methyl-1,4,7-triazacyclononane-N,N',N''- triacetate; (S-Metcta)

The synthesis employed was analogous to that used in preparing tcta but the macrocyclic starting material was different. 2-(S)-methyl-1,4,7-triazacyclononane.3HCl (2.52g, 0.01 moles) was dissolved in 5 mls of water

containing NaOH (0.03 moles). To this solution was added with stirring a second solution of 4.7g (0.034 moles) of bromoacetic acid and 1.2g of sodium hydroxide in 10 mls of water. The resulting solution was heated to 80°C and a third solution, containing 1.2g NaOH in 5 mls of water, was added dropwise. The temperature was maintained for one hour. On cooling the solution was taken to pH = 7 using concentrated HCl. This solution was used in preparing the Metcta complexes since it was found that, as with tcta, neither the free ligand nor its sodium salt could be isolated. The molarity of the solution was calculated to be 0.5M. m/e = 314. (Rotary evaporation gave an oil).

2.3.4.1 CoIII (S-Metcta).$2H_2O$

To 0.107g (4.5×10^{-4} moles) of $CoCl_2.6H_2O$ in 5 mls of water was added, with stirring, 1 ml (5×10^{-4} moles) of the prepared S-Metcta solution, at 80°C. The solution was maintained at 80°C until a bright red colour developed. Addition of 0.5mls of 100 vol. H_2O_2 speeded the process. Unlike the case of CoIII (tcta) no crystals precipitated on cooling. The solution was taken to dryness slowly in order to effect crystallisation.

The major problem of purification was the presence of sodium halides, arising from the ligand solution, which were found to have similar solubility to the complex in all solvents tried. The best purification method was found to be that whereby a concentrated solution of the complex and salt impurity was left in an open beaker whereupon clear salt crystals formed. The mother liquor was carefully

removed by pipette when salt crystal formation was complete. Cooling of the red mother liquor in a refrigerator gave red needle shaped crystals.

Yield 0.11g, 60%.

Found; C 38.3 H 5.6 N 10.3.

Calc. for $C_{13}H_{24}CoN_3O_8$;C 38.1, H 5.8, N 10.3.

2.3.4.2 CrIII(S-Metcta)

To 1 ml (5×10^{-4} moles) of ligand solution was added 0.120g (4.5×10^{-4} moles) of $CrCl_3.6H_2O$ in 1 ml of water. The initially green solution darkened and turned purple on refluxing. Refluxing was maintained for 2 hours after which the solution was observed to have become deep red in colour. As with the cobalt case the precipitation of crystals, observed in [MIII (tcta)] formation, was absent. The red solution was rotary evaporated to dryness and gave a red, hygroscopic, precipitate with a sodium chloride impurity. As in the cobalt case separation of the salt from the complex was difficult and was performed in a similar manner.

Yield 0.10g, 61%

Found; C 42.3, H 5.6, N 11.3.

Calc. for $C_{13}H_{20}CrN_3O_6$; C 42.6, N 5.5, H 11.5.

2.3.4.3 [CuII(S-Metcta)]$^-$

0.109g of $CuCl_2.2H_2O$ was dissolved, with stirring, in 1 ml of the 0.5M ligand solution. The mixture was heated at 50°C for 10 minutes and the pH was adjusted to 7 using solid sodium hydroxide. Addition of ethanol did not result in

crystallisation and it was found necessary to evaporate the water at 60 °C. Recrystallisation from hot ethanol removed the bulk of the sodium chloride and gave a blue precipitate of the copper salt.

The species was identified by its spectroscopic similarity to the analogous complex, $[Cu(tcta)]^-$ (Ref 55).

2.3.4.4 $[Ni(S\text{-}Metcta)]^-$

To 1 ml of the ligand solution was added 0.107g (4.5×10^{-4} moles) of $NiCl_2.6H_2O$. The temperature was raised to 60°C and maintained for twenty minutes during which time a deep purple solution formed. The solution was taken to dryness and redissolved in ethanol to remove sodium chloride. On evaporation of the alcohol purple crystals formed.

As with the Cu(II) complex, identification was inferred from the close similarity between the electronic spectra obtained for "$[Ni(S\text{-}Metcta)]^-$ " and those reported (Ref 55) for $[Ni(tcta)]^-$.

2.3.5 N,N',N''-tris(2-hydroxyethyl)-1,4,7-triazacyclononane hydrochloride (fig 2.7)

The ligand thetacn was prepared by a method loosely based on that first reported by Hancock et al (Ref 58). 2.38g (0.01 moles) tacn.3HCl and 1.2g (0.03 moles) NaOH were dissolved in 1 ml H_2O with cooling. Ethanol (5 mls) was added and the solution was refrigerated overnight. Filtration of the solution removed sodium chloride to give an ethanolic solution of tacn which was cooled to 5 °C. To this solution was added, dropwise, 1.5g (0.034 moles) of

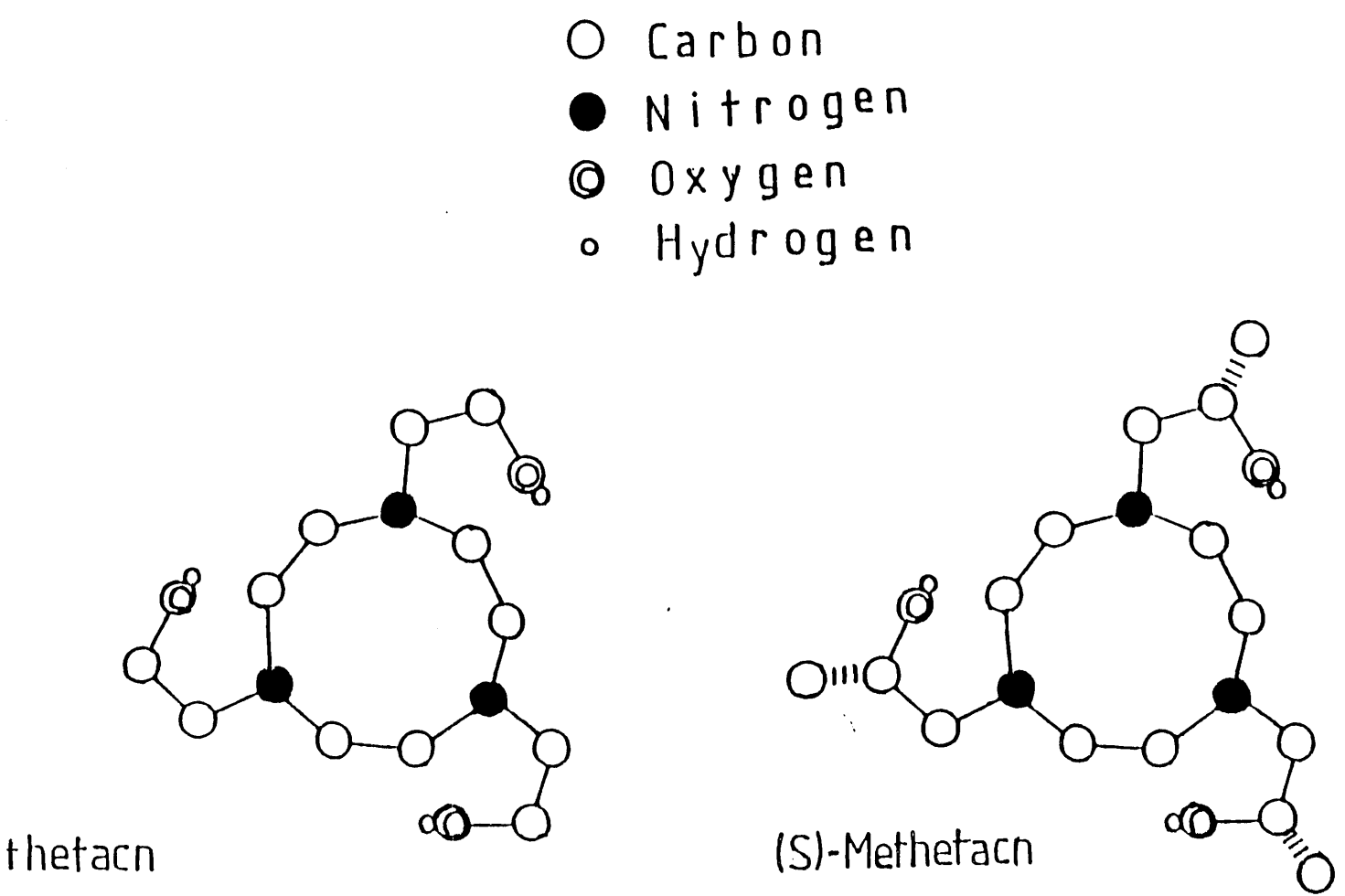

FIGURE 2.7
The ligands thetacn and S-Methetacn.

ethylene oxide which had been refrigerated. Cooling was essential because of the exothermic nature of the reaction and the volatility of the ethylene oxide. The solution was stoppered and left overnight in order to allow the reaction to be completed. On rotary - evaporation to dryness and recrystallisation from isopropanol a white solid was obtained.

Yield 1.9g, 65%;

Found; C 48.7, H 9.5, N 14.5, Cl 11.9

Calc. for $C_{12}H_{27}NO_3.HCl$; C 48.4, H 9.4, N 14.1, Cl 11.9.

m/e = 262.

2.3.5.1 Co(thetacn)Cl_3

To a solution of 0.24g (0.001 moles) of $CoCl_2.6H_2O$ in 10 mls of water was added a second solution of 0.30g (0.001 moles) of thetacn.HCl in 5 mls of water. The cobalt solution immediately turned from purple to rust coloured. 2 mls of 30 vol H_2O_2 was added and the solution was raised to 80°C to effect oxidation to the cobalt(III) species. After 30 minutes the solution had turned intensely purple and was allowed to cool. The complex was isolated by rotary-evaporating the aqueous solution to dryness and redissolving the precipitate in acetonitrile. Filtration removed residual salt so that on drying the purple complex was found to be pure. It was found necessary to store the product in vacuo since it was hygroscopic.

Yield 0.33g, 78%.

Found; C 33.6, H 6.8, N 9.7.

Calc. for $[Co^{III}(C_{12}H_{27}N_3O_3)]Cl_3$; C 33.8, H 6.6, N 9.8.

2.3.6 N,N',N''-tris(2-(S)-hydroxyisopropyl)-1,4,7-triazacyclononane.hydrochloride

The ligand S-Methetacn (Ref 72) was prepared by a method analogous to that used in the preparation of thetacn.

1g (0.017 moles) of S-(-)-propylene oxide was added, by means of cooled apparatus, to a solution of tacn (0.006 moles) in ethanol prepared from 1.35g of tacn.3HCl. Addition was sufficiently slow to prevent loss of the epoxide due to its low boiling point and the exothermic nature of the reaction. The mixture was left for 24 hours in a stoppered flask (this was found to be essential to allow reaction to proceed) after which it was taken to dryness to give an oil containing traces of sodium chloride. The oil was purified by dissolution, filtration and reprecipitation from the minimum volume of isopropyl alcohol and was found to be S-Methetacn.HCl.

Yield 1.29g, 71%.

Found; C 53.1, H 9.7, N 12.4.

Calc. for $C_{15}H_{33}N_3O_3.HCl$; C 53.0, H 9.7, N 12.4.

^{1}H-nmr in $CDCl_3$; m,3.9ppm, 3 protons (methine) ; m, 2.4-2.9 ppm, 18 protons (methylene); d, 1.1ppm, 9 protons (methyl).

m/e = 304.

2.3.6.1 [CoIII(S-Methetacn)]Cl_3

To a solution of 0.24g (1 mmole) of $CoCl_2.6H_2O$ in 10 mls of water was added a second solution of 0.34g (1mmol) of S-Methetacn.HCl in 5 mls of water. From this stage onwards the preparation was identical to that for

[CoIII(thetacn)]Cl_3 except that the optically active complex formed was slightly more hygroscopic. The dry purple solid [CoIII(S-Methetacn)]Cl_3 was most conveniently obtained by placing wet complex in an oven at 100°C for one hour. No decomposition was apparent after this procedure. Both acidic and basic solutions of the title complex were used. These were prepared using concentrated HCl and concentrated NaOH solution respectively. For nuclear magnetic resonance studies deuterated solvent and reagents were required. The solvent used was deuterium oxide (D_2O) which was acidified by deuterochloric acid (DCl) and basified using sodium deuteroxide (NaOD). DCl was produced to the required concentration by addition of thionyl chloride to D_2O and NaOD by addition of sodium metal to D_2O.

Yield of Complex. 0.35g, 74%.

Found; C 38.6, H 7.4, N 9.0.

Calc. for $C_{15}H_{33}CoN_3O_3Cl_3$; C 38.4, H 7.0, N 9.0.

As a result of the hygroscopic nature of the chloride salt of $[CoIII(S\text{-}Methetacn)]^{3+}$ it was found necessary to make another salt which would be open to investigation in the solid state. To this end the tri hexafluorophosphate salt was prepared as follows. To 0.2g (0.42 mmoles) of [CoIII(S-Methetacn)]Cl_3 in 2 mls of water was added with stirring a 1 ml aqueous solution of 0.21g (1.26 mmoles) of ammonium hexafluorophosphate. A precipitate formed immediately and the solution was chilled overnight after which the solution over the precipitate was almost colourless. The precipitate was filtered and washed with

water before being air-dried. It could conveniently be recrystallised from acetonitrile although larger crystals were obtained by slow evaporation of a dimethyl formamide solution of the salt.

Yield 0.33g, 88%.

Analysis from crystal structure (Chapter 4).

2.3.6.2 [CuII(S-Methetacn)]Cl_2

A solution of 0.17g of $CuCl_2.2H_2O$ in 3 mls of water was added to a second solution of 0.34g of S-Methetacn hydrochloride in 3 mls of water. The mixture was heated to 70°C and the pH was adjusted to 8. After 20 minutes the pale blue/green solution was cooled and its pH was adjusted to 11 which resulted in a deep blue colour. The aqueous solution was taken to dryness to give bright blue crystals which could be regrown from chloroform.

Yield 0.31g, 71%.

Found; C 41.1, H 7.63, N 9.5,

Calc. for $CuC_{15}H_{33}N_3O_3Cl_2$;C 41.1, H 7.53, N 9.6

2.3.6.3 [NiII(S-Methetacn)]$Cl_2.3H_2O$

To a solution of nickel (II) chloride hexahydrate (0.24g, 1.0 mmoles) in 3 mls of water was added 0.34 g, 1.0 mmoles of S-Methetacn hydrochloride in 3 mls of water. The pH was adjusted to 7 with KOH. The temperature of the resulting solution was raised to 70°C on a steam bath and maintained for 30 minutes after which the solution was violet in colour. The water was evaporated over several weeks and platy purple crystals formed.

Yield 0.33g, 68%.

Found; C 36.8, H 8.1, N 8.2.

Calc. for $C_{15}H_{39}Cl_2N_3O_6Ni$; C 37.4, H 8.1, N 8.7.

CHAPTER 3

Complexes of tacn

3. COMPLEXES OF tacn

3.1 $Co(tacn)_2Cl_3.5H_2O$

3.1.1 Introduction

The origins of the optical activity in various systems possessing a $Co(III)N_6$ chromophore have been widely investigated over many years (Refs 73, 74 & 75). The work which has been conducted in this area has been largely concerned with Co(III) tris diamines which possess geometries determined, to a large extent, by the size of the chelate rings involved. Rings of up to five members, (for example those containing ethylene diamine) have a ring angle α, between the coordinated bonds within a ring, of less than the 90° expected for perfect octahedral geometry (Ref 41). Rings of six or more members tend to have ring angles of greater than 90°. In complexes where $\alpha < 90°$ there are two geometric consequences 1) a trigonal compression and 2) a trigonal twist. If α is greater than 90° the trigonal twist is accompanied by trigonal elongation. Cobalt bis-triamines are generally elongated as a result of repulsive interactions between the two macrocyclic rings. Originally it was believed that the absence of chelate rings parallel or oblique to the C_3 axis (such as those observed in $[Co(en)_3]^{3+}$), would lead to a trigonal twist of zero (Ref 27). However, crystal structure data (Ref 48) indicated that there was a twist (7.6° in the case of $[Co(R\text{-}Metacn)_2]^{3+}$). This twist has since been explained as being a result of the interactions between the

hydrogens of the two macrocyclic ligands. Like $[Co^{III}(diamine)_3]^{3+}$ the $[(Co^{III}(triamine)_2]^{3+}$ species have optical activity arising both from chelate ring conformation (λ and δ) and from trigonal twist (Λ and Δ). The main difference is that in the triamine case the bulk of the ligands is held in axial regions while in the diamine case it is held in equatorial regions.

In both types of complex the possible combinations of λ and δ for each of up to six chelate rings, and Λ or Δ for the overall twist, gives the potential for a large number of diastereomers. This is particularly true in the case of complexes possessing a chiral centre on the ligands. The effect of such a centre is to lower the symmetry of the molecule and consequently to increase the number of optical isomers. An example of this is the complex $[Co(R\text{-Metacn})_2]^{3+}$ which is not, in fact, a unique species but is rather a mixture of the nine possible isomers resulting both from the position of the methyl group on one ligand relative to that on the other, and from the relative orientations of the two distinct faces on each macrocycle. Five fractions of $[Co(R\text{-Metacn})_2]^{3+}$ have been resolved by column chromatography (Ref 44). However, difficulties in complete resolution and subsequent assignment of the isomers suggest that a simpler system, free from the problems of diastereoisomerism would be a more fruitful source of information on the optical activity of cobalt (III) bis triamines.

In the case above it is the very presence of chiral centres on the ligands which leads to diverse isomerism. It would clearly be preferable to use analogous chiral ligands which could theoretically give a resolvable racemic mixture of the two enantiomers of a metal complex. It is fortunate that for cobalt(III) complexes lability is not a problem so that resolution into enantiomers is possible by a number of methods. For $[Co(en)_3]^{3+}$ such methods as chiral induction (Ref 39), chromatography (Ref 76) and diastereomeric precipitation using a chiral counter ion (Ref 28) have all been successfully applied. However, the separation of chelated amine complexes relies heavily on the conformational stability of the individual chelate rings. In the case of $[Co(tacn)_2]^{3+}$ the barrier to ring flipping is sufficiently low that in solution the two enantiomers are in equilibrium. It is fortunate that racemic mixtures of $[Co(tacn)_2]^{3+}$ give rise to two enantiomeric crystalline forms. These forms are analogous to the two species $[Co(R\text{-}Metacn)_2]^{3+}$ and $[Co(S\text{-}Metacn)_2]^{3+}$ but are free from problems arising from diastereoisomerism. It has been found (Refs 27 & 32) that when one of the six chelate rings in a bis triamine cobalt(III) complex is fixed in a particular conformation in the solid state, the other rings adopt the same conformation. While this finding related to $[Co(R\text{-}Metacn)_2]^{3+}$ it was expected to hold for all cobalt bis triamines and it is supported by the absence of a meso form of $[Co(tacn)_2]^{3+}$ i.e. $(\lambda\lambda\lambda,\delta\delta\delta)$. The meso-form would be expected to predominate in the absence of the postulated synergic effect. In the absence of crystal structure data

solid state circular dichroism, provides a useful tool for investigating the $[Co(tacn)_2]^{3+}$ system.

3.1.2 Results

$[Co(tacn)_2]Cl_3.5H_2O$ was prepared as described in section 2.3.1.1 and was twice recrystallised from the minimum quantity of water to give platey hexagonal crystals. Several crystals were rotated between crossed polarisers on the stage of a polarising microscope and were found to be invariant to rotation. This isotropy in directions perpendicular to the crystals six fold axis indicated that the crystals were uniaxial. A crystal was selected which would give an absorbance close to unity and which was of uniform thickness. The uniformity of thickness was important because the Beer-Lambert Law could not be applied directly in its normal form:

3a) $A = \varepsilon c l$

It has been found useful, in the case of single crystals, (Ref 40) to combine the concentration and path length terms to give unitary cancellation so that

3b) $cl = \text{moles } dm^{-3} cm \equiv \text{moles}/(1000 cm^2)$

Thus application of the Beer-Lambert Law to a single crystal sample requires only a knowledge of the surface area and mass of the crystal. In this instance the area of the crystal was measured using a graticulated eyepiece of

magnification X10. The geometric nature of the sample facilitated accurate calculation of the area which was found to be 0.0168cm^2. The weight of the crystal was 4.0×10^{-4} g, equivalent to 7.78×10^{-7} moles (mol wt. = 513.5) From this information cl may be computed to be 4.63×10^{-2} moles/(1000cm^2). By use of this value in conjunction with an absorption spectrum of the crystal it was possible to obtain values of ε_E, the molar extinction coefficient for light propagated parallel to the crystal's highest fold axis, at any required wavelength. The values obtained differ from solution values because in the single crystal only the $A_1 \rightarrow E$ transition is excited whereas in solution both the $A_1 \rightarrow A_2$ and $A_1 \rightarrow E$ transitions are excited. This is because in crystals of $[Co(tacn)_2]Cl_3.5H_2O$ the molecules are known (Ref 43) to be aligned such that the three fold axis of the complex ion is parallel to the highest fold crystal axis. The result is that light propagated parallel to the unique crystal axis has its electric and magnetic vectors rotating in the xy plane of the complex. These vectors can, from symmetry considerations, excite only those transitions which occur in the xy plane, namely $A_1 \longrightarrow E_x$ and $A_1 \longrightarrow E_y$ so that as a result only the $A_1 \longrightarrow E$ band is observed. In solution spectra what is observed is the result of light passing through an assemblage of randomly oriented chromophores. This randomness has the effect that the observed extinction coefficient represents contributions from $A_1 \longrightarrow A_2$, $A_1 \rightarrow E_x$, and $A_1 \longrightarrow E_y$.

i.e. 3c) $$\varepsilon_{Solution} = \frac{1}{3}\varepsilon_{A_1 \rightarrow A_2} + \frac{1}{3}\varepsilon_{A_1 \rightarrow E_x} + \frac{1}{3}\varepsilon_{A_1 \rightarrow E_y}$$

If this is compared to the single crystal case (equation (3d)) it can be seen that unless $\varepsilon_{A_1 \rightarrow A_2}$ is equal in magnitude to $\varepsilon_{A_1 \rightarrow E_x}$ and $\varepsilon_{A_1 \rightarrow E_y}$ then ε_{SC} will be unequal to $\varepsilon_{Solution}$.

3d) $$\varepsilon_{\text{single crystal}} = \frac{1}{2} \varepsilon_{E_x} + \frac{1}{2} \varepsilon_{E_y}$$

The circular dichroism spectrum is also subject to this phenomenon although the effect is more marked since the $A_1 \rightarrow A_2$ and $A_1 \rightarrow E$ transitions are necessarily oppositely signed. However, circular dichroism provides a technique for obtaining quantitative values for the two contributions. As with absorption spectra the crystal was placed in the sample holder and oriented so that it was perpendicular to the beam. The spectrum was recorded (figure 3.1) and from it a table of values of $\Delta\varepsilon_{\text{single crystal}}$ versus wavelength was compiled (Table 3.1). It has already been noted that the complex $[Co(tacn)_2]^{3+}$ racemises in solution and so no solution spectra could be recorded. In order to obtain values of $\Delta\varepsilon$ for a randomly oriented sample it was necessary to take a single crystal of known enantiomer and mass ($\simeq 1.0 \times 10^{-3}$ g) and to grind it to a microcrystalline state in a matrix of potassium bromide. The powder formed from grinding for five minutes was pressed to form a KBr disk which was found to have a surface area of $1.54 cm^2$. The weight of complex in the disk was checked at the end of the experiment by dissolving the disk in 5 mls of water and

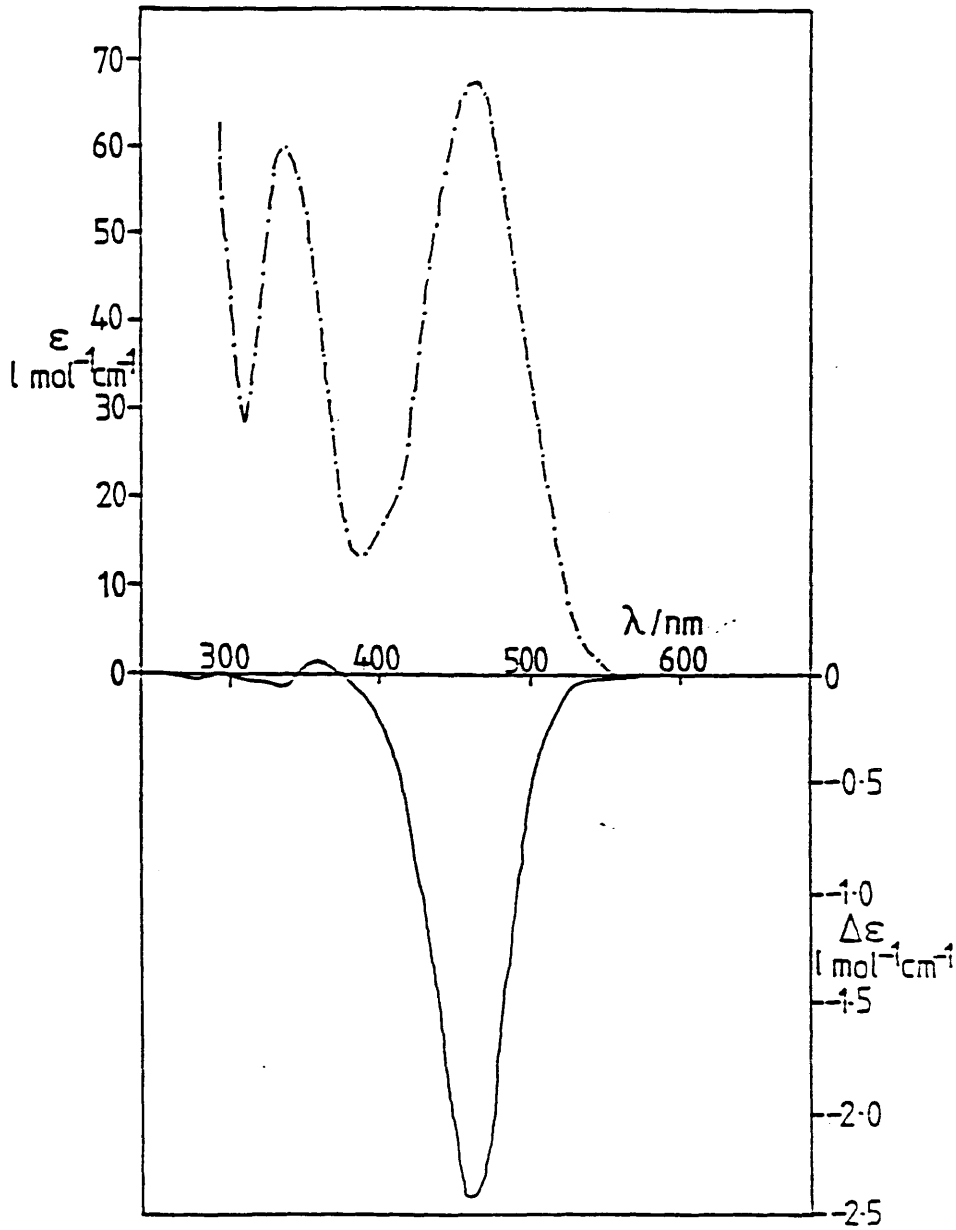

FIGURE 3.1
The absorption (top) and circular dichroism (bottom) spectra of a $[Co(tacn)_2]Cl_3.5H_2O$ single crystal with light propagated parallel to both the highest fold crystal axis and the highest fold molecular axis.

using known values of ε in conjunction with reported absorption spectra. A value of 1.19×10^{-3}g was obtained. Using the surface area of the disk and the number of moles present it was possible to obtain values of $\Delta\varepsilon_{\text{microcrystalline}}$ by application of equation (3b) in conjunction with the c.d. spectrum of the sample. The spectrum obtained using the disk was calibrated from accepted values of ε solution to give figure 3.2. Thus a table of $\Delta\varepsilon_{\text{microcrystalline}}$ versus wavelength was compiled (Table 3.1).

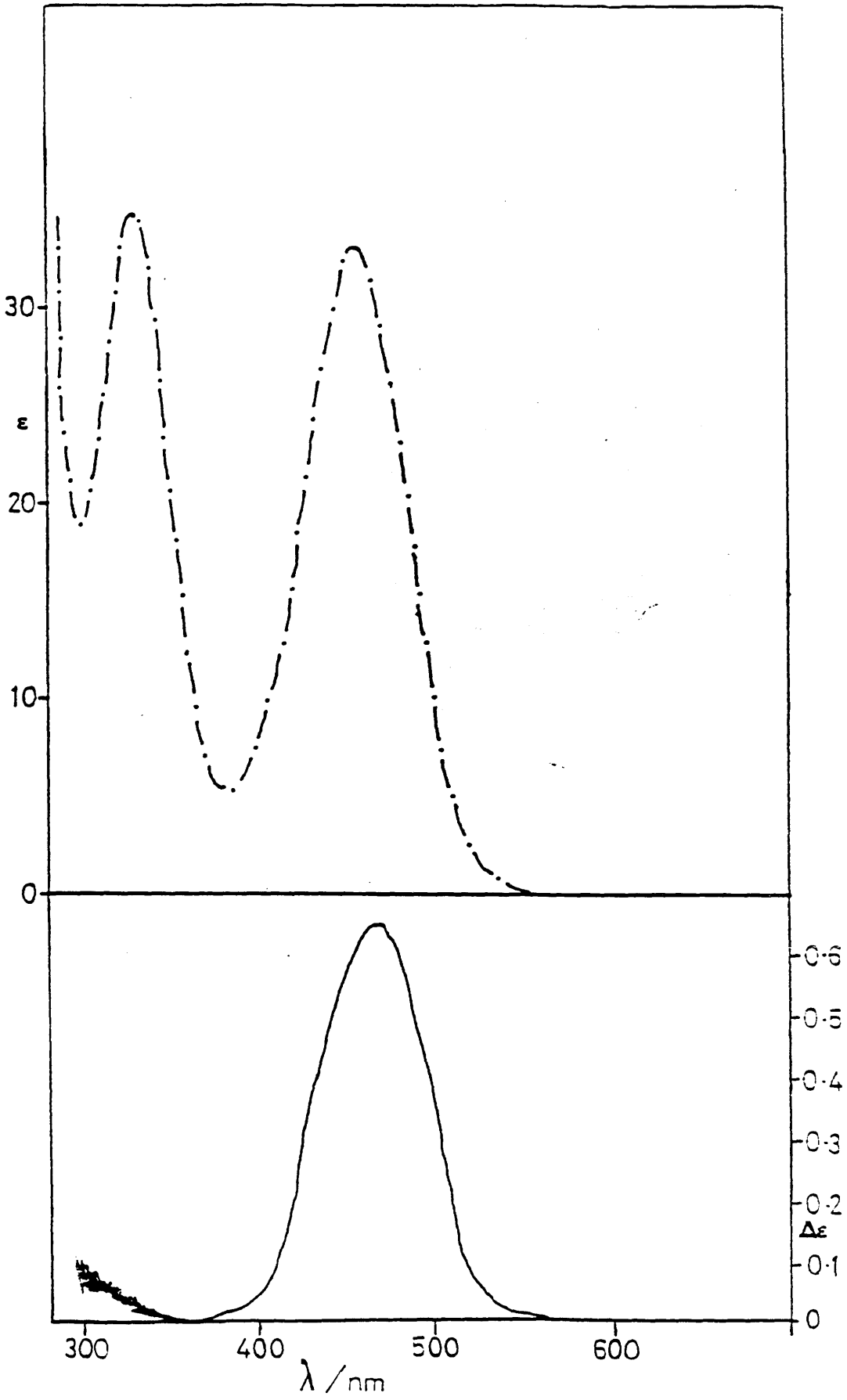

FIGURE 3.2
The absorption (top) and cd (bottom) spectra of microcrystalline $[Co(tacn)_2]Cl_3.5H_2O$.

TABLE 3.1

EXTINCTION COEFFICIENTS IN THE VISIBLE REGION FOR $Co(tacn)_2Cl_3.5H_2O$

λ(nm)	$\Delta\varepsilon_S$	$\Delta\varepsilon_m$	$\Delta\varepsilon_E$	$\Delta\varepsilon_{A_2}$	$\Delta\varepsilon_{T_1}$
286	0	0			
296	0	0			
306	0	0			
316	0	0.005			
326	-0.023	0.009			
336	-0.046	0.011			
346	0.023	0.018			
356	0.069	0.028			
366	0.046	0.037			
376	0	0.051	0	0.153	0.153
386	-0.104	0.074	-0.208	0.430	0.222
396	-0.264	0.094	-0.528	0.810	0.282
406	-0.529	0.161	-1.058	1.541	0.483
416	-0.840	0.299	-1.680	2.577	0.897
426	-1.184	0.409	-2.368	3.595	1.227
436	-1.472	0.547	-2.944	4.585	1.641
446	-2.015	0.628	-4.030	5.914	1.884
456	-2.277	0.646	-4.554	6.492	1.938
466	-2.358	0.612	-4.716	6.552	1.836
476	-2.024	0.501	-4.048	5.551	1.503
486	-1.357	0.359	-2.714	3.791	1.077
496	-0.759	0.232	-1.518	2.214	0.696
506	-0.356	0.129	-0.712	1.099	0.387
516	-0.150	0.074	-0.300	0.522	0.222
526	-0.058	0.051	-0.116	0.269	0.153
536	0	0.037	0	0.111	0.111
546	0	0.025	0	0.075	0.075
556	0	0.013	0	0.039	0.039
566	0	0.005	0	0.015	0.015
576	0	0	0	0	0
586	0	0	0	0	0

Note that A_2 & E do not apply outside the T_1 band

By use of the values for $\Delta\varepsilon$ microcrystalline ($\Delta\varepsilon_m$) and $\Delta\varepsilon$ for the single crystal, $\Delta\varepsilon_s$, it was possible to calculate the extent to which the $A_1 \rightarrow E$ and $A_1 \rightarrow A_2$ transitions contributed to the overall optical activity. The relative order of the energy levels could also be established by reference to the tables.

In the following equations $\Delta\varepsilon_s$ refers to the single crystal sample $\Delta\varepsilon_m$ to the microcrystalline sample, $\Delta\varepsilon(A_2)$ is the differential molar extinction coefficient due to the $A_1 \rightarrow A_2$ transition and $\Delta\varepsilon(E)$ is that due to the $A_1 \rightarrow E$ transition. α is the angle between the highest fold axis of the complex and that of the crystal (zero in the case of $[Co(tacn)_2]Cl_3.5_2O$). It is possible by the following method (devised by Kuroda & Saito (Ref 31)) to decompose the $A_1 \rightarrow T_1$ transition of $CoIIIN_6$ species into its components.

3e) $$\Delta\varepsilon_s = \frac{[(1+\cos^2\alpha)\,\Delta\varepsilon(E_x)]}{4} + \frac{[(1+\cos^2\alpha)\,\Delta\varepsilon(E_y)]}{4} + \frac{[(\sin^2\alpha)\,\Delta\varepsilon(A_2)]}{2}$$

3f) $$\Delta\varepsilon_m = \frac{1}{3}\Delta\varepsilon(E_x) + \frac{1}{3}\Delta\varepsilon(E_y) + \frac{1}{3}\Delta\varepsilon(A_2)$$

For the crystal $Co(tacn)_2Cl_3.5H_2O$ two simplifications may be made. Firstly since the E_x and E_y transitions are degenerate and equivalent $\Delta\varepsilon_{E_x}$ must be equal in magnitude to $\Delta\varepsilon_{E_y}$ and so terms containing these quantities may be combined. Secondly, $\alpha = 0$ so that equation (3e) becomes:

3g) $$\Delta\varepsilon_s = \Delta\varepsilon(E)$$

and equation (3f) becomes

3h) $\Delta\varepsilon_m = \frac{2}{3}\Delta\varepsilon(E) + \frac{1}{3}\Delta\varepsilon(A_2)$

To facilitate calculation of $\Delta\varepsilon(A_2)$ equation (3h) may be rewritten;

3i) $\Delta\varepsilon(A_2) = 3\,\Delta\varepsilon_m - 2\Delta\varepsilon_S$

The above equations (3g) and (3i) represent quantitatively the observation that single crystal spectra involve only the $A_1 \longrightarrow E$ component of the $A_1 \longrightarrow T_1$ transition whereas the spectra of microcrystalline samples include contributions from both $A_1 \longrightarrow A_2$ and $A_1 \longrightarrow E$ components.

In an attempt to obtain solution c.d. spectra of the complex a sample was eluted on a chromatography column with 0.1 molar sodium (+) antimonyl tartrate solution. It was hoped that the optically active tartrate ion might hydrogen bond to the complex and favour one enantiomeric form over the other (Ref 77). In practice the experiment was unsuccessful since the eluted complex did not exhibit circular dichroism in the $d \rightarrow d$ region.

The c.d. and absorption spectra of single crystal and microcrystalline samples are shown in figures 3.1 and 3.2 respectively and tabulated in table 3.1. From the values contained in table 3.1 the magnitudes of $\Delta\varepsilon$ (E), $\Delta\varepsilon$ (A_2) and $\Delta\varepsilon$ (T_1) have been calculated at selected wavelengths by equations (3g) and (3i) and plotted to give figure 3.3.

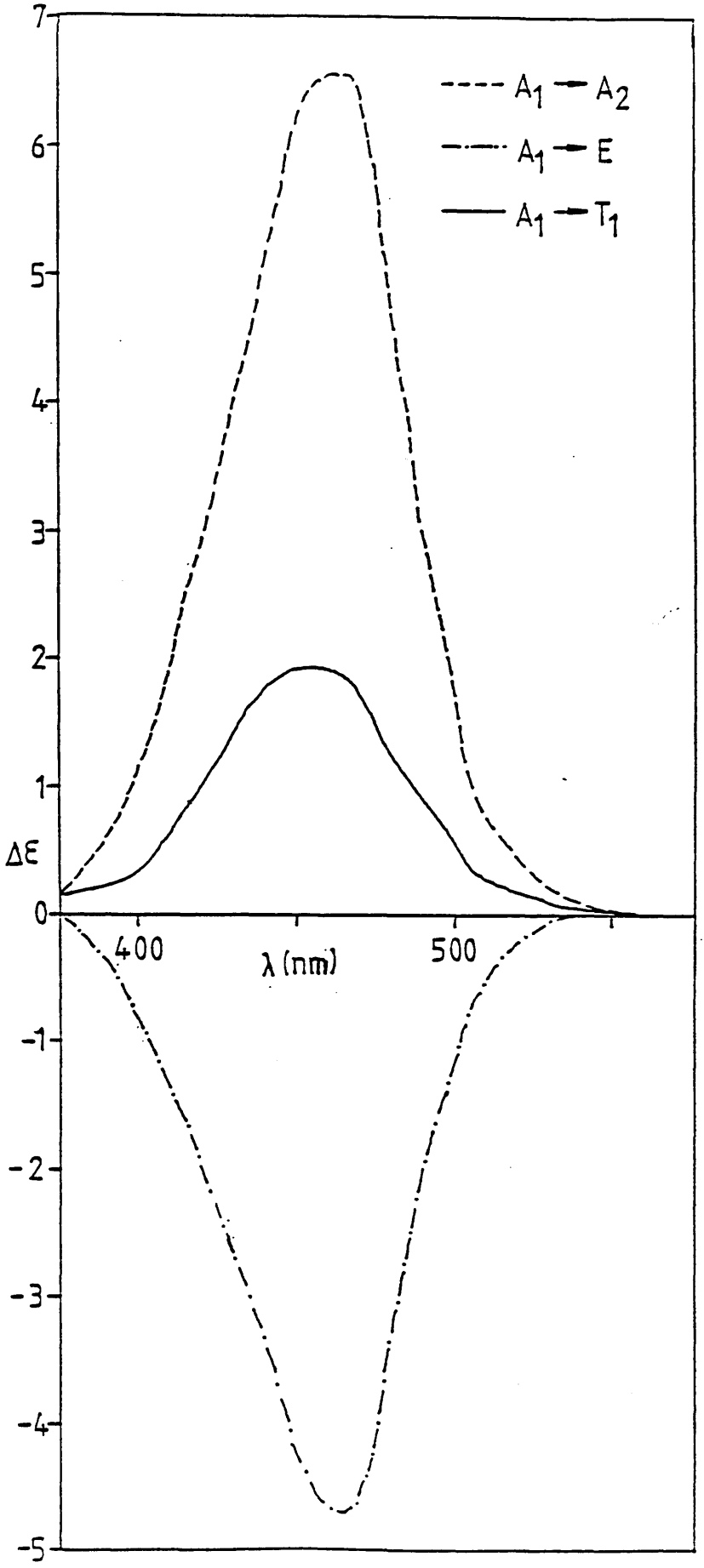

FIGURE 3.3
Measured plots of $\Delta\varepsilon(E)$ and $\Delta\varepsilon(T_1)$ versus wavelength with the resulting calculated plot of $\Delta\varepsilon(A_2)$ versus wavelength.

Using these values it was possible to calculate the rotational strengths, R(E), $R(A_2)$, and $R(T_1)$, of the transitions by means of the equation;

3j) $R = 0.248 \int (\Delta\varepsilon / \nu)\, d\nu$

which may be expressed, approximately as;

3k) $R = 0.248 \dfrac{\Delta\varepsilon_{max}\, \Delta\nu_{1/2}}{\nu_{max}}$ (Debye Bohr Magnetons)

From the calculated spectra values of $\Delta\varepsilon_{max}$, $\Delta\nu_{1/2}$ and ν_{max} were obtained and these appear in table 3.2 along with the resulting values of rotational strength in Debye Bohr Magnetons. It is necessary for purposes of comparison to convert the rotational strengths to c.g.s. units. The values obtained were $R(A_2) = +21.7 \times 10^{-40}$, $R(E) = -14.9 \times 10^{-40}$ and $R(T_1) = 6.9 \times 10^{-40}$ (Note: 1 Debye Bohr Magneton = 9.274×10^{-39} c.g.s. units (Ref 48).

TABLE 3.2

PARAMETERS RELATING TO TRANSITIONS OF $Co(tacn)_2Cl_3.5H_2O$

	$\Delta\varepsilon_{max}$	ν_{max} (Hz)	$\Delta\nu_{1/2}$ (Hz)	R(Γ) DBM	R(Γ) $\times 10^{40}$ c.g.s.
A_2	+6.58	6.50×10^{14}	9.32×10^{13}	+0.235	+21.8
E	-4.72	6.46×10^{14}	8.86×10^{13}	-0.160	-14.8
T_1	+1.94	6.47×10^{14}	10.12×10^{13}	+0.075	+ 7.0

In the region of the higher energy $A_1 \longrightarrow T_2$ transition, which is magnetic dipole forbidden, weak circular dichroism is observed and appears to have both positively and negatively signed components in the single crystal spectrum (Fig 3.1).

3.1.3 Discussion

The two transitions observed in the absorption spectra of the visible region for octahedral Co(III) complexes are labelled $^1A_{1g} \longrightarrow {}^1T_{1g}$ (lower energy) and $^1A_{1g} \longrightarrow {}^1T_{2g}$ (higher energy). In O symmetry the transition may be represented as $^1A_1 \longrightarrow {}^1T_1$ and $^1A_1 \rightarrow {}^1T_2$. These labels both represent transitions from the ground state t_2^6 to an excited state $t_2^5 e$. The $^1A_1 \rightarrow {}^1T_1$ transition represents a triply degenerate excitation of the form; $d_{xy} \longrightarrow d_{x^2-y^2}$, $d_{yz} \rightarrow d_{y^2-z^2}$ or $d_{xz} \longrightarrow d_{x^2-z^2}$. The $^1A_1 \rightarrow {}^1T_2$ label covers the triply degenerate transition set $d_{xy} \longrightarrow d_{z^2}$, $d_{yz} \longrightarrow d_{x^2}$ and $d_{xz} \longrightarrow d_{y^2}$. In the octahedral point group the transition $^1A_{1g} \longrightarrow {}^1T_{1g}$ has symmetry T_{1g} and possesses a zero order magnetic dipole while the transition $^1A_{1g} \longrightarrow {}^1T_{2g}$ has symmetry $^1T_{2g}$ and is magnetic dipole forbidden. Neither transition has a zero order electric dipole: a consequence of being internal transitions within the 3d shell (and thereby breaking the Laporte selection rule; $\Delta l = \pm 1$).

Since $[Co(tacn)_2]^{3+}$ belongs approximately to the point group D_3 the triplet states in octahedral symmetry are no longer degenerate: thus T_1 splits into E and A_2 while T_2 splits into E and A_1. Under the $A_1 \longrightarrow T_1$ (O) band of $[Co(tacn)_2]^{3+}$ lie two transitions, $A_1 \rightarrow A_2$ (D_3) and

$A_1 \rightarrow E(D_3)$ while the T_2 envelope covers $A_1 \rightarrow E$ and $A_1 \rightarrow A_1$ transitions. The $A_1 \rightarrow A_1$ transition possesses no magnetic dipole and is therefore forbidden so that there are three transitions observable in the visible spectra of cobalt(III) species in an approximately D_3 ligand environment.

Light propagated parallel to the C_3 axis of a complex ion of this type has its electric and magnetic vectors rotating perpendicular to its direction of propagation and is therefore capable of exciting only those transitions polarised in the xy plane of the complex (ie $A_1 \rightarrow E$). Similarly, light propagated normal to the C_3 axis excites those transitions with a component in the z-direction (i.e. $A_1 \longrightarrow A_2$). It is known that for a helix, comprising a molecule in a D_n point group, the sense of the helix viewed down the C_n axis is opposite to that of the helices observed when the same molecule is viewed down any one of the nC_2 axes. As a consequence of these two observations the signs of the E and A_2 components, in D_3 symmetry, under any T_n (O) transitions are opposite. The result of the foregoing is that the circular dichroism of a typical Co(III) complex with a D_3 environment (eg $[Co(tacn)_2]^{3+}$) comprises a bisignate couplet to lower energy (460nm) due to $^1A_1 \rightarrow {}^1A_2$ ($^1T_1$) and $^1A_1 \rightarrow {}^1E(^1T_1)$, with a unisignate band to higher energy, $^1A_1 \rightarrow {}^1E(^1T_2)$ (330nm).

The absorption spectra due to $[CoIII(tacn)_2]^{3+}$ in solution (or in the microcrystalline state) comprises two bands, at 456nm and 330nm, corresponding to $^1A_1 \rightarrow {}^1T_1$ (O) and $^1A_1 \longrightarrow {}^1T_2$ (O) respectively. Since the integrated intensity of absorption spectra is proportional to the square of the electric dipole, and since both transitions are electric dipole forbidden, the two bands are of approximately equal intensity. The intensity of circular dichroism spectra, ΔA , on the other hand is proportional to the product of the electric and magnetic dipoles. Since the $^1A_1 \longrightarrow {}^1T_1$ transition is magnetic dipole allowed and the $^1A_1 \longrightarrow {}^1T_2$ transition is magnetic dipole forbidden, the intensity due to the band resulting from the latter is considerably weaker (fig 3.1). In order to gain any intensity the $A_1 \longrightarrow E(T_2)$ transition must borrow magnetic dipole intensity by mixing with a transition of similar symmetry (generally regarded to be $A_1 \rightarrow E(T_1)$). Both of these transitions in the visible region of the spectrum are presumed to derive their electric dipole contributions to intensity by mixing with charge transfer transitions of similar symmetry in the U.V. region.

Plane polarised light may be considered to be the result of in-phase combination of left circularly polarised light and right circularly polarised light. If such light is in contact with a chiral medium one hand of light will be preferentially absorbed so that the emerging light will exhibit rotation of the plane. In this process light is absorbed by a molecule and an electron is promoted to an

excited state which involves a change of dipole and consequently movement of the electron. Since the electron is moving in a chiral field its path must be right or left handed and the ease with which it moves will be determined by the handedness of the incident light quantum. Theoretically an electron displaced along a right handed helical path gives rise to a positive rotational strength. However, it is rarely possible to predict with certainty the path of an electron through a given molecular environment and so empirical procedures are applied in order to ascertain absolute configurations. One such empirical method is that devised by Peacock & Stewart (Ref 41) whereby the sign of the E component of the $^1A_1 \rightarrow {}^1T_1$ transition of Co(III) (or of the $^4A_2 \rightarrow {}^4T_2$ transition of Cr(III) may reliably be related to the smaller of the two angles, viewed down the C_3 axis, between the triangles defined by the upper and lower donor sets.

Using this method for the c.d. spectrum in figure 3.1 a negative E component indicates that the angle ω is positive (i.e. clockwise from above) as shown in figure 1.20.

The results using this method are reliable and are reported to be reproducible by theoretical calculations based on the ligand polarisation correlation model.

It is not possible to use the circular dichroism spectra of species in solution to assign the absolute configuration

unambiguously because of problems in identifying the A_1 and E bands. The observed $^1T_1$ band results from cancellation of the A_2 and E bands (typically 90% cancellation for tris diamine cobalt(III) species and approximately 50% for bis triamine species). Thus, the $A_1 \longrightarrow T_1$ band is very susceptible to change in either the A_2 or E components and therefore assignment of the signs of these transitions is a prerequisite to assignment of the absolute configuration. Early work in this field suggested that the E component was always dominant. However $[Co(Metacn)_2]^{3+}$ and other less exotic complexes proved to be exceptions to this observation. $[Co(tacn)_2]Cl_3.5H_2O$ is also an exception (figure 3.3).

A more reliable method of assigning A_2 and E involved addition, in solution, of a salt such as phosphate or selenite (Ref 42). This has the effect of enhancing the A_2 component by hydrogen bonding to the three axial N - H groups (for example in $[CoIII(diamine)_3]^{3+}$) and thereby increasing the effective elongation of the molecule. This method was inapplicable to the complex $[Co(tacn)_2]^{3+}$ since it required the presence of axial N-H groups which, though a feature of $[Co(diamine)_3]^{3+}$ systems, are absent in $[Co(triamine)_2]^{3+}$ species.

The ability of other species in solution to influence the circular dichroism of metal complexes is well documented (Refs 45 & 46) and illustrates the advantage of microcrystalline samples supported in alkali metal halide

disks over solution samples in that the immediate environment of the complex is identical in the crystal and in the disk. Calculations of relative energies and rotational strengths of the bands are all the more valid as a result of this consistency in the two samples.

The extent to which the circular dichroism of solutions may vary from that of the corresponding crystalline solid is an area which has attracted considerable attention. Woldbye (Ref 78) and Dingle and Ballhausen (Ref 79) believed that while one conformer was present in the crystalline state of chiral complexes (as evidenced by unisignated circular dichroism in the visible region) there were two conformationally related species in solution which gave rise to oppositely signed circular dichroism. This theory was disproved by, among others, Jensen and Galsbol (Ref 80) who doped $[Co(en)_3]^{3+}$ into a crystal of $2[Ir(en)_3]Cl_3.NaCl.6H_2O$ and showed that the spectrum in the solid state with light propagated parallel to the C_3 axis was of opposite sign to that where light was propagated normal to the axis. This showed that the two signs observed at slightly different wavelengths in the circular dichroism solution spectra of $[Co(diamine)_3]^{3+}$ species were due, not to two conformers of one species but, to two separately observable transitions of the same conformer. Unfortunately problems of assessing the concentration of $[Co(en)_3]^{3+}$ in the lattice precluded calculation of the relative intensities of the two transitions. However in addition to offering further confirmation of the existence of two

oppositely signed transitions, the method used in the present work, whereby a randomly oriented sample in a KBr disk allows an orientationally weighted average of the two transitions to be observed, enables calculation of the intensities of the transitions.

No crystal structure data is available to confirm that the enantiomer of $[Co^{III}(tacn)_2]Cl_3 .5H_2O$ with a negative rotational strength due to the $^1A_1 \longrightarrow {}^1E(T_1)$ transition is that with ω positive. However, Dubicki et al (Ref 43) assigned the enantiomer of the above complex as $\delta\delta\delta$ so that where ω is positive, the three chelate rings should be represented by $\lambda\lambda\lambda$. This is in agreement with crystal structure data on the analogous complex $[Co^{III}(R\text{-Metacn})_2]^{3+}$ in which the presence of six λ chelate ring conformations was accompanied by a positive value of ω. The size of the twist angle in the case of the bis-Metacn complex was 7.6° removed from octahedral (i.e. ω = 52.4°) and it is believed that this results from non-bonded interactions between the hydrogens on one macrocycle and those on the other. Evidence for this was offered by Nonoyama et al (Ref 51) who pointed out that for complexes of the type $[Co(R\text{-Metacn})(NH_3)_3]^{3+}$, the maximum differential molar extinction coefficient in solution for the $^1A_1 \rightarrow {}^1T_1$ transition was approximately 20% of that in $[Co(R\text{-Metacn})_2]^{3+}$ (Table 3.3). The inference is that in the absence of a second macrocycle there is insufficient ligand interaction to cause a large (eg 7°) twist and generate intense circular dichroism.

TABLE 3.3

THE $^1A_1 \longrightarrow {}^1T_1$ TRANSITIONS OF VARIOUS $CoIIIN_6$ SPECIES

COMPLEX	$\bar{\nu} / 10^{-3}cm^{-1} (\Delta\varepsilon)$
$[CoIII(R\text{-}Metacn)(NH_3)_3]^{3+}$	21.35 (0.83)
$[CoIII(R\text{-}Metacn)(tacn)]^{3+}$	21.15 (4.02)
$[CoIII(R\text{-}Metacn)_2]^{3+}$	20.9 (4.53)
$[CoIII(tacn)_2]^{3+}$	21.55 (1.94)

It may be significant that $[Co(Metacn)(tacn)]^{3+}$ and $[Co(Metacn)_2]^{3+}$ are reported by Nonoyama to have very similar values of $\Delta\varepsilon_{max_{A_1 \rightarrow T_1}}$: while for $[Co(tacn)_2]^{3+}$ this value is halved. It could be the case that the methyl group on a Metacn ring (where present) not only fixes the complex in one enantiomeric form but also directly affects the circular dichroism. This seems unlikely because of the distance between the methyl group and the chromophore and it is more likely that the differences observed between the Metacn and tacn forms are a manifestation of the extreme sensitivity of the $A_1 \longrightarrow T_1$ band to small changes in its A_2 and E polarised components. Table 3.3 lists the values of $\Delta\varepsilon_{max}$ of the electronic transitions of various complexes as reported by Nonoyama and Sakai (Ref 51). The value for $[Co(tacn)_2]^{3+}$ is included for comparison although caution is advised as it is the only microcrystalline sample represented; the others being in solution.

Two parameters which may yield information about the optical activity and structure of transition metal complexes are the absolute magnitudes of the rotational strengths $R(A_2)$ and R(E): and the relative energies of the band maxima for these two transitions.

In a review of the c.d. spectra of transition metal complexes Peacock and Stewart (Ref 41) gathered information on several $Co(III)N_6$ species for which decomposition into A_2 and E components had been conducted. Table 3.4 shows these values and is incremented by the values obtained in the present work for $[Co(tacn)_2]^{3+}$. On comparison of $[CoIII(tacn)_2]^{3+}$ with related complexes certain features stand out. The value of R(E) is very similar to that for the analogous species $[Co(R\text{-}Metacn)_2]^{3+}$, (-14.9 cf - 14.8) although the values of $R(A_2)$ are + 21.7 in the case of the tacn complex and + 29.7 in the case of the R-Metacn complex. It may be significant that the R(E) values, obtained from the single crystal spectra for both species are in good agreement whereas the $R(A_2)$ values, from the microcrystalline state in the case of $[Co(tacn)_2]^{3+}$ and from the solution state in $[Co(R\text{-}Metacn)_2]^{3+}$ differ markedly. This observation leads to the conclusion, supported by preliminary crystal structure evidence (Refs 31 & 43), that these two species are structurally very similar in the crystalline state. This being the case it is the value of $R(A_2)$ which is anomalously large suggesting effective elongation of the chiral $[Co(R\text{-}Metacn)_2]^{3+}$ chromophore in solution by hydrogen

bonding, ion association or some other mechanism which attracts bulk to the axial areas of the molecule.

It can be seen from Table 3.4 that in the cases where 5 membered chelate rings run oblique to, or parallel to, the C_3 axis, $R(A_2)<R(E)$, for 6 membered chelate rings $R(A_2) \simeq R(E)$ and for 7 membered rings $R(A_2)>R(E)$. Since the bis triamines have no chelate rings connecting the top and bottom donor sets it is not surprising that $R(A_2) >> R(E)$.

TABLE 3.4
THE DECOMPOSED ROTATIONAL STRENGTHS OF VARIOUS $CoIIIN_6$ SPECIES

Complex	R(E) $\times 10^{40}$ c.g.s.u.	$R(A_2)$ $\times 10^{40}$ c.g.s.u.	$R(T_1)$ $\times 10^{40}$ c.g.s.u.	ω°	α°	Energy Order
$\Lambda[Co(en)_3]^{3+}$	+62.9	-58.6	+ 4.3	-54.9	85.4	$E < A_2$
$\Lambda[Co(S\text{-}pn)_3]^{3+}$	+38.1	-36.6	+ 1.5	-55	84.2	$E < A_2$
$\Lambda[Co(S,S\text{-}chxn)_3]^{3+}$	+56.5	-51.1	+ 5.4	-55	86.7	$E < A_2$
$\Lambda[Co(S,S\text{-}cptn)_3]^{3+}$	+57.3	-54.5	+ 2.8	-54.5	86.7	$E < A_2$
$\Lambda[Co(S,S\text{-}ptn)_3]^{3+}$	+12.5	-14.5	- 2.0	-57	89.1	$E < A_2$
$\Lambda[Co(tmd)_3]^{3+}$	+31.1	-38.7	- 7.6	-55.7	89.2	$E < A_2$
$\Lambda[Co(tn)_3]^{3+}$	-10.5	+10.2	- 0.3	+53	91	$E > A_2$
$Co(2R\text{-}Metacn)_2]^{3+}$	-14.8	+29.7	+14.8	+52.4		$E \simeq A_2$
$Co(tacn_{\lambda\lambda\lambda})_2]^{3+}$	-14.8	+21.8	+ 7.0			$E \simeq A_2$

The second parameter which is affected by elongation is the relative energies of the band maxima of the E and A_2 transitions. It has been observed (Ref 41) that in squat molecules E is the lower energy state while in elongated molecules E lies to higher energy. This is in accordance with the necessary degeneracy of A_2 and E in octahedral symmetry. It was noted (Ref 48) that for $[Co(Metacn)_2]^{3+}$ a situation approaching degeneracy was observed. It has now been shown that in the bis tacn analogue the same situation applies since λ_{max} (A_2) occurs at 464 nm while λ_{max} (E) occurs at 462nm. This is surprising since $[Co(R\text{-}Metacn)_2]^{3+}$ is known to be elongated (Ref 38) and $[Co(tacn)_2]^{3+}$ would be expected to be similar. It must be concluded from these two examples that, for the purposes of predicting structure from the relative energies of ^1E (T_1) and $^1A_2(T_1)$, the cobalt bis triamines may not be regarded as analogues of the cobalt tris diamines. Inspection of crystal structure data for $[Co(R\text{-}Metacn)_2]I_3.5H_2O$ reveals a possible reason for this observation. If the $[Co(diamine)_3]^{3+}$ species are assumed to be standard then the $[Co(triamine)_2]^{3+}$ species appear to be more elongated than would be inferred from their c.d. spectra. However if the electron density accompanying the iodide ions were to be included in the chromophore then the elongation is counterbalanced by the equatorial halides. Such close proximity of halides in the equatorial plane of $Co(diamine)_3\ X_3.nH_2O$ is precluded by the presence of chelate rings.

3.1.4 Conclusions

From the values obtained for $R(E(T_1))$ for the species $[Co(tacn)_2]^{3+}$ and $[Co(Metacn)_2]^{3+}$ it would appear that in these two species the chromophore experiences a similar environment. The disparity of the two values observed for $R(A_2(T_1))$ may be rationalised as resulting from the fact that $[Co(tacn)_2]^{3+}$ was investigated in the crystalline state whereas $[Co(Metacn)_2]^{3+}$ was investigated in solution. It would appear that the state of the complex ion is crucial to the magnitude of the rotational strengths of its transitions and consequently calculations may only be expected to yield meaningful results when both axial and randomly oriented spectra are measured in the crystalline state. A trend has been noted whereby compressed $Co(III)(N_6)$ species (eg$[Co(en)_3]^{3+}$) exhibit splitting of the $^1A_1 \longrightarrow {}^1T_1$ energy level such that the E component lies to lower energy than the A_2 component. It is expected that in elongated species the reverse energy ordering would obtain. However, it appears from this work, and from previous work, that for $[Co(triamine)_2]^{3+}$ species the energy levels are close to degeneracy. This phenomenon is explained by the presence of a pseudo octahedral electronic field comprising axial organic groups and equatorial halide ions.

3.2 $Cr(tacn)_2Br_3.5H_2O$

3.2.1 Introduction

3.2.1.1 Preparation

The method first adopted for the preparation of crystals incorporating the $[Cr(tacn)_2]^{3+}$ species was that described by Wieghardt et al (Ref 33). However it was found that, on several occasions, the reaction yielded a green suspension which could not be converted to $[Cr(tacn)_2]^{3+}$ and was presumed to be a mixture of polymeric hydroxo-bridged chromium complexes. The green suspension was optically inactive in the cases where tacn was used although on a number of occasions attempts at generating $[Cr(R\text{-}Metacn)_2]^{3+}$ resulted in a similar suspension which showed circular dichroism in the visible region. The most probable explanation for the difficulty in preparing the title complex lies in the method of formation of the free ligand which, of necessity, differed from the original authors' preparation for reasons of scale. The free ligand in the present work was obtained by reaction of tacn. 3HBr with an excess over three equivalents of potassium hydroxide in the minimum quantity of water. Care was taken to avoid large temperature increases, as a result of the neutralisation, and the solution was allowed to cool completely before further treatment . Extraction of the amine was achieved using an organic layer consisting of toluene, or occasionally benzene. After five extractions the aromatic fractions were combined and the solvent removed slowly

under vacuum in order to avoid exposing the free amine to atmospheric oxygen. The resulting white solid was dissolved in ethanol and the solution was used in the Wieghardt preparative route (Ref 33).

In order to overcome the problems of reproducibility with this route a second preparative method was developed which proved successful for small scale reactions. In aqueous solution a known quantity of tacn.3HBr was neutralised to approximately pH 7 using KOH. The resulting solution containing both free amine and KBr was then added to a volume of DMSO which was raised to 150°C and maintained at that temperature until all of the water and 10% of the DMSO had evaporated. This solution was combined with a solution of $CrCl_3$ in DMSO at 150°C and the resulting solution was raised to 170°C and maintained for one hour at that temperature after which time a yellow crystalline solid was observed to have been deposited from the red solution. The precipitate after three recrystallisations from 10% hydrobromic acid analysed as $Cr(tacn)_2Br_3.5H_2O$ and was identical in all respects to samples obtained by the published method.

3.2.1.2 Crystal Growth

Having obtained small crystals the growth of larger hexagonal crystals was achieved by allowing solutions, dropped onto microscope slides, to crystallise. The best crystals were selected and used to seed solutions formed by dissolution of small or imperfect crystals. Small, well

formed, crystals were used to seed the growth of the various crystal types required (Fig 3.4); (i) large thin plates with a well developed hexagonal face perpendicular to the crystal c-axis, (ii) thick plates with a well developed hexagonal face perpendicular to the crystal c-axis and (iii) crystals with a face developed parallel to the crystal c-axis. Type (i) was obtained easily while perfect examples of types (ii) and (iii) proved difficult to produce.

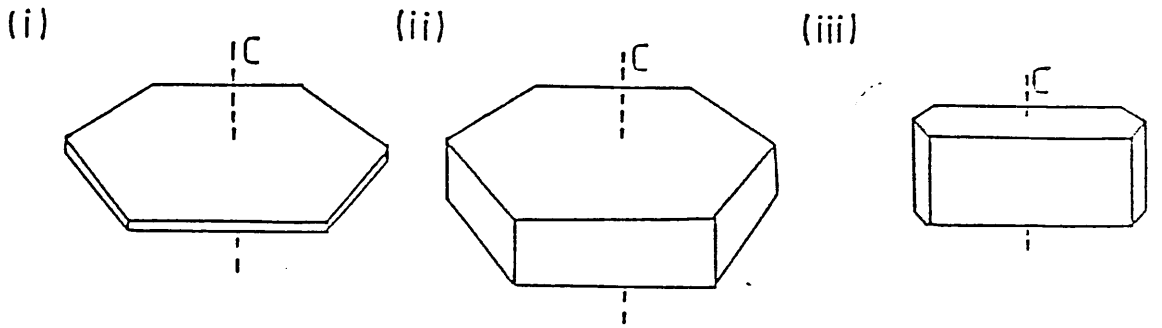

FIGURE 3.4
The three crystal types used in the spectroscopic investigation of $[Cr(tacn)_2]Br_3.5H_2O$.

The crystals obtained from solutions of $Cr(tacn)_2Br_3.5H_2O$ were typically hexagonal prisms which were found, by rotation on the stage of a polarising microscope, to be optically isotropic perpendicular to the crystal c-axis: indicating that they were uniaxial. Examination under 354nm U.V. radiation revealed a red luminescence. Unlike $[Cr(diamine)_3]^{3+}$ analogues the crystals of $[Cr(tacn)_2]Br_3.5H_2O$ showed no tendency to decompose when exposed to ambient sunlight and artificial light over a

period of months. This reinforces the claim of Ditze and Wasgestian (Ref 81) that the $[Cr(tacn)_2]^{3+}$ species is considerably more stable to both photolysis and thermal decomposition than its tris diamine analogues. In these diamine species a red coloration, due to decomposition products, develops on exposure to light. One change which was noted in the bis tacn species was that over a period of months dehydration at the surface caused the normally transparent yellow crystals to become opaque and flakey.

3.2.1.3 Molecular Symmetry

Molecules of $[Cr(tacn)_2]^{3+}$ are presumed to be similar to the cobalt(III) analogue both in sandwich structure and in trigonal symmetry. The main difference was expected to lie in the extent of trigonal twisting which is limited by the degree of ligand field stabilisation. Thus chromium(III) is expected to be more distorted as a consequence of having three electrons in the t_{2g} (O_h) orbitals while cobalt(III) is stabilised by the presence of six d-electrons in the t_{2g} (O_h) orbitals.

3.2.1.4 Spectra

The spectra of Cr(III) species in the visible region are more complicated and consequently richer in information than those of corresponding Co(III) species. The reason for this is the presence of sharp bands arising out of transitions from the quartet ground state to doublet excited states. The full visible region energy level diagram is shown in figure 3.5. This figure also shows the

splitting which results from a decrease in symmetry on going from O_h to D_3 symmetry. The two spin allowed bands observed in chromium(III) spectra are due to the transitions: $^4A_{2g} \longrightarrow {}^4T_{2g}$ (O_h) at lower energy and $^4A_{2g} \longrightarrow {}^4T_{1g}$ (O_h) at higher energy. In D_3 symmetry the transitions become: $^4A_2 \rightarrow {}^4E(T_2)$, $^4A_2 \rightarrow {}^4A_1(T_2)$, $^4A_2 \rightarrow {}^4E$ (T_1) and $^4A_2 \rightarrow {}^4A_2(T_1)$. The symmetries associated with these transitions are E, A_2, E and A_1 respectively (the last of these is not observed). As a consequence of O_h parentage the bands resulting from $^4A_{2g} \longrightarrow {}^4T_{1g}$ are magnetic dipole forbidden, having transitional symmetry T_{2g}, while the other spin allowed band, having a transition of symmetry T_{1g} possesses a zero order magnetic dipole moment. All of the transitions in figure 3.5 are electric dipole forbidden as a result of being internal transitions within the 3d shell of the metal ion.

The three spin forbidden transitions in O_h symmetry, i.e. those to doublet spin states, appear as low intensity sharp lines on absorption spectra. The high energy $^4A_{2g} \longrightarrow {}^2T_{2g}$ transition may be observed as a shoulder on the $^4A_{2g} \longrightarrow {}^4T_{2g}$ band and it is consequently difficult to obtain unambiguous information about it. The two lower energy transitions $^4A_{2g} \longrightarrow {}^2T_{1g}$ and $^4A_{2g} \longrightarrow {}^2E_g$ represent intra-configurational transitions involving changes of spin state within the t_{2g} energy level. Being removed in energy from the broad spin allowed bands these bands are open to spectroscopic analysis and have attracted considerable interest in complexes such as $[Cr(en_3]^{3+}$ (Refs 82, 83 & 84). It is

believed that these spin forbidden transitions borrow both rotational strength and dipole strength from the $^4A_2 \rightarrow {}^4T_2$ transition. The transitions may be observed in luminescence (phosphorescence) as well as by absorption spectroscopy.

As with cobalt(III) the anisotropy of the chromophore, and of the crystal, results in different spectra being obtained depending on the direction of propagation of light and the orientation of the chromophore.

Spectra measured with unpolarised light incident on the hexagonal crystal face (the (001) face) are referred to as α or axial spectra. Two other types of absorption spectra may be obtained, designated π and σ . Both involve propagation of plane polarised light incident normal to the (100) crystal face. In the σ case the plane of the polarised light is parallel to the crystal c-axis while in the π case it is perpendicular. The irradiation conditions for the three spectral types are shown in figure 3.6.

3.2.2 Spin Allowed Transitions

3.2.2.1 Solution Spectra

A single crystal of $Cr(tacn)_2Br_3.5H_2O$ was dissolved to give an aqueous solution which was found to be devoid of circular dichroism showing that, as in the case of $[Co(tacn)_2]^{3+}$ species, dissolution is accompanied by racemisation. It is believed that the racemisation process

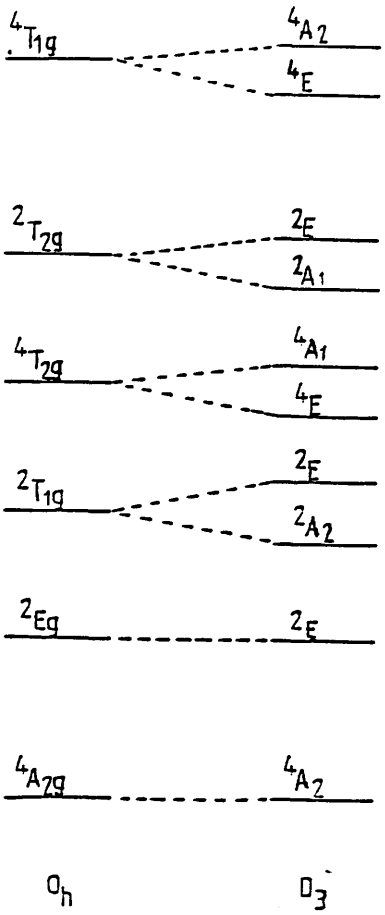

FIGURE 3.5
An energy level diagram for Cr(III) species in octahedral and D_3 environments. (Not to scale).

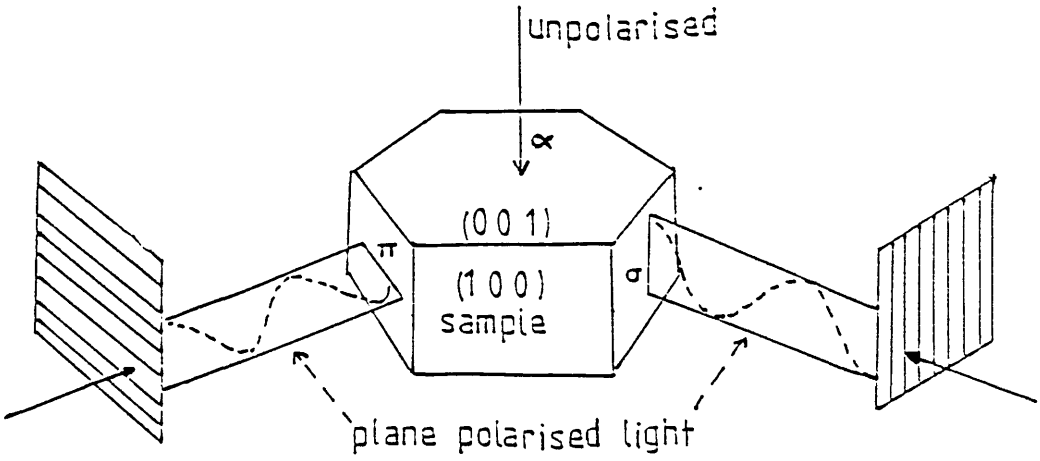

FIGURE 3.6
Directions of propagation and polarisation used to obtain α, σ and π absorption spectra.

involves chelate ring flipping since chromium(III) complexes are generally regarded to be non-labile species. The absorption spectrum of the racemised solution is shown in figure 3.7. In this spectrum the two main bands are due to the transitions $^4A_2 \rightarrow {}^4T_2$ at lower energy, and $^4A_2 \rightarrow {}^4T_1$ at higher energy. A shoulder may be discerned on the lower energy band which has been assigned to the spin forbidden $^4A_2 \rightarrow {}^2T_{2g}$ transition. The solution spectrum of $[Cr(tacn)_2]^{3+}$ was known prior to this work (Refs 33 & 81). However it was remeasured to confirm the identity of the sample and yielded previously unreported information regarding the position of the highest energy spin forbidden transition. The values obtained for the wavelengths of the two main bands were in excellent agreement with those obtained by earlier workers [339, 439; cf 340, 439 (Ref 33) and 342, 439 (Ref 81)]. The molar extinction coefficient for the lower energy band is also in good agreement [88 l $mol^{-1} cm^{-1}$ cf 88 (Ref 33) & 89 (Ref 81)]: although the higher energy band was exaggerated [83 l $mol^{-1} cm^{-1}$ cf 64 (Ref 33) and 64 (Ref 81)], apparently because of overlap with the charge transfer band at higher energy.

3.2.2.2 Solid State Spectra

As a result of the optical inactivity of solvated $[Cr(tacn)_2]^{3+}$ the remainder of the work carried out on this species involved crystalline samples. Figure 3.8 shows the axial single crystal absorption and c.d. spectra obtained using a sample of type (i) in figure 3.4 with light propagated in the $\propto$ direction as defined in figure 3.6. The

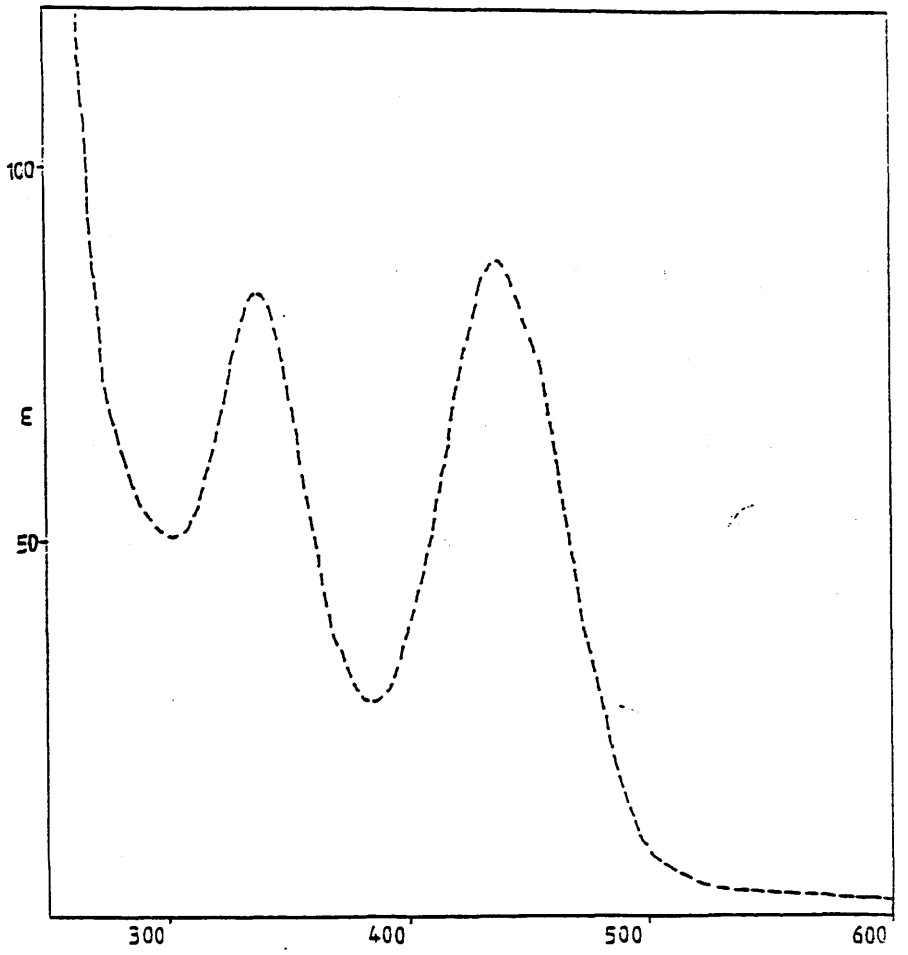

FIGURE 3.7
The aqueous solution absorption spectrum of $[Cr(tacn)_2]^{3+}$.

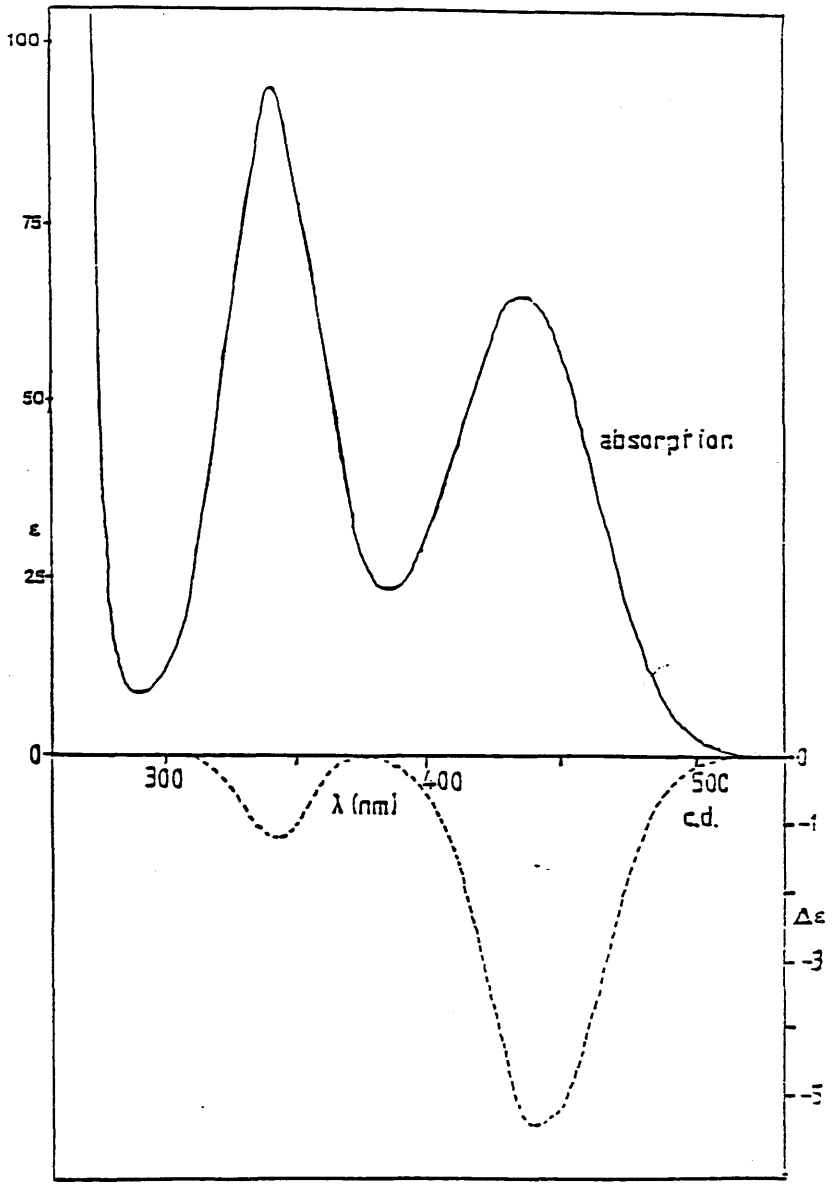

FIGURE 3.8
Axial, absorption and circular dichroism spectra in the visible (spin allowed) region of a single crystal of $[Cr(tacn)_2]Br_3.5H_2O$.

spectra were recorded at room temperature and the wavelengths, extinction coefficients and differential extinction coefficients are listed in Table 3.5 along with derived values of g_{abs} (the Kuhn dissymmetry factor) and R (the rotational strength). (Obtained by use of equation 3k).

Table 3.5

PARAMETERS FROM THE SINGLE CRYSTAL SPECTRA OF $Cr(tacn)_2 Br_3 .5H_2O$

Transition	λ_{max}(abs)	ε_{max}	λ_{max} c.d.	$\Delta\varepsilon_{max}$	g_{max}	R(E)
	nm	l $mol^{-1}cm^{-1}$	nm	l $mol^{-1}cm^{-1}$		$x10^{40}$ cgsu
E (T_1)	435	67	439	5.43	-0.081	-19.9
E (T_2)	339	94	340	1.13	-0.012	-3.8

3.2.3 Spin Forbidden Transitions

In the spin-forbidden region of the spectra of $Cr(tacn)_2 Br_3 .5H_2O$ the bands were, as expected, both sharper and weaker than those arising from spin-allowed transitions. Consequently it was necessary to measure the spectra using a thick crystal of type (ii) in figure 3.4. The molar extinction coefficients were calculated in the same way as those of $Co(tacn)_2 Cl_3 .5H_2O$ by measuring the surface area of a crystal of known weight in order to calculate the (path length x concentration) factor and so to compute ε from absorbance values and $\Delta\varepsilon$ from differential absorbance values.

3.2.3.1 Axial Absorption And c.d. Spectra

Figure 3.9a shows the room temperature axial electronic absorbance spectrum of a single crystal of $Cr(tacn)_2Br_3.5H_2O$. The bands at 682 and 679nm have been assigned to the $^4A_2 \rightarrow {}^2E$ transition which gives rise to two bands because of the presence of two distinct species in the crystal with similar spectroscopic characteristics.

A similar phenomenon has been reported for $[Cr(en)_3]^{3+}$ (Ref 85). The band at 665nm has been tentatively assigned to the $^4A_2 \rightarrow {}^2T_1$ transition. No assignment is made, at this stage, to the remaining band at 673nm. Figure 3.9b shows the circular dichroism due to the ^2E transitions. No optical activity was observed under the band assigned to $^4A_2 \rightarrow {}^2T_1$ in absorbance although the small positive feature at 673nm in the c.d. spectrum may be attributable to the unassigned absorption band at that wavelength. The wavelengths and intensities of the bands are listed in table 3.6. The poor signal to noise ratio in the c.d. spectrum is a consequence of the low absorbance of the sample and was reduced to the level in figure 3.9b by recording the spectrum over a period of 25 minutes (compared to less than 1 minute for spin allowed transitions).

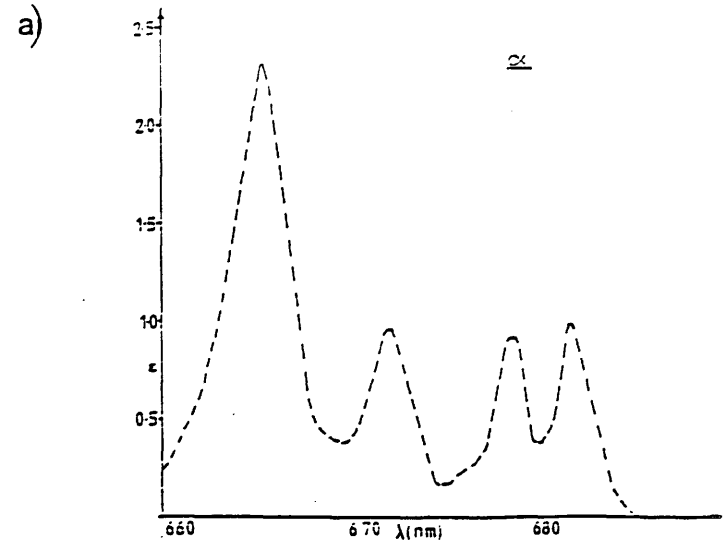

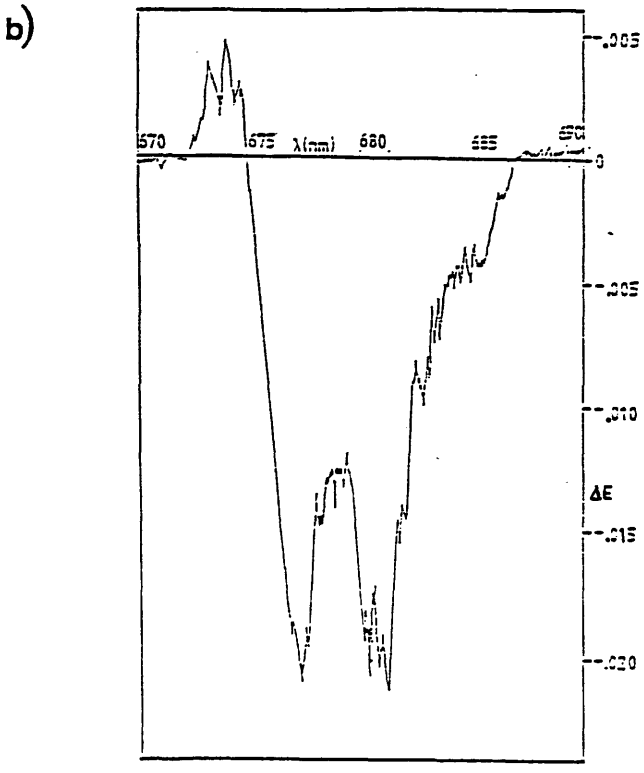

FIGURE 3.9
Spin forbidden region:
a) The absorption spectrum of $[Cr(tacn)_2]Br_3.5H_2O$ with light propagated axially through the crystal
b) The circular dichroism spectrum of the complex with axially propagated light.

TABLE 3.6

THE ABSORPTION SPECTRA OF

$Cr(tacn)_2Br_3.5H_2O$ IN THE SPIN-FORBIDDEN REGION

BAND	λmax abs nm	ε max l mol^{-1} cm^{-1}	λmax c.d nm	Δε max l mol^{-1} cm^{-1}	g_{abs}
$^4A_2 \rightarrow {}^2E$	682	1.00	681	-0.021	-0.021
	679	0.92	677	-0.020	-0.022
?	673	0.96	673	+0.005	+0.005
$^4A_2 \rightarrow {}^2T_1$	665	2.31	—	—	—

3.2.3.2 σ And π Spectra

Additional information regarding transitions in the spin forbidden region in absorption may be obtained by the use of plane polarised light to generate σ and π polarised spectra as shown in figure 3.6. In order to obtain such spectra it was first necessary to grow a crystal of the atypical type (iii) in figure 3.4 and to mount it such that the orientation of the c-crystal axis was known. Three spectra were recorded at 80K on this single crystal and are shown in figure 3.10a, b and c. Figure 3.10a is the σ polarised spectrum in which the plane of polarisation of the light was parallel to the crystal c-axis, figure 3.10b is the π polarised spectrum in which the plane polarised light was perpendicular to the c-axis and figure 3.10c resulted from irradiation of the crystal with unpolarised light incident, as in the previous two cases, on the 100 crystal face. The bands observed may be correlated to those observed in the axial spectra and assigned accordingly. The parameters from figures 3.10 a, b and c are detailed in table 3.7.

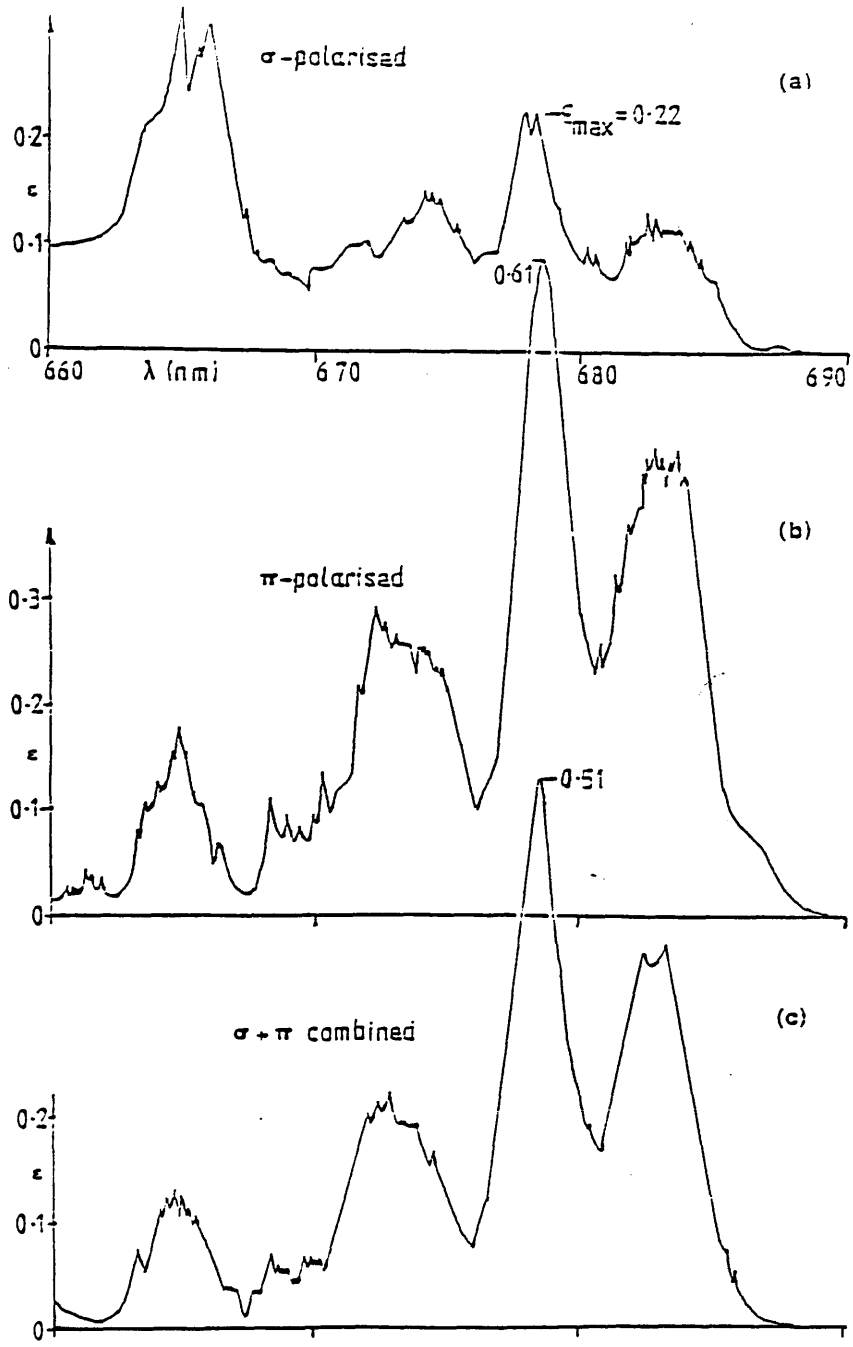

FIGURE 3.10
π, σ and unpolarised absorption spectra in the $^4A_2 \rightarrow {}^2E$ spectral region of a single crystal of $[Cr(tacn)_2]Br_3.5H_2O$.

TABLE 3.7

THE POLARISED ABSORPTION SPECTRA OF $Cr(tacn)_2Br_3.5H_2O$ IN THE SPIN FORBIDDEN REGION

BAND	σ		π		UNPOLARISED	
	ε	λ	ε	λ	ε	λ
$^4A_2 \rightarrow {}^2E$ } two	0.14	683	0.44	683	0.36	683
} species	0.22	678	0.61	679	0.51	678
?	0.15	674	0.29	674	0.22	674
$^4A_2 \rightarrow {}^2T_1$	0.32	665	0.18	665	0.13	665

It was not possible to record circular dichroism spectra corresponding to the absorption spectra in figure 3.10 since light propagated perpendicular to the c-axis of any uniaxial crystal is depolarised.

3.2.3.3 Axial Luminescence Spectra

One of the attractive features of the spin forbidden bands of $Cr(tacn)_2Br_3.5H_2O$ was the accessibility of the bands for investigations, not only in absorption ($^4A_2 \rightarrow {}^2T_1$ and $^4A_2 \rightarrow {}^2E$), but also in the case of the latter transition, in luminescence as $^2E \longrightarrow {}^4A_2$. Investigation of luminescence spectra affords information regarding excited states of molecules which is complementary to the information on the ground state obtained from absorption measurements. In the luminescence spectra of $Cr(tacn)_2Br_3.5H_2O$ discussed below the crystals were oriented such that the laser beam was parallel to the crystal c-axis so that the resulting spectra correspond to the axial absorption and c.d. spectra. At room temperature thermal population of vibronic hot-bands gives rise to broad, featureless luminescence spectra so that it was necessary to cool the sample in

order to observe structure. Cooling to 10K was achieved by means of a Displex closed cycle helium refrigerator comprising a cooling circuit, an optical cell and a thermocouple attachment (to enable monitoring of the cell temperature). The circularly polarised luminescence spectra were also run at low temperature and, indeed, all of the spectra in figures 3.11, 3.12, 3.13 and 3.14 relate to the same crystal so that correlation of bands may be made with certainty. Although the values of I and ΔI quoted are arbitrary, the use of one crystal allows intercorrelations between the various spectra which in turn allows meaningful conclusions to be drawn from changes in intensity with temperature. Values for the emission dissymmetry factor g_{em} (equation 3l) are, unlike the intensity values, absolute and comparable with values from other species. The values of g_{em} were obtained after calibration of spectra against the circular depolarisation ratio measured for the $\nu_1(A_1)$ Raman band of CCl_4.

The relative intensities of the major bands observable on cooling $Cr(tacn)_2Br_3.5H_2O$ from room temperature to 10K have been extracted from figures 3.11, a, b, c, d, e & f, 3.12a and 3.13a. They appear in table 3.8 which also charts the changes in wavelength of the emission bands (origin bands only).

3l) $$g_{em} = \frac{2(I_l - I_r)}{(I_l + I_r)}$$

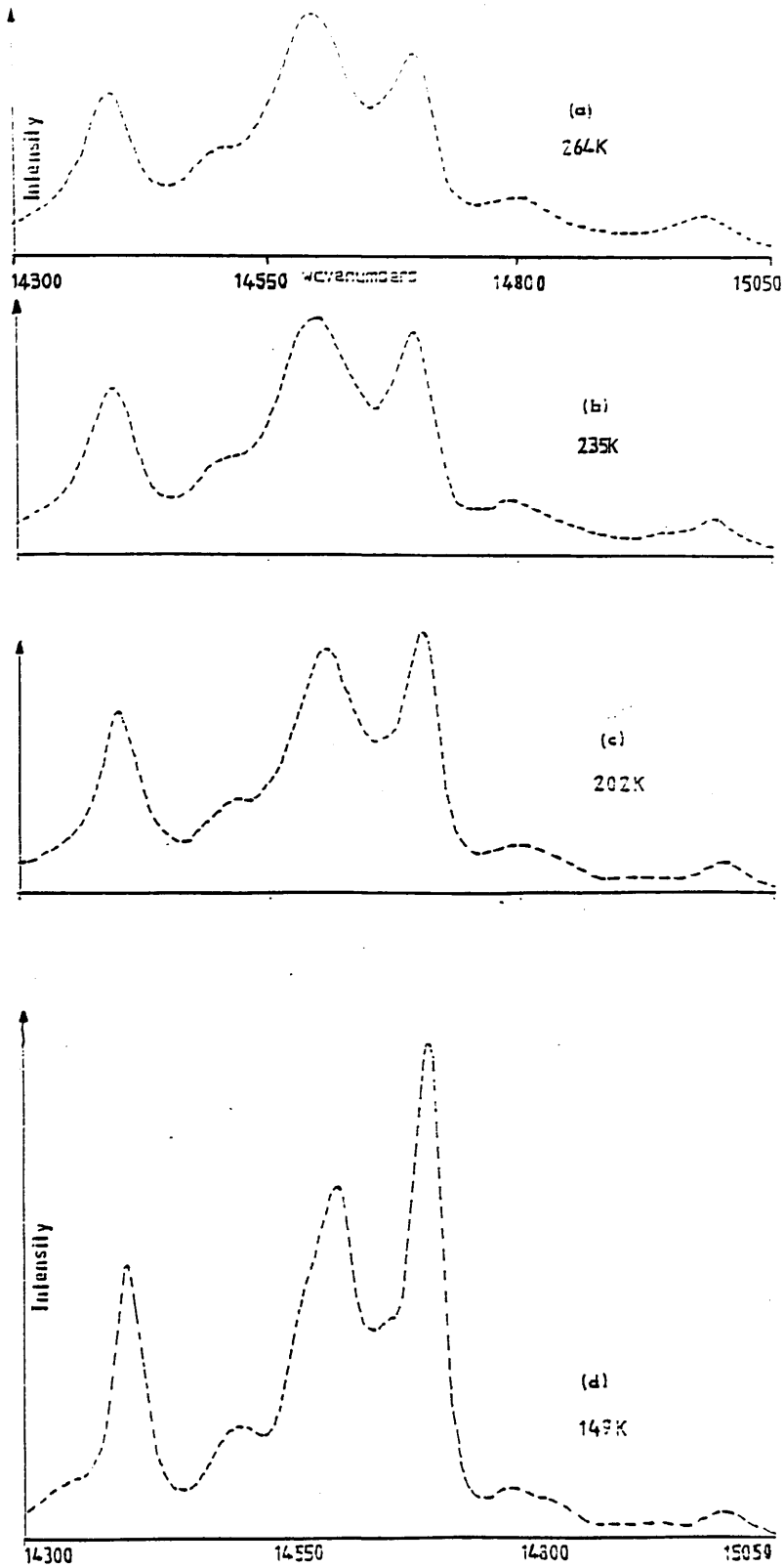

FIGURE 3.11
The axial luminescence spectra of $[Cr(tacn)_2]Br_3.5H_2O$ at a) 264K,b) 235K,c) 202K,d) 149K,e) 86K & f) 63.5K.

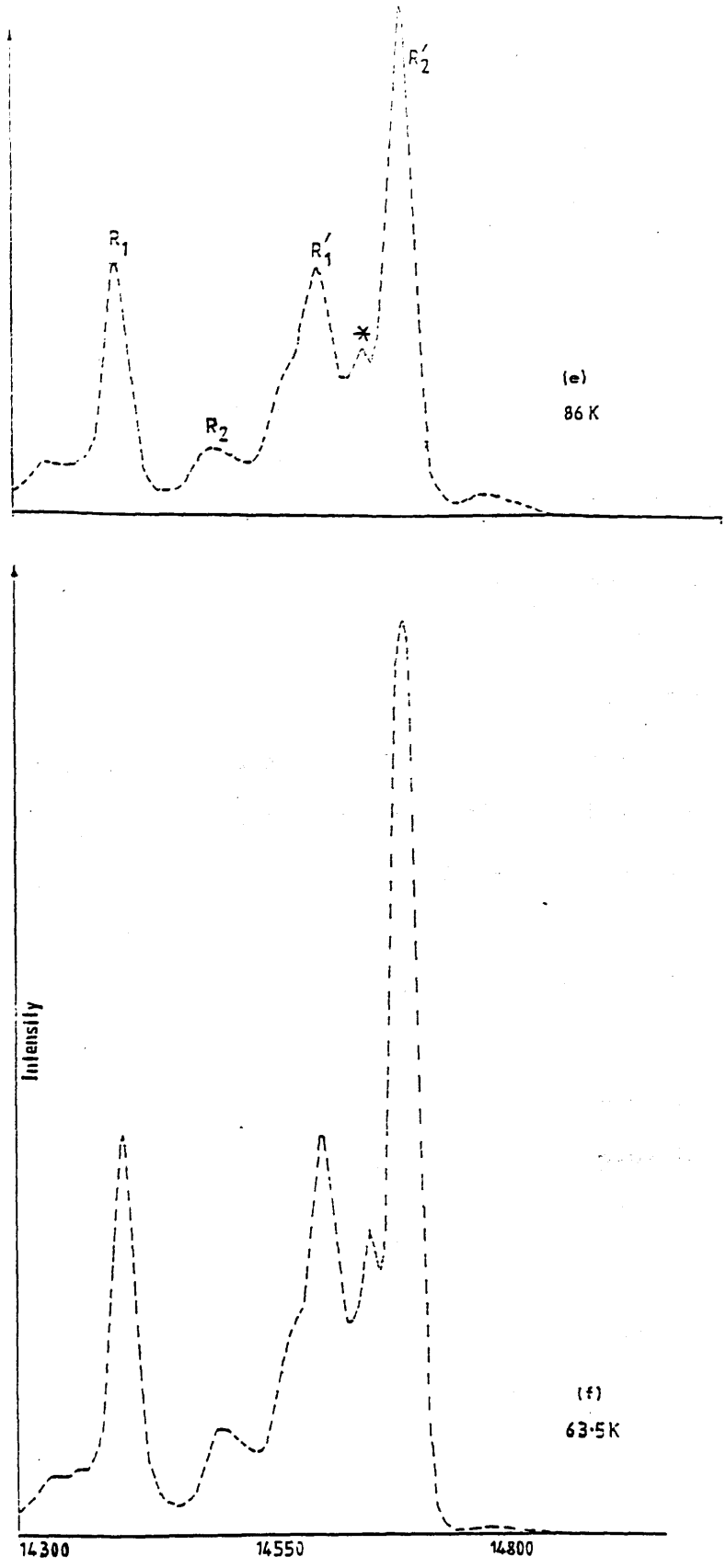

FIGURE 3.11 (Continued)

TABLE 3.8
THE VARIATION OF LUMINESCENCE WITH TEMPERATURE FOR $Cr(tacn)_2Br_3.5H_2O$

	R_2'		*		R_1'		R_2		R_1	
	λ	I	λ	I	λ	I	λ	I	λ	I
Room Temp.	681	80	-	-	685	109				
264K	681	96	-	-	685	113	689	52	695	79
235K	680	106	-	-	685	113	689	47	695	79
202K	680	125	-	sh	684	116	689	47	694	85
149K	680	238	682	sh	684	164	689	52	694	133
86K	680	256	682	sh	684	124	689	31	694	125
63K	680	230	682	78(sh)	684	101	689	27	694	101
10K	680	54	682	208	684	56				

In addition to the origin bands several hot-bands were observed and were identified by the fall-off in their intensities at low temperatures. The 86K spectrum gives the clearest picture of the luminescence and in particular of the thermally populated transitions and so the spectrum at this temperature is listed below with the wavenumbers followed (in brackets) by the relative intensities of all the discernible bands between 15050cm^{-1} and 14050cm^{-1}:

14994(2), 14796(9), 14708(256), 14666(sh),
14619(124), 14588(sh), 14508(31), 14404(125)
14327(22), 14246(8), 14179(16), 14096(26)

The form of the luminescence spectrum changes dramatically on approach to absolute zero: however the bands observed in figures 3.12a) and b) correlate directly with those obtained on cooling. Figure 3.13a) and b) show the room temperature luminescence spectrum: a) before and b) after irradiation at low temperature over a period of approximately three hours. These spectra illustrate the

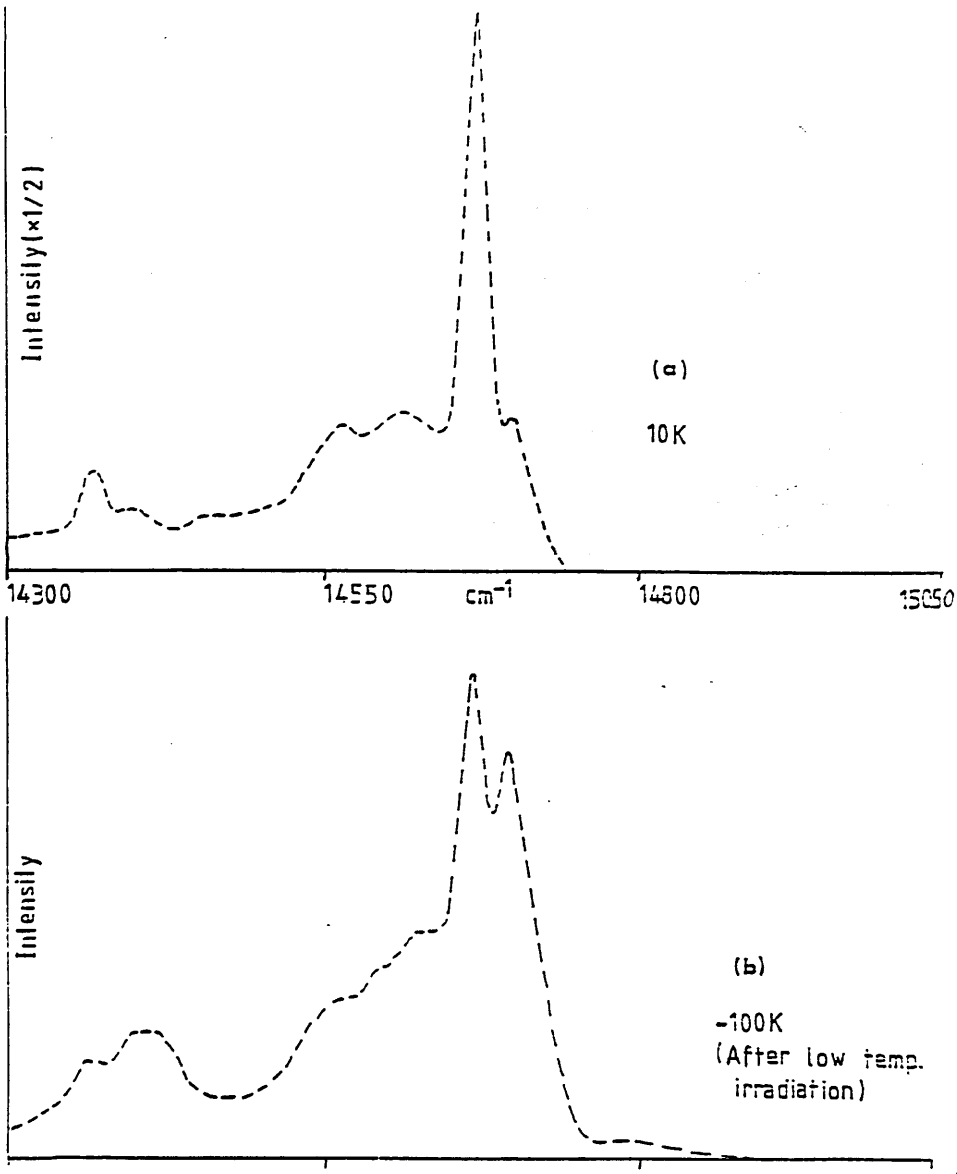

FIGURE 3.12
Axial luminescence spectra a) at 10K and b) after heating to 100K of $[Cr(tacn)_2]Br_3.5H_2O$.

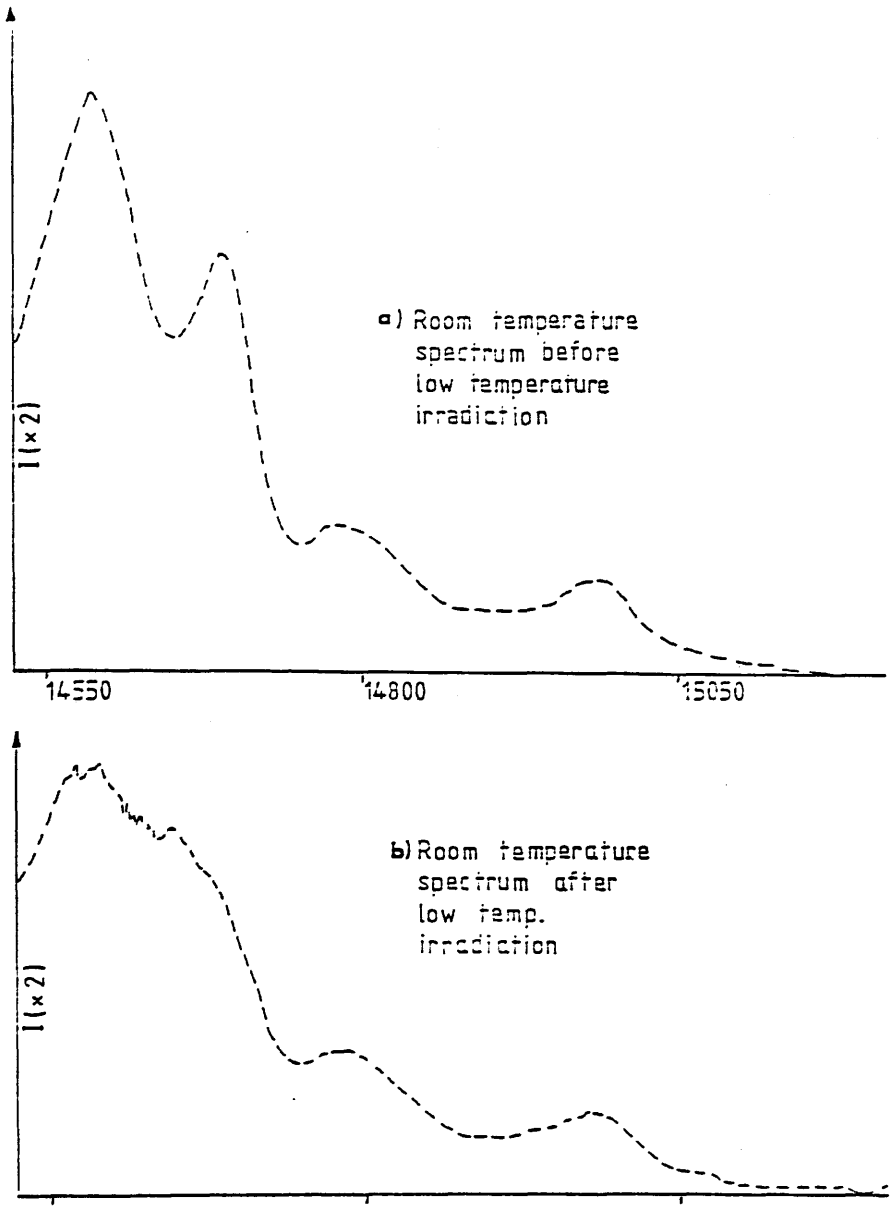

FIGURE 3.13
Room temperature axial luminescence spectra a) before and b) after low temperature LASER irradiation.

(partially) irreversible nature of the postulated low temperature photo-decomposition of $Cr(tacn)_2Br_3.5H_2O$.

The circularly polarised luminescence spectra at three representative temperatures are shown in figures 3.14 a, b and c. These bands may be directly correlated with the luminescence spectra of the same crystal to give values of the luminescence dissymmetry factor g_{em} where;

3m) $g_{em} = 4\ R_{no}/D_{no}$

R_{no} and D_{no} are the Rotational and Dipole strengths respectively of an emission from an excited state n to a ground state o. Table 3.9 lists the differential intensity of each band in the spectrum at 60K along with the corresponding intensity and the luminescence dissymmetry factor.

TABLE 3.9

THE CHIROPTICAL PARAMETERS, IN LUMINESCENCE, OF THE BANDS OF $Cr(tacn)_2Br_3.5H_2O$.

Band	Wavenumber	I	ΔI	g_{em} (x10^3)
?	14775	2	-1.2	-46.0
R_2'	14708	230	93.5	31.1
*	14675	78 (sh)	0	0
R_1'	14620	101.5	18	12.4
R_2	14508	27	2.9	8.2
R_1	14398	100	9.0	6.9
?	14312	15	2.2	5.1

From the wavelengths of the various absorption bands it is possible, by reference to Tanabe-Sugano diagrams, to obtain information on the ligand field strength. The wavenumbers

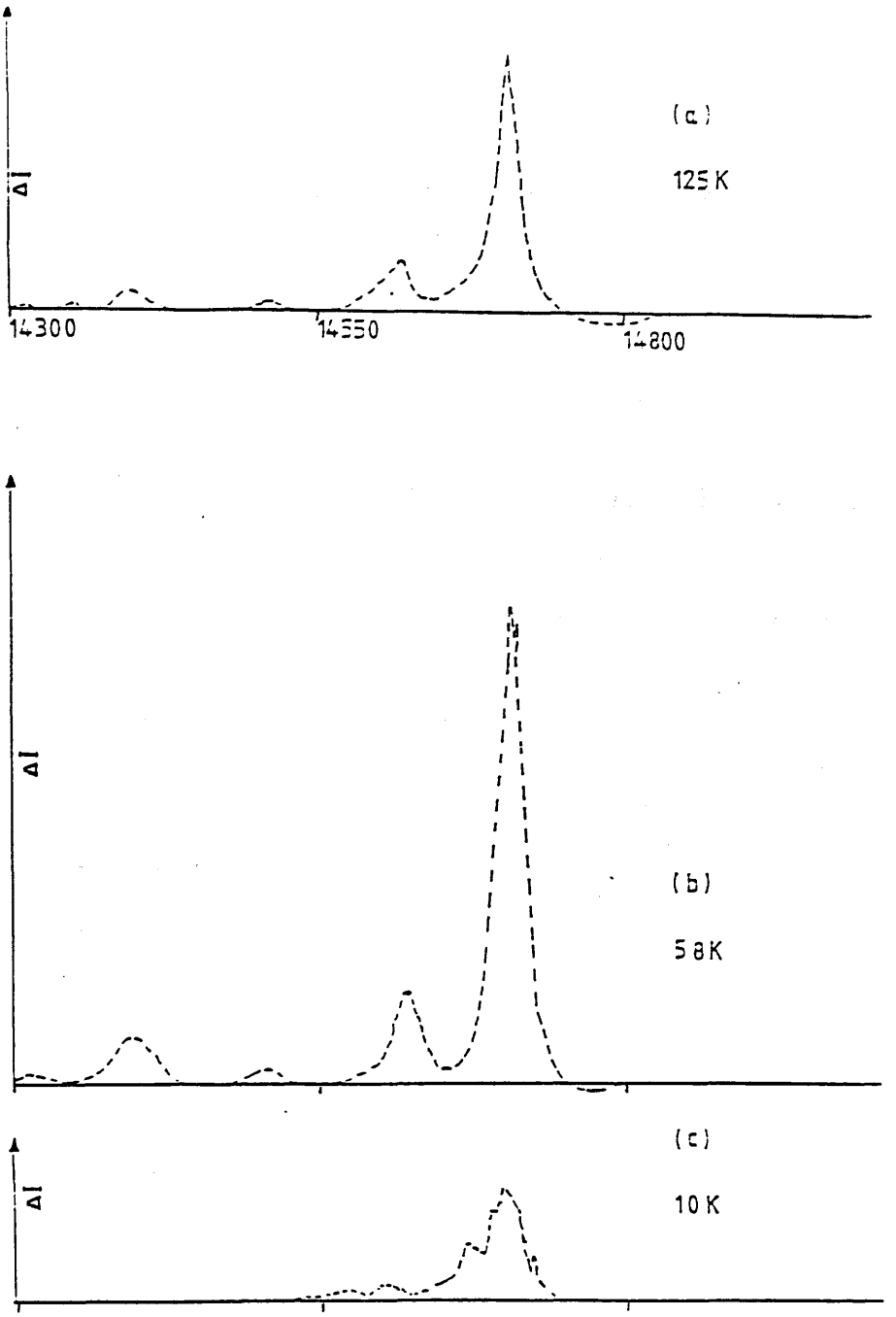

FIGURE 3.14
Axial circularly polarised luminescence spectra of $[Cr(tacn)_2]Br_3.5H_2O$ at a) 125K b) 5.8K and c) 10K.

corresponding to the four assigned transitions are $^4A_2 \rightarrow {}^2E$ 14728cm^{-1}, $^4A_2 \rightarrow {}^2T_1$ 15038cm^{-1}, $^4A_2 \rightarrow {}^4T_2$ 22779cm^{-1}, and $^4A_2 \rightarrow {}^4T_1$ 29498cm^{-1}.

The spin forbidden transition energies are invariant with ligand field strength in Tanabe-Sugano diagrams so that they may be used to obtain a value for the Racah B parameter which in this case, from the ^2E transition, is 675cm^{-1}. From this value the E/B values for the transitions are 21.32, 21.96, 33.27 and 43.08 respectively. The allowed transitions have energies which vary approximately linearly with ligand field splitting allowing estimation of Δ_o.

The ligand field splitting of $Cr(tacn)_2Br_3.5H_2O$ appears to be approximately 14800cm^{-1}. This gives a value for the energy of $^4A_2 \rightarrow {}^2T_2$ of 22260cm^{-1} (449nm) (cf observed wavelength ~454nm).

3.2.4. Discussion

3.2.4.1 Absorbance

The presence of a shoulder on the $^4A_2 \rightarrow {}^4T_2$ transition observed in absorption spectra had previously been reported by Ditze and Wasgestian (Ref 81) who assigned it to the $^4A_2 \rightarrow {}^2T_{1g}$ (O_h) transition. However, Geiser and Gudel (Ref 86) had previously recorded a similar phenomenon in low temperature π and σ polarised single crystal spectra of $[Cr(en)_3]^{3+}$ doped in $2[Ir(en)_3Cl_3].KCl.6H_2O$ which they had

attributed to the transition $^4A_2 \rightarrow {}^2T_2$ and more specifically to the interaction between that inherently sharp band and the much broader $^4A_2 \rightarrow {}^4T_2$ transition giving rise to a negative feature. (They labelled this phenomenon anti-resonance.) In view of the value obtained for Racah B and with regard to Tanabe-Sugano diagrams it is concluded that, as in the case of $[Cr(en)_3]^{3+}$, it is the $^4A_2 \rightarrow {}^2T_2$ transition which gives rise to the shoulder on the $^4A_2 \rightarrow {}^4T_2$ band (and not $^4A_2 \rightarrow {}^2T_1$).

Until the present work was conducted spectroscopic information regarding $[Cr(tacn)_2]^{3+}$ was limited to solution absorption (Refs 80, 81) and solution phosphorescence (Ref 81) spectra. In view of the additional information which may be gleaned from solid state (single crystal) spectra and from investigation of the optical activity of the complex; measurements of crystalline samples were made by absorption, c.d., luminescence and c.p.l. spectroscopies.

The solution absorption spectrum in the spin-allowed region has maxima at 339nm and 439nm while in the crystalline axial spectrum the maxima occur at 339 and 435nm. A property of Co(III) and Cr(III) bis triamines (Ref 43) (and tris diamines (Refs 87 and 88)) is that the C_3 molecular axis often lies parallel to the c-axis of the crystal. In order to see if this was true for $Cr(tacn)_2 Br_3 . 5H_2O$ a crystal was rotated about its c-axis under crossed polarisers to ascertain whether the crystal was uniaxial: it was. A preliminary axial c.d. spectrum showed no

evidence of a negative band (due to A_2 polarised transitions). The solution absorption spectrum represents the effect of light incident on a randomly oriented set of chromophores so that the transitions which comprise, in D_3 symmetry, two non degenerate components with different polarisations are excited to give an orientationally weighted average spectrum. Thus the solution absorption spectrum, Fig 3.7, contains contributions from both A_2 and E polarised transitions; the relative contributions being defined by;

3n) $\varepsilon_{solution} = 2/3\,\varepsilon(E_x) + 1/3\,\varepsilon(A_2)$

where the terms $\varepsilon(E_x)$ and $\varepsilon(A_2)$ represent the total molar extinction coefficients for transitions within a sample which is illuminated isotropically. The terms 2/3 and 1/3 take account of the ability of light propagated in a fixed direction through a randomly oriented sample to excite the E and A components respectively. For an axial sample light propagated parallel to the C_3 molecular axis excites exclusively E polarised transitions so that $\varepsilon(axial) = \varepsilon(E_x)$. As a result of the unequal extinction coefficients due to the E and A_2 polarised transitions, the solution and axial single crystal absorption spectra of D_3 chromophores are generally different in intensity. Since the two transitions to an E state and an A_2 state derived from a T_1 transition in octahedral symmetry are, by their very nature, non-degenerate; it follows that the band maxima in the two spectra would be expected to be different. If this

difference were measurable then a qualitative assessment as to which of the two states occurred at higher energy would be possible. The two bands in the visible region of $Cr(tacn)_2Br_3.5H_2O$ are derived from the $^4A_{2g} \rightarrow {}^4T_{2g}$ (at lower energy) and the $^4A_2 \rightarrow {}^4T_{1g}$ (at higher energy) transitions in octahedral symmetry. In the D_3 symmetry of the chromophore the first of these two transitions decomposes to give $^4A_2 \rightarrow {}^4E$ and $^4A_2 \rightarrow {}^4A_1$ transitions polarised E and A_2 respectively and the second transition decomposes to $^4A_2 \rightarrow {}^4E$ and $^4A_2 \rightarrow {}^4A_2$ giving rise to an E polarised transition and a magnetic dipole forbidden transition. Thus the solution spectrum comprises a lower energy band with E and A_2 polarised contributions and a higher energy band with only an E polarised contribution. The axial absorption spectrum has only E polarised contributions to both transitions and so it is to be expected that the higher energy band should occur at the same wavelength in both spectra: as observed. The lower energy band occurs at 439nm in the solution (2/3 E + 1/3A) spectrum and 435nm in the crystal (E) spectrum. The conclusion is drawn that the $^4A_2 \rightarrow {}^4E(T_2)$ transition is higher in energy than the $^4A_2 \rightarrow {}^4A_1(T_2)$ transition.

From consideration of the intensity of the axial absorbance spectrum in the region of the higher energy band $\varepsilon = 94$, it is possible, on application of equation 3n), to derive a theoretical value of 62.7 (cf litt 64 l $mol^{-1}cm^{-1}$) for the extinction coefficient in solution. This close agreement between the values in solution and the values in the single

crystal indicates that the change in chromophoric environment has had a very small effect on intensity so that there is justification for drawing quantitative conclusions regarding the relative contributions of the A_2 and E components to the molar extinction coefficient observed for the $^4A_2 \rightarrow {}^4T_2$ band. The axial crystal spectrum gives a value for $\varepsilon_{^4A_2 \rightarrow {}^4E(T_2)}$ of 67 l mol^{-1} cm^{-1} which indicates that the contribution from the E polarised components in the solution absorption spectrum is 44.7 l mol^{-1} cm^{-1} so that, by subtraction, the contribution from the A_2 polarised component is approximately 43.3 l mol^{-1} cm^{-1}. It is concluded that the E and A_2 polarised components make approximately equal contributions to the $^4A_2 \rightarrow {}^4T_2$ solution absorbance in $Cr(tacn)_2Br_3.5H_2O$. Since the value for ε_E observed in solution represents 2/3 of the total ε_E whereas the ε_{A_2} observed represents only 1/3 of ε_{A_2} (from equation 3n), it follows from the approximately equal values ε_{A_2} (solution) and ε_E (solution) that the actual value of ε_{A_2} is approximately double that of ε_E.

Peacock and Stewart (Ref 41) concluded, in a review of cobalt(III) species with chelating nitrogen donors, that in cases where the chromophore was compressed along the C_3 axis the E state was lower in energy than the A_2 state and that where the molecules were elongated along the axis the energy levels crossed so that the E state became the higher in energy. From the wavenumbers of the E (21276 cm^{-1}), and A_2 (24509 cm^{-1}), transitions of the compressed molecule $[Cr(-pn)_3]^{3+}$ in the $^4A_2 \rightarrow {}^4T_2$ region (ref 89) and from the

conclusion that the E component is higher in energy for $[Cr(tacn)_2]^{3+}$ than the A_2, it would appear that this trend also holds for $Cr(III)N_6$ species.

The room temperature axial single crystal absorption spectrum in the forbidden region (figure 3.10b) comprises four bands which may also be observed in the 80K σ, π and unpolarised equatorial spectra (figures 3.10 a, b, & c). The bands at 679 and 682nm have been assigned to the transition $^4A_2 \rightarrow {}^2E$ in two distinct but similar species of the complex.

It is interesting to note in the π polarised spectrum that in the case of $[Cr(en)_3]^{3+}$, (Ref 86) the maximum intensity in low temperature absorbance is carried by the higher energy of the two bands. This situation is found to be repeated in the $[Cr(tacn)_2]Br_3 .5H_2O$ case.

The band at 665nm has been assigned to $^4A_2 \longrightarrow {}^2T_1$. In D_3 symmetry this band decomposes to $^4A_2 \longrightarrow {}^2E$ which is E polarised and $^4A_2 \longrightarrow {}^2A_2$ which is magnetic dipole forbidden. It is thus expected that this transition would be most intense in the axial spectrum with reduced intensity in the σ spectrum and with negligible intensity in the π spectrum, as observed for the 665nm band. This is in line with the behaviour reported for $[Cr(en)_3]^{3+}$ (Ref 86). The identity of the band at 673nm is not known although it appears to have a considerable A_2 polarised component since it is enhanced in the π and σ spectra.

3.2.4.2 Circular Dichroism

In order to allow comparison of c.d. spectra in the forbidden region of the spectrum with those in the allowed region, a crystal of type (ii) in figure 3.4 was used to record an axial single crystal c.d. spectrum of the doublet bands. The sign of the circular dichroism of the spin-allowed bands was then determined at the band edge of the $^4A_2 \rightarrow {}^4T_2$ transition and it was found that for any single crystal the c.d. bands were of one sign throughout the spectrum with the exception of a small oppositely signed feature in the vicinity of the $^4A_2 \rightarrow {}^2E$ transition. This concurs with the findings for $[Cr(en)_3]^{3+}$ (Ref 86).

Figure 3.8 shows the absorption and circular dichroism spectra of the $^4A_2 \rightarrow {}^4E(T_2)$ and $^4A_2 \rightarrow {}^4E(T_1)$ transitions of an axial single crystal of $Cr(tacn)_2 Br_3 .5H_2O$. There is some dissymmetry at the lower energy side of the lower energy band which is assigned to the forbidden $^4A_2 \rightarrow {}^2T_2$ transition. The most noticeable feature of these spectra is the lack of intensity in the circular dichroism spectrum of the higher energy band. The reason for this is that although the $^4A_2 \rightarrow {}^4E(T_1)$ transition is polarised E and therefore carries some magnetic dipole intensity: it is nevertheless derived from the $^4A_2 \rightarrow {}^4T_1$ transition in octahedral parentage which is polarised T_2 and, from group theoretical considerations, carries no zero order magnetic dipole intensity. The $^4A_2 \rightarrow {}^4E(T_1)$ transition is observed to have a much stronger c.d. band because it is derived

from the $^4A_2 \rightarrow {}^4T_2$ transition in octahedral symmetry which is magnetic dipole allowed. The extent of the electric dipole and magnetic dipole contributions to the optical activity may be determined by calculation of g_{abs}, the absorption dissymmetry factor at the band maxima.

3o) $$g_{abs\ max} = \Delta\varepsilon_{max} / \varepsilon_{max} = 4R/D$$

R is the rotational strength and D is the dipole strength. From table 3.5 g_{abs} E ($^4A_2 \rightarrow {}^4T_2$) = -0.081 and g_{abs} E ($^4A_2 \rightarrow {}^4T_1$) = -0.012. The rotational strength was calculated using equation 3k to give values of -19.9×10^{-40} cgsu and -3.8×10^{-40} cgsu respectively. By use of equation 3o it is possible to compute the dipole strength D which is 9.83×10^{-38} cgsu in the case of the lower energy transition and 1.27×10^{-37} cgsu in the case of the higher energy transition. This is a quantitative representation of the observation that in the absorption spectra, where intensity depends only on electric dipole, the higher energy band is dominant while in the circular dichroism spectrum, where intensity is dependent on the product of the electric and magnetic dipoles, the lower energy (magnetic dipole allowed) transition dominates.

In the spin forbidden region the only observed circular dichroism was recorded in the vicinity of the $^4A_2 \rightarrow {}^2E$ transition (figure 3.9b) and comprises a doublet (assigned to the transition $^4A_2 \rightarrow {}^4E$ for two similar but distinct species). The g_{abs} values obtained were -0.021 and -0.022

for the higher and lower energy bands respectively. These values will be used in conjunction with luminescence values to draw conclusions about the chirality of the ground state and the emitting state.

The close similarity of the Kuhn dissymmetry factors for the two bands, and the similarity of the absorption and circular dichroism bands from which they are derived, provides evidence of the chemical similarity of the two absorbing species.

The positive feature at 673nm in figure 3.9b is of interest since (from symmetry considerations) it cannot be derived from the $^4A_2 \rightarrow {}^2E$ transition.

Geiser and Gudel (Ref 86) noted a similar feature in the circular dichroism of $[Cr(en)_3]^{3+}$ and attributed it to a conformational isomer with a negative sign sufficiently strong to overturn the sign of the c.d. In complexes involving ethylene diamine this explanation is plausible since conformers such as $\lambda\lambda\delta$ are common. However, in complexes containing two triazacyclononanes (eg tacn and Metacn) there is no evidence for the existence of conformational isomers and so bis tacn complexes are either λ_6 or δ_6 . The presence of enantiomeric impurities in the crystal would not give rise to negative bands but would, rather, decrease the intensity of existing bands. Peacock and Stewart (Ref 85) proposed an explanation of an impurity observed in $[Cr(en)_3]^{3+}$ doped in an iridium tris ethylene

diamine host. The presence of impurities was inferred from luminescence spectra and was explained as molecules of $[Cr(en)_3]^{3+}$ at crystallographically distinct sites in the host lattice. These authors felt that the assignment of the luminescence bands to conformers was incorrect because of the energy differences between bands due to the impurity and the corresponding bands of the dominant emitter.

3.2.4.3 Luminescence

The luminescence due to Cr(III) chromophores occurs because of spin forbidden emission from the ^2E state to the $^4A_2$ ground state and is more precisely labelled phosphorescence. Since ^2E is the lowest energy doublet transition it constitutes the lowest energy to which other doublet transitions may decay by spin allowed transitions and non-radiative decay so it acts as a sink at 14708 cm^{-1} for doublet intensity. In $[Cr(tacn)_2]Br_3 .5H_2O$ the next lowest energy level ($^2T_1$) lies at 15037cm^{-1} (from absorbance spectra) and is therefore significantly thermally populated.

Calculations using the Boltzmann equation;

$$3p)\quad N(^2T_1)/N(^2E) = (g_{T_1}/g_E)\ \exp -\frac{\Delta E}{kT}$$

N_x is the population of state x

g_x is the degeneracy of state x

ΔE is the energy separation (in this case 329cm^{-1})

k is the Boltzmann constant

and T is the temperature in Kelvin

indicate that at 10K the population of the upper state is $4x10^{-21}$ times that of the lower state. However at 298K 23.66% of molecules shared by these states exist in the upper state.

The most widely studied $Cr(III)N_6$ system is $[Cr(en_3]^{3+}$ for which all of the main bands have been assigned. It is worth considering the luminescence spectrum of $[Cr(en)_3]^{3+}$ in order to compare it with the luminescence observed for $[Cr(tacn)_2]^{3+}$. In figure 3.11 the origin bands observed by Peacock and Stewart (Ref 85) in the luminescence of $Cr(en)_3Cl_3$ doped in a lattice of $2[Rh(en)_3Cl_3].NaCl.6H_2O$ at 40K are shown. Several features are worth noting. The bands marked * were not present when the low temperature spectra were first run but gradually grew in intensity on irradiation at low temperature over a period of time and were consequently assigned to decomposition products. The lines labelled R_1 and R_2 correspond to the partially resolved electronic origins $^4A_2 \leftarrow \overline{E}$ (^2E) and $^4A_2 \leftarrow \overline{2A}$ (^2E) respectively. It was proposed that the lines labelled R_1' and R_2' resulted from the same conformer of $[Cr(en)_3]^{3+}$ $[\Lambda(\delta\delta\delta)]$, but were in different crystal sites. It was postulated that the R′states might result from clusters of CrN_6 chromophores in the host lattice with the R states presumably being due to isolated $[Cr(en)_3]^{3+}$ ions in the lattice.

The luminescence spectra, on cooling, of $Cr(tacn)_2Br_3.5H_2O$

are shown in figures 3.11 a, b, c, d, e & f and 3.12a. On cooling the bands become progressively sharper as a result of lower population of the higher vibrational levels within each electronic potential energy well. Certain bands gain in intensity while others lose intensity and with some reservations these bands may be assigned as origin bands and 'hot-bands' respectively. Hot bands correspond to transitions which possess a combination of electronic and vibrational character and as a result occur at slightly different wavelength from the corresponding purely electronic origin band. One other type of hot band which may be present in spectra 3.11 a, b, c, & d is that due to a forbidden electronic state lying sufficiently close to the lowest forbidden excited state to be thermally populated. In the case of $[Cr(tacn)_2]^{3+}$ the $^2T_1$ state might be expected to exhibit luminescence at approximately $15037cm^{-1}$ and indeed at temperatures as low as 149K a hot band centred at $\sim 14990cm^{-1}$ but with appreciable intensity up to $\sim$ 15040 was observed.

As the temperature of the sample was decreased a band, not previously present, grew steadily in intensity from being a shoulder on the R_2' line at 149 K to being greater than three times more intense than the next most intense band at 10K. The growth of this band was accompanied by collapse of the genuine origin bands and was most pronounced between 60K and 10K. The rapid change in the luminescence spectrum of $[Cr(en)_3]^{3+}$ below 50K is well documented (Ref 86), and is generally regarded as being caused by low temperature

traps associated with crystal imperfections.

It is common practice, as a result of low temperature collapse of luminescence spectra, to record spectra at around 60K in order to achieve a compromise between decomposition and resolution. For this reason the spectrum 3.11e will be considered.

The labelling of bands has been conducted in accordance with the system adopted by Peacock and Stewart (Ref 85) (fig 3.15), however some major differences are envisaged between the spectra.

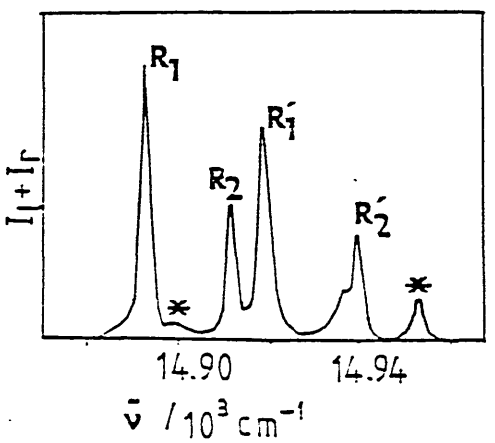

FIGURE 3.15
The unpolarised emission spectrum of ~10% Λ-(+)-$[Cr(en)_3]Cl_3$ doped in a single crystal lattice of $2[Rh(en)_3].NaCl.6H_2O$ at 40K.
(Taken from ref. 85).

In the Peacock and Stewart assignment R_1' and R_2' are attributed to $[Cr(en)_3]^{3+}$ ions in two distinct sites (possibly as clusters). In the $[Cr(tacn)_2]^{3+}$ case it would appear that the R′ states have become dominant although

this may not represent a difference between the two species but may alternatively be a function of the concentration of the chromophore in the crystal lattice [100% for $Cr(tacn)_2Br_3.5H_2O$: ~10% for $[Cr(en)_3Cl_3]$. This latter possibility is supported by the expectation that a rise in concentration would give greater scope for clustering.

As the sample was heated towards room temperature luminescence spectra were recorded which showed a gradual, but incomplete, loss of intensity from the decomposition product band. This transfer of intensity could indicate that the lower energy decomposition product band represents a low energy trap which prevents population of the slightly higher R_2' band at the lowest temperatures. However, if this were the case it would be expected that on raising the temperature to a particular point during heating the intensity of the decomposition product band would be identical to its intensity at the same temperature in spectra recorded during cooling of the sample. This is not the case since the decomposition product band retains considerable intensity. It is concluded therefore that the decomposition product is in equilibrium at low temperatures with molecules in the R′ environment. The room temperature luminescence spectra before and after irradiation are shown in figures 3.13a & b and illustrate the irreversible nature of the decomposition. On removing crystals from the evacuated sample holder after prolonged low temperature irradiation a red coloration was observed to have developed at the point of contact of the laser beam with the crystal.

CrIII N_3O_3 species are red and it may be that the formation of the decomposition product involved reaction of the $[Cr(tacn)_2]^{3+}$ species with its water of crystallisation.

3.2.4.4. Circularly Polarised Luminescence

Because of practical difficulties involved in recording circularly polarised luminescence of single crystals only two examples exist in the literature of such spectra $NaUO_2(MeCO_2)_3$, (Ref 90) and $[Cr(en)_3Cl_3]$ doped in a rhodium tris (ethylene diamine) matrix (Ref 85).

Figures 3.15 a, b, and c show how the circularly polarised emission of $Cr(tacn)_2Br_3.5H_2O$ varies with temperature. The increase in intensity at lower temperatures is in line with the luminescence spectrum: however it is noted that, as reported in the case of $[Cr(en)_3]^{3+}$ (Ref 85) the decomposition product carries no measurable optical activity; a fact witnessed by the collapse of c.p.l. in the 10K spectrum (Fig 3.14c) despite considerable decomposition product intensity in the luminescence spectrum.

The emission dissymmetry factors for the origin bands of $[Cr(tacn)_2]^{3+}$ are listed in table 3.9. The transitions represented by $^4A_2 \rightleftharpoons {}^2E$ occur within the t_2 energy level and should therefore involve flipping of the spin of an electron without a change in structure of the molecule. As a result of the common origin (t_2^3) of these states it is to be expected that their potential energy curves will be vertically disposed with respect to one another on an

energy level diagram. Hilmes, Brittain and Richardson (Ref 83) recorded g_{abs} and g_{em} for solution samples of $(-)[Cr(en)_3]Cl_3$ in ethylene glycol / water at room temperature and obtained values for $^4A_2 \rightleftharpoons {}^2\bar{E}$ of -0.031 and -0.046 respectively. The values for g_{abs} and g_{em} obtained for $Cr(tacn)_2Br_3.5H_2O$ were;

g_{abs} R= -0.021, g_{em} R_1 = 0.007, g_{em} R_2 = 0.008

g_{abs} R' = -0.022, g_{em} R_1' = 0.012, g_{em} R_2' = 0.031

(The absorption experiments and emission experiments were carried out on enantiomeric crystals).

The values for g_{abs} are averages over the two non-degenerate transitions $\bar{E}$ (R_1) and $\overline{2A}$ (R_2) since the bands due to these transitions could not be resolved in absorption. The values are most meaningfully related to the average of g_{em} over the two transitions resulting from a given species as in Table 3.10.

TABLE 3.10

COMPARISON OF THE DISSYMMETRY FACTORS IN ABSORBANCE AND EMISSION OF THE BANDS R AND R'.

	R	R'
g_{abs}	-0.021	-0.022
g_{em}	0.008	0.022

Assuming a negligible change in the asymmetry of the molecule between emitting and ground states g_{em} and g_{abs} should be equal for given species. The values obtained for the species designated R′ are identical and do not express adequately experimental error. However, the values obtained for the species labelled R are outwith the bounds of experimental error and require explanation. Superficially they point to a greatly depleted chiral field in the emitting state, however the magnitude of the change in the dissymmetry factor, coupled with the interconfigurational nature of the transition, render this possibility unlikely. One possible mechanism to explain the observed phenomenon might be that species of the type represented by R are, by virtue of their different crystalline environment, more susceptible to racemisation. However this would be expected to result in a time dependent diminution of R with respect to R′ which is not observed. No satisfactory explanation is possible until the differences between the two absorbing and emitting species R and R′ are more fully understood.

Temperature changes observed in the spectra of $[Cr(en)_3]^{3+}$ are due to decomposition, racemisation, or a combination of the two. It is clear from the irreversible growth of a new band in the low temperature luminescence of $Cr(tacn)_2Br_3.5H_2O$ that decomposition is significant. However, in order to assess the importance of racemisation it is necessary to observe the change in the circularly polarised luminescence spectra, and more specifically the g_{em} values, with temperature. Table 3.10 shows how g_{em} varies from 125K to 63.5K.

TABLE 3.11

COMPARISON OF THE DISSYMMETRY FACTORS, AT 125K AND 63.5K, FOR $Cr(tacn)_2Br_3.5H_2O$

g_{em}	R_1	R_2	R_1'	R_2'
125K	0.005	0.007	0.010	0.030
63.5	0.007	0.008	0.012	0.031

The increase in the dissymmetry factor at low temperature documented in Table 3.11 indicates the higher chirality of the electronic origins compared to that of the attendant unresolvable vibronic side bands.

In the c.p.l. spectra at 125K and 63.5K a negative feature may be observed at the high energy side of the R′ band. This band has been noted in the corresponding c.d. spectrum (Fig 3.9b) and in the c.d. spectra of $[Cr(en)_3]^{3+}$ (Ref 86). Geiser and Gudel assigned it to a conformer in the $[Cr(en)_3]^{3+}$ case. Although no species other than λ_6 and δ_6 $[M(tacn)_2]^{n+}$ has been reported in crystal samples the existence of species adopting a mixture of λ and δ conformations must be involved in solution racemisation, if only as transient intermediates.

The presence of such species is more plausible in samples subjected to intense irradiation (as in the c.p.l. spectra). It is tempting to postulate the existence of such a species in the present study and to attribute the

negative c.p.l. feature to it. Such a species would emit at slightly different energy from the main conformer and would have lower point symmetry and appears to be the most likely explanation of the anomalous c.p.l. and c.d. results.

3.2.5. Conclusions

The elongated nature of $[Co(R\text{-}Metacn)_2]^{3+}$ observed in its crystal structure may be regarded as similar to the geometry expected for the species $[Cr(tacn)_2]^{3+}$ since the main cause postulated for the elongation, non-bonded hydrogen interactions, is present in both species. Spectroscopic evidence is offered which shows that the E component of the $^4A_2 \rightarrow {}^4T_2$ transition is at higher energy than the A_2 component, in contrast to the situation prevalent among compressed $[Cr(\overset{\frown}{N\ N})_3]^{3+}$ species. Observations (Ref 41) of $[Co(\overset{\frown}{N\ N})_3]^{3+}$ species and of the species $[Co(R\text{-}Metacn)_2]^{3+}$ suggest that in the cobalt case E lies to lower energy than A_2 for squat species and to higher energy than A_2 for trigonally elongated species. The present work allows this rule of thumb to be extended to $Cr(III)N_6$ chromophores.

This reversal of the two substates arising from an octahedral triply degenerate state is an inevitable consequence of passing from the squat form, through a notional pseudo degenerate (and pseudo octahedral) form to the elongated form.

The value of 10Dq estimated for $Cr(tacn)_2Br_3.5H_2O$ ($\sim 14{,}800 cm^{-1}$) allows assignment of the shoulder on the

$^4A_2 \rightarrow {}^4T_2$ absorption band to the intraconfigurational transition $^4A_2 \rightarrow {}^2T_2$ at 454nm.

By comparison of the dissymmetry factors in emission and absorption it may be deduced that there is, as expected, little change in the chirality of the major $Cr(tacn)_2 Br_3 .5H_2O$ species (R') in its ground and excited states. The same has not been found for the species R which appears to be considerably less chiral in its emitting state. It should be borne in mind that the absorption and emission spectra relate to two different crystals so that the relative proportions of the two species was not necessarily the same in both cases. (Although if this were the reason for the depletion in R it should have resulted in a compensatory increase in R' which is not observed). It is concluded that the emitting state in the R case must be markedly less chiral than the ground state. The absorption spectral data (and c.d. spectrum) provide evidence that R and R' are very similar so that the lower dissymmetry factor in the case of the species R is all the more puzzling. One possibility, which cannot be overlooked, is that a species, represented by the absorption band and the positive c.d. feature at 673nm was also responsible for the negative c.p.l. feature of the enantiomer at 676nm and, more importantly, for exageration of the band assigned to R_2'. For both the lower energy $[Cr(tacn)_2 Br_3 .5H_2O]$ emitting species and the $[Cr(en)_3]^{3+}$ emitting species (Ref 85), R_1 was more intense than R_2. The fact that this situation is reversed in the higher energy $[Cr(tacn)_2]^{3+}$ species suggests that some interference has taken place. The high

intensity associated with this impurity in low temperature c.p.l. spectra, coupled with the c.d. and c.p.l. features of unexpected sign, would point to the existence of a conformer in the crystal lattice.

Three species appear to be present in crystals of $Cr(tacn)_2Br_3.5H_2O$, as grown from solutions obtained by the Wieghardt (Ref 33) preparation. Two, labelled R and R′, appear to be molecules of the preferred conformer (λ_6 or δ_6) in distinct lattice sites, while the third has been assigned as a conformer. On extended irradiation at low temperatures a fourth species grows in intensity at the expense of the others and remains, to some extent, as the temperature is raised. This species has been assigned as a decomposition product, possibly a $CoN_{6-n}O_n$ chromophore.

CHAPTER 4

N,N',N''-tris(hydroxyalkyl)-1,4,7-triazacyclononanes and Related Complexes

4. N,N',N''-tris(hydroxyalkyl)-1,4,7-triazacyclononanes and Related Complexes

4.1 Introduction

The attractiveness of tacn as a ligand has been demonstrated in the previous chapter. However, in addition to being an excellent ligand, tacn is also the synthetic starting material for a number of interesting ligands. Of the various possible derivatives, those possessing three hydroxyalkyl pendant arms (recently prepared in 1983 (Ref 58)) were selected as being of particular interest. The metal complexes of tris(hydroxyalkyl) triazacyclononanes were expected to adopt configurations of trigonal symmetry. Estimation of chelate ring strain in such complexes suggested that there would be a pronounced trigonal twist (analogous to that in ethylene diamine) and that consequently these species would exhibit strong circular dichroism. By virtue of the predicted hexadenticity of the $[M(N_3O_3)]^{3+}$ species and considering contributions from the chelate ring and macrocyclic effects it was considered that these complex ions would have enhanced stability in solution and would therefore be accessible to detailed spectroscopic investigation.

4.2 N,N',N''-tris(2-(S)-hydroxyisopropyl)-1,4,7-triazacyclononane.

The title ligand, abbreviated (S)-Methetacn, (figure 2.7) was prepared by a synthetic route analogous to that used by Hancock et al (Ref 58) in the preparation of the ligand thetacn which is N,N',N''-tris(2-hydroxyethyl)-1,4,7-triazacyclononane. For the purposes of these investigations it was desirable that the ligands used should possess chiral centres. In designing (S)-Methetacn care was taken to ensure that all three chiral centres would be of the same sign in order to avoid problems of diastereoisomerism. By using the optically active ligand (S)- Methetacn in complex formation it was possible to ensure that the species formed would be optically active and optically pure.

The ligand was prepared from tacn by use of the chiral reagent S-(-)-propylene oxide in basic ethanolic solution. The formation of optically pure ligand relied on observations made on the cleavage of epoxides. The general rule applying to this type of reaction is that for acid catalysed cleavage attack occurs at the epoxide ring carbon which can more easily accommodate a positive charge: for base catalysed cleavage attack occurs at the less hindered carbon atom by a single step S_N2 mechanism (figure 4.1).

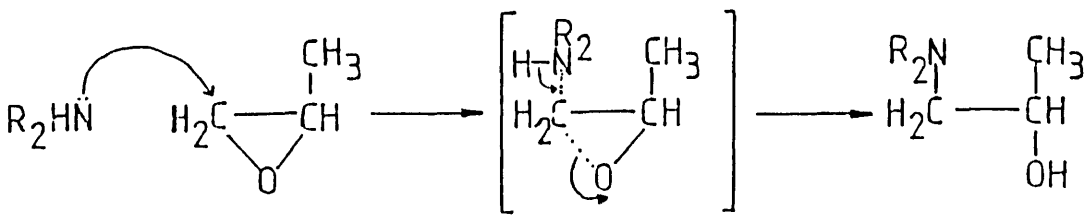

FIGURE 4.1
The ring opening of propylene oxide during an S_N2 reaction involving attack by an amine. The regio-specificity of the reaction ensures the optical purity of the product.

In the reaction of tacn with S-(-)-propylene oxide attack takes place at the less hindered ring carbon so that the configuration of the remaining ring carbon is unaffected during the course of the reaction with the result that the S configuration is retained in all three arms of the ligand. It follows from this reaction mechanism that regio-specificity must be accompanied by stereospecificity so that S-(-)-propylene oxide reacted with tacn to yield Methetacn with three chiral centres sharing a common S configuration. In the course of the work R-(+)-propylene oxide was used on one occasion and yielded R-Methetacn. The regio-specificity of the reaction may be observed in the sharpness of the 200MHz p.m.r. spectrum of the ligand (figure 4.2) and was confirmed by X-ray crystal structure analysis on a cobalt complex of the ligand.

The resonances due to S-Methetacn in the p.m.r. spectrum represented in figure 4.2 have been assigned as follows; 1.1 ppm, doublet, 9 protons, CH_3; 2.4-2.9 ppm, multiplet, 18 protons, CH_2; 3.4 ppm, multiplet, ~1 proton, NH; 3.9 ppm, multiplet, 3 protons, CH. The sharpness of the doublet at 1.1 ppm (J=6.18Hz) is significant in ascribing regio-specificity to the reaction.

From the above it may be deduced that each molecule of S-Methetacn possesses three chiral centres with a common S configuration so that unlike the ligand R-Metacn, which necessarily introduces asymmetry into its complexes,

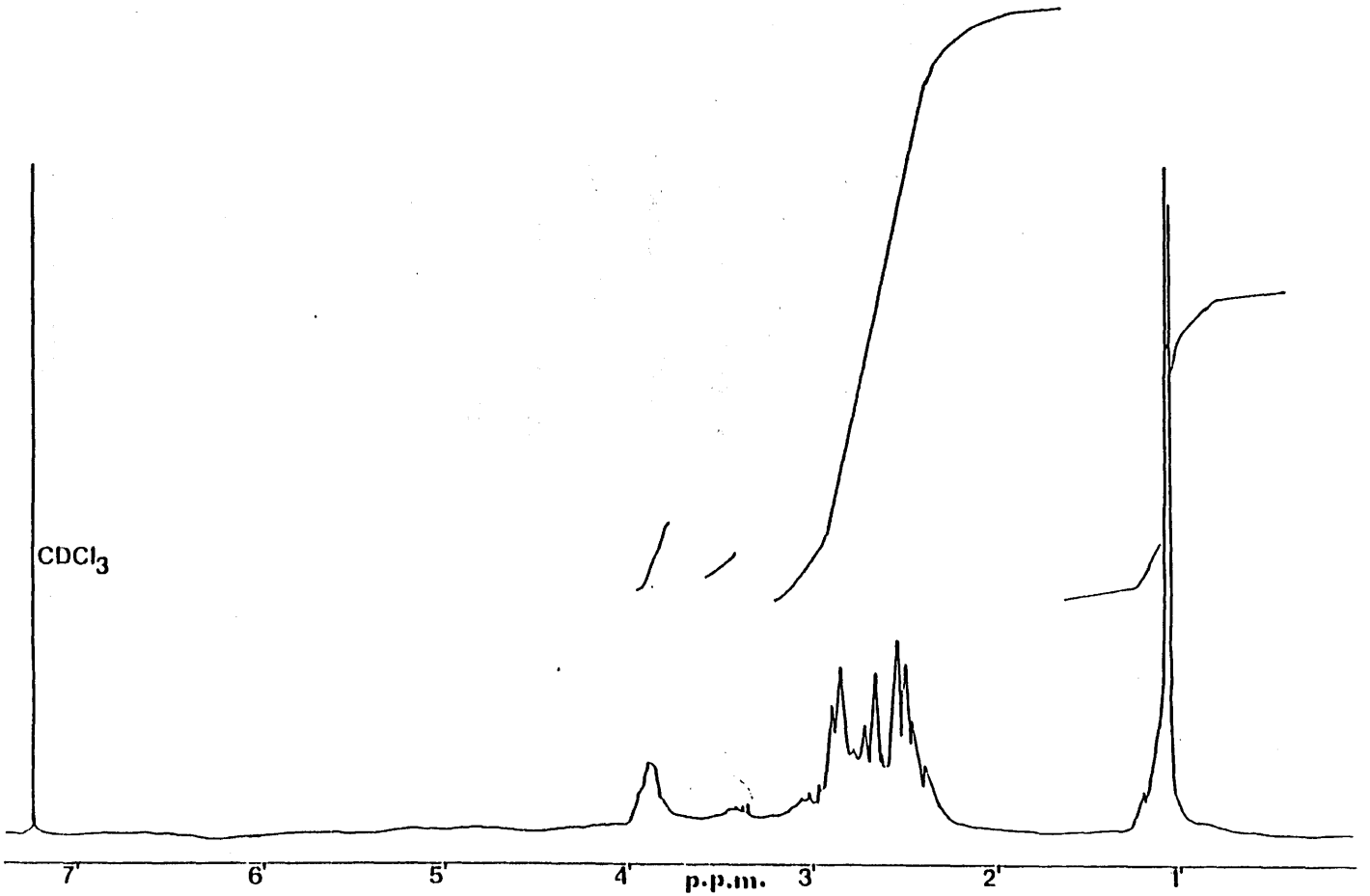

FIGURE 4.2
The p.m.r. spectrum of S-Methetacn.HBr in deutero-chloroform.

S-Methetacn allows complex ions in which it participates to adopt full trigonal symmetry.

The spectra of several first row transition metal complexes of Methetacn are discussed below. Attempts to prepare chromium complexes with S-Methetacn by methods used to prepare similar CrN_3O_3 species (Ref 55) proved unsuccessful.

4.3 [CoIII((S)-Methetacn)]$^{3+}$ - Results

4.3.1 Purification

The cobalt(III) complex of (S)-Methetacn was prepared as described in Chapter 2 and, as a means of purification, it was subjected to column chromatography on an SP-Sephadex C25 ion exchange column (80cm) using 0.3M NaCl solution as eluent. From the apparently pure solution there separated three bands on the column. The fast band was purple in colour and was followed by two red bands in close proximity to one another (~1 cm apart after passing down the column). The absorption and c.d. spectra of the species are shown in figure 4.3 and were found to be unchanged after 21 hours in solution at room temperature indicating that there was no significant thermal equilibrium among the three species represented in the spectra. Addition of acid or base significantly changed the spectra such that addition of base gave spectra of the type attributable to the purple band while acid addition gave a spectrum similar to the first red band. It was not found possible, by addition of

acid or base, to regenerate the species responsible for the second red band. From the circular dichroism spectra in figure 4.3 the second red band appears to be intermediate between the acidic (red) species and the basic (purple) species. It should be borne in mind that the low intensity of the second red band is probably a concentration effect. The wavelengths and dissymmetry factors of the bands in all three spectra are listed in Table 4.1.

TABLE 4.1

THE ABSORPTION AND C.D. CHARACTERISTICS OF THREE FRACTIONS OBTAINED BY COLUMN CHROMATOGRAPHY OF $[Co(S\text{-}Methetacn)]^{3+}$

Transition	Chromatography Band	Positive Feature λ_{max}	Positive Feature g_{max} ($\times 10^3$)	Negative Feature λ_{max}	Negative Feature g_{max} ($\times 10^3$)	Absorption λ
	Purple	551	6.51	–	–	540
$^1A_1 \rightarrow {}^1T_1$	Red 1	575	2.69	514	-10.12	530
	Red 2	559	5.50	5.00	-3.33	532
	Purple	410	3.92	–	–	395
$^1A_1 \rightarrow {}^1T_2$	Red 1	398	4.92	–	–	382
	Red 2	403	2.67	–	–	375

4.3.2 pH Dependence of the Spectra

The species represented in figure 4.3 could not be isolated from solution. However, an extremely hygroscopic purple solid could be obtained from basified aqueous solutions which allowed calculation of molar extinction coefficients in both the acidic and basic forms.

The spectra obtained from species in acidic and basic solutions constitute figure 4.4. Acidity was generated in solution by addition, with stirring, of concentrated

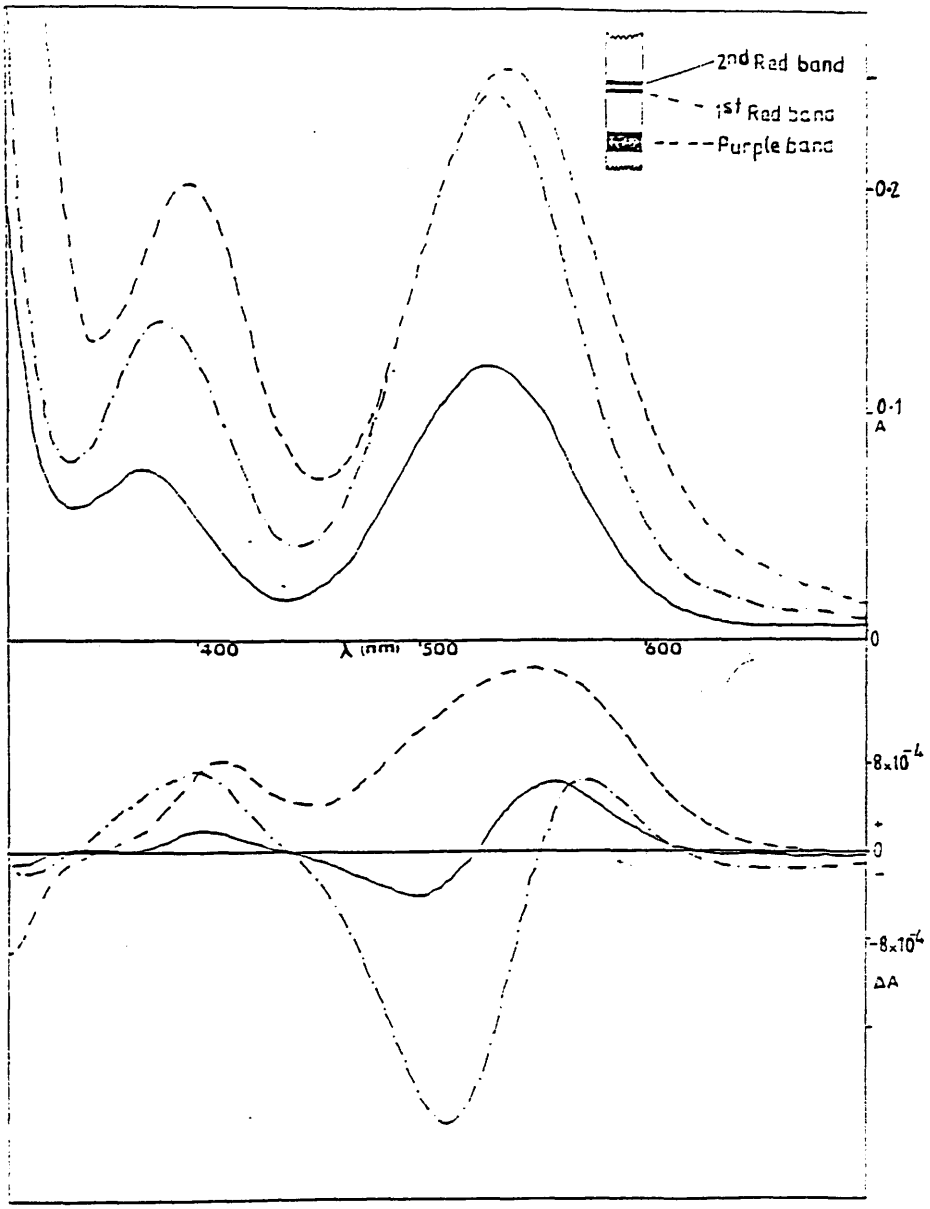

FIGURE 4.3
Column chromatography of a newly prepared aqueous solution of $[Co(S\text{-}Methetacn)]^{3+}$ gave three bands with distinct absorption and circular dichroism characteristics.

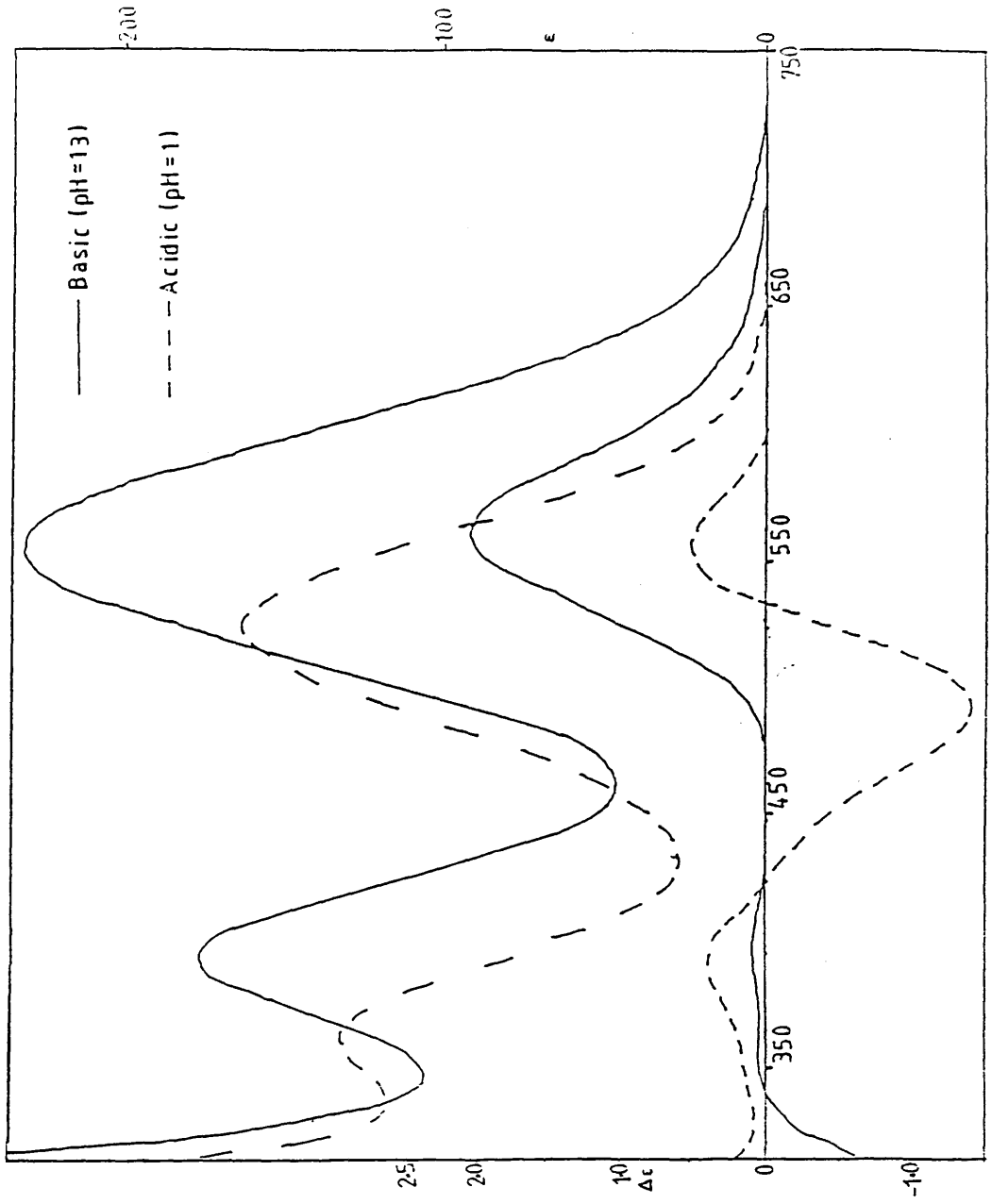

FIGURE 4.4
The absorption (top) and circular dichroism (bottom) spectra of acidic and basic aqueous solutions of $[Co(S\text{-}Methetacn)]^{3+}$.

hydrochloric acid: basicity being generated in an analogous manner by addition of sodium hydroxide solution. The resulting solutions were pink and purple respectively. In order to examine the observed change in absorption with pH a series of 38 absorption spectra, with corresponding c.d. spectra, were recorded using buffered solutions from pH 2.5-12. The graphs resulting from plots of pH against various spectral features did not in any case give a classical pKa stepped slope; instead the result was an uneven curve irrespective of the feature plotted. This behaviour is typical of chelated species (Ref 91) and is brought about by a buffering mechanism whereby raising of the pH causes loss of protons in the solution which act against the rise in pH in the vicinity of the complex. The circular dichroism spectra at selected pH values are shown in figure 4.5. From figures 4.3 and 4.5, and from the complex nature of pKa curves associated with this reaction it has been deduced that more than two species are involved. This deduction is supported by the absence of an isosbestic point in figure 4.6 which shows the absorbance associated with the c.d. bands in figure 4.5. Figure 4.7 is a typical plot of pH versus an absorption characteristic (in this case the absorbance at 600nm). The plot aludes to a pKa for one of the species involved of ~8.2 ; however as a result of strong chelation the plateau is not sufficiently well defined to allow accurate assignment. The absence of further plateaux is attributed to the wavelength chosen for sampling. The use of lower wavelengths resulted in incomprehensible plots as a result of the number of species involved.

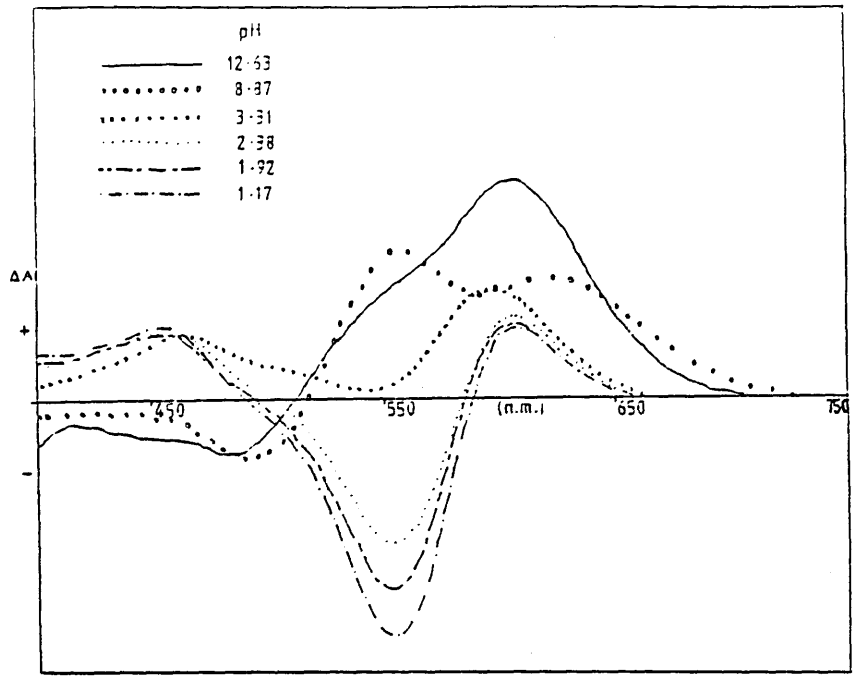

FIGURE 4.5
The c.d. spectra of $[Co(S\text{-}Methetacn)]^{3+}$ at selected (buffered) pH values.

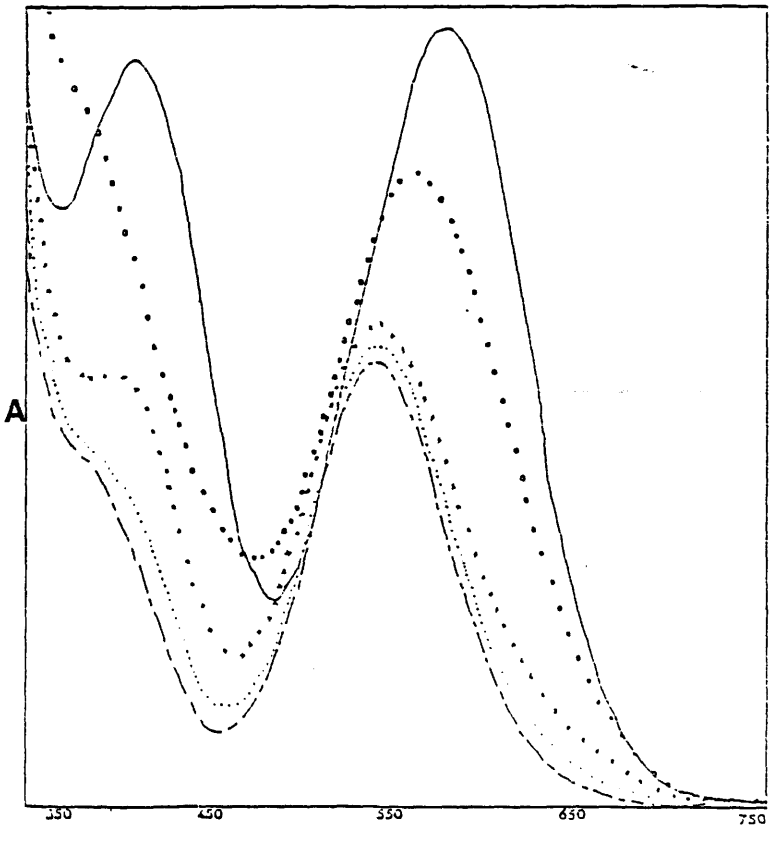

FIGURE 4.6
The absorption spectra corresponding to figure 4.5.

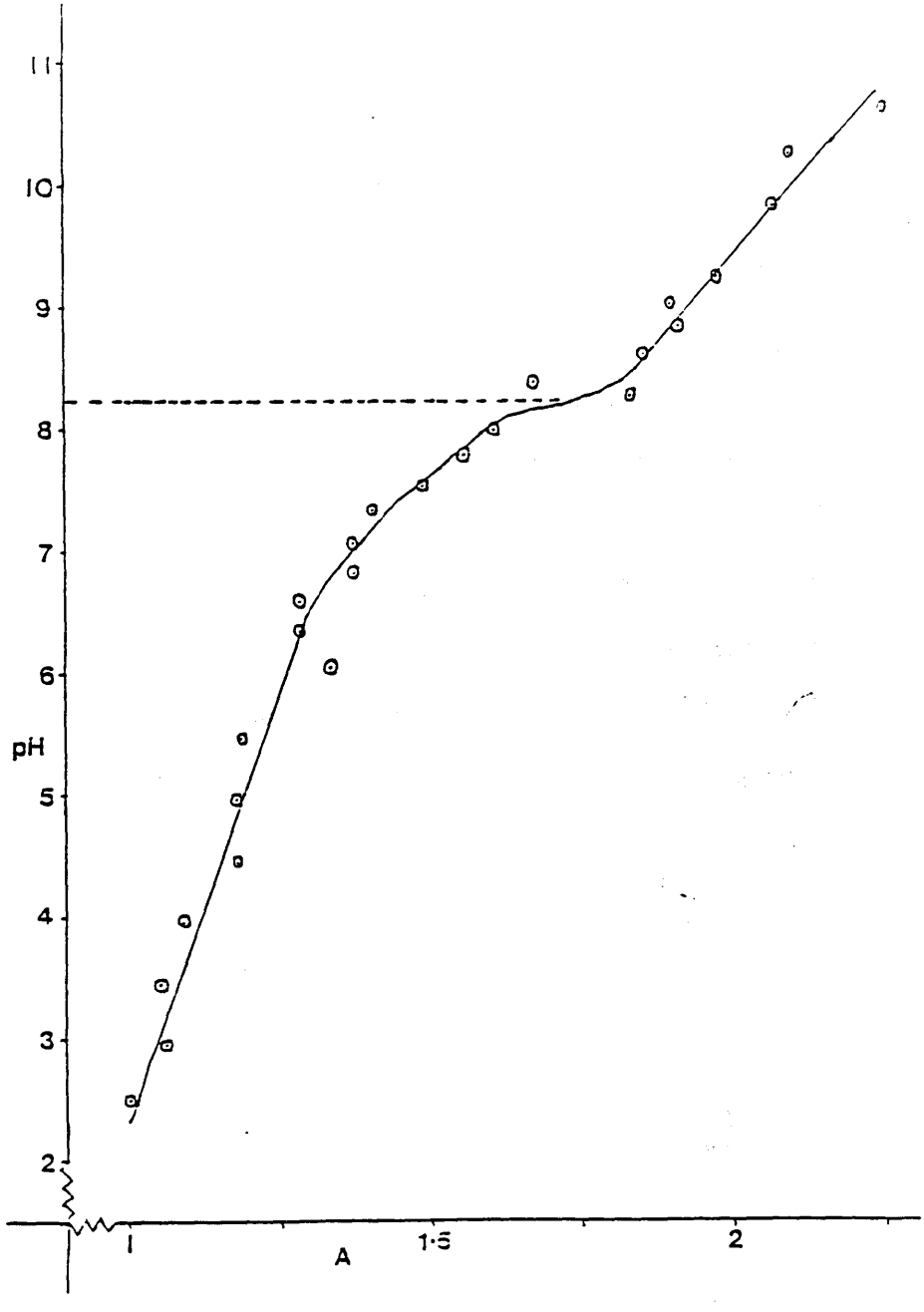

FIGURE 4.7
Plot of pH versus absorbance at 600nm showing a marked change in absorbance between pH=9 and pH=7.

4.3.3. Spectra In Non-Aqueous Solvents

The hygroscopic nature of $[Co^{III}(S\text{-Methetacn})]^{3+}$ as its chloride salt made it desirable to prepare a salt with a lower affinity for water. Several such salts were prepared including the hexafluoroantimonate salt, the hexaflurophosphate salt and tetrafluoroborate salt. Of these the hexafluorophosphate salt and the tetrafluoroborate salt proved to be insoluble in water. The former was consequently examined in various non-aqueous media. A summary of the spectra of the hexafluorophosphate salt of the complex in various solvents is provided in table 4.2. Also included, for comparison, are parameters abstracted from the various aqueous spectra of the chloride salt and the spectra recorded using a KBr disk containing the hexafluorophosphate salt.

TABLE 4.2
SPECTRAL FEATURES OF SAMPLES OF $[Co(S\text{-Methetacn})]^{3+}$ IN VARIOUS SOLVENTS

	$^1A_1 \longrightarrow {}^1T_1$					$^1A_1 \longrightarrow {}^1T_2$		
	λcd(nm) +ve max	g(x10³) +ve max	λcd(nm) -ve max	g(x10³) -ve max	λabs(nm)	λcd(nm)	g(x10³) +ve	λabs(nm)
Red 1	575	2.69	514	-10.12	530	398	4.92	382
Red 2	559	5.50	500	-3.33	532	403	2.67	375
Purple	551	6.51	—	—	540	410	3.92	395
EtOH	574	5.56	—	—	557	384	0.22	390
CH_2Cl_2	578	6.05	—	—	555	398	0.49	390
DMF	603	5.25	527	-2.12	558	418	3.80	402
CH_3CN	578	5.90	454	-0.12	555	398	0.55	386
KBr	615	8.90	528	-2.98	555	433	4.12	397

In the case of the spectra obtained by dissolution of $[\{Co^{III}(S\text{-Methetacn})\}_2(\mu H)_3](PF_6)_3$ in acetonitrile (figure 4.8) a purple residue remained beneath the pink solution. In all other cases dissolution was complete.

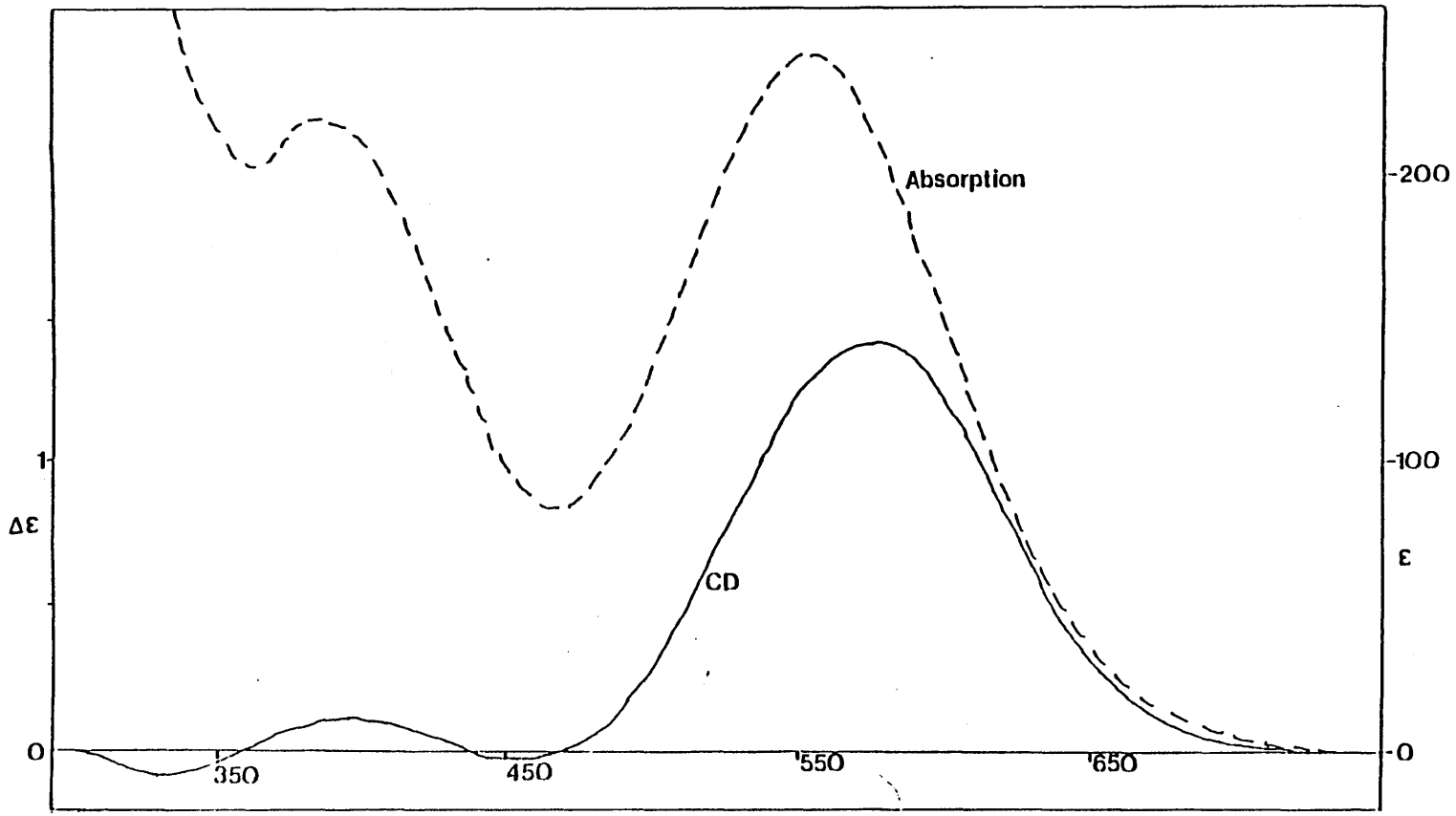

FIGURE 4.8
The absorption and circular dichroism spectra of $[\{Co(S\text{-Methetacn})\}_2(\mu H)_3](PF_6)_3$ in acetonitrile.

4.3.4. Polarisable Oxyanions

As a means of distinguishing between the two non-degenerate transitions observed in the $^1A_1 \rightarrow {}^1T_1$ region in the circular dichroism spectra of acidic and basic aqueous solutions, sodium selenite was added to each solution. This is a commonly applied procedure (Refs 46,47 and 48) which relies on the ability of the selenite ion (for example) to hydrogen bond to aminic or alcoholic protons in metal complexes, provided that the protons in question are suitably disposed. In the case of $[Co(Methetacn)]^{3+}$, i.e. the monomer with three alcoholic protons bonded to coordinating oxygens, it was envisaged that the selenite ion would be capable of capping the complex to give an effectively axially elongated chromophore. This would result, spectroscopically, in an enhancement of the intensity of the $^1A_1 \rightarrow {}^1A_2(T_1)$ transition with a corresponding diminution of the $^1A_1 \rightarrow {}^1E$ transition. The results of addition of sodium selenite to the two solutions are shown in figure 4.9. In each case the polarisable oxyanion was added to give a final concentration of 0.1M in selenite.

4.3.5. ^{1}H-n.m.r. Spectra

Figures 4.10 and 4.11 represent the 200 MHz proton n.m.r. spectra of acidified and basified samples of the cobalt complex. The acidified sample was produced by addition of deuterochloric acid, prepared by reaction of sulphonyl chloride with D_2O, to an aqueous (D_2O) solution of the

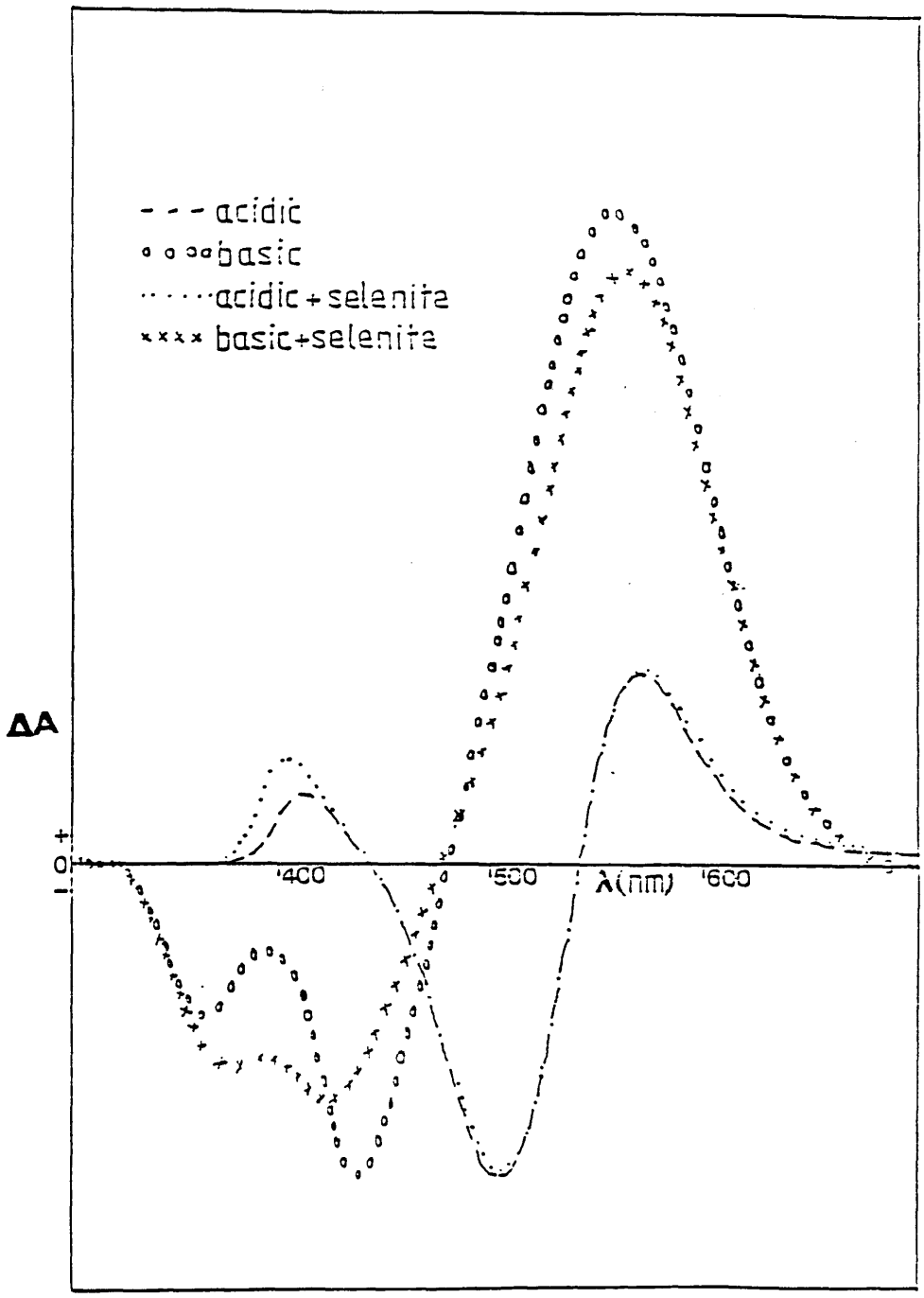

FIGURE 4.9
The effect of addition of sodium selenite to both acidic and basic aqueous solutions of $[Co(S\text{-}Methetacn)]^{3+}$.

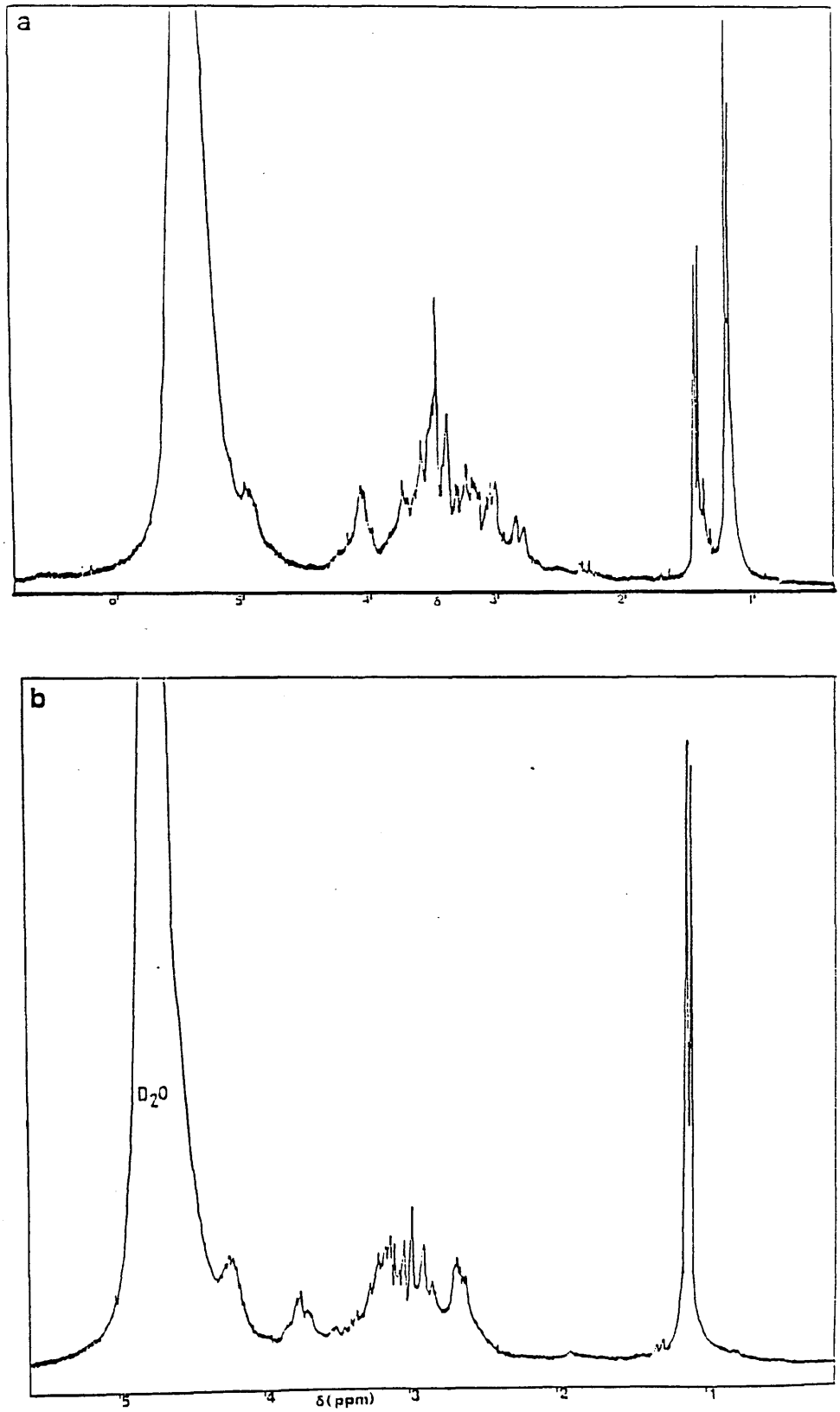

FIGURE 4.10
The 200MHz ^{1}H-nmr spectrum of a) acidified and b) basified aqueous solutions of $[Co(S\text{-}Methetacn)]^{3+}$.

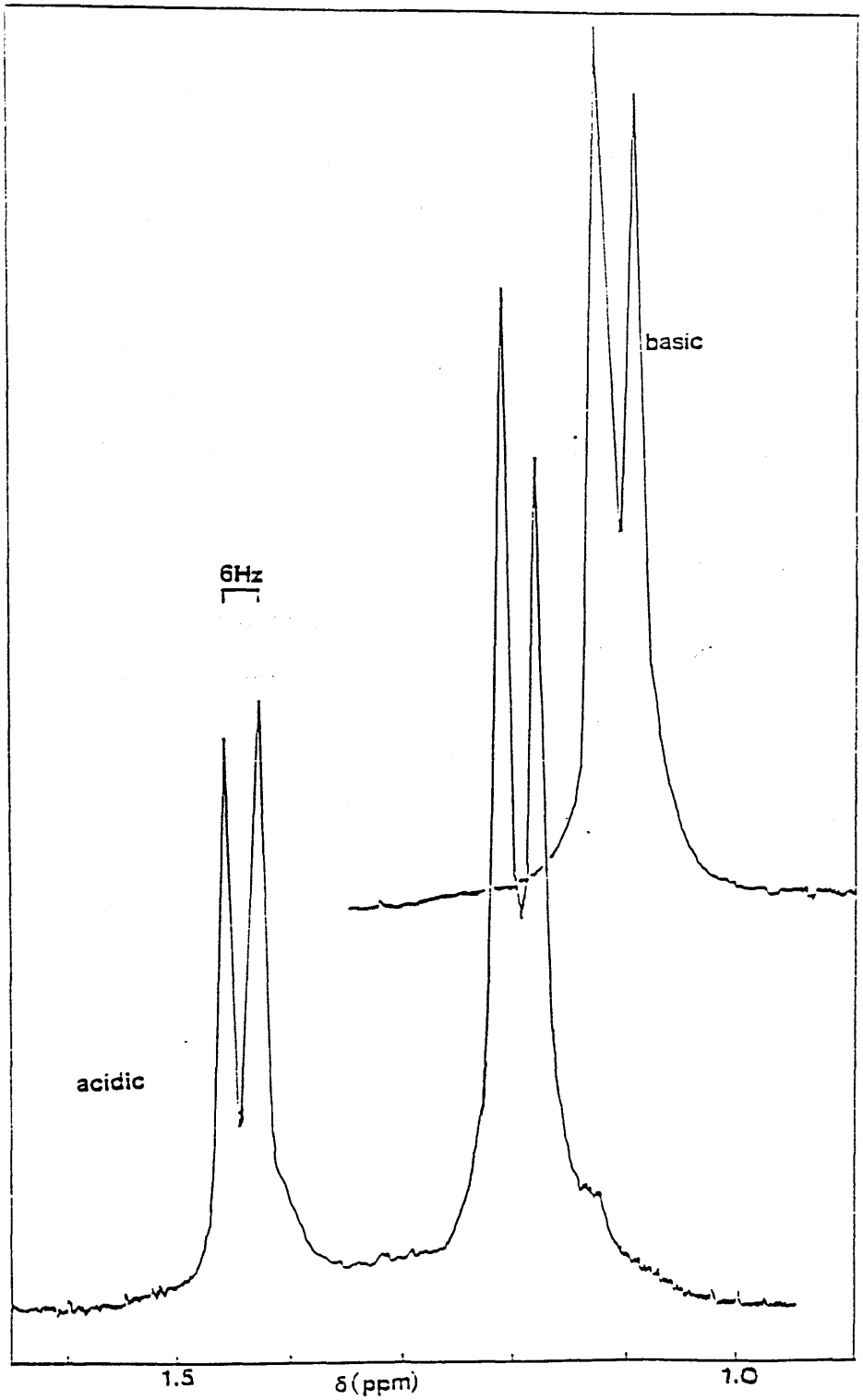

FIGURE 4.11
Expanded ^{1}H-nmr spectra ,in the methyl region, of acidic (lower) and basic (upper) aqueous solutions of $[Co(S\text{-}Methetacn)]^{3+}$ with $CDCl_3$ as external reference.

complex. The basified sample was produced by addition of sodium deuteroxide, prepared by addition of clean sodium metal to D_2O, to a solution of the complex. Because of the expected susceptibility of the resonant frequency of water soluble internal standards to change, on addition of strong acid or base, an external standard was used. The standard consisted of a finely drawn capillary tube containing deutero chloroform. The technique involved recording the n.m.r. spectrum of a sample with no external standard present and then immediately repeating the experiment with the external standard mounted centrally in the n.m.r. tube. Thus for both acidic and basic samples the spectra, though free from interfering reference species resonances, have been fixed relative to deuterochloroform. The pH values of the acidic and basic solutions were not evaluated (due to problems of sample size) but were estimated to be pH 2 and pH 12 respectively. The details of the resonances in both spectra ware listed in table 4.3, along with assignments (the values for the ligand hydrobromide salt are included for comparison).

TABLE 4.3
^1H-n.m.r. SPECTRA OF THREE Methetacn CONTAINING SPECIES.

	Acidic Co(III) Complex	Basic Co(III) Complex	Ligand Hydrobromide
Methyl	1.2 & 1.45	1.1	1.1
Methylene	2.7-3.8	2.5-3.5	2.4-2.9
Methine	4.1	3.4	3.9
Amino	-	-	3.4

The expanded n.m.r. spectra in the region of the methyl resonances for the acidic and basic forms are superimposed for ease of comparison in figure 4.11. In a separate experiment the dimeric hexafluorophosphate salt of the complex was dissolved in d^3 acetonitrile and the 90 MHz n.m.r. spectrum recorded. The resulting resonances which are displayed graphically in figure 4.12 have been assigned: 1.1ppm, doublet, relative intensity 9, methyl; 2.5-3.2ppm, multiplet, relative intensity 18, methylene; and 4.0 ppm, multiplet, relative intensity 3, methine.

4.4 $[\{Co(S\text{-}Methetacn)\}_2(\mu H)_3](PF_6)_3$:Crystal Structure.

4.4.1. Preparation of crystals

The title complex was precipitated from aqueous solution by addition of an excess of ammonium hexafluorophosphate to a strong solution of $[Co^{III}(Methetacn)]^{3+}$ in the presence of chloride ions. The precipitation of a fine purple powder took place overnight to leave a pink aqueous solution. The pink solution had a positive c.d. maximum at 550nm with minima at 439nm and 369nm and was very similar spectroscopically to basified solutions containing the chloride salt of the complex (e.g. figure 4.4), despite the fact that no base had been added. The purple solid was air dried and recrystallised from the minimum amount of acetonitrile over approximately one day. There followed a more protracted crystallisation procedure in which dimethylformamide was used as solvent in order to allow crystallisation to occur over a period of about one month.

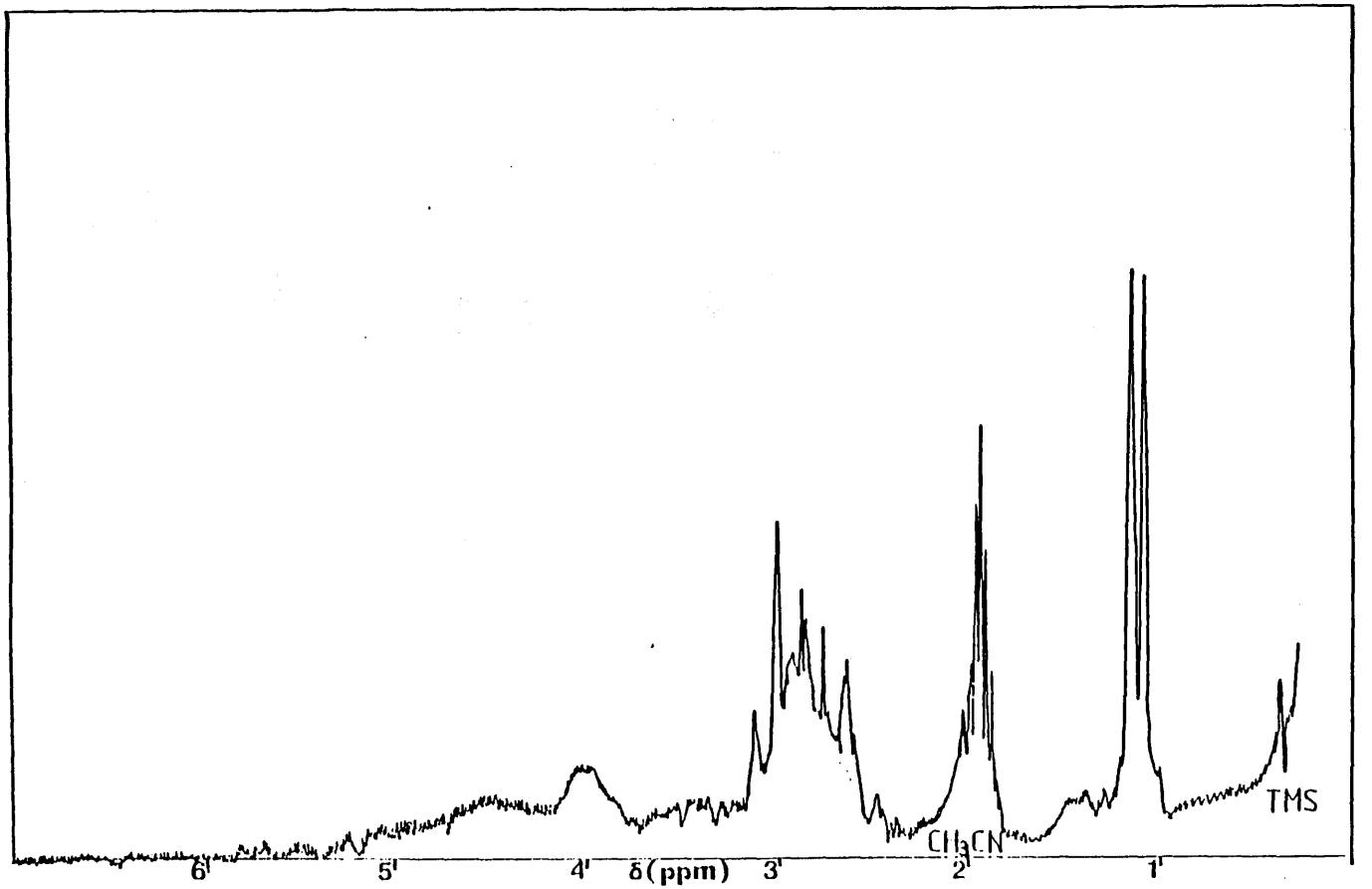

FIGURE 4.12
The proton nmr spectrum of in deutero-acetonitrile of $[\{Co(S\text{-}Methetacn)\}_2(\mu H)_3](PF_6)_3$. (Referenced to TMS).

The result was truncated pyramidal crystals which appeared, from micro-analysis, to have 1.5 hexafluorophosphate ions per ligand unit. Five such crystals were subjected to examination and the finest example, with no visible sign of twinning, was selected for X-ray crystal analysis.

4.4.2. Crystal Data

The chosen crystal measured 0.3x0.32x0.3mm and was mounted on a glass fibre. The crystal data comprised in brief $[\{CoC_{15}H_{30}N_3O_3\}_2(\mu H)_3](PF_6)_3$, formula weight 1157.14, cubic, space group $P2_13$, a=b=c=16.277(3), D 1.78, U 4312(1), Z 4, μ 10.01 cm^{-1}, F(000) 2376, T= ambient.

Intensity data were collected in the range $4^\circ<2\theta<50^\circ$. Standard reflections were remeasured after the collection of every 200 reflections and showed a decay factor of 1.2% in 10,000. 1704 independent reflections were measured of which 950 were used for refinement (cut-off value 2.5σ). The final discrepancy factors were R=0.0379 and R'=0.0347.

The final least squares positional parameters for $[\{Co(S\text{-}Methetacn)\}_2(\mu H)_3](PF_6)_3$ are shown in table 4.4.

Bond lengths are listed in table 4.5 and selected bond angles in table 4.6. From these data it is possible to ascertain the twist angle, that is the extent to which the molecule has been distorted from octahedral geometry. The twist represents a displacement of 11.2° in the anti-clockwise direction of the bottom donor set (viewed

	X/A	Y/B	Z/C	U
CO(1)	-.08126(6)	-.08126	-.08126	.030
CO(2)	.08331(7)	.08331	.08331	.033
C(11)	-.2188(5)	.0166(5)	-.0724(5)	.038
C(12)	-.2003(5)	.0023(5)	.0168(5)	.033
C(13)	-.2096(5)	.0790(5)	.0673(5)	.046
C(14)	-.1841(5)	-.0404(6)	-.2086(5)	.046
C(15)	-.2477(5)	-.1284(5)	-.1037(5)	.042
C(21)	.2242(5)	.0611(5)	-.0050(6)	.044
C(22)	.0164(5)	.1994(5)	-.0286(5)	.035
C(23)	.2123(5)	-.0792(6)	-.0582(5)	.064
C(24)	.1985(5)	.2028(5)	.0401(6)	.041
C(25)	.2473(6)	.0982(6)	.1404(6)	.056
N(1)	-.1919(4)	-.0554(4)	-.1182(4)	.038
N(2)	.1977(4)	.1145(4)	.0644(4)	.042
O(1)	-.1169(3)	-.0304(3)	.0204(3)	.036
O(2)	.0422(4)	.1165(4)	-.0235(4)	.041
P(1)	.3051(2)	.3051	.3051	.054
P(2)	-.30117(19)	-.30117	-.30117	.044
P(3)	.4973(4)	.4973	.4973	.071
F(1)	.3329(4)	.2832(4)	.3956(4)	.072
F(2)	.2150(4)	.2762(5)	.3267(5)	.085
F(3)	-.3945(4)	-.3210(4)	-.2635(4)	.074
F(4)	-.2059(4)	-.2815(4)	-.3165(4)	.074
F(5A)	.4449(14)	.5454(16)	.5602(17)	.177
F(5B)	.5737(19)	.5054(23)	.5580(25)	.122
F(6A)	.466(3)	.432(2)	.552(2)	.242
F(6B)	.483(3)	.418(3)	.451(5)	.137
H(1)	-.051(4)	.024(4)	.072(4)	.02(2)
H(11A)	-.18660	.07003	-.09375	.050
H(11B)	-.28349	.02570	-.08083	.050
H(12A)	-.24161	-.04333	.04001	.050
H(14A)	-.24377	-.04378	-.23645	.050
H(14B)	-.15911	.01974	-.21861	.050
H(15A)	-.30635	-.10753	-.08190	.050
H(15B)	-.25635	-.16133	-.16018	.050
H(21A)	.19455	.08004	-.06072	.050
H(21B)	.28951	.06512	-.01296	.050
H(22A)	.06580	.23666	-.05118	.050
H(24A)	.25947	.22743	.04549	.050
H(24B)	.17810	.20959	-.02220	.050
H(25A)	.30503	.07149	.12318	.050
H(25B)	.25351	.15531	.17147	.050
H(13A)	-.19640	.06878	.13110	.050
H(13B)	-.27146	.10091	.06152	.050
H(13C)	-.16829	.12483	.04412	.050
H(23A)	.22709	-.09632	-.12012	.050
H(23B)	.15184	-.10536	-.05364	.050
H(23C)	.25393	-.12172	-.02980	.050

TABLE 4.4
The fractional coordinates of atoms in the unit cell of $[\{Co(S\text{-Methetacn})\}_2(\mu H)_3](PF_6)_3$.

CO(1)	- N(1)	1.944(7)	CO(1)	- N(1)	1.944(7)
CO(1)	- N(1)	1.944(7)	CO(1)	- O(1)	1.939(6)
CO(1)	- O(1)	1.939(6)	CO(1)	- O(1)	1.939(6)
CO(2)	- N(2)	1.954(8)	CO(2)	- N(2)	1.954(8)
CO(2)	- N(2)	1.954(7)	CO(2)	- O(2)	1.939(6)
CO(2)	- O(2)	1.939(7)	CO(2)	- O(2)	1.939(7)
C(11)	- C(12)	1.501(12)	C(11)	- N(1)	1.456(11)
C(11)	- H(11A)	1.073(9)	C(11)	- H(11B)	1.073(8)
C(12)	- C(13)	1.501(12)	C(12)	- O(1)	1.461(9)
C(12)	- H(12A)	1.073(8)	C(13)	- H(13A)	1.073(9)
C(13)	- H(13B)	1.073(8)	C(13)	- H(13C)	1.073(9)
C(14)	- C(15)	1.514(13)	C(14)	- N(1)	1.497(12)
C(14)	- H(14A)	1.073(9)	C(14)	- H(14B)	1.073(10)
C(15)	- N(1)	1.513(11)	C(15)	- H(15A)	1.073(9)
C(15)	- H(15B)	1.073(9)	C(21)	- C(22)	1.553(12)
C(21)	- N(2)	1.490(12)	C(21)	- H(21A)	1.073(9)
C(21)	- H(21B)	1.073(8)	C(22)	- C(23)	1.482(12)
C(22)	- O(2)	1.416(11)	C(22)	- H(22A)	1.073(9)
C(23)	- H(23A)	1.073(10)	C(23)	- H(23B)	1.073(9)
C(23)	- H(23C)	1.073(10)	C(24)	- C(25)	1.521(14)
C(24)	- N(2)	1.492(12)	C(24)	- H(24A)	1.073(9)
C(24)	- H(24B)	1.073(10)	C(25)	- N(2)	1.561(12)
C(25)	- H(25A)	1.073(10)	C(25)	- H(25B)	1.073(11)
O(1)	- H(1)	1.62(7)	O(2)	- H(1)	.90(7)
P(1)	- F(1)	1.581(7)	P(1)	- F(1)	1.581(7)
P(1)	- F(1)	1.581(7)	P(1)	- F(2)	1.581(8)
P(1)	- F(2)	1.581(8)	P(1)	- F(2)	1.581(8)
P(2)	- F(3)	1.579(7)	P(2)	- F(3)	1.579(7)
P(2)	- F(3)	1.579(7)	P(2)	- F(4)	1.603(8)
P(2)	- F(4)	1.603(7)	P(2)	- F(4)	1.603(8)
P(3)	- F(5A)	1.55(3)	P(3)	- F(5A)	1.55(3)
P(3)	- F(5A)	1.55(3)	P(3)	- F(5B)	1.59(4)
P(3)	- F(5B)	1.59(4)	P(3)	- F(5B)	1.59(5)
P(3)	- F(6A)	1.49(4)	P(3)	- F(6A)	1.49(4)
P(3)	- F(6A)	1.49(4)	P(3)	- F(6B)	1.51(7)
P(3)	- F(6B)	1.51(7)	P(3)	- F(6B)	1.51(5)

TABLE 4.5
Bond lengths in the species
$[\{Co(S\text{-Methetacn})\}_2(\mu\text{-III})_3](PF_6)_3$.

N(1)	- Co(1)	- N(1)	88.9(3)	N(1)	- Co(1)	- N(1)	88.7(3)
N(1)	- Co(1)	- O(1)	84.0(3)	N(1)	- Co(1)	- O(1)	170.7(3)
N(1)	- Co(1)	- O(1)	96.8(3)	N(1)	- Co(1)	- N(1)	88.9(3)
N(1)	- Co(1)	- O(1)	96.8(3)	N(1)	- Co(1)	- O(1)	84.0(3)
N(1)	- Co(1)	- O(1)	170.7(3)	N(1)	- Co(1)	- O(1)	170.7(3)
N(1)	- Co(1)	- O(1)	96.8(3)	N(1)	- Co(1)	- O(1)	84.0(3)
O(1)	- Co(1)	- O(1)	91.0(3)	O(1)	- Co(1)	- O(1)	91.0(3)
O(1)	- Co(1)	- O(1)	91.0(3)	N(2)	- Co(2)	- N(2)	86.7(3)
N(2)	- Co(2)	- N(2)	86.7(3)	N(2)	- Co(2)	- O(2)	96.6(3)
N(2)	- Co(2)	- O(2)	170.9(3)	N(2)	- Co(2)	- O(2)	85.0(3)
N(2)	- Co(2)	- N(2)	86.7(3)	N(2)	- Co(2)	- O(2)	85.0(3)
N(2)	- Co(2)	- O(2)	96.6(3)	N(2)	- Co(2)	- O(2)	170.9(3)
N(2)	- Co(2)	- O(2)	170.9(3)	N(2)	- Co(2)	- O(2)	85.0(3)
N(2)	- Co(2)	- O(2)	96.6(3)	O(2)	- Co(2)	- O(2)	92.1(3)
O(2)	- Co(2)	- O(2)	92.1(3)	O(2)	- Co(2)	- O(2)	92.1(3)
C(12)	- C(11)	- N(1)	108.1(7)	C(12)	- C(11)	- H(11A)	109.9(7)
C(12)	- C(11)	- H(11B)	109.9(7)	N(1)	- C(11)	- H(11A)	109.9(7)
N(1)	- C(11)	- H(11B)	109.9(7)	H(11A)	- C(11)	- H(11B)	109.0(8)
C(11)	- C(12)	- C(13)	112.4(7)	C(11)	- C(12)	- O(1)	106.3(7)
C(11)	- C(12)	- H(12A)	108.8(7)	C(13)	- C(12)	- O(1)	110.0(7)
C(13)	- C(12)	- H(12A)	108.8(7)	O(1)	- C(12)	- H(12A)	108.4(7)
C(12)	- C(13)	- H(13A)	110.4(8)	C(12)	- C(13)	- H(13B)	108.8(7)
C(12)	- C(13)	- H(13C)	108.8(7)	H(13A)	- C(13)	- H(13B)	108.8(8)
H(13A)	- C(13)	- H(13C)	108.8(7)	H(13B)	- C(13)	- H(13C)	109.0(8)
C(15)	- C(14)	- N(1)	110.7(8)	C(15)	- C(14)	- H(14A)	109.5(8)
C(15)	- C(14)	- H(14B)	109.5(8)	N(1)	- C(14)	- H(14A)	109.5(8)
N(1)	- C(14)	- H(14B)	109.5(8)	H(14A)	- C(14)	- H(14B)	109.5(9)
C(14)	- C(15)	- N(1)	108.9(7)	C(14)	- C(15)	- H(15A)	109.7(8)
C(14)	- C(15)	- H(15B)	109.7(8)	N(1)	- C(15)	- H(15A)	109.7(7)
N(1)	- C(15)	- H(15B)	109.7(8)	H(15A)	- C(15)	- H(15B)	109.0(8)
C(22)	- C(21)	- N(2)	107.7(7)	C(22)	- C(21)	- H(21A)	110.0(8)
C(22)	- C(21)	- H(21B)	110.0(8)	N(2)	- C(21)	- H(21A)	110.0(7)
N(2)	- C(21)	- H(21B)	110.0(8)	H(21A)	- C(21)	- H(21B)	109.0(8)
C(21)	- C(22)	- C(23)	107.6(7)	C(21)	- C(22)	- O(2)	105.0(7)
C(21)	- C(22)	- H(22A)	110.1(7)	C(23)	- C(22)	- O(2)	114.3(8)
C(23)	- C(22)	- H(22A)	110.1(8)	O(2)	- C(22)	- H(22A)	109.6(7)
C(22)	- C(23)	- H(23A)	161.0(10)	C(22)	- C(23)	- H(23B)	95.5(7)
C(22)	- C(23)	- H(23C)	95.5(7)	H(23A)	- C(23)	- H(23B)	95.5(8)
H(23A)	- C(23)	- H(23C)	95.5(8)	H(23B)	- C(23)	- H(23C)	109.0(9)
C(25)	- C(24)	- N(2)	106.7(8)	C(25)	- C(24)	- H(24A)	110.3(8)
C(25)	- C(24)	- H(24B)	110.3(8)	N(2)	- C(24)	- H(24A)	110.3(8)
N(2)	- C(24)	- H(24B)	110.3(8)	H(24A)	- C(24)	- H(24B)	109.5(8)
C(24)	- C(25)	- N(2)	111.5(8)	C(24)	- C(25)	- H(25A)	109.1(9)
C(24)	- C(25)	- H(25B)	109.1(8)	N(2)	- C(25)	- H(25A)	109.1(8)
N(2)	- C(25)	- H(25B)	109.1(9)	H(25A)	- C(25)	- H(25B)	109.0(9)
Co(1)	- N(1)	- C(11)	107.1(5)	Co(1)	- N(1)	- C(14)	105.1(5)
Co(1)	- N(1)	- C(15)	109.8(5)	Co(1)	- N(1)	- C(11)	107.1(5)
Co(1)	- N(1)	- C(14)	105.1(5)	Co(1)	- N(1)	- C(15)	109.8(5)
Co(1)	- N(1)	- C(11)	107.1(5)	Co(1)	- N(1)	- C(14)	105.1(5)
Co(1)	- N(1)	- C(15)	109.8(5)	C(11)	- N(1)	- C(14)	113.4(7)
C(11)	- N(1)	- C(15)	111.8(7)	C(14)	- N(1)	- C(15)	109.4(7)
Co(2)	- N(2)	- Co(2)	.0(1)	Co(2)	- N(2)	- Co(2)	.0(1)
Co(2)	- N(2)	- C(21)	104.1(5)	Co(2)	- N(2)	- C(24)	107.5(6)
Co(2)	- N(2)	- C(25)	109.7(6)	Co(2)	- N(2)	- Co(2)	.0(1)
Co(2)	- N(2)	- C(21)	104.1(5)	Co(2)	- N(2)	- C(24)	107.5(6)
Co(2)	- N(2)	- C(25)	109.7(6)	Co(2)	- N(2)	- C(21)	104.1(5)
Co(2)	- N(2)	- C(24)	107.5(6)	Co(2)	- N(2)	- C(25)	109.7(6)
C(21)	- N(2)	- C(24)	111.0(7)	C(21)	- N(2)	- C(25)	111.5(7)
C(24)	- N(2)	- C(25)	112.6(7)	Co(1)	- O(1)	- Co(1)	.0(1)
Co(1)	- O(1)	- Co(1)	.0(1)	Co(1)	- O(1)	- C(12)	113.6(5)
Co(1)	- O(1)	- H(1)	118.5(23)	Co(1)	- O(1)	- Co(1)	.0(1)
Co(1)	- O(1)	- C(12)	113.6(5)	Co(1)	- O(1)	- H(1)	118.5(23)
Co(1)	- O(1)	- C(12)	113.6(5)	Co(1)	- O(1)	- H(1)	118.5(23)
C(12)	- O(1)	- H(1)	116.0(24)	Co(2)	- O(2)	- C(22)	114.9(5)
Co(2)	- O(2)	- H(1)	109.7(42)	Co(2)	- O(2)	- C(22)	114.9(5)
Co(2)	- O(2)	- H(1)	109.7(42)	Co(2)	- O(2)	- C(22)	114.9(5)
Co(2)	- O(2)	- H(1)	109.7(42)	C(22)	- O(2)	- H(1)	129.4(42)

TABLE 4.6
Selected bond angles from the crystal structure of $[\{Co(S\text{-Methetacn})\}_2(\mu H)_3](PF_6)_3$.

F(1)	P(1)	F(2)	179.3(4)	F(1)	P(1)	F(2)	89.5(4)
F(1)	P(1)	F(2)	90.3(4)	F(1)	P(1)	F(2)	90.3(4)
F(1)	P(1)	F(2)	179.3(4)	F(1)	P(1)	F(2)	89.5(4)
F(2)	P(1)	F(2)	89.8(4)	F(2)	P(1)	F(2)	89.8(4)
F(2)	P(1)	F(2)	89.8(4)	F(3)	P(2)	F(3)	90.9(4)
F(3)	P(2)	F(3)	90.9(4)	F(3)	P(2)	F(4)	178.4(4)
F(3)	P(2)	F(4)	90.7(4)	F(3)	P(2)	F(4)	89.1(4)
F(3)	P(2)	F(3)	90.9(4)	F(3)	P(2)	F(4)	89.1(4)
F(3)	P(2)	F(4)	178.4(4)	F(3)	P(2)	F(4)	90.7(4)
F(3)	P(2)	F(4)	90.7(4)	F(3)	P(2)	F(4)	89.1(4)
F(3)	P(2)	F(4)	178.4(4)	F(4)	P(2)	F(4)	89.4(4)
F(4)	P(2)	F(4)	89.4(4)	F(4)	P(2)	F(4)	89.4(4)
F(5A)	P(3)	F(5A)	108.0(14)	F(5A)	P(3)	F(5A)	108.0(14)
F(5A)	P(3)	F(5B)	88.7(17)	F(5A)	P(3)	F(5B)	83.8(16)
F(5A)	P(3)	F(5B)	38.3(14)	F(5A)	P(3)	F(6A)	77.0(17)
F(5A)	P(3)	F(6A)	169.8(16)	F(5A)	P(3)	F(6A)	61.8(16)
F(5A)	P(3)	F(6B)	132.8(23)	F(5A)	P(3)	F(6B)	111.5(23)
F(5A)	P(3)	F(6B)	83.4(27)	F(5A)	P(3)	F(5A)	108.0(13)
F(5A)	P(3)	F(5B)	38.3(17)	F(5A)	P(3)	F(5B)	88.7(16)
F(5A)	P(3)	F(5B)	83.8(17)	F(5A)	P(3)	F(6A)	61.8(20)
F(5A)	P(3)	F(6A)	77.0(17)	F(5A)	P(3)	F(6A)	169.8(16)
F(5A)	P(3)	F(6B)	83.4(25)	F(5A)	P(2)	F(6B)	132.8(23)
F(5A)	P(3)	F(6B)	111.5(25)	F(5A)	P(3)	F(5B)	83.8(17)
F(5A)	P(3)	F(5B)	38.3(18)	F(5A)	P(3)	F(5B)	88.7(17)
F(5A)	P(3)	F(6A)	169.8(20)	F(5A)	P(3)	F(6A)	61.8(16)
F(5A)	P(3)	F(6A)	77.0(18)	F(5A)	P(3)	F(6B)	111.5(28)
F(5A)	P(3)	F(6B)	83.4(24)	F(5A)	P(3)	F(6B)	132.8(30)
F(5B)	P(3)	F(5B)	93.2(20)	F(5B)	P(3)	F(5B)	93.2(18)
F(5B)	P(3)	F(6A)	87.5(21)	F(5B)	P(3)	F(6A)	90.3(21)
F(5B)	P(3)	F(6A)	136.6(17)	F(5B)	P(3)	F(6B)	120.0(25)
F(5B)	P(3)	F(6B)	158.6(25)	F(5B)	P(3)	F(6B)	143.2(31)
F(5B)	P(3)	F(5B)	93.2(20)	F(5B)	P(3)	F(6A)	136.6(21)
F(5B)	P(3)	F(6A)	87.5(20)	F(5B)	P(3)	F(6A)	90.3(20)
F(5B)	P(3)	F(6B)	143.2(26)	F(5B)	P(3)	F(6B)	120.0(27)
F(5B)	P(3)	F(6B)	158.6(24)	F(5B)	P(3)	F(6A)	90.3(19)
F(5B)	P(3)	F(6A)	136.6(20)	F(5B)	P(3)	F(6A)	87.5(18)
F(5B)	P(3)	F(6B)	158.6(31)	F(5B)	P(3)	F(6B)	143.2(24)
F(5B)	P(3)	F(6B)	120.0(29)	F(6A)	P(3)	F(6A)	113.1(18)
F(6A)	P(3)	F(6A)	113.1(24)	F(6A)	P(3)	F(6B)	68.6(30)
F(6A)	P(3)	F(6B)	103.3(26)	F(6A)	P(3)	F(6B)	55.7(32)
F(6A)	P(3)	F(6A)	113.1(19)	F(6A)	P(3)	F(6B)	55.7(26)
F(6A)	P(3)	F(6B)	68.6(26)	F(6A)	P(3)	F(6B)	103.3(30)
F(6A)	P(3)	F(6B)	103.3(28)	F(6A)	P(3)	F(6B)	55.7(24)
F(6A)	P(3)	F(6B)	68.6(26)	F(6B)	P(3)	F(6B)	50.7(32)
F(6B)	P(3)	F(6B)	50.7(29)	F(6B)	P(3)	F(6B)	50.7(37)
P(2)	F(3)	P(2)	.0	P(2)	F(3)	P(2)	.0
P(2)	F(3)	P(2)	.0	P(2)	F(4)	P(2)	.1(1)
P(2)	F(4)	P(2)	.1(1)	P(2)	F(4)	P(2)	.1(1)
P(3)	F(5A)	F(5B)	73.4(26)	P(3)	F(5A)	F(5B)	73.4(26)
P(3)	F(5A)	F(5B)	73.4(26)	P(3)	F(5B)	F(5A)	68.3(24)
P(3)	F(5B)	F(5A)	68.3(24)	P(3)	F(5B)	F(5A)	68.3(24)
P(3)	F(6A)	P(3)	.1(1)	P(3)	F(6A)	P(3)	.1(1)
P(3)	F(6A)	F(6B)	63.0(23)	P(3)	F(6A)	P(3)	.1(1)
P(3)	F(6A)	F(6B)	63.0(25)	P(3)	F(6A)	F(6B)	63.0(25)
P(3)	F(6B)	F(6A)	61.3(26)	P(3)	F(6B)	F(6B)	64.6(39)
P(3)	F(6B)	F(6B)	64.6(37)	P(3)	F(6B)	F(6A)	61.3(26)
P(3)	F(6B)	F(6B)	64.6(39)	P(3)	F(6B)	F(6B)	64.6(37)
P(3)	F(6B)	F(6A)	61.3(26)	P(3)	F(6B)	F(6B)	64.6(39)
P(3)	F(6B)	F(6B)	64.6(37)	P(6A)	F(6B)	F(6B)	77.5(41)
F(6A)	F(6B)	F(6B)	121.4(50)	F(6B)	F(6B)	F(6B)	60.0(47)
O(1)	N(1)	O(2)	157.7(63)				

TABLE 4.6 (Continued)

down the C_3 axis in figure 4.13) relative to the top donor set. The complex has adopted the Δ configuration (defined by the exocyclic chelate rings). The angle ω, as defined by Peacock and Stewart (Ref 41), has been found to be + 11.2°.

The angle ∝ , defined as the angle enclosed by each of the exocyclic chelate rings, was found to be 83.95°. The angles $\hat{NCo}C_3$ and $\hat{OCo}C_3$ were found to be 53.95° and 55.47° respectively. The complex was found to exist in the solid state as a hydrogen bridged dimer (fig 4.14) with three (PF_6^-) counter ions balancing the overall charge of +3. The structure was sufficiently well refined that determination of absolute configuration was possible using the Bijvoet method (Refs 92 & 93).

4.5 Discussion of Cobalt Complexes of Methetacn

4.5.1. Solution Behaviour

The original aim of the investigation of $[CoIII(Methetacn)]^{3+}$ was to relate the circular dichroism spectrum to the physical structure of the complex. It was believed that all six donor atoms of the ligand would coordinate to the cobalt ion to give a trigonally symmetric chromophore which would be accessible for spectroscopic investigation. It became obvious soon after preparation of the complex that the chemistry was more interesting than initially envisaged. One preliminary observation: that basic solutions were purple while acidic solutions were red, led to the hypothesis that one of the hydroxyisopropyl

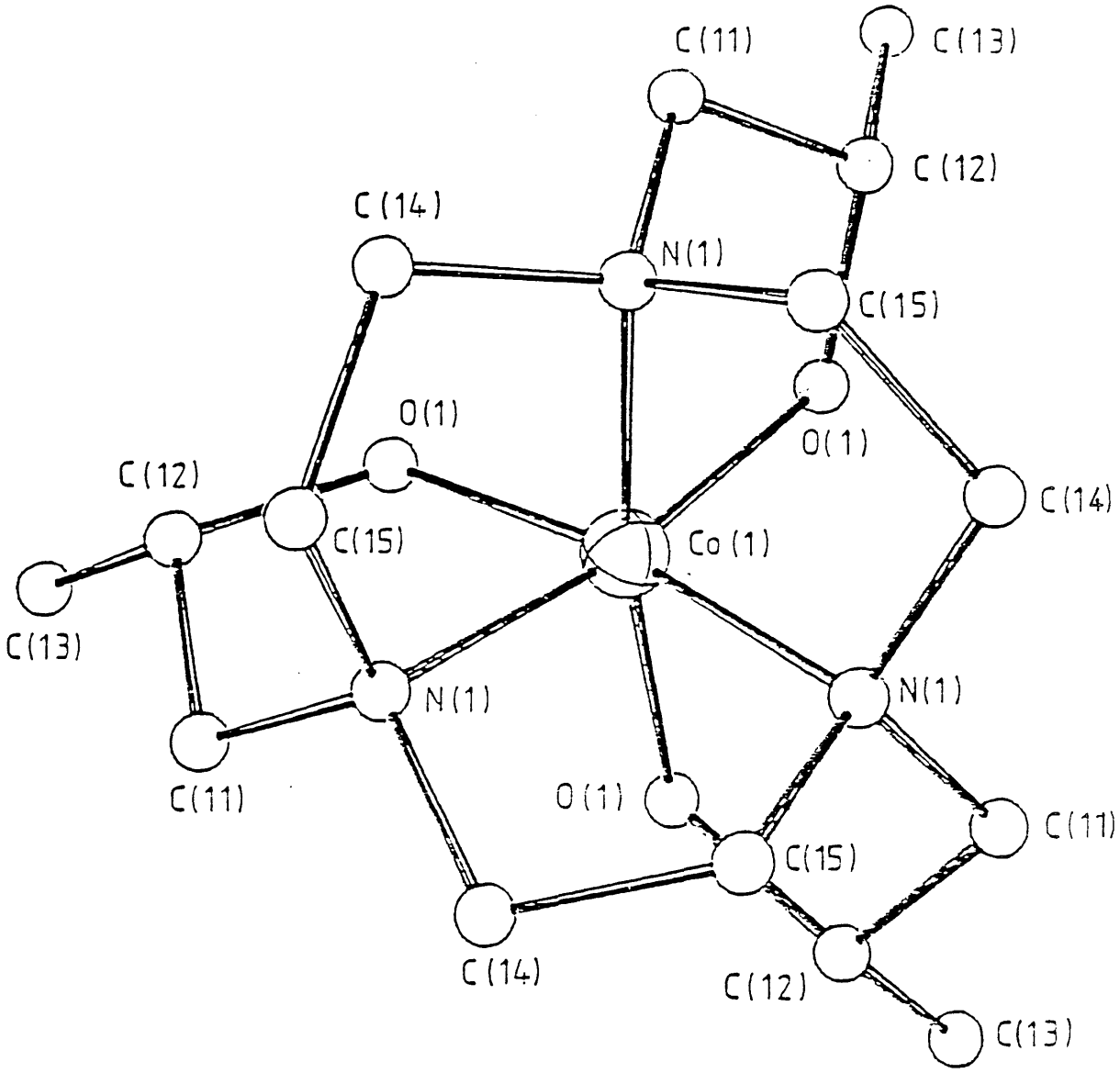

FIGURE 4.13
The view down the C_3 axis of a $[Co(S\text{-}Methetacn)]^{3+}$ unit showing clockwise rotation of the rear donor set (relative to a trigonal prismatic configuration).

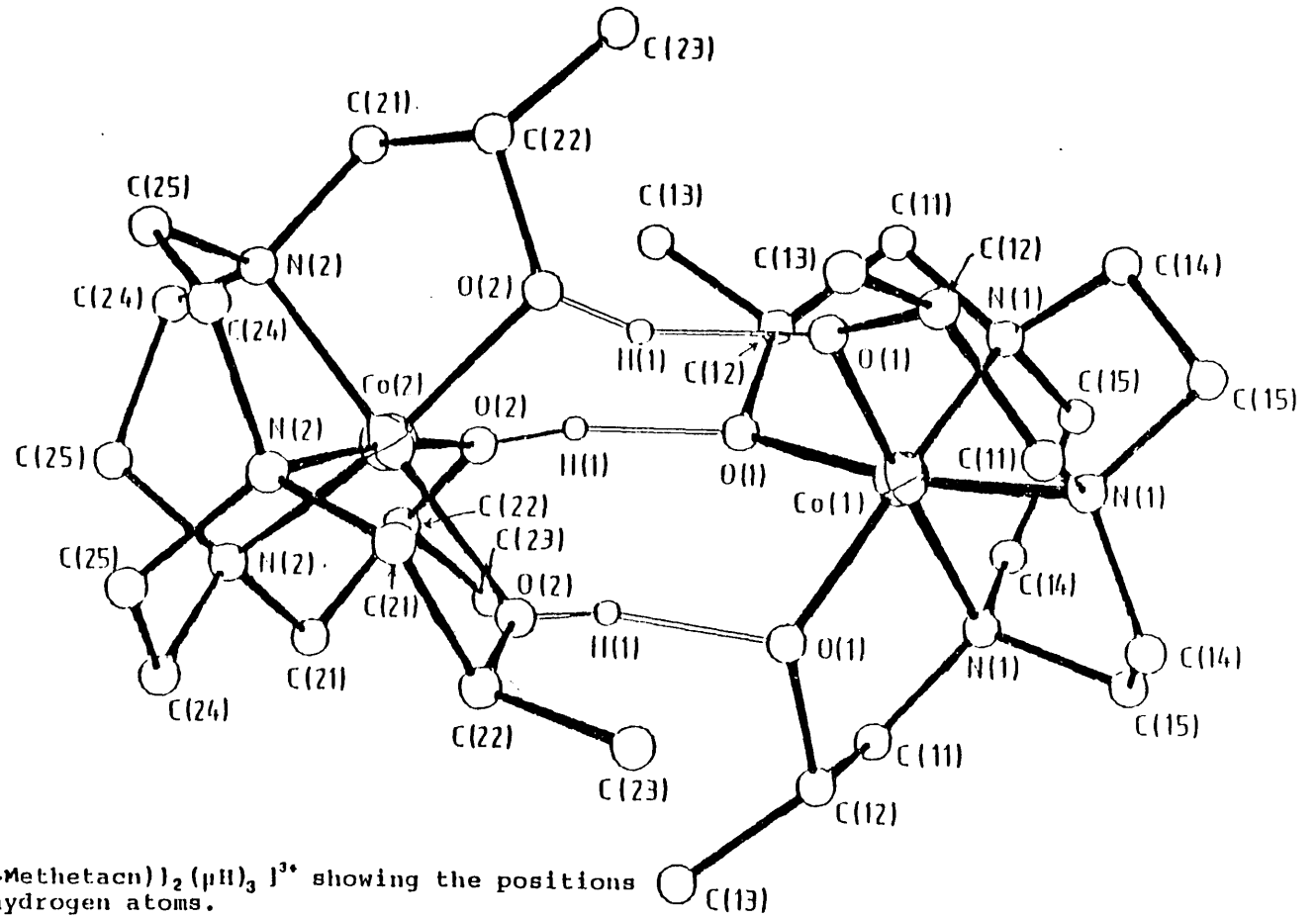

FIGURE 4.14
The dimer $[(Co(S\text{-}Methetacn))_2(\mu H)_3]^{3+}$ showing the positions of the bridging hydrogen atoms.

arms of the ligand was dissociating by protonation in acidic solution. Clearly the protonated alcohol would carry a positive charge and would consequently be expelled from the inner coordination sphere. The question arose as to which species would fill the resulting coordination vacancy. The two ligands present in significant concentration were water and chloride ion. In order to test for chloride ion coordination acidifications were conducted using trifluoroacetic acid, sulphuric acid and hydrobromic acid. In each case the absorption and circular dichroism spectra showed, within experimental error, no deviation from those obtained on acidification with hydrochloric acid. Later experiments involving solvents such as chloroform, ethanol, acetonitrile and dimethyl formamide showed that in the absence of water the solution behaviour of the complex was markedly different.

In order to examine further the aqueous solution behaviour of the Co(III) complexes of (S)-Methetacn, n.m.r. spectra were obtained. Although the methylene and methine resonances were very confused the methyl group, originally introduced only to impart chirality, provided useful evidence. In the basic form (figure 4.10b) there is one resonance due to the methyl group, a doublet at 1.1ppm (J=6.5Hz). This is closely similar to the situation in the free ligand (fig 4.2) although the resonance is at slightly higher chemical shift for the cobalt complex. The sharpness of the doublet indicates that all three methyl groups are equivalent which for this complex implies trigonal

symmetry. The situation obtaining in acidic solutions of the complex is quite different. N.m.r. spectra of such solutions invariably revealed the presence of two distinct methyl environments with integral ratio 2:1 (figure 4.10a). This is taken to be indicative of a situation in which one pendant arm of the ligand differs from the other two and where, in addition, interconversion between the two distinct pendant arm environments, (e.g. by exchange of protons), is sufficiently slow that there is no significant line broadening and two separate resonances are to be observed in the methyl region. It would be expected that, in the form of the complex with one arm dissociated, that arm, being protonated, would carry a positive charge and would thus be responsible for a more electron withdrawn methyl group (figure 4.15).

FIGURE 4.15
The withdrawal of electron density from a methyl group resulting from proximity to a protonated alcohol group.

The consequence of this in the n.m.r. spectrum would be the presence of two methyl resonances (i.e. in the ratio 2:1) with the unique methyl resonance lying to lower field. This

is important because in the unlikely event of two hydroxyisopropyl arms being protonated, the integral ratio of the two doublets would be the reverse of that observed. There is evidence in the literature for dangling hydroxyl arms being replaced by water molecules in a kinetically controlled process in aqueous solution (Ref 94). In the present work there was no perceivable delay between addition of acid or base and observed colour change: nor were the visible/U.V. spectra subject to time dependent change. It would appear from the p.m.r. spectra that in acidic solution dissociation was complete while in strongly basic solution there was negligible dissociation. In aqueous solution the protonation/deprotonation reaction was found to be completely reversible. It is interesting to note that in deutero-acetonitrile solution the hexafluorophosphate salt of the complex presented a unique doublet due to methyl groups indicating that in that environment all three arms were symmetrically equivalent.

4.5.2. Spectroscopy

The vis./U.V. spectra of Co(III)-Methetacn complexes in solution, particularly the circular dichroism spectra, do much to identify the presence of several distinct species and go some way toward identifying these species. The aqueous spectra are of interest because of their pH dependence (figure 4.5 & 4.6). As in the case of $[Co^{III}(tacn)_2]^{3+}$ these are two observed $d \rightarrow d$ transitions neither of which has a zero order electric dipole. The lower energy $^1A_1 \rightarrow {}^1T_1$ transition has symmetry T_1 and is

consequently magnetic dipole allowed while the higher energy transition has symmetry T_2 and is m.d. forbidden. The actual symmetry of the complex is not octahedral but is, rather, C_3 (approximately D_3) so that the degeneracy of these two triply degenerate states in octahedral symmetry is removed to give A_2 and E polarised transitions to the lower energy level and A_1 (forbidden) and E to the higher level. Since no uniaxial single crystal spectra could be obtained, all spectra show the total intensity due to all of the transitions. This is a particularly important factor in the case of c.d. spectra where cancellation of the two oppositely signed transitions under any triplet state (in octahedral symmetry) can give various effects. In octahedral symmetry it is to be expected that the $E(T_1)$ and $A_2(T_1)$ states should be degenerate. It has been found for CoN_6 chromophores that as the chromophore is elongated along its C_3 axis E moves to higher energy than A_2 (Ref 41). The reverse is true when a compression trend is followed through a number of complexes involving CoN_6 chromophores. Another structural factor which may be inferred from c.d. spectra is the absolute configuration. It has already been mentioned that the sign of the twist angle of cobalt complexes may be directly related to the sign of the E and A_2 transitions in $^1A_1 \rightarrow {}^1T_1$ region (a negative twist angle leads to a negative value for $R(A_2)$ and a positive value for R(E)). For any given chromophore it may be further stated that $R(A_2)$ will grow in magnitude if the complex is elongated (e.g. by addition of phosphate ion) at the expense of R(E). This last observation is the

most tentative of the three and cannot be extended to allow comparisons between species.

It is known, from chemical reasoning and from absolute configurational determination on a single crystal sample using the Bijvoet method, (Ref 92) that the organic chiral centres on the ligand (S)-Methetacn have a common (S) configuration. It is also known that the angle, ω, defined as the smaller of the two possible angles between the upper and lower donor sets when viewed down the C_3 axis has a positive sign in the solid state of the complex $[\{Co(S\text{-Methetacn})\}_2 (\mu H)_3](PF_6)_3]$.

From this information it is expected that R(E) would be negative in sign and $R(A_2)$ positive. In the c.d. spectra of the basic form of cobalt(III) complexes of (S)- Methetacn there was no indication of the presence of a negatively signed band. This was of interest because it strongly suggested that the A_2 band had the dominant intensity in the T_1 region. This situation had previously been noted in the cases of $[Co(Metacn)_2]^{3+}$ (Ref 39) and $[Co(tacn)_2]^{3+}$ but was contrary to corresponding results for tris diamine cobalt(III) species. The twist observed in the complex was clockwise (down the C_3 axis) which is conventionally described as Δ . Hammershoi and Sargeson (Ref 59) reported circular dichroism spectra of Δ-$[Co(taetacn)](ClO_4)_3$ in aqueous solution and found it to be bisignate with the E component at lower energy. Taetacn is the N_6 analogue of thetacn. It had also been reported (Ref 43) that the

complex Δ[Co(sep)]$^{3+}$ had only a positive band in the c.d. spectrum in that region which was assigned to dominance of the circular dichroism spectrum by the A_2 transition. The dominance by the A_2 (T_1) component transition appears to be real from consideration of the proximity of the c.d. band maximum to the absorption band maximum of basic samples (e.g. figure 4.4). The acidic samples of Co(III) complexes of (S)-Methetacn recorded invariably had two component bands in circular dichroism in the T_1 region; a positively signed low energy band and a negatively signed higher energy band. In the T_2 region a single positive band was generally observed. The spectra obtained bear a striking similarity, allowing for the blue shift of CoN_6 species, to c.d. spectra of [Co(taetacn)]$^{3+}$. It may be assumed, following the conclusions of Peacock and Stewart (Ref 41) that the lower energy (positive) band is due to the A_2 transition while the higher energy E transition has the negative sign associated with a positive twist angle, ω :assuming no inversion takes place on dissolution. The fact that only one sign is observed for the basic solution of the T_1 region points, not only to A_2 dominance, but also to the near degeneracy of the A_2 and E transitions. The variation in c.d. of acidic solutions of the complex in this region is a measure of the sensitivity of the observed spectra, resulting from cancellation of the two oppositely signed transitions, to change.

An empirical observation is widely quoted (e.g. Ref 41), whereby the degree of elongation of a complex has a bearing

on which of $E(T_1)$ or $A_2(T_1)$ occurs at higher energy. For example in $[Co(\widehat{N\ N})_3]^{3+}$ type complexes it is generally regarded that if the chelate ring angle α is less than 90° the E component should come at lower energy and conversely if $\alpha > 90$ then A_2 should be at lower energy. Several cases are now known where this rule of thumb does not apply (Refs 42 & 48) and [Co((S)-Methetacn)]$^{3+}$ constitutes another such example ($\alpha = 83.95^\circ$). It would appear that although it is true to say that elongation lowers the energy of the A_2 transition relative to that of the E polarised transition it is unrealistic to draw a rigorous dividing line at $\alpha = 90^\circ$. Many factors affect the effective chromophoric symmetry and must be taken into account. For example, in the case of [Co((S)-Methetacn)]$^{3+}$, methyl groups project parallel to the C_3 axis of the complex giving effective elongation without markedly altering the angle, α. It is interesting to note that the angle $N\hat{C}oC_3$ is smaller than the angle $O\hat{C}oC_3$ indicating that the "tacn" half of the complex is elongated while the hydroxyalkyl end is compressed. A similar situation was found to exist in the case of [CoIII(taetacn)]$^{3+}$.

If the assumption is made that for any given cobalt(III) complex elongation results in a rise in energy of the E component relative to the A_2 component, then it would appear that on going from the basic to the acidic form of the complex there is some elongation. In molecules such as $[Co(en)_3]^{3+}$ with three "exocyclic" chelate rings the final shape is a compromise between the tendency of the metal ion

to enforce an octahedral ligand field and the tendency of the chelate rings to axially compress the molecule. Opening of one of the $\overline{MN(C_2H_4)OH}$ chelate rings in the complex $[Co((S)\text{-Methetacn})]^{3+}$ might be envisaged, by release of chelate ring strain, to facilitate elongation. The observed $^1A_1 \rightarrow {}^1T_1$ circular dichroism spectrum is reported to be very sensitive to slight changes in chromophoric environment (Ref 60). In the foregoing C_3 symmetry has been assumed and has been found to be an adequate representation, so far as can be ascertained.

The spectra of the basic and acidic forms have been assigned to hexadentate coordination and effective pentadentate coordination respectively. In an attempt to answer the question as to which species filled the remaining coordination site, various acids were used to effect protonation from basic solutions in order to determine whether there was an observable change from the acidic type species obtained in the presence of hydrochloric acid. In a series of experiments sulphuric acid, trifluoroacetic acid and hydrobromic acid all gave products which were indistinguishable from the HCl form. This was taken as evidence (though far from conclusive) that the sixth coordination site was not occupied by a chloride ion. The most likely alternative was that the sixth ligand was water. It was expected therefore that in solution in the absence of water the generation of the acidic form of the complex would result in some displacement of the absorption maxima (relative to aqueous

samples). The result was much as expected. In order to obtain non-aqueous samples the complex was dried in the case of the chloride salt or precipitated as the PF_6^- salt. In the former case redissolution in ethanol was followed by a second dessication prior to solvent addition in order to expel water: whereas in the latter case recrystallisation from DMF in vacuo was used. It was invariably noted that on solvation absorption due to $^1A_1 \rightarrow {}^1T_1$ occurred at lower energy for solvent samples than for aqueous samples. From table 4.2 two solvent groups may be delineated: those with unisignate c.d. in the T_1 region for the complex (ethanol and chloroform), and those with a bisignate c.d. (CH_3CN and DMF). It is felt that this is significant only in highlighting the sensitivity of the observed circular dichroism in this region to small changes in the two component transition intensities. It is interesting to note that the n.m.r. spectrum of the PF_6^- salt of the complex dissolved in deutero acetonitrile (fig 4.12) showed no inequivalence of the methyl groups while the c.d. spectrum was of the bisignate form.

4.5.3. The Nature of the Species in Solution

In view of the dimeric nature discovered in the solid state the question arises as to the nature of the complex in solution: particularly since micro-analysis of a chloride salt of the complex implied the monomeric species $[Co(S\text{-Methetacn})]Cl_3$. The addition of sodium selenite provided a potential means of distinguishing between monomeric and dimeric species in solution. However the

results of experiments based on selenite addition were inconclusive in establishing the existence of monomeric solution species. Interestingly Evreev (Ref 95) postulated that in solution the complex $[Co(MEA)_3]X_3$, where MEA is monoethanolamine, can form $[Co_2(MEA\text{-}H)_3(MEA)_3]^{3+}$. This species is exactly analogous to that found in the $[\{Co(S\text{-}Methetacn)\}_2(\mu H)_3](PF_6)_3$ crystal structure. The relative intensities of the $A_2(T_1)$ and $E(T_1)$ bands in circular dichroism would tend to indicate that the species existing in basic solution were more elongated than those in acid solution. However, care is required in deriving conclusions from the relative strengths of the intensities of these transitions because of cancellation effects.

Another question which arises relates to the number of species in solution. Column chromatography distinguished three species originating from a neutral aqueous solution of the complex. Two of these species gave bisignate circular dichroism in the T_1 region and one gave unisignate c.d. spectra. It was apparent that the wavelength of maximum absorption of the purple species was less than that obtained using strongly basic solution implying the presence of at least one other species beyond those separated on the column. Figures 4.5 and 4.6 show typical c.d. and absorption spectra at selected pH values. The absence of an isosbestic point is only one of the features which points to the presence of more than two species in solution. The c.d. spectra are much more sensitive to small changes and it is in the optical activity that the presence

of species other than those prevailing in strongly acidic or basic solution is most obvious. In figure 4.5 the spectra at acidic pH were consistent through to pH ~ 3.3 where the spectrum was entirely positive in sign. At pH 8.37 the feature at ~550nm was a positive band whereas in acidic solution a negative band had its maximum at that wavelength. As the pH was raised further the positive ingrowth at 550nm declined so that by pH 12.5 the dominant positive band was that at ~610nm. In order to explain the observed trend it has been assumed that the lower energy band belongs to the $^1A_1 \longrightarrow {}^1A_2$ transition while the higher energy band is that belonging to the $^1A_1 \longrightarrow {}^1E$ transition. The band maxima observed are not those of the two transitions since cancellation of the two bands plays an important part in determining the observed spectra. The interpretation attached to these spectra is that at low pH values the E polarised transition is dominant and cancels out all but the low energy tail of the A_2 band. As the pH is raised the molecule is effectively elongated so that A_2 becomes progressively more intense at the expense of E until pH 3.31. The energy of the E component is then markedly decreased to ~600nm cancelling the centre of the A_2 band but leaving the wings with sufficient intensity to give the appearance of two peaks. A further increase in pH reverses the migration of the $^1A_1 \rightarrow {}^1E$ transition and is accompanied by the continued growth of A_2 at the expense of E. The spectra shown represent a selection from approximately forty recorded throughout the pH range and it should be appreciated that the c.d. spectrum at pH 8.87

(and the accompanying absorption spectrum) while superficially anomalous, are nevertheless supported by similar spectra in the same pH range. It would appear therefore that a third species exists in solution between pH 7.5 and 9.3.

The solvent spectra (table 4.2) relating to the cobalt species (as both chloride and hexafluorophosphate salt) show a regularity in absorption spectra, particularly for the $A_1 \rightarrow T_1$ region, which is accompanied by an equally marked irregularity in the circular dichroism spectra. This has been interpreted as another manifestation of sensitivity of the orientationally averaged $A_1 \rightarrow T_1$ circular dichroism to small changes in environment. What is more significant is the shift ($\sim$15nm with respect to the basic form) to higher wavelength of absorption which was invariably found to accompany solution in organic solvents. Perhaps even more significant was the observation that a potassium bromide disk containing the dimeric complex $[\{Co((S)\text{-Methetacn})\}_2(\mu H)_3](PF_6)_3$ also showed a shift to lower energy in absorbance compared to aqueous samples (also table 4.2). While the absorption spectra of the dimer bore a strong similarity to those of solvent samples the same could not be said of the c.d. spectra. The solid state (randomly oriented) circular dichroism spectra of $[\{Co(S\text{-Methetacn})\}_2(\mu H)_3](PF_6)_3$ showed much stronger optical activity (as measured by the dissymmetry factor, g). The reason for this could be an increase of dissymmetry about the chromophore imposed by the lattice. However the

effect has undoubtedly been exaggerated by an increased energy gap between the E and A_2 polarised transitions which has reduced the cancellation of c.d. intensity resulting from these two oppositely signed bands.

4.5.4. The Crystal Structure

The crystal structure of $[\{Co(S\text{-Methetacn})\}_2 (\mu H)_3](PF_6)_3$ shows several interesting features not least of which is the H-bonded dimerisation involved. The O-H distance measured was 1.62Å which compares with $\sim$ 1.38Å for the hydrogen bonds between water molecules. The absence of three protons (relative to the species expected in basic aqueous solutions) decreases the number of counter ions required from six to three. These ions (hexafluorophosphates) are positioned along the extended C_3 axes of the molecules.

The aspects of the structure relating to optical activity are of particular interest. The dimer in figure 4.14 shows six asymmetric carbon atoms, all in the expected S-configuration. This confirms the stereospecificity of the ligand synthesis. The conformations of the chelate rings are important in determining the form of the circular dichroism spectrum - if only because they determine the sign and extent of the chromophoric twist. In $[Co(S\text{-Methetacn})]^{3+}$ two distinct chelate ring types may be differentiated. The endocyclic rings are those encompassed by the macrocyclic moiety while the exocyclic rings are those with a ligating oxygen atom. The crystal structure

shows the endocyclic rings to be fixed, without exception, in the λ conformation (N-C-C-N torsion angle = 45·4) : the exocyclic chelate rings are, again without exception, in the δ conformation (N-C-C-O torsion angle = 45.5°). The sign of the twist in each of these rings is dictated by the chirality of the asymmetric carbon atom although the effect of the chiral centre on the magnitude of the twist is thought to be minimal. In other words the thetacn analogue of $[Co(S\text{-}Methetacn)]^{3+}$ should have approximately the same geometry as that depicted in the crystal structure of its chiral analogue but would be racemic in solution. Observation of figure 4.13 reveals that the twist about the cobalt atom is clockwise looking down the C_3 axis. This form is designated Δ . The overall symmetry of the complex may be summarised as $[(S)_3\ \Delta\ (\lambda\delta)]_2$. The first lower case Greek letter refers to the endocyclic rings, the second to the exocyclic rings.

4.5.5. Comparison to $[Co(taetacn)](ClO_4)_3$

It is instructive to compare the structure found in the case of $[Co(S\text{-}Methetacn)]^{3+}$ with that reported (Ref 60) for the related species $[Co(taetacn)]^{3+}$. Taetacn is tris-(2-aminoethyl)-1,4,7-triazacyclononane.

$[Co(taetacn)]^{3+}$ was found to adopt a Δ(λδ) geometry which is exactly that found in the $[Co(S\text{-}Methetacn)]^{3+}$ case. This similarity is, in part, coincidence since the crystal of the $Co(N_6)$ species selected might equally well have been the enantiomer Λ (δ λ) : the same is not true in the case of Co(S-Methetacn).

Taylor, Snow and Hambley conducted energy minimisation calculations on the conformational isomers of $[\Delta\text{-Co(taetacn)}]^{3+}$ (Ref 60). Having identified sixteen possible conformers they eliminated twelve because of the absence of C_3 symmetry. The remaining four: $\Delta(\delta\delta)$, $\Delta(\lambda\delta)$, $\Delta(\delta\lambda)$ and $\Delta(\lambda\lambda)$, were subjected to energy minimisation calculations which confirmed $\Delta(\lambda\delta)$ as the lowest energy conformer. The model employed to calculate the minimum energy conformation used the following energy terms; bond length deformation (E_b), non-bonded interactions (E_{nb}), valence angle deformation (E_θ) and torsion angle strain (E_ϕ). It was found that the low energy of the $\Delta(\lambda\delta)$ conformation relied largely on the minimisation of non-bonded interactions and torsional strain energy. There is every reason to expect that the same terms dominate the conformational energy considerations of $[\text{Co(S-Methetacn)}]^{3+}$. In addition to confirming the solid state structure the energy minimisation calculations indicated that the geometry observed in the crystal structure was not a consequence of lattice constraints and was equally likely to predominate in solution.

The solution circular dichroism spectrum of $[\Delta\text{-Co(taetacn)}]^{3+}$ was reported (Ref 59) and was remarkably similar to that of acidified $[\text{Co(S-Methetacn)}]^{3+}$.

Some important parameters, derived from the structures of

$[\{Co(S\text{-}Methetacn)\}_2(\mu H)_3](PF_6)_3$ and $[Co(taetacn)](ClO_4)_3$ are listed in table 4.7.

The angle (N or O)$\hat{C}oC_3$ is very similar in the two cases and represents slight compression of the complex in the region of the exocyclic ligating group. This is in contrast to the N$\hat{C}oC_3$ angle which shows elongation of the molecule (relative to the octahedral situation of 54.73°) at the end possessing the macrocyclic moiety. This situation was expected on the basis of observations on species such as $[Co(en)_3]^{3+}$ and $[Co(R\text{-}Metacn)_2]^{3+}$. The angle α, at the cobalt atom in the exocyclic chelate rings, is smaller in the case of $[Co(S\text{-}Methetacn)]^{3+}$ than in the CoN_6 analogue, presumably as a result of the requirement to include the shorter Co-O bonds, at the expense of the Co-N bonds, into the chelate rings.

TABLE 4.7

SOME PARAMETERS OBTAINED FROM CRYSTAL STRUCTURES

	$[Co(S\text{-}Methetacn)]^{3+}$	$[Co(taetacn)]^{3+}$
(N or O)$\hat{C}oC_3$	55.47°	55.42°
N$\hat{C}oC_3$	53.95°	52.86°
α	83.95°	84.89°
Trigonal Twist	11.2°	11.1°
Co-(O or N)	1.939Å	2.009Å
Co-N	1.949Å	1.963Å

4.6 Conclusions Relating to Cobalt Complexes of Methetacn.

The aim of this project was to relate structural parameters to observed circular dichroism and it is therefore most convenient to start with the complex for which the crystal structure data are available and to progress to other more tentative structures. The crystal structure was sufficiently well resolved to allow determination of absolute configuration (figure 4.13). Each of the organic chiral centres was found, as expected, to be in the (S) configuration. The complex would be expected to be twisted such that a helical disposition of the nitrogen donor triangle with respect to that of the oxygens would be observed. The presence of the methyl groups would not be expected to add significantly to the magnitude of the twist: however it would ensure that all of the chromophores experienced the same direction of twist (i.e. racemisation would be very unlikely). The observed twist on going from the top donor set to the bottom donor set was clockwise (ω is therefore positive). From the empirical rule devised by Peacock and Stewart (Ref 41) a positive value of ω should be accompanied by a negative differential extinction coefficient of the $A_1 \rightarrow E(T_1)$ band. This being the case it is concluded that the E polarised transition comes at higher energy than the A_2. There is an empirical rule relating elongation of a Co(III) chromophore to the relative energy levels of the $E(T_1)$ and $A_2(T_1)$ transitions. It has been suggested that when the angle α, in this case spanned by the exocyclic chelate rings, was

90° the two levels should reach degeneracy : at angles of less than 90° the E component has often been found at lower energy (Refs 31 & 73). However the present findings support others which suggest that an inflexible 90° value of α at the cross-over point is unrealistic bearing in mind the effects on the circular dichroism of the position of the ligand bulk and the nature of the ligating species. It was concluded in consideration of the structure elucidated by X-ray analysis, and of the circular dichroism spectrum of a KBr disk of the same sample, that the lower energy band was the $^1A_1 \rightarrow {}^1A_2$ transition with a positive sign and that the higher energy band corresponded to the oppositely signed $^1A_1 \rightarrow {}^1E$. In the $^1A_1 \rightarrow {}^1T_2$ region the E polarised transition was found to have a positive sign. This is in good agreement with the findings of Hammershoi and Sargeson (Ref 59) for the enantiomeric form Δ-[Co(taetacn)]$^{3+}$ and confirms their statement that small variations in atomic position can be crucial to the observed energy orderings.

The various solvent samples, obtained by dissolution of chloride and hexafluorophosphate salts of the complex, show strong similarity in the wavelength of the $^1A_1 \rightarrow {}^1T_1$ absorption band which occurred at around 555nm. It is tempting to conclude that in solvent samples the dimeric cation [{Co((S)-Methetacn)}$_2$ (μH)$_3$]$^{3+}$ predominates. However it should be borne in mind that micro-analysis indicated the presence of a monomer, with chloride counter ions, isolated from aqueous solution. Of the non-aqueous solutions only that with DMF as solvent is sufficiently similar to the

solid sample, spectroscopically, to be labelled, with any degree of certainty, as a dimer. In both the KBr disk and DMF solution spectra a considerable splitting is observable between the energies of the two $^1A_1 \rightarrow {}^1T_1$ component bands and possibly as a consequence of this the residual wing intensities due to the $^1A_1 \rightarrow {}^1E$ and $^1A_1 \rightarrow {}^1A_2$ bands were stronger in these two cases than in others encountered. The other solvent spectra (in ethanol, chloroform and acetonitrile) showed remarkable spectral similarity with band maxima in absorption at 555-557nm (T_1) and 386-390nm (T_2) and positive, approximately unisignate, circular dichroism in the T_1 region. The chemistry of these species was not extensively investigated: however, from n.m.r. spectra in CD_3CN and $CDCl_3$, it would appear that all three methyl groups were equivalent indicating trigonal symmetry. The unisignate nature of the c.d. points to near degeneracy of the E and A_2 states which in turn implies a lowered trigonal splitting and possibly a less pronounced twist at the cobalt atom than in the solid state complex.

The aqueous solution behaviour of this species is at the same time intriguing and complex. In strongly basic samples (fig 4.4) the species which exists has absorption bands at 558nm and 395nm and could arguably be assigned to the same dimeric structure observed in the crystal, on the basis of absorption spectroscopy. The p.m.r. spectrum of a basic sample showed three equivalent methyl groups. Column chromatography of a neutral sample resulted in three bands (fig 4.3) the first of which was typical of a basic type

c.d. spectrum, both in purple colour and in the dominance of the A_2 transition. However, the maximum intensity of the $A_1 \rightarrow T_1$ absorption band occurred at 540nm, some 15nm below that of strongly basic solutions. If it is assumed that the purple band from the chromatography column represented a single species then the conclusion must be drawn that another purple form of the complex exists at higher pH. In acidic solutions the absorption is somewhat less intense than in basic samples. A migration of λ_{max} to 528nm, with concommitant colour change, was also observed on acidification. The circular dichroism of acidic samples was invariably found to be bisignate with the higher energy, negative, and presumably E polarised, transition dominant. The n.m.r. spectra of strongly acidic samples (eg fig 4.10a) showed two distinct methyl resonances in the ratio 2:1 from which it was concluded that one of the hydroxyisopropyl arms of the complex had become dissociated. The sharpness of the resonances due to the methyl groups is a measure of the stability of the arm-dissociated form in acidic solution. The growth to dominance of the E polarised transition in the c.d. spectrum on acidification indicates an increase in bulk about the equatorial region of the complex, possibly due to the presence of a ligating water molecule in addition to the dissociated pendant arm.

The pKa curve obtained spectroscopically for this system (fig 4.7) is slightly less regular than would be expected for a straight-forward acid/base (2 species) reaction. The

presence of more than two species is evidenced by the absence of an isosbestic point in the absorption spectra recorded over a range of pH values.

It is postulated that with increasing acidity a dimeric species, similar to that observed in the solid state, decomposes to form two trigonally symmetric monomers in which the ligand is hexadentate and that at still lower pH these monomers become non-trigonally symmetric, by a mechanism which involves dissociation of one pendant arm on each monomer and its replacement by a water molecule.

The existence of a trigonally symmetric monomer was supported by analyses of basified aqueous samples which had been oven dried at $\sim 60^{\circ}C$. The analyses suggested (Section 2.3.6.1) that the species thus obtained was [Co((S)-Methetacn)]Cl_3 which was found to be extremely hygroscopic.

4.7 [Co(thetacn)]$^{3+}$

The species [Co(thetacn)]$^{3+}$ was prepared as outlined in Section 2.3.5.1. It was purified by passing it down a 30cm chromatography column charged with SP-Sephadex using 0.1M sodium chloride solution as eluent. There was some evidence of partial resolution into a red and a (faster) blue fraction on the column. The eluted samples were evaporated to dryness under vacuum and the cobalt complex was extracted from the alkali halide by use of ethanol. Reprecipitation gave a brittle purple film which was found

to be extremely hygroscopic, like its chiral analogue. The sample was stored under vacuum and weighed samples were removed to enable calculation of extinction coefficients. Two separate determinations of ε were carried out: one at pH 10.93 and the other at pH 1.15. The technique used was to make up a solution from a known weight of dry sample and a pipetted volume of water. From this stirred sample, two aliquots were pipetted into volumetric flasks which were then topped up with hydrochloric acid solution or sodium hydroxide solution as appropriate. The resulting solutions were stirred to ensure homogeneity and small samples were used for spectroscopic examination: the remainder being used to measure the pH. The two absorption spectra obtained are shown figure 4.16. In the basic spectrum (dashed line) the two bands $A_1 \rightarrow T_1$ and $A_1 \rightarrow T_2$ occurred at 560nm and 399nm with extinction coefficient of 198 l mol^{-1} cm^{-1} and 136 l mol^{-1} cm^{-1} respectively. In the acidic form the lower energy band had its maximum at 530 nm (ε =149) and the higher energy band peaked at 369nm (ε = 96). Clearly there are close similarities between the chemistry of $[Co(thetacn)]^{3+}$ and $[Co(Methetacn)]^{3+}$. The basic form of the latter has bands at 558nm (ε = 232) and 397nm (ε = 178) while the acidic form has maxima at 527nm (ε = 164) and 388nm (ε= 134). A comparison of the absorption spectra of solutions of these two species reveals that the extinction coefficients due to $[Co(S\text{-}Methetacn)]^{3+}$ species are on average 25% stronger than those of thetacn analogues. This is considered too large a difference to have resulted from experimental errors and must therefore

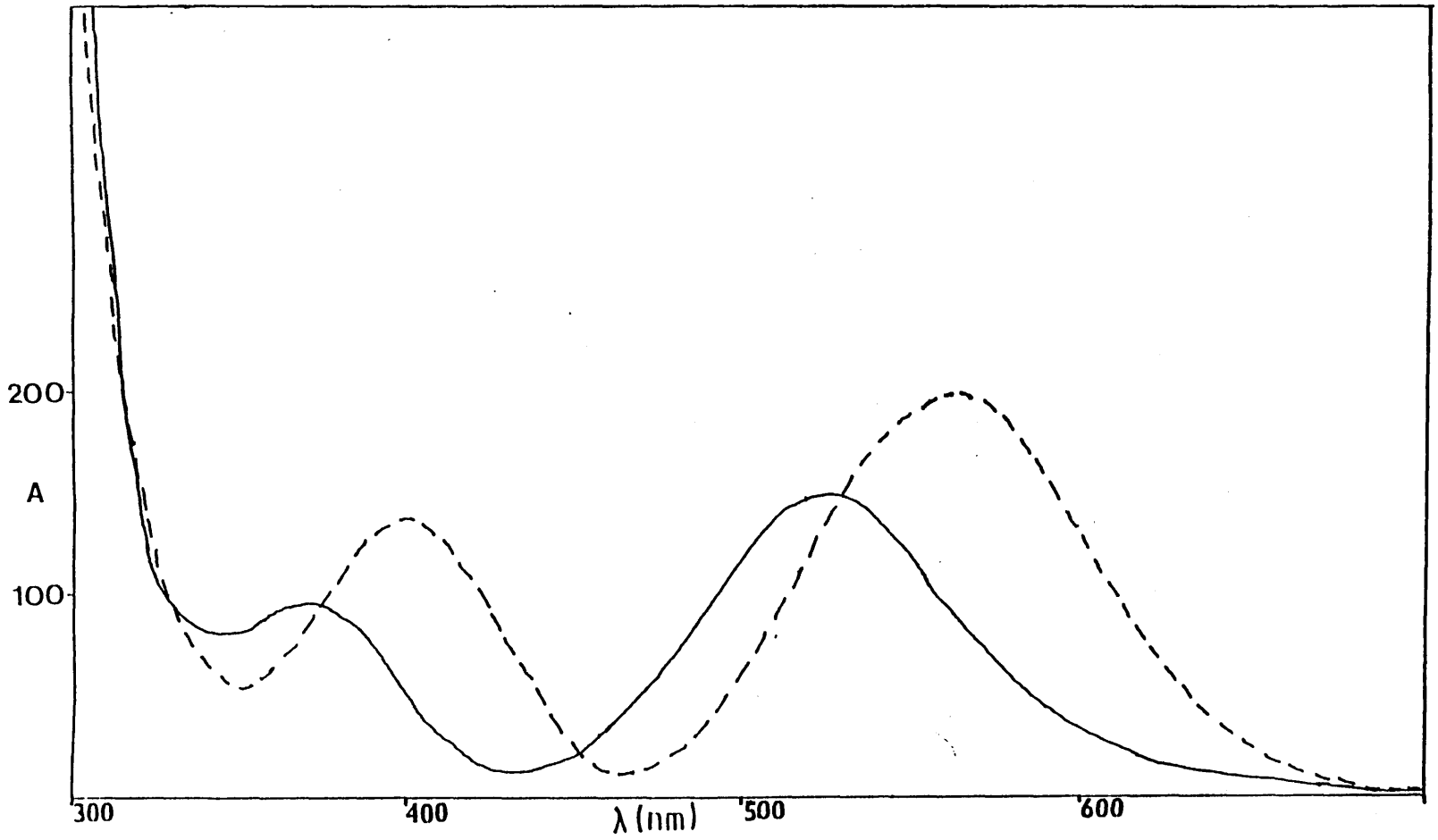

FIGURE 4.16
The absorption spectra of acidic (——) and basic (---) aqueous solutions of $[Co(thetacn)]^{3+}$.

have resulted from greater dissymmetry of the complex in the case with hydroxyisopropyl arms. This would suggest lower symmetry about the chromophore in the chiral sample which would not be expected since the methyl groups on chelate rings are significantly removed from the chromophore.

The positions of the band maxima of the basic forms show very good agreement with a slightly weaker ligand field indicated, perhaps surprisingly, for the thetacn complex. It may be that the lower extinction coefficients and lower energy ligand field are caused by ring-flipping between the two enantiomeric extrema. The situation in the spectra of the acidic solution is complicated by a rising background. However it would appear, on the evidence of the $A_1 \longrightarrow T_1$ band, that in this form also it is the Methetacn complex which has the stronger ligand field. The acidic form in each case was found to have an apparently stronger field than the basic form. However, circular dichroism spectra of $[Co((S)\text{-Methetacn})]^{3+}$ showed that the change accompanying protonation resulted in a change in the intensities of the two component transitions which was observed in absorption as a change in the energy of the band. There is every reason to believe that $[Co(thetacn)]^{3+}$ behaves likewise.

Resolution of racemic $[Co(thetacn)]^{3+}$ into two enantiomers was attempted by column chromatography. A basified sample of the complex was charged on a 90cm column packed with SP-Sephadex ion exchange resin which had previously been

washed with 0.01M sodium antimonyl-(+)-tartrate. The column was eluted, over a period of four days, with approximately 4 litres of 0.01M sodium antimonyl-(+)-tartrate during which time a single deep purple fraction moved down the column. On elution the band spanned some 3cm of column and so it was possible to test for optical activity in the early and late fractions by transferring samples to optical cells and recording circular dichroism spectra. No circular dichroism was observed. It may be possible to resolve $[Co(thetacn)]^{3+}$: however all attempts made in the course of this work failed.

An attempted generation of optically active $[Co(thetacn)]^{3+}$ from thetacn.HCl and [Co((+)-tartrate)] by chiral induction failed to give a reaction.

4.8. Copper Complexes of (S)-Methetacn

A copper complex of (S)-Methetacn was formed as outlined in Section 2.3.6.2 and was recrystallised from chloroform *in vacuo* (because of the hygroscopic nature of the blue complex). The resulting solid was weighed and an aqueous solution made up to allow calculation of the molar extinction coefficient by the same method as that previously used for $[Co(thetacn)]^{3+}$. The spectra of copper(II) complexes are simplified by application of the positive hole formalism which allows them to be treated in the same way as d^1 systems.

Thus, a single broad band is observed in the visible region of copper(II) complexes although the asymmetry of the band often gives the impression that more than one transition is involved and indeed the lack of symmetry in the band is a manifestation of the Jahn Teller effect acting on the chromophore. Conventionally Cu(II) species distort by elongation along the Z-axis. $[CuII((S)Methetacn)]^{2+}$ was not well suited to this geometry since the facial binding of the tacn moiety ensured that one of the amine donors was situated on a Z-axis site. However, in view of the propensity of the analogous Co(III) species to dissociate a hydroxyalkyl arm, it was expected that the tendency towards weak bonding in the Z direction would result in protonation of an arm in the Cu(II) complex at relatively high pH.

The spectra in figure 4.17 (absorption and circular dichroism) of aqueous solutions of $[Cu((S)-Methetacn)]^{2+}$ at pH 11.96 (dotted line) and 4.90 (full line) represent the observation that at high pH solutions of the complex were deep blue while at low pH the solutions appeared to be almost colourless. As with the cobalt(III) case it was found that conversion between acidic and basic forms was completely reversible.

Table 4.8 summarises the main parameters determined for the acidic and basic forms of the species.

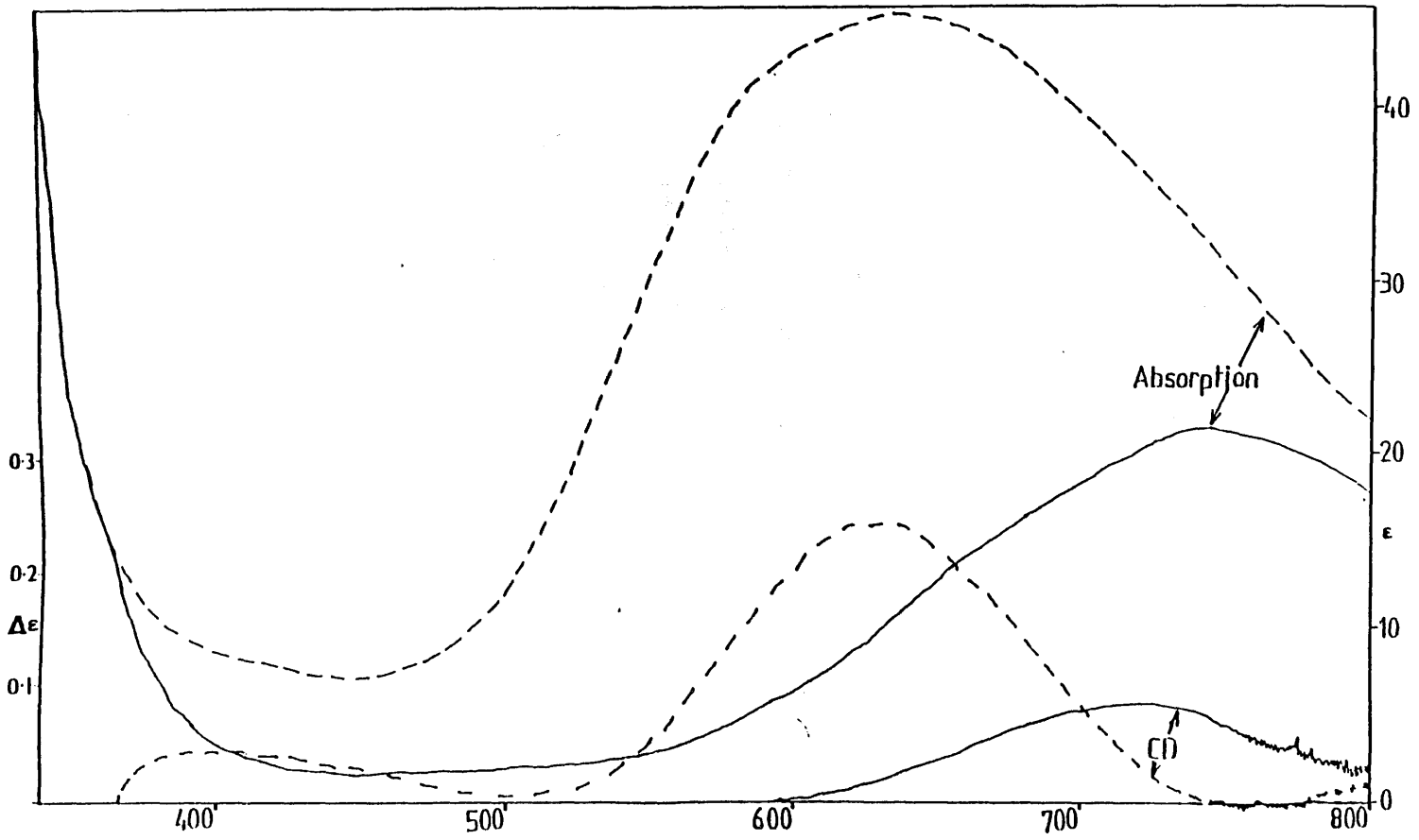

FIGURE 4.17
The absorption and c.d. spectra of the copper complexes of S-Methetacn in solution at pH=11.96 (- - -) and pH=4.90 (——).

TABLE 4.8

THE VARIATION OF $[Cu(S\text{-}Methetacn)]^{-}$ SPECTRA WITH pH

pH	λmax abs	εmax	λmax c.d.	Δεmax	g
4.90	741nm	21.7	716nm	86.8×10^{-3}	4.0×10^{-3}
11.96	636nm	45.2	629nm	0.244	5.4×10^{-3}

Since Cu(II) species can be treated as having a single d-electron it follows that, ignoring the Jahn Teller effect, the position of the single $d \rightarrow d$ transition represents Δ_o, the ligand field strength. Thus from table 4.8 it may be concluded that the Δ_o of the basic form of the complex is $15723cm^{-1}$: while that of the acidic form is $13495cm^{-1}$. This difference is to be expected in consideration of the presumed hexadentate nature of the ligand in the former case and its presumed pentadentate nature in the latter. Approximate D_3 symmetry is postulated for the basic complex so that E polarised transitions should be excited by light propagated along the Z axis while A polarised transitions should be excited by light propagated in the XY plane. In practice a unisignate positive c.d. spectrum was recorded in each case indicating the dominance of the positive component transition. The separation between the absorption and c.d. maxima in each case gave a measure of the extent of trigonal splitting of the ligand field which was greater for the form existing in basic solutions. This splitting ($471cm^{-1}$ in the basic case: $175cm^{-1}$ in acidic solutions) was postulated to result from

the additional twist about the chromophore occasioned by the imposition of a third exocyclic chelate ring. The lessening in intensity with lowering of pH was monitored by means of a series of buffered solutions and the results constitute figures 4.18 and 4.19. Figure 4.18 shows the spectra recorded at eight representative pH values while figure 4.19 shows the variation of the absorbance at 600nm with pH. The latter figure shows that the most pronounced changes in absorption with pH occurred at around pH 11 supporting the initial expectation that the Jahn Teller distortion of the complex would facilitate dissociation of a hydroxy-isopropyl arm. The observed pseudo pKa in the copper(II) case was in the region of the value of 11.52+0.04 measured by Hancock et al (Ref 58) for the free ligand thetacn.

4.9. [NiII(S)-Methetacn)]$^{2+}$

[NiII(S)-Methetacn)]$Cl_2.3H_2O$ was prepared by the method outlined in Section 2.3.6.3 and was purified by column chromatography on an SP-Sephadex column using 0.1M NaCl as eluent. The eluted samples were combined and taken to dryness (in a rotary evaporator). Separation from sodium chloride was effected by extraction into ethanol and reprecipitation by evaporation. The resulting purple acicular solid was weighed and dissolved in a known volume of water in order to allow calculation of molar extinction coefficient values. The spectra of the complex were found to be invariant over the pH range investigated (1-12). Hancock et al (Ref 56) reported that oxidation of the

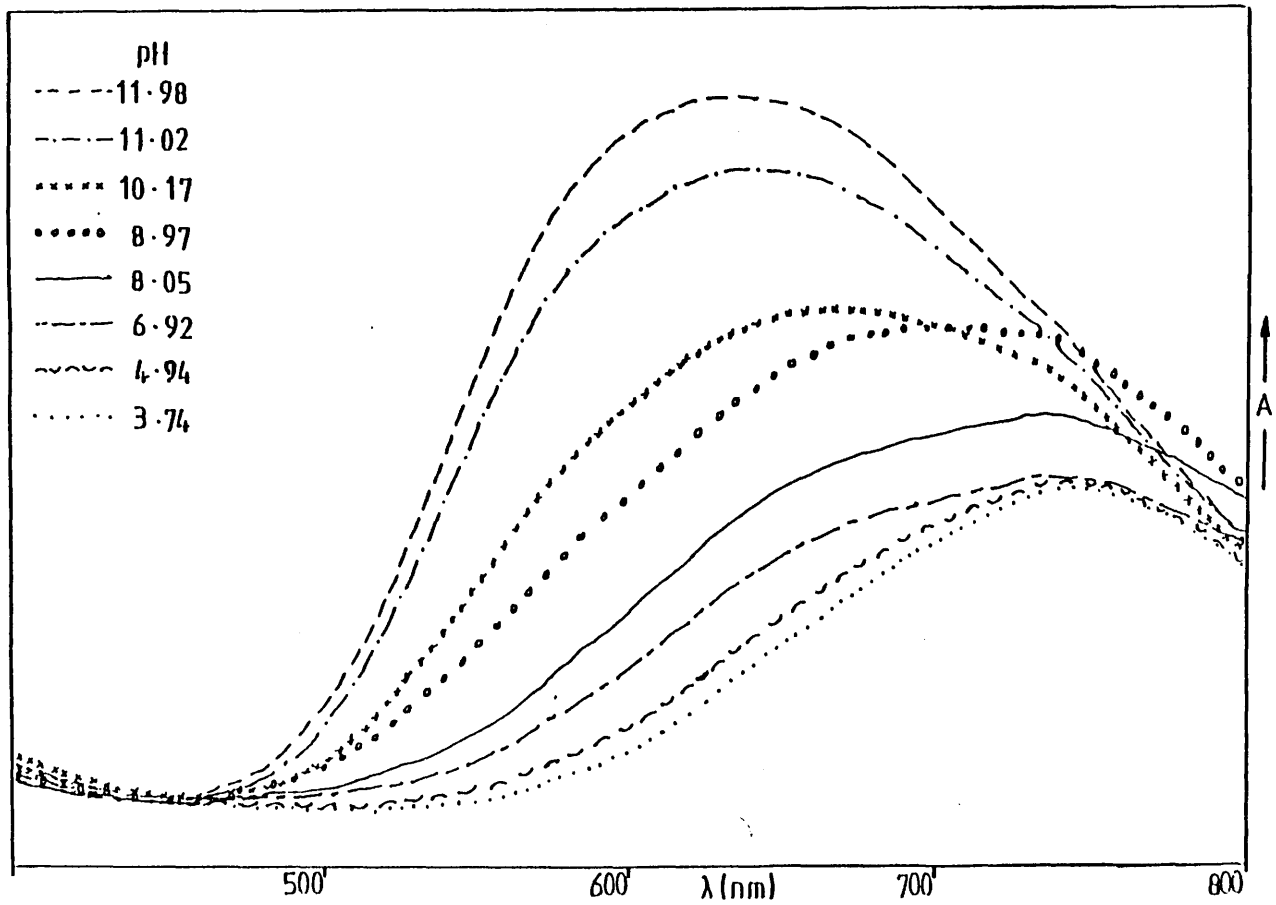

FIGURE 4.18
The absorption spectra of $[Cu(S\text{-}Methetacn)]^{2+}$ at eight representative pH values.

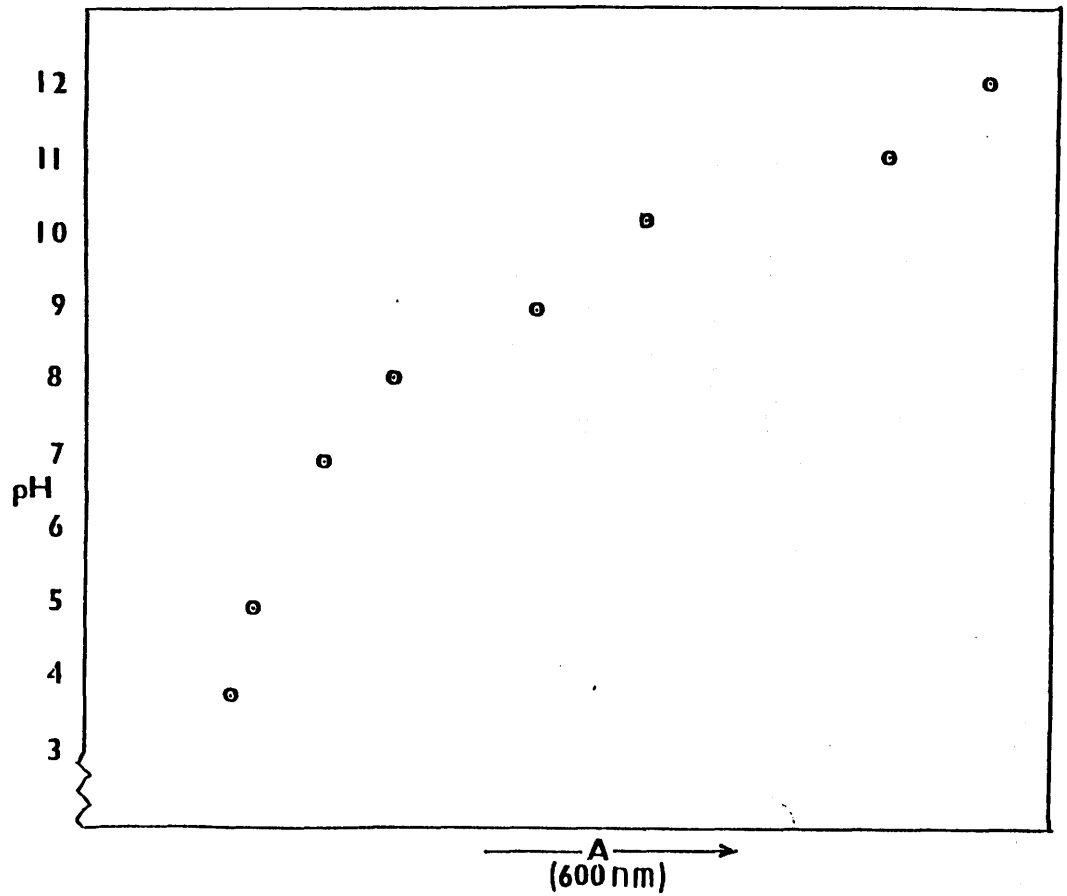

FIGURE 4.19
The plot of pH versus (absorbance at 600nm) for $[Cu(S\text{-}Methetacn)]^{2+}$.

related species [NiII(tcta)]$^{2+}$ to [NiIII(tcta)]$^{3+}$ could be achieved by prolonged exposure to dilute nitric acid: this technique did not prove to be applicable to [NiII (S)-Methetacn)]$^{2+}$.

The electronic spectra of NiIII complexes in the vis/NIR region comprise three spin allowed bands and one spin-forbidden band. Examples of spectra of a $NiIIN_6$ and a $NiIIO_6$ chromophore are shown in figure 4.20. By the rule of average environment the spectrum of the nickel complex of (S)-Methetacn, being a NiN_3O_3 system, would be expected to be intermediate between these two extremes. Three broad bands are distinguishable in each case. The lowest in energy results from transitions from the ground $^3A_2$ state to the $^3T_2$(F) state. The middle band corresponds to the $^3A_2 \rightarrow {}^3T_1$ (F) transition while the highest energy transition observed is $^3A_2 \rightarrow {}^3T_1$ (P). An important feature of the electronic spectrum of [Ni$(H_2O)_6$]$^{2+}$ is the shoulder at ~690nm on the $^3A_2 \rightarrow {}^3T_1$ (F) band. This effect results from spin-orbit coupling which mixes the $^3T_1$ (F) band and the nearby spin-forbidden $^3A_2 \rightarrow {}^1E$ transition. The effect is also present in the [Ni$(NH_3)_6$]$^{2+}$ spectrum although it is less pronounced as the ^1E band lies at the higher energy edge of the $^3A_2 \rightarrow {}^3T_2$ (F) band.

Figure 4.21 shows the absorption spectrum for [NiII ((S)-Methetacn)]$^{2+}$ along with the corresponding c.d. spectrum. The band features from the spectra are detailed in table 4.9.

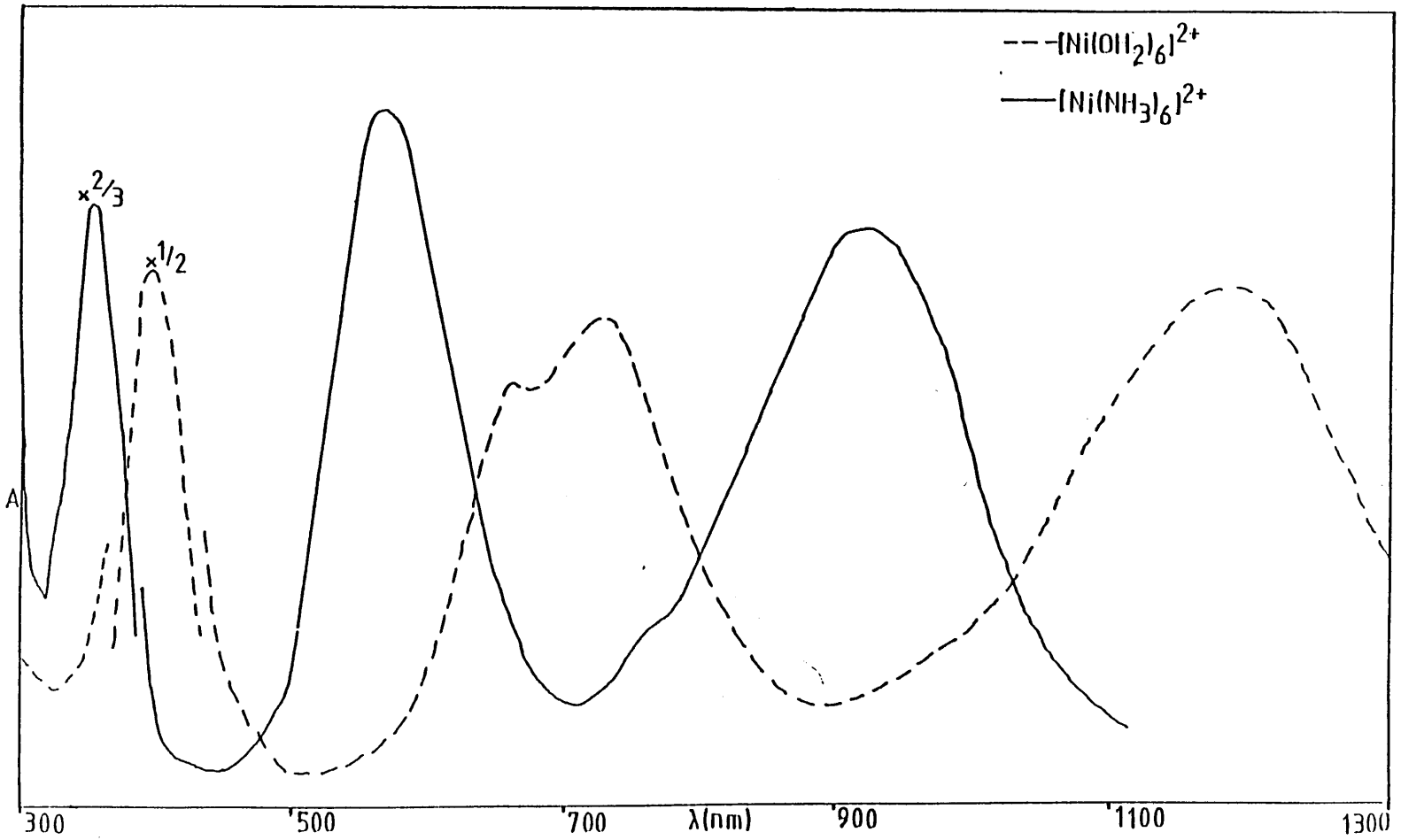

FIGURE 4.20
The absorption spectra of a $Ni^{II}O_6$ chromophore and a $Ni^{II}N_6$ chromophore.

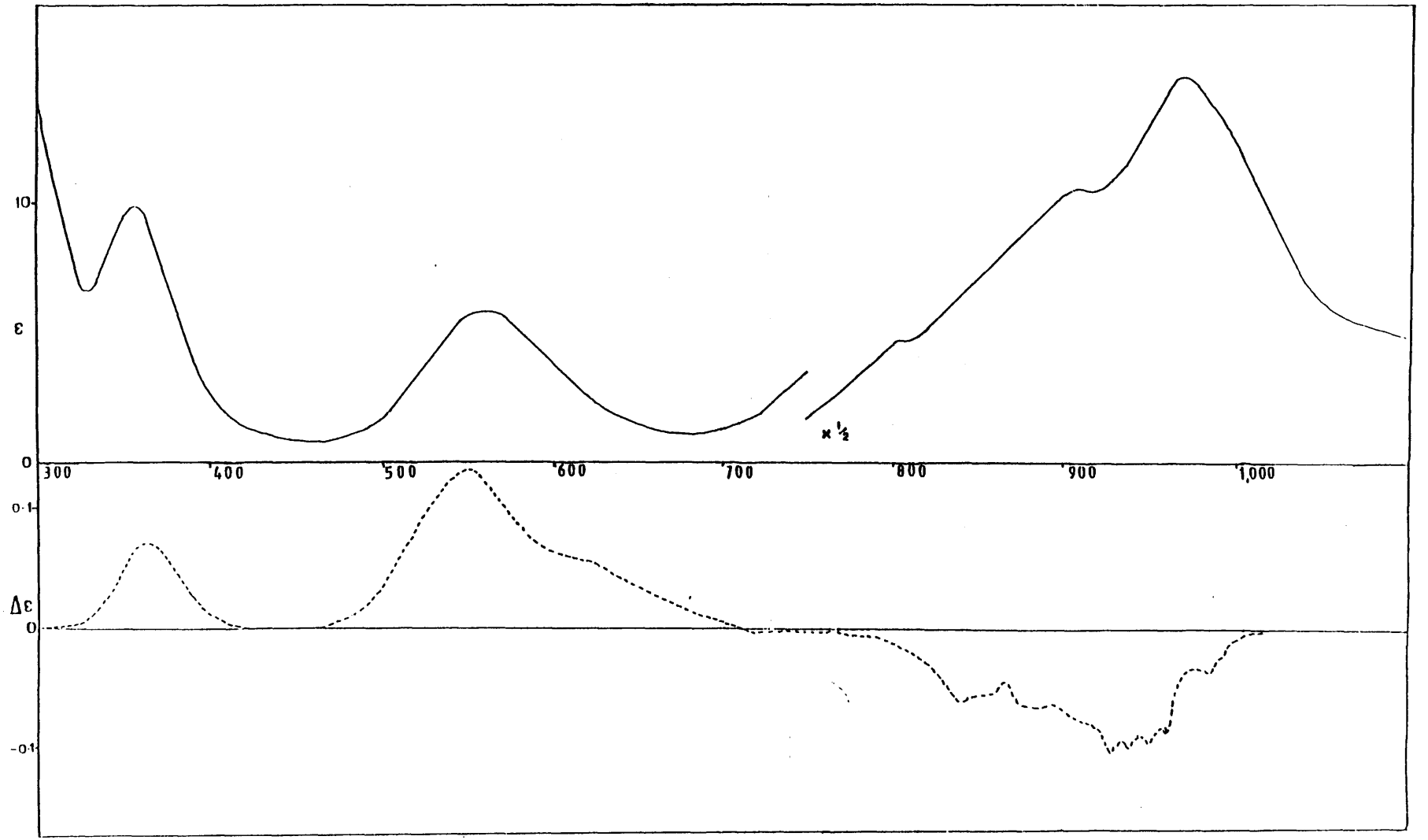

FIGURE 4.21
The absorption and c.d. spectra of $[Ni(S\text{-}Methetacn)]^{2+}$.

TABLE 4.9

THE ABSORPTION AND c.d. SPECTRA OF $[Ni(S\text{-}Methetacn)]^{2+}$

Band	abs.		c.d.		g
	λ(nm)	ε	λ(nm)	Δε	
$^3A_2 \rightarrow {}^3T_2$ (F)	966	29	930	0.1	3.4×10^{-3}
$^3A_2 \rightarrow {}^3T_1$ (F)	562	5.84	622	0.062 sh	—
			546	0.132	2.3×10^{-2}
$^3A_2 \rightarrow {}^3T_1$ (P)	358	10.36	364	0.073	7.0×10^{-3}

The extent of spin-orbit coupling in the nickel complex is witnessed by the multitude of bands under the lowest energy transition. There should theoretically be three spin-orbit states associated with the $^3A_2 \rightarrow {}^3T_2$ (F) band; presumably corresponding to the two shoulders and the main peak observed in the absorbance spectrum. The four closely spaced bands in the circular dichroism spectra of the lowest energy transition are difficult to assign and may be the result of operation of the spectrometer at regions lower in energy than those for which it was intended. From these spectra the value of Δ_o has been estimated as $\sim 10{,}700\ cm^{-1}$.

One interesting consequence of this rough estimate is that it predicts that the $^3A_2 \rightarrow {}^1A$ spin-forbidden transition should occur at ~625nm. In the absorption spectrum the band at 562nm is clearly asymmetric with a slower intensity fall-off to lower energy. In the circular dichroism spectrum the effect is more marked with a very definite shoulder in the region around 620nm. Despite the lack of sharpness associated with this feature it may be attributed to the $^3A_2 \rightarrow {}^1A_1$ transition.

The absorption spectrum is unexceptional in the position of bands in that those of the $[NiN_3O_3]^{2+}$ species are sandwiched by those of the $[NiN_6]^{2+}$ and the $[NiO_6]^{2+}$ species (in figure 4.20). The exception to this observation is the $^3A_2 \rightarrow {}^3T_1$ (F) band which occurs at higher energy than the corresponding N_6 system band. This anomally is thought to have been brought about as a result of loss of intensity resulting from spin-orbit coupling, at the lower energy end of the band, to the $^3A_2 \rightarrow {}^1A_1$ transition. The approximate extinction coefficients of the bands of $[Ni((S)\text{-Methetacn})]^{2+}$ along with those of the two octahedral model species are listed in table 4.10.

TABLE 4.10

THE EXTINCTION COEFFICIENTS OF THE TRANSITIONS OF SOME Ni(II) SPECIES

	$[Ni(NH_3)_6]^{2+}$	$Ni((S)Methetacn)]^{2+}$	$[Ni(OH_2)_6]^{2+}$
$^3A_2 \rightarrow {}^3T_2$ (F)	3.2	29.1	5.1
$^3A_2 \rightarrow {}^3T_1$ (F)	4.0	5.8	2.5
$^3A_2 \rightarrow {}^3T_1$ (P)	5.3	10.4	2.6

The extra intensity associated with the $[NiN_3O_3]^{2+}$ species may be attributed to lower symmetry arising from the twist about the chromophore caused by the chelate rings.

CHAPTER 5

The Ligands tcta and Metcta and their Metal Complexes

5.1 Introduction

Since tcta was first reported in 1973 (Ref 54) its highly symmetrical nature has attracted attention (Refs 55 & 56). However, analyses of the crystal structures of several first row transition metal complexes have revealed another feature, of particular interest to those working in the field of circular dichroism spectroscopy: the tendency of tcta to twist the chromophoric environment of chelated metal ions. Since tcta, as a derivative of tacn, clearly fell within the scope of this project, and since the reported twist might be expected to yield interesting and pronounced circular dichroism features, it was decided that an investigation of tcta and similar acetate ligands, in their first row transition metal complexes, would be of interest. Two strategies were followed in the quest for optically active metal complexes of tcta type ligands: the first involved the use of the ligand tcta itself, which is inherently non-chiral, but which might be expected to yield optically stable complexes with Co(III) and Cr(III); the second involved the use of the ligand S-Metcta (fig 2.6) which would give chiral complexes. The second strategy had the advantage that it would inevitably give optically pure product (although a and b type complexation (Ref 37) would be expected to result in 2 distinct species). However, the synthetic route via S-Metacn made preparation of S-Metcta difficult. The preparation of optically pure [Co(tcta)] or [Cr(tcta)] would require 100% chiral induction which would be unlikely to be achieved. Alternative resolutions of tacn/acetate complexes reported in the literature had

included chromatographic separation (Ref 96) and fixing of the tacn chelate rings by the presence of a chiral ligand (Ref 97).

5.2 [Co(tcta)]

5.2.1 Racemic [Co(tcta)]

Racemic [Co(tcta)] was prepared by the method of Wieghardt et al (Ref 55) with a view to resolving the two enantiomeric components. The species was known to crystallise in the space group C_{2h}^5-$P2_1/n$ so that spontaneous resolution on crystallisation would not be possible. Nor would formation of a diastereomeric salt be possible, since the species was neutral. An attempt was made to separate the two enantiomers by chromatography on an SP-Sephadex ion exchange column using 0.01M sodium antimonyl tartrate as eluent. However, since the species was neutral its residence time on the column was short and no separation was observed. The species produced by the preparation was spectroscopically identical to that prepared by the original authors (Ref 55).

5.2.2 Optically Active [Co(tcta)]

It was known that optically active $[Co(en)_3]^{3+}$ could be prepared by reaction of ethylene diamine with [Co(d-tartrate)] (Ref 39), the asymmetric synthesis being brought about as a result of chiral induction by the optically active tartrate. Although the title ligand differs greatly from ethylene diamine, critically in its

charge, the application of the technique (Section 2.3.3.2) yielded an optically active complex which was spectroscopically indistinguishable from racemic samples of [Co(tcta)]. An attempt to prepare [Co(tcta)] from [Co(cysteine)] proved unsuccessful with no discernable reaction after 2 hours of refluxing at 80 degrees centigrade. A precipitate of very fine acicular red crystals was obtained via the [Co(tartrate)] route. The crystals were filtered and air dried before being used to obtain quantitative spectral information.

5.2.3 Spectra of [Co(tcta)]

The absorption and circular dichroism spectra are shown in figure 5.1 and the $^1A_1 \longrightarrow {}^1T_1$ area in the c.d. spectrum is of immediate interest due to the apparent presence of two positive bands. These spectra pertain to a sample prepared by reaction of the ligand with [CoII(l(-)-tartrate)]. It was generally found that syntheses involving (-) tartrate gave a completely positive circular dichroism spectrum (experiments involving (+) tartrate led to wholly negative circular dichroism phenomena).

It should be noted that the spectra in figure 5.1 relate to a sample which had been cleaned by elution, using methanol, on an LH20 chromatography column. The result was the separation of a purple band, identified as unreacted starting material, [CoII((-)tart)], from the main [Co(tcta)] fraction. On rotary evaporation of solvent from the main fraction, a red powder was obtained which was dissolved in distilled water and gave the spectra in figure 5.1. Later

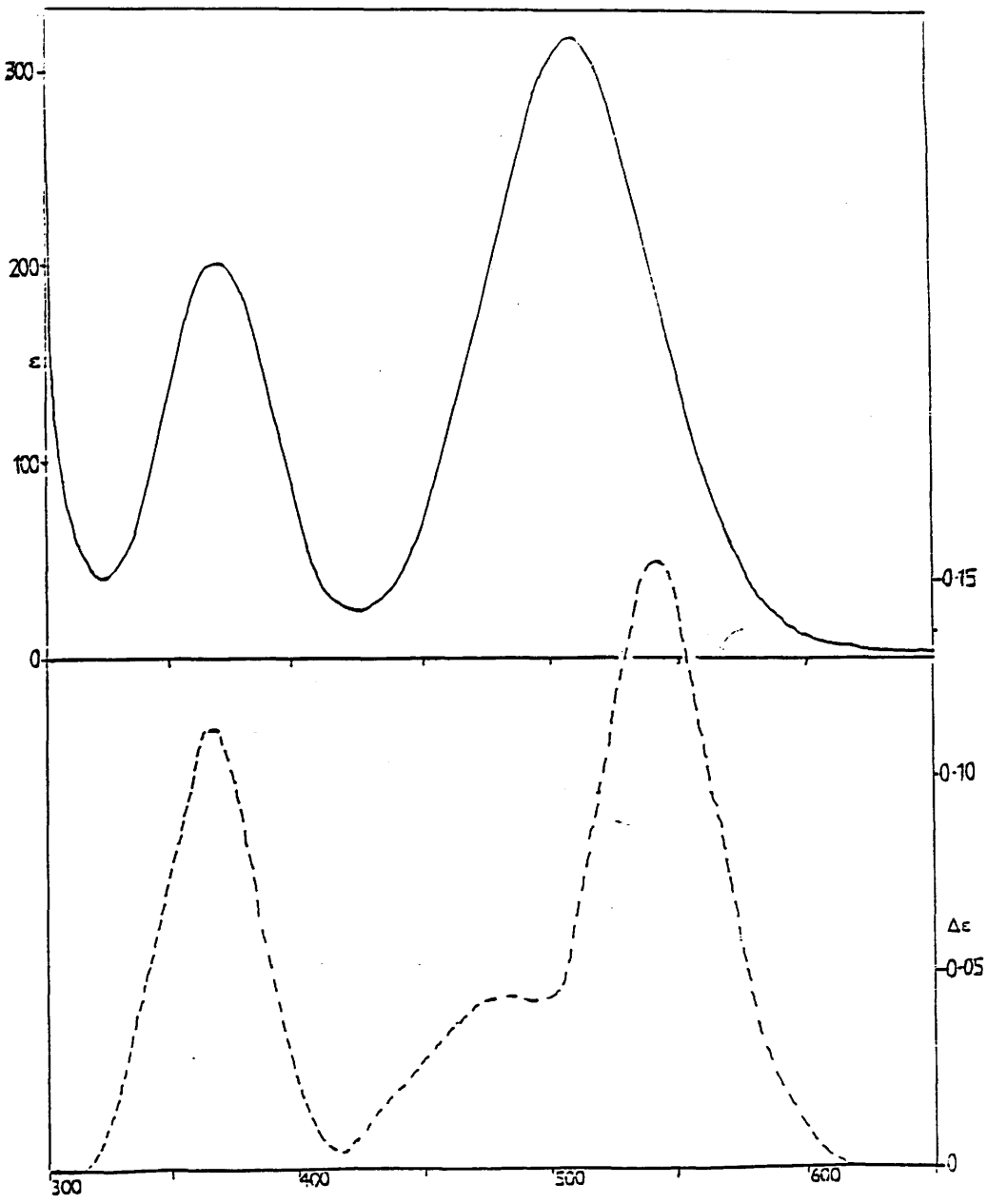

FIGURE 5.1
Absorption (——) and circular dichroism (- - -) spectra of enantiomerically impure [Co(tcta)] prepared from [Co(l-tartrate)].

attempts to further separate the [Co(tcta)] into components proved unsuccessful and provided evidence that the spectra obtained related to a single species. Table 5.1 represents the bands in the spectra of [Co(tcta)].

Table 5.1

The spectra of [Co(tcta)] prepared with l-tartaric acid.

	$^1A_1 \longrightarrow {}^1T_2$	$^1A_1 \longrightarrow {}^1T_1$	
λabs(ε)	371nm(200)	511nm(318)	
λc.d.($\Delta\varepsilon$)	363nm(+0.108)	480nm(+0.041)	540nm(+0.155)
g	$+0.54\times10^{-3}$	$+0.13\times10^{-3}$	$+0.49\times10^{-3}$

In dilute solutions the g-factors were found to be constant with time indicating that, as expected, racemisation was negligible. It was noted that while the shapes of the bands in the spectra were consistent over several batches the g-factors were not. (In practice using the $^1A_1 \longrightarrow {}^1T_2$ band as a measure they ranged from 2.2×10^{-4} - 6.6×10^{-4}). This showed that the chiral induction was not 100% efficient and led to the question of how purification might be effected. It had been found by Wieghardt et al (Ref 55) that [Co(tcta)] formed racemic crystals and so a saturated solution was placed in a refrigerator with a view to precipitating the racemate so that the g-factor of the resulting solution would rise. Some success was achieved with initial precipitation of acicular crystals leaving the solution more optically active. However, after a time, very

small hexagonal platy crystals could be detected which could not be separated physically from the racemic form. The formation of these crystals signalled the end of the rise in g-factor. The maximum value of the g-factor (in the T_1 region) obtained for [Co(tcta)] was $+1.2 \times 10^{-3}$.

5.3 [Co(S-Metcta)]

[Co(S-Metcta)] was prepared in order to provide a chiral cobalt complex with an N_3O_3 donor set. It possessed an advantage over the analogous tcta complex in that its optical purity was imparted by the ligand and could be assumed to be one hundred percent. The disadvantage of this particular ligand (Fig 2.6) was that, although it gave complexes with approximately C_3 symmetry, the methyl group on the macrocycle could theoretically give two isomeric species depending on whether it adopted mode a or mode b as defined in figure 1.21. The complex was similar to [Co(tcta)] in many respects although it crystallised with two waters of crystallisation.

5.3.1 Spectra of Co(S-Metcta)

The absorption and c.d. spectra of the species [Co(S-Metcta)] in aqueous solution are shown in figure 5.2 and the main features are listed in Table 5.2. The spectra bear strong similarity to those obtained from [Co(tcta)], however three differences should be noted. [Co(S-Metcta)] has a negative sign while [Co(tcta)] made by use of l(-)tartrate has a positive sign, there is a greater energy gap between the two apparent negative bands under the

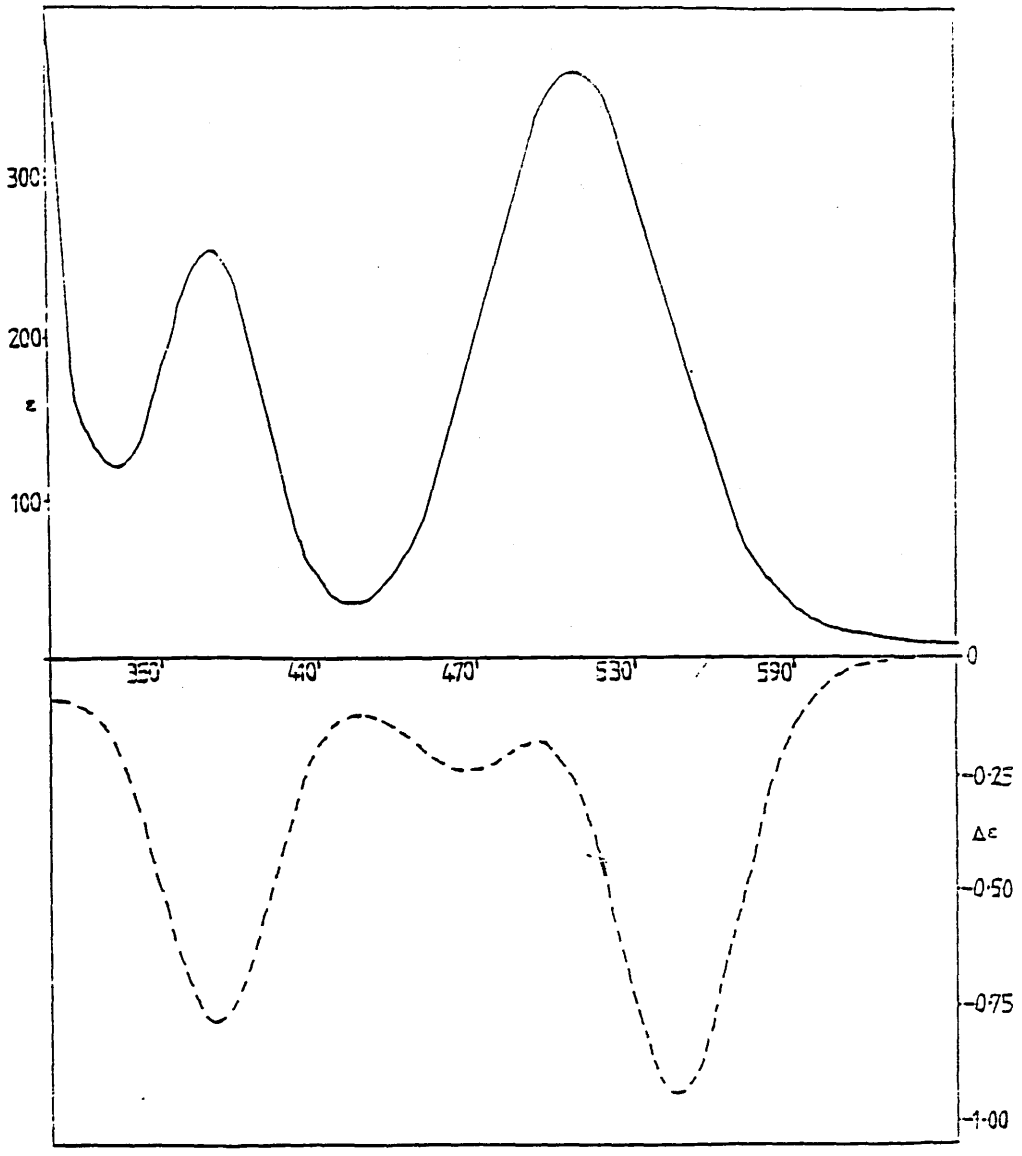

FIGURE 5.2
Absorption (——) and circular dichroism (- - -) spectra of [Co(S-Metcta)] in aqueous solution.

$^1A_1 \longrightarrow {}^1T_1$ transition in the S-Metcta case and the g-factor is roughly five times as great in the S-Metcta case. The visible absorption spectra of the two species are remarkably similar with the S-Metcta species having slightly larger extinction coefficients.

Table 5.2

The Spectra of [Co(S-Metcta)].

	$^1A_1 \rightarrow {}^1T_1$	$^1A_1 \rightarrow {}^1T_2$
abs.(ε)	372nm(260)	510nm(366)
c.d.(Δε)	370nm(-0.79)	461nm(-0.24),541(-0.95)
g	-3.0×10^{-4}	-6.6×10^{-4} -2.6×10^{-3}

5.4 Discussion of [Co(tcta)] and [Co(S-Metcta)]

In the case of [Co(S-Metcta)] the optical activity derives from the asymmetric carbon which, on complexation, determines the sense of each of the other chiral features of the complex and specifically the twist about the chromophore. From the crystal structure of $[Co(R\text{-}Metacn)_2]^{3+}$ it is known that an R chiral centre on an endocyclic ring gives rise to endocyclic chelate rings in the conformation λ (Ref 45). Observations of various crystal structures (Refs 55 & 72) suggest that where the LFSE is high (eg for Co(III)) the geometry adopted by tcta (or thetacn) type complexes is type I as defined by Hancock (Ref 57). It follows that a δ conformation of the endocyclic rings causes a Λ configuration and consequently a

negative twist angle as defined by Peacock (Ref 40). By this line of reasoning, and from the empirical observation that a negative twist angle leads to a positively signed E component in the $^1A_1 \longrightarrow {}^1T_1$ region of the circular dichroism spectrum, it is to be expected that the sign of the A_2 component in the spectrum of [Co(S-Metcta)] should be negative. Since the negative component is dominant in the [Co(S-Metcta)] c.d. spectrum it would appear that, as in the cases of $[Co(tacn)_2]^{3+}$, $[Co(R\text{-}Metacn)_2]^{3+}$ (Ref 45), $[Co(S\text{-}Methetacn)]^{3+}$ (Ref 72) and $[Co(taetacn)]^{3+}$ (Ref 60) the A_2 component dominates the $A_1 \longrightarrow T_1$ region of the c.d. spectrum. Since the spectra of [Co(tcta)] bore a strong resemblance to those of [Co(S-Metcta)] it was concluded that the two species were, as expected, very similar: with the methyl group of Metcta constituting a minor perturbation.

It was expected that [Co(tcta)], being a Co(III) complex of a hexadentate ligand, would not suffer from labilisation. However, since racemisation was theoretically possible by chelate ring flipping it was necessary to conduct experiments to determine whether racemisation was a significant process. In practice no change was observed in the circular dichroism spectra of dilute solutions, produced from [Co((-)tart)], over a period of two weeks. It was found that when l(-)-tartrate was used in preparations the c.d. spectrum of the resulting [Co(tcta)] was positive but that when d(+)-tartrate was used the [Co(tcta)] produced had a negative sign. Thus d(+)-tartrate gave rise

to [Co(tcta)] the configuration of which was, by correlation with [Co(S-Metcta)], $\Lambda(\delta)$. Conversely [Co(l(-)-tartrate)] was found to give rise to a species consistent with a $\Delta(\lambda)$ [Co(tcta)] configuration.

The most puzzling feature of the c.d. spectra in figures 5.1 and 5.2 is the apparent presence of two positive bands under the $A_1 \longrightarrow T_1$ transition. This phenomenon has previously been noted in the case of α-Co(+ala) (Ref 98). This is most probably the result of cancellation of the A_2 and E components. However, this being the case, the band widths of the two components appear to be significantly different with the lesser E component being the narrower. (The relative energy ordering of A_2 and E is the same as that found for $[Co(Methetacn)]^{3+}$.) If the c.d. spectrum is not the result of different band widths of the two components of the T_1 transition then it would be necessary to postulate the presence of two substantially dissimilar species in solution. The symmetry of the absorption bands is evidence against this possibility.

The optical purity of the [Co(tcta)] formed by reaction of [Co(l-tart)] with tcta was clearly not 100%. The Kuhn dissymmetry factor of the T_1 transition of various newly prepared samples ranged from 2.2×10^{-4} to 6.6×10^{-4} indicating a maximum optical excess of 25% (calculated by reference to [Co(S-Metcta)]) of the Δ configuration (i.e. 62.5% : 37.5%). It was found to be possible, by selective crystallisation of racemic crystals from solution, to raise

the maximum g-factor to $+1.2\times10^{-3}$. The g-factor of Co(S-Metcta) was found to be -2.6×10^{-3} so that, assuming the g-factor of [Co(tcta)] and [Co(S-Metcta)] to be approximately equal in magnitude for optically pure solutions, selective racemic crystallisation was capable of raising the optical excess to ~45%.

5.5 [Cr(tcta)]

[Cr(tcta)] was prepared, in the first instance, by the method of Wieghardt et al (Ref 55): however attempts to resolve the resulting racemic solution into the enantiomeric components by column chromatography proved to be unsuccessful. As a result the technique of chiral induction, which had been applied in the case of the cobalt (III) complex, was again tried. The experiment was equally successful. The spectra in figure 5.3 were obtained from a freshly prepared sample and the important features are listed in Table 5.3.

Table 5.3

The spectra of [Cr(tcta)] prepared with l-tartaric acid.

	$^4A_2 \longrightarrow {}^4T_1$	$^4A_2 \longrightarrow {}^4T_2$
abs(ε)	388nm(249)	512nm(340)
c.d.(Δε)	412nm(+0.39)	538nm(-0.94), 614(+0.33)
g	$+1.6\times10^{-3}$	-2.8×10^{-3} $+0.97\times10^{-3}$

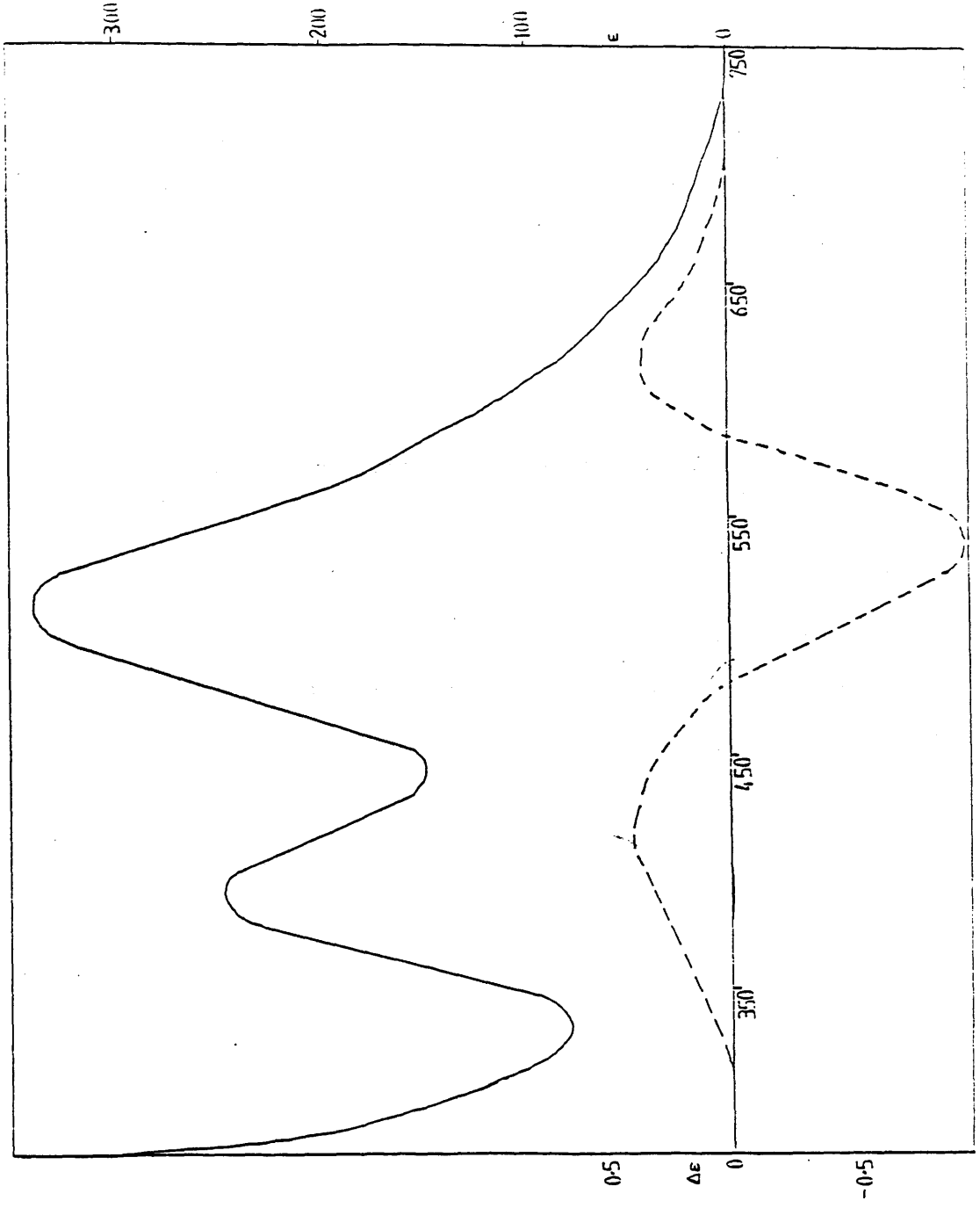

FIGURE 5.3
Absorption (——) and circular dichroism (– – –) spectra of enantiomerically impure [Cr(tcta)] prepared in the presence of l-tartaric acid.

The spectra (Fig 5.3) are from a solution prepared using l-tartaric acid. The solution was taken to dryness when the reaction was complete and the resulting solid was found to be intimately mingled with white material. The [Cr(tcta)] was preferentially dissolved in dmso and the solution formed was passed down an LH20 column to ensure purity of the sample. The eluted fraction was taken to dryness by rotary evaporation and redissolved in water to allow the aqueous spectra (Fig 5.3) to be obtained.

As a check that the observed product was not a tartrate complex the preparation described in section 2.3.3.2 was carried out in detail except that no tcta was added. The resulting solution had an absorption spectrum comprising two bands; 417nm (A=1.20) and 572nm (A=1.03). The circular dichroism spectrum consisted of two positive bands at 583nm ($\Delta A=7.4\times10^{-4}$) and 450nm ($6.4\times10^{-4}$). The solution was blue in colour.

5.6 [Cr(S-Metcta)]

[Cr(S-Metcta)] was prepared as described in section 2.3.4.2. A sample of dried material was weighed and then dissolved in distilled water and used to obtain the spectra shown in figure 5.4. The salient features of the spectra are listed in table 5.4.

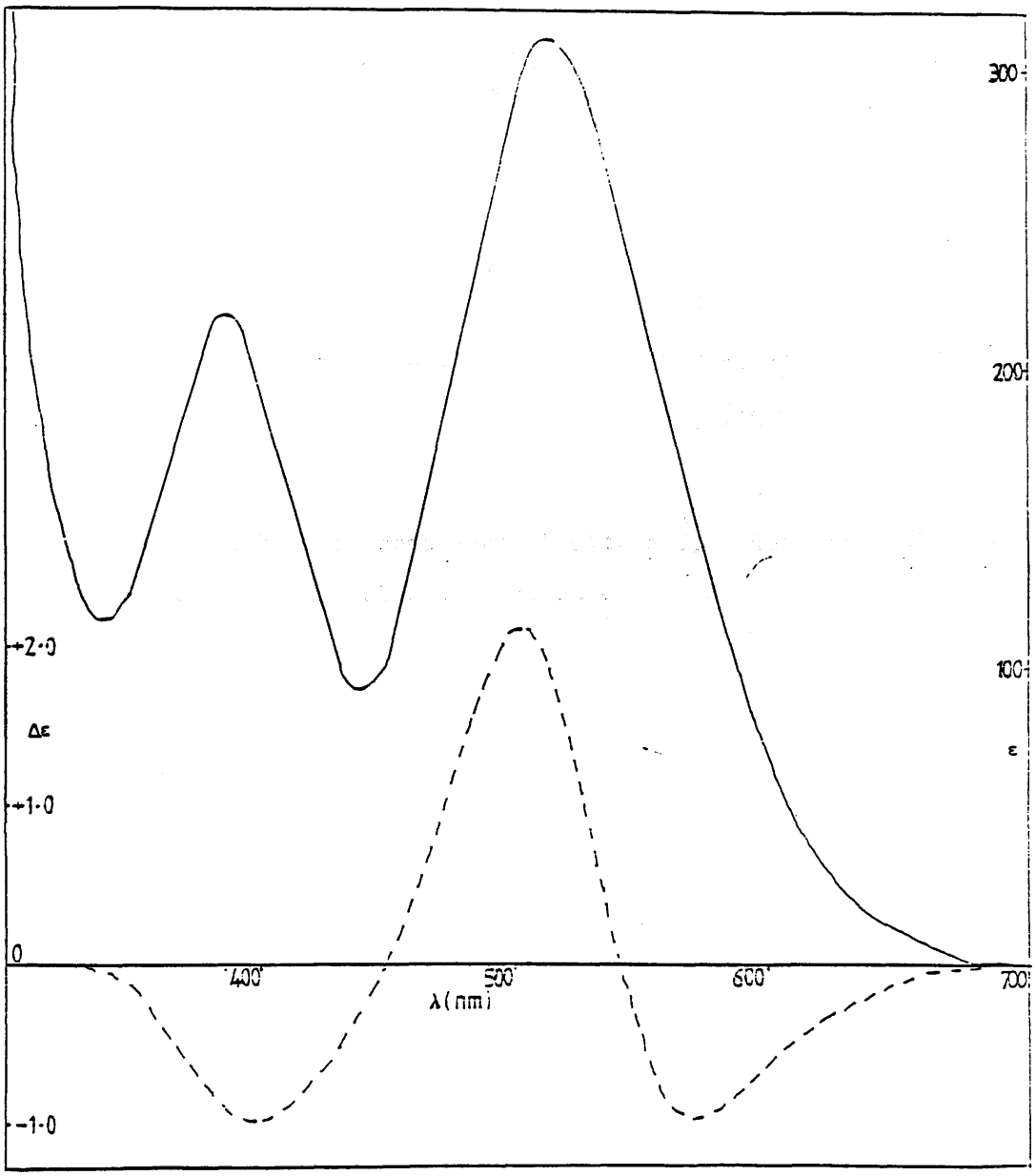

FIGURE 5.4
Absorption (——) and circular dichroism (– – –) spectra of [Cr(S-Metcta)].

Table 5.4

The spectra of [Cr(Metcta)]

	$^4A_2 \longrightarrow {}^4T_1$	$^4A_2 \longrightarrow {}^4T_2$	
abs(ε)	385 (226)	512(310)	
c.d.(Δε)	395 (-1.01)	500(+2.11)	570(-0.99)
g	-4.47×10^{-3}	$+6.8\times10^{-3}$	-3.2×10^{-3}

As with the complexes [Co(tcta)], [Co(S-Metcta)] and [Cr(tcta)] addition of acid or base had no effect, other than by dilution, on the spectra.

5.7 Discussion of [Cr(tcta)] and [Cr(S-Metcta)]

As in the cobalt(III) case the spectra of [Cr(tcta)] and [Cr(S-Metcta)] were superficially very similar to one another. In the circular dichroism spectra the highest and lowest energy bands were of like sign (and comparable intensity) with, in each case, the intermediate energy band being of opposite sign and approximately twice the intensity. It is tempting, on this evidence, to assign the two lower energy bands to the two components of the $^4A_2 \longrightarrow {}^4T_2$ transition and the highest energy component to the magnetic dipole allowed $^4A_2 \longrightarrow {}^4E(T_2)$ transition. However, in the case of [Cr(tcta)] this assignment does not explain the observed spectra. The circular dichroism in the $^4A_2 \longrightarrow {}^4T_2$ region for [Cr(tcta)] has band maxima at 538nm and 614nm

whereas the absorption maximum occurred at 512nm. Normally the band maxima of the two component transitions in the c.d. spectrum would lie one to higher energy and one to lower energy than the absorption maximum. On observation of figure 5.3 a possible reason for this phenomenon is apparent; namely that the c.d. band under the $^4A_2 \rightarrow {}^4T_1$ absorption band comprises two components; one from the $^4A_2 \rightarrow {}^4T_1$ band itself, the other a residual wing from the $^4A_2 \rightarrow {}^4T_2$ band. This explanation may also be applied to the spectra of [Cr(Metcta)] and goes some way to explaining the strong asymmetry of the $^4A_2 \rightarrow {}^4T_1$ circular dichroism band which peaks at lower energy than would be expected if only one transition was involved. It should be noted that if the absorption band for $^4A_2 \rightarrow {}^4T_2$ were symmetrical then intensity due to it would be expected down to 410nm. It would appear that the circular dichroism of these chromium complexes is similar to their cobalt analogues in that the circular dichroism of the lower energy electronic transition does not comprise one band (as in the cases of $[Co(tacn)_2]^{3+}$ and $[Co(R\text{-}Metacn)_2]^{3+}$ (Ref 27)); nor does it comprise two bands (as in the cases of $[\{Co(S\text{-}Methetacn)\}_2(\mu H)_3]^{3+}$ or $(Cr((-)pn)_3]^{3+}$ (Ref 99)). Instead three bands are visible. In order for three bands to be observed it is necessary that the two electronic transitions giving rise to the bands should be close in energy and that the bands should have markedly different band widths.

The band shapes in the T_1 transitions of the four complexes so far discussed may be rationalised by postulating that

for the cobalt complexes the transition with the narrower band width, $A_1 \rightarrow E(T_1)$ also carried the minor intensity giving rise to figure 5.1 and 5.2: whereas for the chromium complexes the transition with the narrower band width, $^4A_2 \rightarrow {}^4E(T_1)$ possessed the major intensity. The reason for the different band widths of the two bands in each molecule is unknown. Differences in Doppler broadening due to two orientations of the same molecule are presumed to be insignificant as are differences in lifetime.

It is worth noting that, as in the case of the cobalt complexes the Cr(tcta) formed in the presence of l-tartaric acid is of the opposite enantiomer to the chromium complex of S-Metcta. It is expected that the disposition of the methyl group on the S chiral centre of the Metacn moiety of S-Metcta would cause the endocyclic chelate ring to which it was bonded to adopt a δ conformation. This expectation follows on the observation that in $[Co(R\text{-Metacn})_2]^{3+}$ an R chiral centre on an endocyclic ring caused all of the chelate rings in the macrocycle to adopt a common conformation, λ(Ref 32). From information gained from crystal structure data (Refs 55 & 57) on tcta complexes and in particular for [Cr(tcta)] it is known that a δ conformation in each of the endocyclic chelate rings should result in a Λ configuration and, for c.d. purposes, a negative twist value, ω . Thus it is predicted that the E component of the $^4A_2 \rightarrow {}^4T_2$ transition should have a positive sign in circular dichroism. From the spectra it may be observed that for [Cr(S-Metcta)] the E

component, being positive, is the component with the narrower band-width.

The optical purity of the [Cr(tcta)] obtained by preparation in the presence of l-tartaric acid may be assessed by comparison to the necessarily optically pure analogue [Cr(S-Metcta)]: assuming the methyl group on the latter complex to be of negligible significance to observed circular dichroism. This comparison is inherently inaccurate because of the susceptibility of the T_1 c.d. spectrum observed to small changes in the two component bands. However in the absence of a suitable technique for enantiomeric separation it provides a rough guide to the success of the chiral induction.

The average amplitude of the g-factors over the three bands of [Cr(tcta)] was 35% of that for [Cr(S-Metcta)] indicating an optical excess of 35% of the Δ isomer favoured by l-tartaric acid (i.e. 67.5% :32.5%). As in the case of Co(tcta) initial crystallisation of samples gave rise to higher g factors, in one case indicating a 65% optical excess. However, there came a point in each set of crystallisations where no further increase in optical activity was achieved. Since the g-factor on reaching this stage varied it is considered unlikely that optically pure [Cr(tcta)] had been produced.

5.8 The Rôle of Tartrate in Chiral Induction

Although the inspiration for the optical resolution of tcta complexes came from the work of Broomhead, Dwyer and Hogarth (Ref 39) it became evident that the principles underlying their syntheses were inapplicable in the present study, despite the apparent effectiveness of the technique. The two methods of chiral induction utilised in reference 39 are chiral association of the metal complex with the tartrate ion in solution and steroeselective precipitation of a diasteroemeric tartrate salt. The latter appears from micro-analysis to be an insignificant process in the preparation of optically active Co(III) and Cr(III) complexes of tcta. Association of tartrate with the complex cannot take place by ion pairing, as in the case of $[CoII(en)_3]^{3+}$(d-tart) (Ref 39). Yoneda (Ref 77) reported that three crystal structures of the type involving $[MIII(en)_3]^{3+}$ and (d-tart) had each shown a face to face arrangement of the ion pair such that four oxygen atoms of the tartrate group project towards the complex and face three $-NH_2$ groups. From the inferred hydrogen bonded association it was postulated that chromatographic separation of fac-[Co(β-ala)$_3$], an uncharged species, should be possible. Resolution of this species was subsequently achieved by use of d-tart. In the light of this hypothesis it is all the more intriguing that [Co(tcta)] and [Cr(tcta)], both uncharged species with no amino hydrogens, should be subject to chiral induction in the presence of tartrate ions. It is possible, by use of models, to show that each form of tartaric acid

(protonated) could theoretically hydrogen bond to the oxygens of tcta which directly coordinate the metal ions. The mechanism for the introduction of optical activity would be similar to that involved when amino hydrogen-bonding is invoked. It is envisaged that this process should occur while the tcta complex was in the process of formation since after this stage the complex was found to be optically non-labile. Another more likely possibility is that the tcta approaches a complex of [CoII(l-tart)], for example, and the amine moiety coordinates while the tartrate group is still bound to the metal. The influence of the tartrate would be expected to impart a preferred common conformation on the three chelate rings of the macrocycle; which would remain as the oxygen donor atoms of the tcta replaced those of the tartrate. It is interesting that although the tacn moiety can interconvert freely among the various diastereomeric forms possible (c.f. $[Co(tacn)_3]^{3+}$) the coordination of the acetate groups in a type I structure should fix the chirality. (Since conversion to the enantiomer without dissociation would involve passing through the higher energy type II structure.)

5.9 [Cu(S-Metcta)]$^-$

[Cu(S-Metcta)]$^-$ was prepared by addition of a sub-stoichiometric quantity of $CuCl_2.2H_2O$ to an aqueous solution of S-Metcta. Attempts to crystallise the product proved unsuccessful, however the close similarity (in both wavelength and extinction coefficient) of samples to

[Cu(tcta)]$^-$ allowed the species to be identified. The extinction coefficient was measured by use of an aqueous solution of known concentration of $CuCl_2$ to which was added an excess of S-Metcta. The absorption and circular dichroism spectra obtained are shown in figure 5.5 and the important features are listed in Table 5.5. Despite the positive hole formalism which allows Cu(II) species to be treated as one electron systems, the spectra of such species are difficult to assign because of the low symmetry resulting from Jahn Teller distortion.

Table 5.5

spectra of [Cu(S-Metcta)]

abs(ε) 743(71)

c.d.($\Delta\varepsilon$) 644(-0.18), 747(+0.12)

In the spectra recorded the main band in absorption may, simplistically, be assigned to the $t_{2g} \longrightarrow e_g$ transition and on this basis Δ_o computes as 13333cm^{-1} however the asymmetry of the circular dichroism spectrum highlights the inadequacy of such an assignment. The asymmetry of the single band at 743nm in absorption is attributable to Jahn Teller distortion. The species is presumed, on the basis of a crystal structure of the analogous species [Cu(tcta)]$^-$, to be six coordinate comprising a $Cu(N_3O_3)$ chromophore in a trigonal prismatic configuration. This configuration has been attributed by Wieghardt et al (Ref 47) to the dominance of chelate ring strain over the ligand field

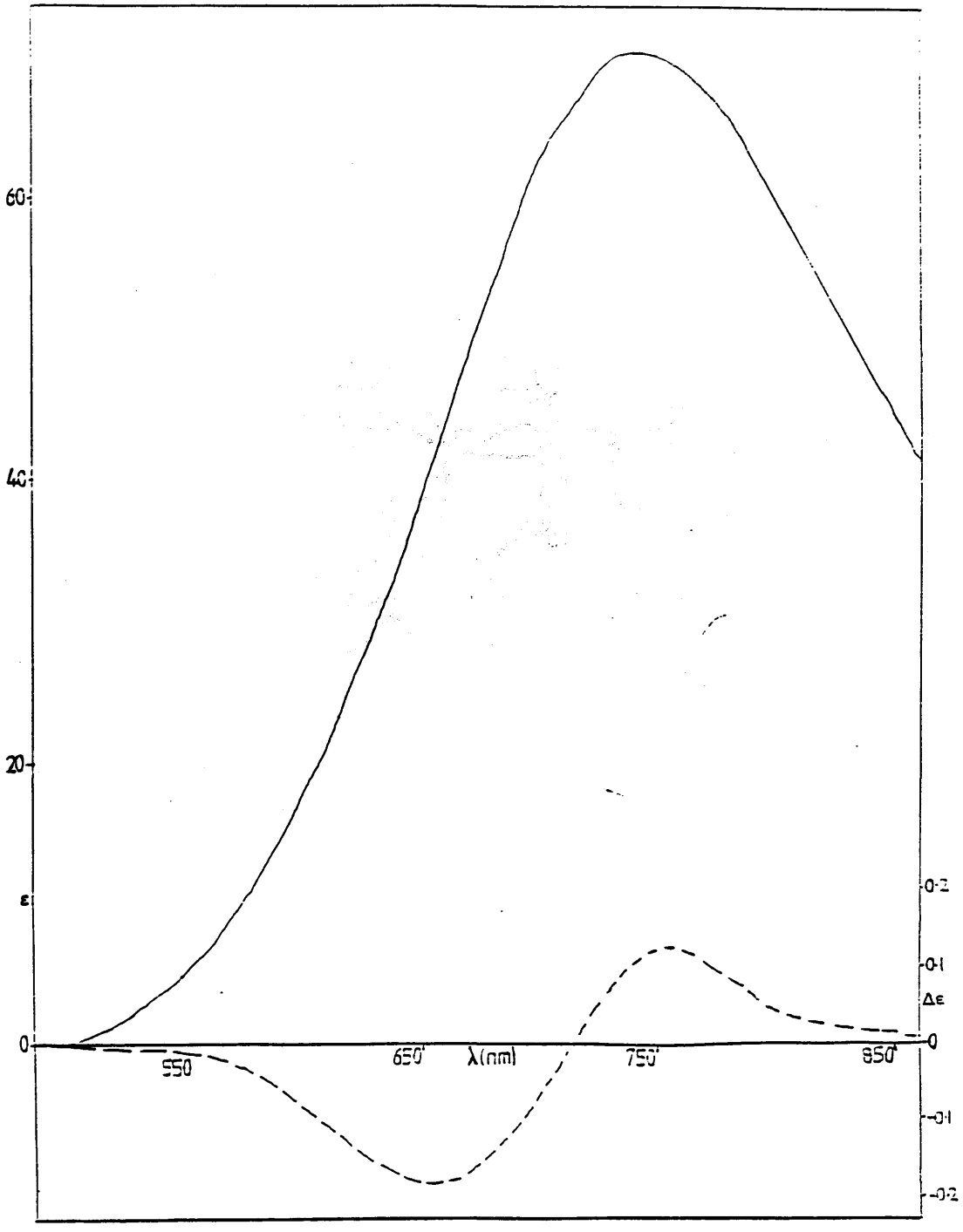

FIGURE 5.5
Absorption (——) and circular dichroism (- - -) spectra of $[Cu(S\text{-}Metcta)]^-$.

stabilisation energy. The absorption spectrum obtained from $[Cu(S\text{-}Metcta)]^-$ shows surprising symmetry in comparison to related Cu spectra : eg $[Cu(tacn)_2]^{3+}$ exhibits two bands (Ref 100) .

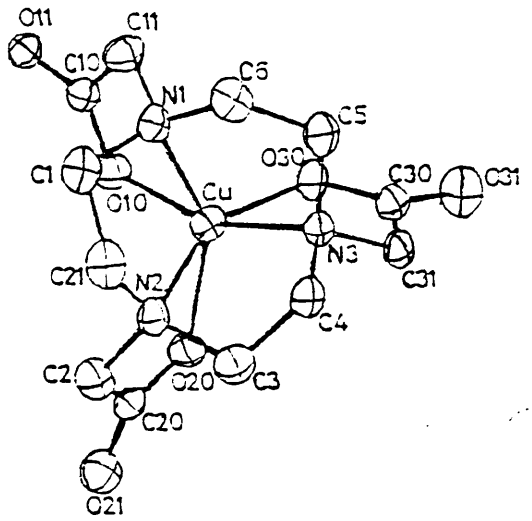

FIGURE 5.6
Apical perspective on the anionic complex $[Cu(tcta)]^-$.(Taken from ref.55)

The c.d. spectrum of $[Cu(S\text{-}Metcta)]^-$ is bisignate consisting of a negative band to higher energy and a positive band to lower energy. From an apical perspective on the crystal structure of [Cu(tcta)] (Fig 5.6) it is clear that there is a considerable distortion from octahedral symmetry and a helical displacement of the donor atoms. In addition to this lowering of symmetry by a twist mechanism the atomic positions show Jahn Teller asymmetry within the N_3 and O_3 groups so that the actual symmetry of the complex is low. Nevertheless the principle that the twist direction (the sign of ω) determines the sign of the

circular dichroism should still apply. In this case an S chiral centre on an endocyclic chelate ring, would be expected to result in a δ conformation of that ring and a Δ configuration about the chromophore: since the complex has a type II structure. In this case the exocyclic chelate rings are short and so a positive value of ω inevitably results. It is to be expected from observations of the circular dichroism of [Cu(S-Metcta)]$^-$ that a positive value of ω will give rise to a negative c.d. band to higher energy and a positive band to lower energy for analogous CuN_3O_3 species. [Cu(S-Methetacn)]$^{2+}$ falls into this category and should possess a configuration opposite to that of [Cu(S-Metcta)]$^-$, i.e. Λ(λδ) as opposed to Δ(δ) . In figure 4.17 the circular dichroism spectrum of the basic form of [Cu(S-Methetacn)]$^{2+}$ shows a single positive band at higher energy than the corresponding absorption band indicating the presence of a latent lower energy band of negative sign: as predicted.

5.10 [Ni(S-Metcta)]$^-$

The species [Ni(S-Metcta)]$^-$ was generated from $NiCl_2.6H_2O$ and was sufficiently similar, spectroscopically, to [Ni(tcta)]$^-$ to allow positive identification. Calculations of ε and Δε were carried out using values obtained by reacting an accurately weighed sample of $NiCl_2.6H_2O$ in an aqueous excess of S-Metcta. The results appear in Table 5.6 while figure 5.7 contains the relevant spectra.

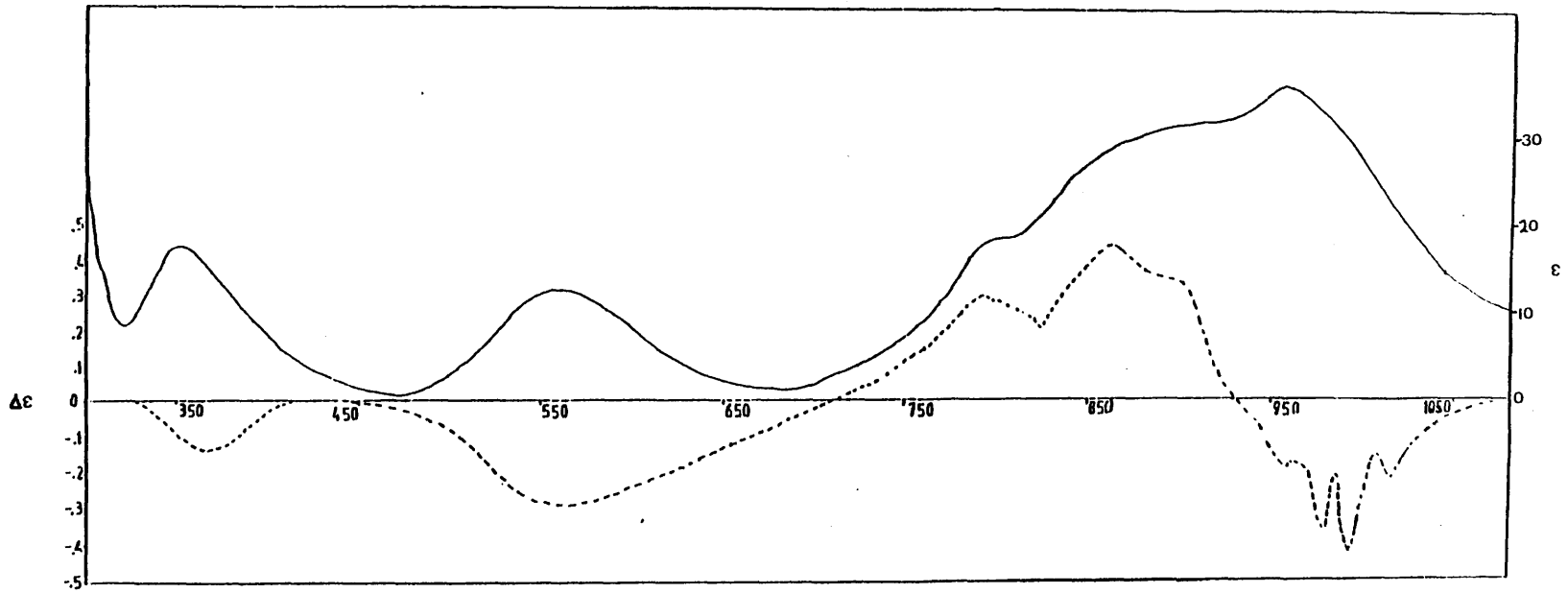

FIGURE 5.7
Absorption (——) and circular dichroism (- - -) spectra of [Ni(S-Hutota)]$^{-}$.

Table 5.6

The Spectra of [Ni(S-Metcta)]

	$^3A_2 \longrightarrow {}^3T_1(P)$	$^3A_2 \longrightarrow {}^3T_1(F)$	$^3A_2 \longrightarrow {}^1E(D)$	$^3A_2 \longrightarrow {}^3T_2(F)$	
$\lambda_{abs}(\varepsilon)$	351(18.2)	555(13.1)	614*	803	(19.0)
				922	(30.0)
				958	(36.4)
				791	(0.28)
$\lambda_{c.d.}(\Delta\varepsilon)$	354(-0.14)	550(-0.29)		862	(0.42)
				954	(-0.18)
				978	(-0.36)
				991	(-0.42)
				1013	(-0.22)

*Estimated from Δ_o

Estimation of Δ_o and Racah parameter B yielded values of 10,920cm^{-1} and 910cm^{-1} respectively. From these values, and by use of a Tanabe Sugano diagram, it was estimated that the spin-forbidden $^3A_2 \longrightarrow {}^1E$ transition should occur at about 614nm. Based on this calculation the asymmetry under the $^3A_2 \longrightarrow {}^3T_1$ (F) band in the c.d. spectrum may be assigned to $^3A_2 \longrightarrow {}^1E$. At lower energy the $^3A_2 \longrightarrow {}^3T_2$ (F) transition comprises three bands. It is probable that these bands are the product of spin-orbit coupling whereby the ^3F state is split into three components $^3F_4$, $^3F_3$ and $^3F_2$. The c.d. spectrum shows greater complexity than the absorption spectrum. This is because the species $[Ni(S\text{-}Metcta)]^-$ is

not a perfectly octahedral chromophore but is more closely represented by D_3 symmetry. As such the two highest energy bands in the visible region have only one component ($^3A_2 \longrightarrow {}^3E$ in each case). However, the $^3A_2 \longrightarrow {}^3T_2$ transition is magnetic dipole allowed and has two components, of opposite sign in the c.d. spectrum, ($^3A_2 \longrightarrow {}^3E$ and $^3A_2 \longrightarrow {}^3A_1$). As a consequence each of the three spin-orbit coupling terms should have a positive and a negative component. This explanation appears to be sufficient to describe the structure of the two higher energy terms which each have a dominant positively signed c.d. band to higher energy and a lesser negative band to lower energy. The lowest energy term is more difficult to explain, being predominantly negative in sign and comprising a major negative component and three narrow positive components.

The spectra of $[Ni(S\text{-}Metcta)]^-$ bear a resemblance, allowing for pseudo enantiomerism, to those of $[Ni(S\text{-}Methetacn)]^{2+}$. The designation of the former may be taken to be $\Lambda(\delta)$ while that of the latter should be $\Delta(\lambda\delta)$, so that the S-Metcta species should have a negative twist angle and the S-Methetacn species should have a positive twist angle. It should be possible on the basis of these two chiral NiN_3O_3 species, whose configurations are known with some certainty, to predict the configuration of other chiral species possessing the same chromophore.

5.11 Conclusions

The empirical rule (Ref 41) relating the signs of the $A_2(T_1)$ and $E(T_1)$ transitions of Co(III) and Cr(III) species to the sense of the twist angle ω were found to be applicable to the species [Co(S-Metcta)] and [Cr(S-Metcta)] for which chemical reasoning allowed the absolute configuration to be inferred. Subsequently the rule was applied to the analogous species [Co(tcta)] and [Cr(tcta)], both prepared in the presence of l-tartrate, in order to elucidate the absolute configuration conferred on them by chiral induction. In something of an extension to this empirical rule it was found that the pairs of pseudo - enantiomers, $[Ni(S\text{-}Metcta)]^-$ and $[Ni(S\text{-}Methetacn)]^{2+}$ and also $[Cu(S\text{-}Metcta]^-$ and $[Cu(S\text{-}Methetacn)]^{2+}$ had, in each case, opposite signs for each band in their circular dichroism spectra. These findings may now be used to infer, by use of c.d. spectra, the absolute configuration of $Cu(N_3O_3)$ and $Ni^{II}(N_3O_3)$ species.

The preparation of optically active [Co(tcta)] and [Cr(tcta)] was achieved using l-tartaric acid as a chiral inductant. The most likely mechanism for this reaction, the product of which possesses neither charge nor amino protons in either case, is one in which the tacn moiety of tcta coordinates to the Co(III) while the tartrate unit remains attached. It is envisaged that replacement of the tartrate by the acetate arms would then occur. Irrespective of the mechanism it appears that for both Co(III) and Cr(III) species the presence of l-tartrate during complex formation induces a positive twist angle about the metal ion.

A puzzling feature of the cobalt (III) and chromium (III) spectra reported in this chapter was the nature of the T_1 transition bands in the c.d. spectra. (For example two negative maxima are observed for [Co(S-Metcta)] while for [(Cr(S-Metcta)] the c.d. spectrum in this region comprises two negative bands and one positive band.) These observations have been rationalised by the postulation that the bandwidth of the E component in each case is narrower than that of the A_2 component. No satisfactory explanation has been found for this phenomenon.

References

1. Pedersen C.J., J. Am. Chem. Soc., 1967, 87, 7017-7036.
2. Sellmann D. and Zapf L., Angew. Chem., 1984, 23, No. 10, 807-8, (Eng).
3. Ashby M.T. and Lichtenberger D.L., Inorg. Chem., 1985, 24, 636-638.
4. Richman J.E. and Atkins T.J., J. Am. Chem. Soc., 1974, 96, 2268-2270.
5. Atkins T.J., Richman J.E. and Oettle W.F., Org. Synth., 1979, 58, 86-98.
6. Dietrich B., Lehn J.M. and Sauvage J.P., J. Chem. Soc., Chem. Commun., 1970, 1055-1056.
7. Christensen J.J., Eatough D.J. and Izatt R.M., Chem. Revs., 1974, 74, 351-384.
8. Muller F.R. and Handel H., Tet. Letts., 1982, 23, 2769-2772.
9. Kaden T.A., Topics in Current Chemistry, 1984, 121, 157-179.
10. Lotz T.J. and Kaden T.A., Helv. Chim. Acta., 1978, 61(4), 1376-1387.
11. Stetter H. and Roos E.E., Chem. Ber., 1954, 87, 566-571.
12. Bosnich B., Poon C.K. and Tobe M.L., Inorg. Chem., 1965, 4, 1102-1108.
13. Collman J.P. and Schneider P.W., Inorg. Chem., 1966, 5, 1380-1384.
14. Izatt R.M., Bradshaw J.S., Nielsen S.A., Lamb J.D., Christensen J.J. and Sen D., Chem. Revs., 1985, 85, 271-339.
15. Hancock R.D. and McDougall G.J., J. Am. Chem. Soc., 1980, 102, 6551-6553.
16. Fabbrizzi L., Paoletti P. and Clay R.M., Inorg. Chem., 1978, 17, 1042-1046.

17. Koyama H. and Yoshino T., Bull. Chem. Soc. Jap., 1972, 45(2), 481-484.

18. Peacock D.H. and Gwan Y.S., J. Chem. Soc., 1937, 1468-1471.

19. Graham P.G. and Weatherburn D.C., Aust. J. Chem., 1983, 36, 2345-2354.

20. Searle G.H. and Geue R.J., Aust. J. Chem., 1984, 37, 959-970.

21. Hay R.W. and Norman P.R., J. Chem. Soc. Dalton Trans., 1979, 1441-1445.

22. Fabbrizzi L., J. Chem. Soc. Dalton Trans., 1979, 1857-1861.

23. McAuley A., Norman P.R. and Olubuyide O., Inorg. Chem., 1984, 23, 1938-1943.

24. Margulis T.M. and Zompa L.J., J. Chem. Soc. Chem. Commun., 1979, 430-431.

25. Angley M.E., Dwyer M., Lincoln S.F., Searle G.H., Geue R.J. and Keene R.F., Inorg. Chim. Acta., 1980, 45, L91-L93.

26. Graham P.G. and Weatherburn D.C., Aust. J. Chem., 1981, 34, 291-300.

27. Mason S.F. and Peacock R.D., Inorg. Chim. Acta., 1976, 19, 75-77.

28. Dwyer F.P., Garvan F.L. and Shulman A., J. Am. Chem. Soc., 1959, 81, 290-294.

29. Nonoyama M., Trans. Met. Chem., 1980, 5, 269-271.

30. Barefield E.K., Carrier A.M. and Vanderveer D.G., Inorg. Chim. Acta., 1980, 42(2), 271-275.

31. Kuroda R. And Saito Y., Bull. Chem. Soc. Jap., 1976, 49(2), 433-436.

32. Mikami M., Kuroda R., Konno M. and Saito Y, Acta. Cryst., 1977, B33, 1485-1489.

33. Wieghardt K., Schmidt W., Herrmann W. and Kuppers H.J., Inorg Chem., 1983, 22, 2953-2958.

34. Wieghardt K. and Koppen M., J. Chem. Soc. Dalton Trans., 1983, 1869-1872.

35. Wieghardt K., Schmidt W., Endres H. and Wolfe R.C., Chem. Ber., 1979, 112, 2837-2846.

36. "Molecular Optical Activity and the Chiral Discriminations", Mason S.F., Cambridge University Press, 1982.

37. "Absolution Configuration of Metal Complexes", Hawkins C.J., Wiley Interscience, New York, 1971.

38. Yoshikawa Y. and Yamasaki K., Coord. Chem. Revs., 1979, 205-229.

39. Broomhead J.A., Dwyer F.P. and Hogarth J.W., Inorg. Synth., 1960, VI, 186-188.

40. Peacock R.D., J. Chem. Soc. Dalton Trans., 1983, 291-294.

41. Peacock R.D. and Stewart B., Coord. Chem. Revs., 1982, 46, 129-157.

42. Gollogly J.R. and Hawkins C.J., J. Chem. Soc. Chem, Commun., 1968, 689-690.

43. Dubicki L., Ferguson J., Geue R.J. and Sargeson A.M., Chem. Phys. Letts., 1980, 74(3), 393-397.

44. Nonoyama M., Inorg. Chim. Acta., 1978, 29, 211-215.

45. Kuroda R. and Mason S., Chem. Letts., 1978, 1045-1048.

46. Mason S.F. and Norman B.J., J. Chem. Soc. (A), 1966, 307-312.

47. Mason S.F. and Norman B.J., Proc. Chem. Soc., 1964, 339-340.

48. Drake A.F., Kuroda R. and Mason S.F., J. Chem. Soc. Dalton Trans., 1979, 1095-1100.

49. Shimba S., Fujinami S. and Shibata M., Chem. Letts., 1979, 783-784.

50. Fujinami S., Hosokawa T. and Shibata M., Bull. Chem. Soc. Jap., 1983, 56, 113-121.

51. Nonoyama M. and Sakai K., Inorg. Chim. Acta., 1983, 72, 57-60.

52. Wainwright K.P., J. Chem. Soc. Dalton Trans., 1980, 2117-2120.

53. Hama H. and Takamoto S., Nip. Kag. Kai., 1975, 1182-1185.

54. Takahashi M. and Takamoto S., Bull. Chem. Soc. Jap., 1977, 50(12), 3413-3414.

55. Wieghardt K., Bossek U., Chaudhuri P., Herrmann W., Menke B.C. and Weiss J., Inorg. Chem., 1982, 21, 4308-4314.

56. Van Der Merwe M.J., Boeyens J.C.A. and Hancock R.D., Inorg. Chem., 1983, 22, 3490-3492.

57. Van Der Merwe M.J., Boeyens J.C.A. and Hancock R.D., Inorg. Chem., 1985, 24, 1208-1213.

58. Sayer B.A., Michael J.P. and Hancock R.D., Inorg. Chim. Acta., 1983, 77, L63-64.

59. Hammershoi B.A. and Sargeson A.M., Inorg. Chem., 1983, 22, 3554-3561.

60. Taylor S.G., Snow M.R. and Hambley T.W., Aust. J. Chem., 1983, 36, 2359-2368.

61. "The Spectrum in Chemistry", Crooks J.E., Academic Press, London, 1978. (p.125).

62. Mason S.F., Chemistry in Britain, 1965, 1965, 245-249.

63. Drake A.F., J. Phys. E: Sci. Instrum., 1986,19, 170.

64. Pasteur L., Alembic Club Reprint, No14, Edinburgh, 1910.

65. Haidinger W., Annalen der Physic, 1847, 70, 531.

66. Drude P., "Lehrbuch der Optik", Leipzig 1900. Translation "The Theory of Optics", 1902, Mann C.R. and Milliken R.A., 400-417.

67. Cotton A., Comptes Rendus de L'Academie des Sciences, 1895, 120, 989 & 1044.

68. Rosenfeld L., Z. Phys., 1928, 52, 161.

69. Richardson F.S. and Riehl J.P., Chem. Revs., 1977, 77, 773-792.

70. Bencini A., Fabbrizzi L. and Poggi A., Inorg. Chem., 1981, 20, 2544-2549.

71. Arishima T., Hamada K. and Takamoto S., Nip. Kag. Kai., 1973, 1119-1121.

72. Robb J. and Peacock R.D., Inorg. Chim. Acta., 1986, 121, L15-17.

73. Mc Caffery A.J. and Mason S.F., Molec. Phys., 1963, 6, 359-371.

74. Mc Caffery A.J., Mason S.F., Norman B.J. and Sargeson A.M., J. Chem. Soc. (A), 1968, 1304-1310.

75. Hearson J.A., Mason S.F. and Seal R.H., J. Chem. Soc. Dalton Trans., 1977, 1026-1034.

76. Yoshikawa Y. and Yamasaki K., Inorg. Nucl. Chem. Letts., 1970, 6, 523-526.

77. Yoneda H., Chimika Chronika (New Series), 1986, 36-39.

78. Woldbye F., Rec. Chem. Prog., 1963, 24, 197.

79. Dingle R. and Ballhausen C.J., Kgl. Dan. Vidensk. Selsk. Mat.-Fys. Medd., 1967, 35, No. 12, (26pp).

80. Jensen H.P. and Galsbol F., Inorg. Chem., 1977, 16, (No 6), 1294-1297.

81. Ditze A. and Wasgestian F., J. Phys. Chem., 1985, 89, 426-428.

82. Flint C.D. and Matthews P.A., J. Chem. Soc. Faraday Trans., 2, 1976, 72, 579-589.

83. Hilmes G.L., Brittain H.G. and Richardson F.S., Inorg. Chem., 1977, 16(3), 528-533.

84. Kuhn K., Wasgestian F. and Kupka. H., J. Phys. Chem., 1981, 85, 665-670.

85. Peacock R.D. and Stewart B., J. Chem. Soc. Chem. Commun., 1982, 295-296.

86. Geiser U. and Gudel H.U., Inorg. Chem., 1981, 20, 3013-3019.

87. Saito Y., Nakatsu K., Shiro M. and Kuroya H., Bull. Chem. Soc. Jap., 1957, 30, 795-798.

88. Iwasaki H. and Saito Y., Bull. Chem. Soc. Jap., 1966, 39, 92-100.

89. Mc Caffery A.J., Mason S.F. and (in part) Ballard R.E., J. Chem. Soc., 1965, 2883-2892.

90. Murata K., Yamakazi Y. and Morita M., J. Lumin., 1979, 18/19, 407.

91. Kirk Othmer Encyclopedia of Chemical Technology, Wiley Interscience, New York, 1979, Vol 5, 355-357. (3rd Ed.)

92. Bijvoet J.M., Peerdeman A.F. and Van Bommel A.J., Nature, 1951, 168, 271-272.

93. Saito Y., Nakatsu K., Shiro M. and Kuroya H., Acta. Cryst., 1955, 8, 729-730.

94. Okamoto M.S. and Barefield E.K., Inorg. Chim. Acta., 1976, 17, 91-96.

95. Evreev V.N., Russian Journal of Inorganic Chemistry, 1967, 12(8), 1112-1116.

96. Fujinami S., Matsunami Y., and Shibata M., Bull. Chem. Soc. Jap., 1982, 55, 2101-2106.

97. Sato S., Ohba S., Shimba S., Fujinami S., Shibata M. and Saito Y., Acta Cryst, 1980, B36, 43-47.

98. Larsen E. and Mason S.F., J. Chem. Soc. (A), 1966, 313-316.

99. Harnung S.E., Kallesoe S., Sargeson A.M. and Schaffer C.E., Acta. Chem. Scand., 1974, A28, 385-398.

100. Yang R. and Zompa L.J., Inorg. Chem., 1976, 15(7), 1499-1502.